



**HAL**  
open science

**Electrochemical Advanced Oxidation Processes for  
removal of Pharmaceuticals from water : Performance  
studies for sub-stoichiometric titanium oxide anode and  
hierarchical layered double hydroxide modified carbon  
felt cathode**

Soliu Ganiyu

► **To cite this version:**

Soliu Ganiyu. Electrochemical Advanced Oxidation Processes for removal of Pharmaceuticals from water : Performance studies for sub-stoichiometric titanium oxide anode and hierarchical layered double hydroxide modified carbon felt cathode. Geophysics [physics.geo-ph]. Université Paris-Est, 2016. English. NNT : 2016PESC1116 . tel-01540817

**HAL Id: tel-01540817**

**<https://theses.hal.science/tel-01540817>**

Submitted on 16 Jun 2017

**HAL** is a multi-disciplinary open access archive for the deposit and dissemination of scientific research documents, whether they are published or not. The documents may come from teaching and research institutions in France or abroad, or from public or private research centers.

L'archive ouverte pluridisciplinaire **HAL**, est destinée au dépôt et à la diffusion de documents scientifiques de niveau recherche, publiés ou non, émanant des établissements d'enseignement et de recherche français ou étrangers, des laboratoires publics ou privés.

Joint PhD degree in Environmental Technology

UNIVERSITÉ  
— PARIS-EST

Docteur de l'Université Paris-Est  
Spécialité : Science et Technique de l'Environnement



Dottore di Ricerca in Tecnologie Ambientali



**UNESCO-IHE**

Institute for Water Education

Degree of Doctor in Environmental Technology

Thèse – Tesi di Dottorato – PhD thesis

Soliu Oladejo GANIYU

**Electrochemical Advanced Oxidation Processes for Removal of Organic pollutants from Water: Performance Studies for Sub-stoichiometric Titanium Oxide Anode and Hierarchical Layered Double Hydroxide Modified Carbon-felt Cathode**

To be defended December 2<sup>nd</sup>, 2016

In front of the PhD committee

Prof. Eric BRILLAS COSO

Prof. Jean PINSON

Prof. Marc CRETIN

Prof. Mehmet A. OTURAN

Hab. Dr. Eric van HULLEBUSCH

Prof. Dr. Ir. Piet LENS

Prof. Giovanni ESPOSITO

Reviewer

Reviewer

Examiner

Promotor/Thésis director

Co-promotor

Co-promotor

Co-promotor



Erasmus Joint doctorate programme in Environmental Technology for Contaminated Solids, Soils and Sediments (ETeCoS<sup>3</sup>)



Erasmus Joint doctorate programme in Environmental Technology for Contaminated Solids, Soils and Sediments (ETeCoS<sup>3</sup>)

## Acknowledgement

Many thanks to the Université Paris-Est and Université Paris-Est Marne-La-Vallée, and other collaborating institution involved in Environmental Technologies for Contaminated Solids, Soils and Sediments (ETeCoS<sup>3</sup>) programme for the opportunities, exposures and all logistic supports during my studies, and more importantly the European Commission and ANR (French National Research Agency) for funding my doctoral degree studies in Europe.

I sincerely acknowledge my thesis director (promotor) Prof. Mehmet A. Oturan for given me the opportunity to conduct this research work in his laboratory. All technical, scientific and administrative support as well as your trust during the course of this work is highly appreciated.

My sincere and profound gratitude goes to Dr. Nihal OTURAN, who always gave me unconditional support, technical assistance, guidance, wise cancelling and emotional support throughout the period of my study.

My sincere appreciation goes to the members of ETeCoS<sup>3</sup> committee, starting from the coordinator, Dr. Hab. Giovanni ESPOSITO (University of Cassino and Southern Lazio, Italy) Dr. Hab. Eric D. van HULLEBUSCH (Université Paris Est, France), and Prof. Piet LENS (UNESCO IHE, The Netherlands) for given me the opportunity to participate in this Erasmus Mundus Joint Doctoral Degree Programme.

I also acknowledge the co-promoters of this thesis, Dr. Hab. Eric D. van HULLEBUSCH and Dr. Hab. Giovanni ESPOSITO for their scientific, technical and administrative assistance, guidance and directions during the course of this work. It is also imperative to acknowledge Prof. Marc CRETIN and his colleague Dr. Mikhael BECHELANY for hosted and supported me technically and otherwise during my stage at Institut Européen des Membranes (IEM), Université de Montpellier, France. Stéphane Raffy (SAINT-GOBAIN CREE – Cavaillon, France) is acknowledged for her technical assistance in the production of Ti<sub>4</sub>O<sub>7</sub> electrode.

I wish to express my gratitude to reviewers of this thesis, Prof. Eric BRILLAS (University of Barcelona) and Prof. Jean PINSON (Université Paris Diderot-Paris 7) for accepting to read and evaluate this work.

Special thanks to Prof. Stéphanie ROSSANO, the director of the Laboratoires Géomatériaux et Environnement and her entire staff for their cooperation, assistance and hospitality during the course of this work.

I acknowledge the assistance and support of my colleagues – Clément TRELLU, Dr. Oleksandra GANZENKO, Dr. Hugo OLEVERA-VARGAS, Thi-Xuan-Huong LE, Nguyen LINH and Roséline ESMILAIRE for their contribution to the success of this thesis work.

Finally, my appreciation goes to my family and friends for their prayers, understanding and supports during my stay in Europe.

Soliu Oladejo Ganiyu

## Abstract

Pharmaceuticals residues as emerging pollutants have become a major concern due to their persistence and continuous accumulation in various environmental compartments and their removal is one the major challenges of this century. Electrochemical advanced oxidation processes (EAOPs) such as anodic oxidation (AO) and electro-Fenton (EF) have shown to be efficient techniques for complete degradation and mineralization of this class of pollutants. A substoichiometric titanium oxide ( $\text{Ti}_4\text{O}_7$ ) deposited on titanium alloy by plasma elaboration was investigated as an alternative stable and efficient low cost anode materials for application in AO and EF degradation of pharmaceuticals amoxicillin (AMX) and propranolol (PPN) and mineralization of their aqueous solutions. Excellent mineralization of both pharmaceuticals was achieved with  $\text{Ti}_4\text{O}_7$  anode compared to dimensional stable anode (DSA) and platinum (Pt) anodes at similar experimental conditions, but less efficient when compared with boron doped diamond (BDD) anode during AO treatment. Almost complete mineralization (96%) was attained with  $\text{Ti}_4\text{O}_7$  anode in EF degradation of PPN at 120 mA after 8 h of electrolysis. Several aromatic, bicyclic and other intermediate byproducts were identified and quantified during the electrochemical treatment of both pharmaceuticals, with the final end products in the treated solutions being short-chain carboxylic acids and inorganic ions. Plausible mineralization pathways for both pharmaceuticals were proposed based on the identified intermediates, released inorganic ions and carboxylic acids as well as TOC data. Initial AMX solution shows relatively high inhibition to *V. fischeri* bacteria, which further increased at the early stage of electrooxidation due to formation of cyclic intermediates that are more toxic than mother molecules, but sharply decreased at the later stage of electrolysis. Since the  $\text{Ti}_4\text{O}_7$  is produced mainly from  $\text{TiO}_2$  which is very cheap and highly abundant material, this anode material could be an interesting alternative electrode in industrial wastewater treatment by electrochemical oxidation. On the other hand, CoFe-layered double hydroxide modified carbon-felt (CoFe-LDH/CF) cathode synthesized by solvothermal process was studied as a heterogeneous catalyst/electrode for degradation of organic pollutant Acid Orange II (AO7) over a wide pH range. Excellent mineralization of this azo dye solution was achieved in pH range 2 – 7.1, with TOC removal much higher than corresponding homogeneous EF with raw carbon-felt (CF) at all pH studied. The prepared cathode exhibited good reusability and can constitute an alternative for the treatment of wastewater effluents at neutral pH values.

## Résumé

Les polluants émergents que sont les résidus de produits pharmaceutiques sont devenus une problématique majeure de par leur persistance et leur accumulation continue dans les différents compartiments de l'environnement. Leur élimination est un des challenges majeurs de ce siècle. Les procédés électrochimiques d'oxydation avancée (PEOA) tel que l'oxydation anodique (AO) et l'électro-Fenton (EF) ont démontré leur efficacité pour la dégradation et la minéralisation complète de cette classe de polluant. Un oxyde de titane sous-stœchiométrique déposé par plasma sur un alliage de titane a été étudié comme anode alternative peu coûteuse, stable et efficace au cours des procédés d'OA et d'EF pour la dégradation et la minéralisation de deux pharmaceutiques, l'amoxicilline (AMX) et le propranolol (PPN). Une excellente minéralisation de ces deux composés a été atteinte avec l'anode  $Ti_4O_7$  comparé à l'utilisation d'une anode dimensionnellement stable (ADS) et d'une anode de platine (Pt) avec des conditions expérimentales similaires, mais une plus faible efficacité a été observé par comparaison à une anode de diamant dopé au bore (DDB) au cours du procédé d'OA. Une quasi-total minéralisation (96%) du PPN a été atteinte avec l'anode  $Ti_4O_7$  au cours du procédé EF après 8 h d'électrolyse à 120 mA. Plusieurs intermédiaires aromatiques, bicycliques et autres ont été identifiés et quantifiés au cours du traitement électrochimique des deux composés pharmaceutiques, ainsi que des acides carboxyliques à chaîne courte et des ions inorganique comme produits finaux de dégradation. Des voies plausibles de dégradation ont été proposées à partir des intermédiaires identifiés, des ions inorganiques libérés ainsi que des données obtenues sur les acides carboxyliques et le COT. La solution initiale d'AMX a mené à une relativement forte inhibition de la bactérie *V. fischeri*, qui a ensuite augmenté au cours des premiers stades de l'électro-oxydation de par la formation d'intermédiaires cycliques plus toxiques que la molécule mère, avant de diminuer nettement au cours des étapes suivantes de l'électrolyse. Puisque le  $Ti_4O_7$  est produit principalement à partir du  $TiO_2$ , un matériau bon marché et abondant, ce matériau d'anode pourrait être une alternative intéressante pour le traitement des eaux usées industrielles par oxydation électrochimique. Par ailleurs, une cathode de feutre de carbone modifiée par des composés hydroxydes à double couche CoFe (CoFe-LDH/CF) et synthétisée par un procédé solvothermique a été étudiée come catalyseur/électrode pour la dégradation du polluant organique Acide Orange II (AO7) par le procédé EF sur une gamme large de pH. Une excellente minéralisation de ce colorant a été atteinte pour des pH allant de 2 à 7.1, avec une élimination du

COT largement supérieure à celle atteinte en utilisant le procédé EF avec une cathode de feutre de carbone brut, quel que soit le pH étudié. La cathode préparée a montré une bonne capacité de réutilisation et peut constituer une alternative pour le traitement des eaux usées à des valeurs de pH neutre.



## Sintesi

I residui farmaceutici sono diventati una delle principali minacce per la salute ambientale, a cause della loro lunga persistenza e continuo accumulo in vari settori ambientali. La rimozione di queste sostanze è una delle sfide più difficili di questo secolo. I processi elettrochimici di ossidazione avanzata (EAOPs), come l'ossidazione anodica (AO) e l'elettro-Fenton (EF), si sono rivelati efficienti al fine di ottenere la completa decomposizione e mineralizzazione di questo tipo di inquinanti. L'obiettivo di questo studio è stato quello di testare un materiale anodico alternativo, efficiente ed economico per i processi AO ed EF. Una quantità substechiometrica di ossido di titanio ( $Ti_4O_7$ ) depositata su lega di titanio tramite elaborazione al plasma è stata utilizzata al fine di ottenere la decomposizione di sostanze farmaceutiche quali amoxicillina (AMX) ed propranololo (PPN) e la mineralizzazione delle rispettive soluzioni liquide. L'utilizzo di un anodo con  $Ti_4O_7$  ha prodotto una migliore mineralizzazione di entrambe le sostanze rispetto a quella ottenuta con un anodi dimensionalmente stabili (DSA) e di platino (Pt) nelle stesse condizioni sperimentali. Tuttavia, la mineralizzazione si è dimostrata meno efficiente se paragonata a quella ottenuta mediante AO con un anodo BDD (boron-doped diamond). Una quasi completa mineralizzazione (96%) è stata ottenuta mediante EF ed un anodo con  $Ti_4O_7$  durante la degradazione del propranololo a 120 mA dopo 8 h di elettrolisi. Diversi composti aromatici, biciclici ed altri prodotti intermedi sono stati identificati e quantificati durante il trattamento elettrochimico delle due sostanze farmaceutiche. I prodotti finali nelle soluzioni trattate sono stati acidi carbossilici a catena corta e ioni inorganici. Un possibile meccanismo di mineralizzazione è stato proposto per entrambe le sostanze sulla base degli intermedi di reazione identificati, degli ioni inorganici ed acidi carbossilici prodotti e dei risultati dell'analisi sul carbonio organico totale (TOC). La soluzioni iniziale di AMX ha prodotto un'elevata inibizione dell'attività del batterio *V. fisheri*, che è ulteriormente aumentata all'inizio del processo di elettro-ossidazione a causa della formazione di composti intermedi ciclici più tossici delle molecole di provenienza. Al contrario, l'inibizione è rapidamente diminuita nell'ultima fase dell'elettrolisi. Il  $Ti_4O_7$  è prodotto principalmente dal biossido di titanio ( $TiO_2$ ), il quale è un materiale molto economico ed abbondante. Per questo motivo, l'utilizzo di  $Ti_4O_7$  come materiale anodico può diventare un'alternativa interessante per il trattamento di reflui industriali tramite ossidazione elettrochimica. In questo studio, un catodo CoFe-LDH/CF (CoFe-layer double hydroxide modified carbon-felt) sintetizzato tramite un processo solvotermico è stato utilizzato

come elettrodo/catalizzatore per la degradazione dell'inquinante organico Acid Orange II (AO7) in un ampio intervallo di pH. Un'eccellente mineralizzazione di questa soluzione azo dye è stata ottenuta in un intervallo di pH compreso tra 2 e 7.1, con una rimozione di TOC molto maggiore di quella ottenuta mediante EF e catodo carbon-felt (CF) a tutti i valori di pH studiati. Il nuovo catodo sintetizzato in questo studio ha mostrato una buona riusabilità e può costituire un'interessante alternativa per il trattamento dei reflui a pH neutro.

## Samenvatting

Pharmaceuticals resten opkomende verontreinigende stoffen hebben een belangrijke zorg geworden als gevolg van hun persistentie en continue accumulatie in verschillende milieu compartimenten en de uitslag is een van de grote uitdagingen van deze eeuw. Elektrochemische geavanceerde oxidatieprocessen (EAOPs) zoals anodische oxidatie (AO) en elektro-Fenton (EF) hebben aangetoond dat efficiënte technieken voor volledige afbraak en mineralisatie van deze klasse van stoffen zijn. Een substoichiometrisch titaniumoxide ( $Ti_4O_7$ ) op titanium legering afgezet door plasma uitwerking werd onderzocht als alternatief stabiele en efficiënte low cost anode materialen voor toepassing in AO en EF afbraak van geneesmiddelen amoxicilline (AMX) en propranolol (PPN) en mineralisatie van hun waterige oplossingen. Uitstekende mineralisatie van beide geneesmiddelen werd bereikt met  $Ti_4O_7$  anode tegenover dimensionaal stabiele anode (DSA) en platina (Pt) anodes soortgelijke experimentele omstandigheden, maar minder efficiënt in vergelijking met borium gedoteerd diamant (BDD) anode tijdens AO behandeling. Bijna volledige mineralisatie (96%) werd verkregen met  $Ti_4O_7$  anode EF afbraak van PPN bij 120 mA na 8 uur elektrolyse. Verschillende aromatische bicyclische en andere intermediaire bijproducten werden geïdentificeerd en gekwantificeerd tijdens de elektrochemische behandeling van beide geneesmiddelen, met het uiteindelijke eindproducten in de behandelde oplossing wordt kortketenige carbonzuren en anorganische ionen. Plausibele mineralisatie routes voor beide geneesmiddelen werden voorgesteld op basis van de geïdentificeerde tussenproducten, vrijgegeven anorganische ionen en carbonzuren evenals TOC data. Initiële AMX oplossing zijn tamelijk hoog remming *V. fischeri* bacteriën, die verder vergroot in een vroeg stadium van elektro-oxidatie door vorming van organische tussenproducten die giftiger dan moeder moleculen, maar sterk gedaald in de latere fase van elektrolyse. Aangezien de  $Ti_4O_7$  hoofdzakelijk wordt geproduceerd  $TiO_2$  die zeer goedkoop en zeer overvloedige materiaal mag deze anodemateriaal een interessant alternatief elektrode in industrieel afvalwater door elektrochemische oxidatie. Anderzijds, CoFe-gelaagd dubbel hydroxide gemodificeerd koolstof vilt (CoFe-LDH / CF) kathode gesynthetiseerd door solvothermal werkwijze werd bestudeerd als heterogene katalysator / elektrode voor afbraak van organische verontreinigende Acid Orange II (AO7) over een breed pH-traject. Uitstekende mineralisatie van deze azokleurstof oplossing werd bereikt bij pH 2-7,1, met TOC verwijdering veel hoger dan overeenkomstige homogene EF rauwe koolstof vilt (CF) in alle onderzochte pH. De bereide kathode vertoonde goede

herbruikbaarheid en een alternatief voor de behandeling van afvalwater afvalwater bij neutrale pH-waarden vormen.

## Table of Contents

<b>ACKNOWLEDGEMENT</b> .....	<b>i</b>
<b>ABSTRACT</b> .....	<b>iii</b>
<b>RÉSUMÉ</b> .....	<b>iv</b>
<b>SINTESI</b> .....	<b>vi</b>
<b>SAMENVATTING</b> .....	<b>viii</b>
<b>TABLE OF CONTENTS</b> .....	<b>x</b>
<b>LIST OF TABLES</b> .....	<b>xiv</b>
<b>LIST OF FIGURES</b> .....	<b>xv</b>
<b>LIST OF ABBREVIATION</b> .....	<b>xiv</b>
<b>CHAPTER 1 INTRODUCTION</b> .....	<b>1</b>
<b>1.1 Background</b> .....	<b>2</b>
<b>1.2 Challenges</b> .....	<b>3</b>
<b>1.3 Selection of pharmaceuticals</b> .....	<b>4</b>
<b>1.4 Objectives</b> .....	<b>4</b>
<i>1.4.1 Electrochemical oxidation using <math>Ti_4O_7</math> ceramic anode</i> .....	<b>5</b>
<i>1.4.2 Heterogeneous electro-Fenton with modified carbon felt cathode</i> .....	<b>5</b>
<b>1.5 Novelty of the thesis</b> .....	<b>6</b>
<b>1.6 Structure of the thesis</b> .....	<b>7</b>
<b>References</b> .....	<b>9</b>
<b>CHAPTER 2 LITERATURE REVIEW</b> .....	<b>14</b>
<b>Abstract</b> .....	<b>16</b>
<b>2.1 Introduction</b> .....	<b>17</b>
<b>2.2 Pharmaceuticals: Occurrence, fate and toxicity</b> .....	<b>19</b>
<i>2.2.1 Occurrence of PhACs in aquatic environment</i> .....	<b>19</b>
<i>2.2.2 Fate of PhACs in aquatic environment</i> .....	<b>21</b>
<i>2.2.3 Toxicity of PhACs in aquatic environment</i> .....	<b>21</b>
<b>2.3 Dyes Stuff in environment: Occurrence and Toxicity</b> .....	<b>22</b>
<b>2.4 Removal of pharmaceutical residues from aqueous solution by EAOPs</b> .....	<b>24</b>
<i>2.4.1 Electrooxidation/Anodic oxidation</i> .....	<b>24</b>
<i>2.4.2 Electro-Fenton Process</i> .....	<b>27</b>

2.4.3 Electrode materials for electrochemical oxidation.....	29
2.4.3.1 Carbon and graphite electrodes.....	29
2.4.3.2 Ruthenium, Thallium and Iridium oxides – based electrodes .....	30
2.4.3.3 Platinum electrodes .....	32
2.4.3.4 Doped-Tin oxides ( $\text{SnO}_2$ ) based electrodes .....	33
2.4.3.5 Lead oxide ( $\alpha\text{-PbO}_2$ ) based electrodes.....	34
2.4.3.6 Boron doped diamond electrodes.....	34
2.4.3.7 Doped and substoichiometric titanium oxides based electrode.....	36
2.4.4 Heterogeneous electro-Fenton process.....	38
2.4.4.1 Heterogeneous electro-Fenton process using added catalyst.....	40
2.4.4.2 Heterogeneous electro-Fenton process using catalyst impregnated electrode.....	43
<b>2.5 Conclusions .....</b>	<b>44</b>
<b>References .....</b>	<b>46</b>
<b>CHAPTER 3 ELECTROOXIDATION USING SUB-STOICHIOMETRIC TITANIUM OXIDE (<math>\text{Ti}_4\text{O}_7</math>) ANODE .....</b>	<b>68</b>
<b>Abstract .....</b>	<b>70</b>
<b>3.1 Introduction .....</b>	<b>71</b>
<b>3.2 Materials and Methods .....</b>	<b>73</b>
3.2.1 Chemicals .....	73
3.2.2 Preparation and characterization of $\text{Ti}_4\text{O}_7$ electrode .....	73
3.2.3 Electrolytic system .....	76
3.2.4 Instruments and analytical procedures .....	77
<b>3.3 Results and Discussion .....</b>	<b>79</b>
3.3.1. Kinetic studies of AMX degradation.....	79
3.3.2 Mineralization of AMX solution.....	82
3.3.3 Evolution of the oxidation byproducts of AMX and mineralization pathways .....	87
3.3.5 Evolution of toxicity of AMX solution during electrooxidation treatment.....	92
<b>3.4 Conclusions .....</b>	<b>93</b>
<b>References .....</b>	<b>94</b>
<b>CHAPTER 4 SUBSTOICHIOMETRIC TITANIUM OXIDE (<math>\text{Ti}_4\text{O}_7</math>): A NEW ELECTRODE IN EF PROCESS .....</b>	<b>101</b>

<b>Abstract .....</b>	<b>103</b>
<b>4.1 Introduction .....</b>	<b>104</b>
<b>4.2 Experimental .....</b>	<b>107</b>
4.2.1 <i>Chemicals .....</i>	<i>107</i>
4.2.2 <i>Instruments and analytical procedures.....</i>	<i>107</i>
4.2.3 <i>Electrolytic systems .....</i>	<i>109</i>
<b>4.3 Results and discussion .....</b>	<b>110</b>
4.3.1 <i>Comparative mineralization of PPN solution by AO and EF processes .....</i>	<i>110</i>
4.3.2 <i>Degradation kinetics of PPN.....</i>	<i>114</i>
4.3.3 <i>Identification and evolution of the oxidation by-products.....</i>	<i>120</i>
4.3.4 <i>Reaction sequence for PPN mineralization.....</i>	<i>124</i>
<b>4.4 Conclusions .....</b>	<b>126</b>
<b>References .....</b>	<b>127</b>
<b>CHAPTER 5 HETEROGENEOUS ELECTRO-FENTON DEGRADATION OF ORGANIC POLLUTANTS AT CIRCUMNEUTRAL pH .....</b>	<b>133</b>
<b>Abstract .....</b>	<b>135</b>
<b>5.1 Introduction .....</b>	<b>137</b>
<b>5.2 Experimental Procedures .....</b>	<b>139</b>
5.2.1 <i>Reagents and Materials .....</i>	<i>139</i>
5.2.2 <i>Electrode preparation.....</i>	<i>140</i>
5.2.3 <i>Characterization.....</i>	<i>140</i>
5.2.4 <i>EF experiment .....</i>	<i>141</i>
5.2.5 <i>Instrument and analytic procedure .....</i>	<i>141</i>
<b>5.3 Results and Discussion .....</b>	<b>142</b>
5.3.1 <i>Preparation of CoFe-LDH/CF electrode .....</i>	<i>142</i>
5.3.2 <i>Structural and morphological properties of the CoFe-LDH/CF.....</i>	<i>142</i>
5.3.3 <i>Electrochemical behavior of the CoFe-LDH/CF .....</i>	<i>148</i>
5.3.4 <i>Mineralization of AO7 by EF process using CoFe-LDH/CF cathode over wide pH range .....</i>	<i>150</i>
5.3.5 <i>Effect of hydrothermal treatment parameters on mineralization of AO7.....</i>	<i>153</i>
5.3.6 <i>Catalyst leaching and stability of the CoFe-LDH/CF.....</i>	<i>155</i>

5.3.7 Mechanism of Efficient removal of AO7 with CoFe-LDH/CF cathode in EF oxidation...	158
<b>5.4 Conclusions</b> .....	<b>160</b>
<b>Reference</b> .....	<b>162</b>
<b>CHAPTER 6 GENERAL CONCLUSIONS AND FUTURE PERSPECTIVES</b> .....	<b>168</b>
<b>6.1 General conclusions</b> .....	<b>169</b>
6.1.1 Electrooxidation of pharmaceutical residues using sub-stoichiometric titanium oxides...	169
6.1.2 Substoichiometric titanium oxides as suitable anode materials for electro-Fenton degradation of pharmaceuticals .....	170
6.1.3 Heterogeneous electro-Fenton process – an efficient alternative .....	171
<b>6.2 Future perspectives</b> .....	<b>171</b>
6.2.1 High current density application of plasma $Ti_4O_7$ electrode .....	171
6.2.2 Coupling of membrane nanofiltration and EAOPs using reactive membranes .....	172
6.2.3 Enhancing the stability of the modified cathode and assessing the toxicity of the solution.....	172
6.2.4 Treatment of real wastewater effluents .....	173
<b>ANNEXES</b> .....	<b>xxii</b>
<b>Annex 1</b> .....	<b>xxiii</b>
<b>Valorization of the PhD research</b> .....	<b>xxiii</b>
<b>Annex 2</b> .....	<b>xxvi</b>
<b>Curriculum Vitae</b> .....	<b>xxvi</b>



## List of Tables

### CHAPTER 2 LITERATURE REVIEW

**Table 2-1**– summary of some recent studies on heterogeneous EF treatment with added catalyst .....41

### CHAPTER 3 ELECTROOXIDATION USING SUB-STOICHIOMETRIC TITANIUM OXIDE (Ti<sub>4</sub>O<sub>7</sub>) ANODE

**Table 3-1** – Apparent rate constants ( $k_{app,AMX}$ ) for the electrooxidation of AMX by M( $\bullet$ OH) ...81

### CHAPTER 4 SUBSTOICHIOMETRIC TITANIUM OXIDE (Ti<sub>4</sub>O<sub>7</sub>): A NEW ELECTRODE IN EF PROCESS

**Table 4-2**– Apparent rate constants ( $k_{app,PPN}$ ) for the electrochemical degradation of PPN by  $\bullet$ OH assuming pseudo first-order reaction .....119

### CHAPTER 5 HETEROGENEOUS ELECTRO-FENTON DEGRADATION OF ORGANIC POLLUTANTS AT CIRCUMNEUTRAL PH

**Table 5-3**– concentration of Co and Fe after 8h during EF treatment at different pHs .....152

## List of Figures

<b>CHAPTER 1 INTRODUCTION .....</b>	<b>1</b>
<b>Figure 1-1– Structure of the thesis .....</b>	<b>8</b>
<b>CHAPTER 2 LITERATURE REVIEW.....</b>	<b>15</b>
<b>Figure 2-1– Origin and transport of PhACs in environment .....</b>	<b>20</b>
<b>Figure 2-2– Color change due to dyes contamination of surface water and landfill .....</b>	<b>23</b>
<b>CHAPTER 3 ELECTROOXIDATION USING SUB-STOICHIOMETRIC TITANIUM OXIDE (Ti<sub>4</sub>O<sub>7</sub>) ANODE .....</b>	<b>68</b>
<b>Figure 3-1 – X-ray diffraction pattern of the powder used in preparing Ti<sub>4</sub>O<sub>7</sub> anode .....</b>	<b>74</b>
<b>Figure 3-2 – TiO<sub>x</sub> particle size distribution used in preparation of Ti<sub>4</sub>O<sub>7</sub>.....</b>	<b>75</b>
<b>Figure 3-3 – SEM image of the prepared Ti<sub>4</sub>O<sub>7</sub> anode (a) surface, and (b) cross-section .....</b>	<b>76</b>
<b>Figure 3-4 – Effect of applied current: (-■-) 10 mA (-●-) 30 mA, (-▲-) 60 mA and (-▼-) 120 mA on AMX concentration decay vs. electrolysis time for the electrooxidation treatment of 0.1 mM AMX in 0.05 M Na<sub>2</sub>SO<sub>4</sub> using (a) Ti<sub>4</sub>O<sub>7</sub> and (b) BDD anode and carbon-felt cathode .....</b>	<b>80</b>
<b>Figure 3-5 – Contribution of in-situ generated H<sub>2</sub>O<sub>2</sub> to the decay of AMX concentration vs time with stainless steel cathode (-■-) and carbon-felt cathode (-●-) for the electrooxidation at 120 mA of 0.1 mM AMX in 0.05 M Na<sub>2</sub>SO<sub>4</sub> using (a) Ti<sub>4</sub>O<sub>7</sub> and (b) BDD anode .....</b>	<b>82</b>
<b>Figure 3-6 – Effect of applied current: (-■-) 10 mA (-●-) 30 mA, (-▲-) 60 mA and (-▼-) 120 mA on TOC removal (a, b) and mineralization current efficiency(c, d) vs. electrolysis time during the electrooxidation of 0.1 mM (19.6 mg L<sup>-1</sup> initial TOC) AMX in 0.05 M Na<sub>2</sub>SO<sub>4</sub> using Ti<sub>4</sub>O<sub>7</sub>, (a, c) and BDD (b, d) anode and carbon-felt cathode .....</b>	<b>84</b>
<b>Figure 3-7 – (a) Effect of in-situ generated H<sub>2</sub>O<sub>2</sub> on the mineralization of 0.1 mM AMX (19.6 mg L<sup>-1</sup> TOC) in 0.05 M Na<sub>2</sub>SO<sub>4</sub> medium at applied current of 60 mA, (-■-) without H<sub>2</sub>O<sub>2</sub> (stainless steel cathode) and (-●-) with H<sub>2</sub>O<sub>2</sub> generation using Ti<sub>4</sub>O<sub>7</sub> anode. (b) Stability of activity of Ti<sub>4</sub>O<sub>7</sub> with usage time for mineralization of 0.1 mM AMX (19.6 mg L<sup>-1</sup> TOC) in 0.05 M Na<sub>2</sub>SO<sub>4</sub> medium at applied current of 60 mA: (-▲-) &lt; 25 h, (-◆-) &gt; 200 h of usage .....</b>	<b>86</b>

**Figure 3-8** – Time-course of the identified inorganic ions: (-■-)  $\text{NH}_4^+$  (-●-)  $\text{NO}_3^-$  and (-▲-)  $\text{SO}_4^{2-}$  during the electrooxidation of 0.1 mM AMX in 0.05 M  $\text{K}_2\text{SO}_4$  (for  $\text{NH}_4^+$ ) and NaCl (for  $\text{SO}_4^{2-}$ ) analyses during constant current electrolysis at 120 mA using (a)  $\text{Ti}_4\text{O}_7$  and (b) BDD anode and carbon-felt cathode .....88

**Figure 3-9** – Time-course of the identified short-chain carboxylic acids: (-■-) oxalic; (-●-) maleic; (-▲-) malonic (-▼-) oxamic; (-◀-) acetic; (-▶-) glyoxylic during the electrooxidation of 0.1 mM AMX in 0.05 M  $\text{Na}_2\text{SO}_4$  solution at 120 mA using (a)  $\text{Ti}_4\text{O}_7$  and (b) BDD and carbon-felt cathode .....89

**Figure 3-10** – Proposed reaction mechanism for the total mineralization of AMX by electrooxidation using  $\text{Ti}_4\text{O}_7$  anode .....91

**Figure 3-11**– Toxicity evolution of 0.1 mM AMX solution during electro-oxidation with  $\text{Ti}_4\text{O}_7$  anode at 120 mA in terms of Inhibition of luminescence of *V. fischeri* bacteria after (-■-) 5 min and (-●-) 15 min exposure time .....92

**CHAPTER 4 SUBSTOICHIOMETRIC TITANIUM OXIDE ( $\text{Ti}_4\text{O}_7$ ): A NEW ELECTRODE IN EF PROCESS .....101**

**Figure 4-1**- Decay of the TOC vs electrolysis time during the degradation of 0.1 mM PPN (corresponding to  $19.2 \text{ mg L}^{-1}$  initial TOC) in 0.05 M  $\text{Na}_2\text{SO}_4$  solution at pH 3 by anodic oxidation (a-c) and electro-Fenton (d) using (a) DSA and (b-d)  $\text{Ti}_4\text{O}_7$  anode. Current: (a, b, and d) 60 mA, and (c) 120 mA .....111

**Figure 4-2**- Effect of applied current on the decay of TOC (a, b) and mineralization current efficiency (MCE) (c, d) vs electrolysis time for the mineralization of 0.1 mM PPN ( $19.2 \text{ mg L}^{-1}$  initial TOC) in 0.05 M  $\text{Na}_2\text{SO}_4$  with 0.1 mM  $\text{Fe}^{2+}$  at pH 3 using (a, c)  $\text{Ti}_4\text{O}_7$  and (b, d) DSA anodes at applied current of (■) 10 mA, (●) 30 mA, (▲) 60 mA, and (▼) 120 mA .....113

**Figure 4-3**- Effect of initial PPN concentration on the decay of TOC (a) and mineralization current efficiency (MCE) (b) vs electrolysis time for the mineralization of PPN in 0.05 M  $\text{Na}_2\text{SO}_4$  with 0.1 mM  $\text{Fe}^{2+}$  using  $\text{Ti}_4\text{O}_7$  anode and applied current of 60 mA; (■) 0.05 mM ( $9.6 \text{ mg L}^{-1}$  TOC), (●) 0.1 mM ( $19.2 \text{ mg L}^{-1}$  TOC), and (▲) 0.2 mM ( $38.4 \text{ mg L}^{-1}$  TOC) .....114

**Figure 4-4**- (a) Decay of PPN concentration vs electrolysis time for the treatment of 0.1 mM PPN at 60 mA and pH 3 using  $\text{Ti}_4\text{O}_7$  anode, (■) EF and (●) AO- $\text{H}_2\text{O}_2$ ; (b, c) effect of current and (d) effect of initial PPN concentration on the decay of PPN concentration vs electrolysis time for

the EF treatment at pH 3 using (b) Ti<sub>4</sub>O<sub>7</sub>, (c) DSA anodes at initial concentration of 0.1 mM and applied current of (■) 10 mA, (●) 30 mA, (▲) 60 mA, and (▼) 120 mA; and (d) Ti<sub>4</sub>O<sub>7</sub> anode at applied current of 60 mA and initial concentration of (◆) 0.05 mM, (◀) 0.1 mM and (▶) 0.2 mM .....116

**Figure 4-5-** Time course of the concentration of main aromatic intermediates: (a) phthalic acid and (b) 1-naphthol accumulated during the EF treatment with Ti<sub>4</sub>O<sub>7</sub> anode of 0.1 mM PPN in 0.05 M Na<sub>2</sub>SO<sub>4</sub> with 0.1 mM Fe<sup>2+</sup> at pH 3 and applied current of (■) 10 mA, (●) 30 mA, (▲) 60 mA, and (▼) 120 mA .....121

**Figure 4-6-** Time course of the concentration of the short-chain carboxylic acids: (■) oxalic, (●) oxamic, (▲) glyoxylic, and (▼) maleic acids accumulated during the treatment of 0.1 mM PPN in 0.05 M Na<sub>2</sub>SO<sub>4</sub> with 0.1 mM Fe<sup>2+</sup> at pH 3 and applied current of 60 mA using (a) Ti<sub>4</sub>O<sub>7</sub> and (b) DSA anodes .....122

**Figure 4-7-** Time-course of concentration of nitrogenated inorganic ions: (■) NH<sub>4</sub><sup>+</sup> and (●) NO<sub>3</sub><sup>-</sup>, during the treatment of 0.1 mM PPN in 0.05 M Na<sub>2</sub>SO<sub>4</sub> (K<sub>2</sub>SO<sub>4</sub> for NH<sub>4</sub><sup>+</sup>) with 0.1 mM Fe<sup>2+</sup> at pH 3 and applied current of 60 mA using (a) Ti<sub>4</sub>O<sub>7</sub> and (b) DSA anodes .....123

**Figure 4-8-** Proposed reaction sequence for complete mineralization of PPN by EF process assuming ·OH as the main oxidizing agent .....125

**CHAPTER 5 HETEROGENEOUS ELECTRO-FENTON DEGRADATION OF ORGANIC POLLUTANTS AT CIRCUMNEUTRAL PH .....133**

**Figure 5-1.** SEM images of (a) raw CF, (b) CoFe-LDH/CF – 70 °C for 7 h (c) CoFe-LDH/CF – 90 °C for 4 h (d) CoFe-LDH/CF – 90 °C for 7 h (e) magnified image of (d), (f) CoFe-LDH/CF – 90 °C for 21 h (g) CoFe-LDH/CF – 120 °C for 7 h and (h) CoFe-LDH/CF – 90 °C for 7 h. Note: (a-f) – 25:12.5 and (h) – 50: 25 (Co<sup>2+</sup>/Fe<sup>3+</sup>) .....144

**Figure 5-2–** TEM images of CoFe-LDH .....145

**Figure 5-3–** (a) XRD pattern of the powder CoFe-LDH (red curve) and CoFe-LDH/CF electrode (black curve), (b) FTIR – spectrum of the powder CoFe-LDH and (c) N<sub>2</sub> adsorption isotherm CoFe-LDH .....147

**Figure 5-4–** XPS spectra for (a) Co 2p, (b) Fe 2p of CoFe-LDH/CF, (c) C1s and (d) existential state of Co, Fe, C, O and N of CoFe-LDH/CF .....148

**Figure 5-5**– (a) CVs of CoFe-LDH/CF (synthesized at 90 °C for 7 h), in 50 mM Na<sub>2</sub>SO<sub>4</sub> at scan rate 50 mVs<sup>-1</sup>: Curves at (a) pH 5.83, (b) pH 3 and (c) pH 2; and (b) electrochemical impedance spectra of raw and CoFe-LDH modified CF .....149

**Figure 5-6.** (a) Effect of initial solution pH on the mineralization of AO7 using CoFe-LDH/CF synthesized at 90 °C, for 7 h and 25:12.5 molar concentration, (■) pH 2, (●) pH 3, (▲) pH 5.83, and (▼) pH 7.1, (b) Comparison between heterogeneous EF with CoFe-LDH/CF cathode and homogeneous EF with raw CF cathode and Fe<sup>2+</sup>/Co<sup>2+</sup> at different pH .....151

**Figure 5-7**– Degradation of AO7 at pH 3 (■) Fe<sup>2+</sup>, (●) Co + Fe (1:1), (▲) Co + Fe (2:1) (▼) CoFe-LDH/CF.....153

**Figure 5-8**– Effect of hydrothermal treatment parameters on the mineralization of AO7 at pH 3: (a) temperature (■) 70 °C, (●) 90 °C and (▲) 120 °C; (b) time (▼) 4 h, (◆) 7 h, (◀) 14 h and (▶) 21 h; and (c) initial molar concentration of growth solution (Co<sup>2+</sup>:Fe<sup>3+</sup>) (□) 10:5, (△) 25:12.5 and (◇) 50:25 (Co<sup>2+</sup>:Fe<sup>3+</sup>). (RSD: 2%) .....154

**Figure 5-9.** (a) Evolution of the concentration of Fenton’s catalyst/co-catalyst in the treated solution (RSD: 1%); (■) Co and (●) Fe and (b) TOC removal (RSD: 2%) after 2 h vs number of cycles for the EF treatment using CoFe-LDH/CF synthesis at optimal conditions.....156

**Figure 5-10.** (a) SEM image of CoFe-LDH/CF; XPS spectra for (b) Co 2p and (d) Fe 2p of CoFe-LDH/CF after used in EF degradation of AO7 at pH 3 for 8 h .....158

**Figure 5-9.** Schematic illustration of AO7 degradation in heterogeneous EF system with CoFe-LDH/CF cathode .....158

## List of abbreviations

ETeCoS <sup>3</sup>	Environmental Technologies for contaminated solids, soils and sediments
ANR	French National Research Agency
IEM	Institut Européen des Membranes
EAOPs	electrochemical advanced oxidation processes
AO	anodic oxidation
EF	electro-Fenton
AMX	amoxicillin
PPN	propranolol
DSA	dimensional stable anode
Pt	platinum
BDD	boron-doped diamond anode
Ti <sub>4</sub> O <sub>7</sub>	sub-stoichiometric titanium oxide
TOC	total organic carbon
CoFe-LDH/CF	cobalt-iron layered double hydroxide modified carbon felt
AO7	acid orange II
CF	carbon-felt
WWTPs	wastewater treatment plants
UV	ultra-violent
AOPs	advanced oxidation processes
<sup>•</sup> OH	hydroxyl radical

LDH	layered double hydroxide
PhACs	pharmaceutical active compounds
V	voltage
SHE	standard hydrogen electrode
LC-MS	liquid chromatography coupled with mass spectroscopy
HPLC-MS	high performance liquid chromatography coupled with mass spectroscopy
GC-MS	gas chromatography coupled with mass spectroscopy
NE	north east
STPs	sewage treatment plants
NOM	natural organic matter
ROS	reactive oxygen species
POPs	persistence organic pollutants
ROC	reverse osmosis concentrate
GDEs	gas diffusion electrodes
ACF	activated carbon felt
Sb	antimony
Ar	argon
B	boron
Bi	bismuth
F	fluorine
Cl	chlorine
eV	electron volt
NDR	niobium-doped rutile TiO <sub>2</sub>
COD	chemical oxygen demand
p-NP	p-nitrophenol
2,4-DCP	2,4-dichlorophenol
RSD	relative standard deviation
AHPS	4-amino-3-hydroxy-2- <i>p</i> -tolylazo-naphthalene-1-sulfonic acid
PTFE	polytetrafluoroethylene
SEM	scanning electron microscopy
DC	direct current

MCE	mineralization current efficiency
$k_{app}$ ,	apparent rate constant
SCE	standard calomel electrode
IC	ionic chromatography
XRD	X-ray diffraction spectroscopy
SEM-EDX	scanning electron microscopy connect of energy dispersive X-ray spectroscopy
FTIR	Fourier transform infra-red
XPS	X-ray photoelectron spectroscopy
CV	cyclic voltammetry
EIS	electrochemical impedance spectroscopy
ICP-OES	optical emission spectrometer coupled Inductively Coupled Plasma
$R_{ct}$	interfacial charge-transfer resistance



# **CHAPTER 1**

---

## **INTRODUCTION**

## CHAPTER 1

### 1.1 Background

Pharmaceuticals as emerging pollutants have been found in wastewater, surface, tap and underground water bodies [1–6]. The major route via which pharmaceuticals enter into the aquatic environment is effluent of municipal wastewater treatment plants (WWTPs) due to insufficient capability of treatment techniques employed to completely remove this pollutants [7–13]. Other sources include indiscriminate disposal of expired drugs, site contamination, hospital wastewater, field treatment and livestock impoundments and treatments in aqua culture [12,14–17]. Several authors have reported the potential toxicological effects of pharmaceuticals released into the environment on aquatic organisms, although the effects of these pollutants on health and safety of human are not well understood [18–24].

Several remediation techniques have been studied for the removal of pharmaceuticals from aquatic environment. Both physical and physicochemical techniques such as adsorption, coagulation-flocculation and membrane filtration and biological treatment are inadequate for the removal of this pollutants because pharmaceuticals are xenophobic and refractory in nature [25]. Chemical oxidation technique like chlorination, peroxidation (UV-peroxidation) and ozonation usually leads to the formation of several stable intermediate by-products, which are sometimes more toxic and harmful compared to the parent compounds [9,26]. Recently research has been focused on the application of Advanced Oxidation Processes (AOPs), which are based on *in-situ* production of hydroxyl radical ( $\cdot\text{OH}$ ) for the treatment of pharmaceutical residues and pharmaceutical wastewater [25,27–30]. Among the AOPs, Electrochemical Advanced Oxidation Processes (EAOPs) have been extensively studied for treating low concentration pharmaceutical wastewaters due to their high versatility, efficiency and environmental compatibility [31–34]. These techniques are based on electrochemical production of  $\cdot\text{OH}$ , either directly via water oxidation at the anode or indirectly by electrochemically assisted Fenton's reaction with *in-situ* production of  $\text{H}_2\text{O}_2$  and regeneration of  $\text{Fe}^{2+}$  [35–38]

## 1.2 Challenges

The efficiency of EAOPs (Anodic oxidation (AO) and electro-Fenton (EF) processes) is greatly influenced by the nature of anode materials. Over the years, commercially available electrodes such as platinum (Pt), Dimensional Stable Anode (DSA), doped oxides of tin and lead ( $\text{SnO}_2\text{-Sb}$  and  $\alpha\text{-PbO}_2$ ), carbonaceous matrix and Boron Doped Diamond (BDD) have been successfully used in electrochemical wastewater treatment both on laboratory and pilot-plant scale [31,37,39]. However, there are some drawbacks encountered with the use of these electrodes, even though some of them have been applied in electrochemical wastewater treatment on commercial scale. For instance, the high cost of BDD electrode and scarcity of suitable substrate on which it can be deposited limit its large-scale application, although it still remains most technically efficient electrode for electrochemical oxidation of organic pollutants [37,40]. Furthermore, relatively short service life of  $\text{SnO}_2\text{-Sb}$  based electrodes and high risk of lead contamination by chemical leaching of  $\text{PbO}_2$  based electrodes have reduced their practical applications, even though both electrodes are relatively effective for electrooxidation of organic pollutants [31,41–43]. Other commercial electrodes like Pt, DSA and carbon matrix are relatively efficient in Fenton based EAOPs but very poor in electrooxidation treatment of organics [37,44].

Sub-stoichiometric titanium oxides recently developed represent efficient and low-cost alternative electrodes in electrochemical wastewater treatment due to their exciting chemical and electrical properties as well as the inexpensive feedstock from which it is prepared [45–47]. Although few studies have reported application of different configurations (plate and tubular) of compacted powder and resin bounded substoichiometric  $\text{TiO}_2$  on substrate in anodic oxidation, only medium mineralization efficiency could be achieved [48–50]. Further, the high possibility of mechanical wearing of compacted or resin bounded substoichiometric  $\text{TiO}_2$  is another challenge that is yet to be overcome. Beside at very acid pH, chemical wearing of  $\text{TiO}_x$  may occur and thus preventing the possibility of applying this electrode in Fenton based EAOPs because Ti forms complexes with  $\text{H}_2\text{O}_2$ .

On the other hand, EF process with heterogeneous catalyst (heterogeneous EF) was recently developed to enhance the performance as well as overcome some major challenges encountered

in traditional/homogeneous EF process. For instance homogeneous EF is only optimal at very narrow pH window (pH 2.5 – 3.5), as such working outside this pH drastically reduces the efficiency of the process. However, heterogeneous EF system can be performed at wide pH range even at basic pH because the oxidation of the organics is mainly controlled by surface-catalyzed process and Fe-catalysts are indissolvable at this pH [51–54]. Further, the use of heterogeneous catalyst ensures the reusability and recyclability of the heterogeneous EF system since the catalysts are indissolvable. Also the need for post-treatment neutralization, precipitation and separation of the catalyst in homogeneous EF system is completely eliminated with the use of heterogeneous catalyst.

### 1.3 Selection of pharmaceuticals and dye

The selection of appropriate and representative pharmaceuticals was a crucial aspect of preparation for this research work. The criteria used in selection of the two representative molecules were:

- ❖ belonging to different therapeutic classes and different mode of administration, i.e., out of hospital care or at home, characteristic of one type of effluent,
- ❖ molecules that have high potential risk (high index PBT) with a persistence in the environment or in relation to biological treatment, and
- ❖ molecules likely to be found in high concentration (high production volume chemicals) for which analytical tools are available or accessible.

Based on these criteria, the two selected pharmaceuticals are: antibiotic "**Amoxicillin**" and a beta-blocker: "**Propranolol**".

Acid orange 7 or orange II, a common azo-dye which is very soluble but persistence and hard to degrade in aqueous solution was selected as other model pollutant.

## 1.4 Objectives

The main aim of this thesis work is to experiment and investigate the removal of pharmaceutical residues from aqueous solution by electrochemical oxidation with the focus on performance studies of plasma deposited sub-stoichiometric titanium oxide ceramic electrode ( $\text{Ti}_4\text{O}_7$ ) and heterogeneous electro-Fenton process with hierarchical layered double hydroxide modified carbon-felt cathode. The low cost of the principal raw materials –  $\text{TiO}_2$  and coke from which  $\text{Ti}_4\text{O}_7$  is prepared make this electrode a cost-effective alternative compared to other commercial available electrode.

### *1.4.1 Electrochemical oxidation using $\text{Ti}_4\text{O}_7$ ceramic anode*

AO and EF degradation of some selected pharmaceuticals will be carried out using plasma deposited  $\text{Ti}_4\text{O}_7$  anode. The specific objectives set to achieve this aim are to:

- ❖ prepare  $\text{Ti}_4\text{O}_7$  powder from a mixture of  $\text{TiO}_2$  and coke, which are low cost and relatively abundant feedstock,
- ❖ prepare a thin film of  $\text{Ti}_4\text{O}_7$  via plasma deposition on a sand-blasted titanium alloy substrate at elevated temperature,
- ❖ characterize the prepared  $\text{Ti}_4\text{O}_7$  anode using X-ray diffraction spectroscopy and scanning electron microscopy, and
- ❖ investigate the performance of the prepared  $\text{Ti}_4\text{O}_7$  anode by electrooxidation and electro-Fenton degradation of some selected pharmaceuticals at natural and acidic pH respectively. Operation parameters such as applied current, initial pollutant concentration and *in-situ* generated  $\text{H}_2\text{O}_2$  on the degradation and mineralization efficiency will be studied.

### *1.4.2 Heterogeneous electro-Fenton with modified carbon felt cathode*

A self-catalyzed heterogeneous electro-Fenton process with layered double hydroxide modified carbon-felt as cathode as well as catalyst source will be investigated for the removal of organic pollutants. The specific objectives set to achieve this aim are to:

- synthesize a layered double hydroxide modified carbon-felt cathode,
- study the structural and electrochemical properties of the prepared electrode,
- investigate the performance of the electrode in terms of mineralization efficiency using acid orange II as a model pollutants,
- study the influence of synthesis parameters on properties and performance of the prepared electrode,
- compare the performance of the prepared electrode with homogeneous EF with raw carbon-felt cathode,
- study the stability and reusability of the prepared electrode.

### 1.5 Novelty of the thesis

EAOPs have been extensively studied in recent years for the removal of pharmaceuticals because of their high oxidation potential for complete destruction of refractory compounds compared to other AOPs and reducing operation costs. In fact, prominent EAOPs like AO and EF process have been applied on industrial scale for wastewater treatment using different commercially available electrodes such as Pt, DSA, doped SnO<sub>2</sub>,  $\alpha$ -PbO<sub>2</sub> and BDD anodes. Ti<sub>4</sub>O<sub>7</sub> anode, recently developed in USA, represents a low cost alternative electrode material compared to other commercially available once because it is prepared from TiO<sub>2</sub>, which is one of the most abundant feedstock on planet. Although electrooxidation of simple organics using compacted/sintered powder or thin film powder of Ti<sub>4</sub>O<sub>7</sub> bound to Ti substrate have been reported in literature, treatment of complex molecules like pharmaceuticals have not been investigated. Additionally plasma deposited Ti<sub>4</sub>O<sub>7</sub> electrode which is highly resistant to abrasion/wear compared to compacted or resin bind Ti<sub>4</sub>O<sub>7</sub> anode and also consist of lower quantities of other phases due to ultra-high temperature at which it is produce, which allows the conversion of other sub oxide of titanium to Ti<sub>4</sub>O<sub>7</sub>, has not been studied in electrooxidation of organic pollutants. Further, to the best of our knowledge, no study has investigated the use of this electrode in EF process. This is understandable because sintered powder or resin bounded Ti<sub>4</sub>O<sub>7</sub>

electrode has low mechanical strength and can easily wear into the treated solution. At the acidic pH of EF process, the sub-oxide of titanium dissolve with the titanium react with hydrogen peroxide, which is one the Fenton reagent to forming yellow complex.

Another novelty of this thesis is the study of heterogeneous EF with layered double hydroxide modified carbon felt cathode. There is no report in the literature on the use of this material in EF process, although some studies have reported chemically or electrochemically prepared Fe-impregnated carbon-based matrix for degradation of organic pollutants. This study is unique because the layered double hydroxide (LDH) grown on the carbon-felt not only contains Fe but also other transition metal (Co), which can serve as catalyst and/or co-catalyst in electro-Fenton process.

## **1.6 Structure of the thesis**

The structure of the thesis, which is entitled "Electrochemical Advanced Oxidation Processes for removal of Pharmaceuticals from water: Performance studies for sub-stoichiometric titanium oxide anode and hierarchical layered double hydroxide modified carbon felt cathode" is shown in Fig. 1.1.

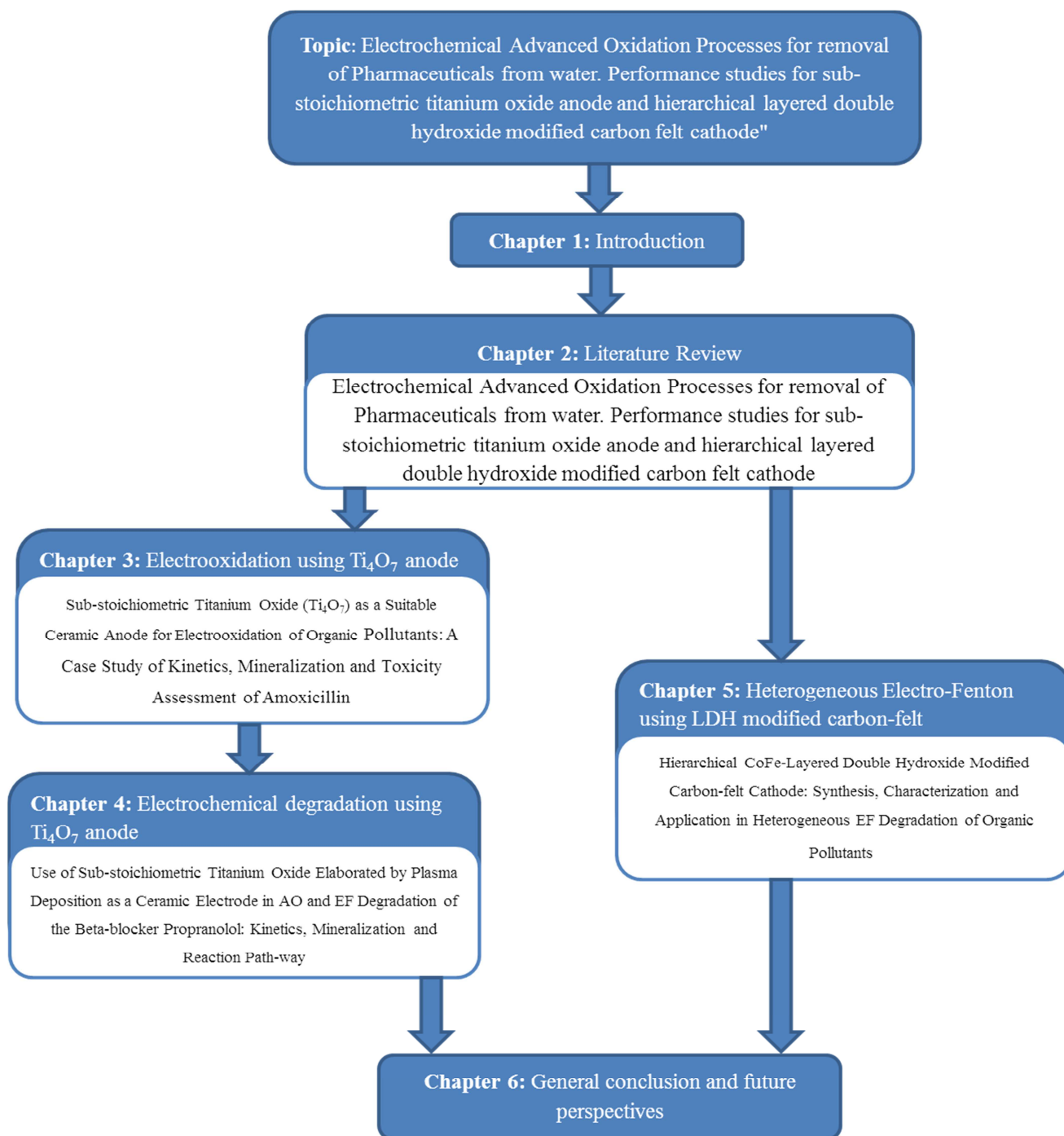


Figure 1-1–Structure of the thesis



---

**References**

- [1] T. Heberer, Occurrence, fate, and removal of pharmaceutical residues in the aquatic environment: a review of recent research data, *Toxicol. Lett.* 131 (2002) 5–17.
- [2] R. Hirsch, T. Ternes, K. Haberer, K.L. Kratz, Occurrence of antibiotics in the aquatic environment, *Sci. Total Environ.* 225 (1999) 109–118.
- [3] T.A. Ternes, Occurrence of drugs in German sewage treatment plants and rivers: Dedicated to Professor Dr. Klaus Haberer on the occasion of his 70th birthday.1, *Water Res.* 32 (1998) 3245–3260.
- [4] D. Bendz, N.A. Paxéus, T.R. Ginn, F.J. Loge, Occurrence and fate of pharmaceutically active compounds in the environment, a case study: Höje River in Sweden, *J. Hazard. Mater.* 122 (2005) 195–204.
- [5] M. Kołodziejska, J. Maszkowska, A. Białk-Bielińska, S. Steudte, J. Kumirska, P. Stepnowski, S. Stolte, Aquatic toxicity of four veterinary drugs commonly applied in fish farming and animal husbandry, *Chemosphere.* 92 (2013) 1253–1259.
- [6] C. Carlsson, A.-K. Johansson, G. Alvan, K. Bergman, T. Kühler, Are pharmaceuticals potent environmental pollutants?, *Sci. Total Environ.* 364 (2006) 67–87.
- [7] C.G. Daughton, T.A. Ternes, Pharmaceuticals and personal care products in the environment: agents of subtle change?, *Environ. Health Perspect.* 107 (1999) 907–938.
- [8] O.A.H. Jones, N. Voulvoulis, J.N. Lester, Human pharmaceuticals in the aquatic environment a review, *Environ. Technol.* 22 (2001) 1383–1394.
- [9] R. Andreozzi, M. Canterino, R. Marotta, N. Paxeus, Antibiotic removal from wastewaters: The ozonation of amoxicillin, *J. Hazard. Mater.* 122 (2005) 243–250.
- [10] K. Kümmerer, Antibiotics in the aquatic environment – A review – Part I, *Chemosphere.* 75 (2009) 417–434.
- [11] K. Kümmerer, The presence of pharmaceuticals in the environment due to human use – present knowledge and future challenges, *J. Environ. Manage.* 90 (2009) 2354–2366.
- [12] L.H.M.L.M. Santos, M. Gros, S. Rodriguez-Mozaz, C. Delerue-Matos, A. Pena, D. Barceló, M.C.B.S.M. Montenegro, Contribution of hospital effluents to the load of pharmaceuticals in urban wastewaters: Identification of ecologically relevant pharmaceuticals, *Sci. Total Environ.* 461-462 (2013) 302–316.

- [13] A. Ziyilan, N.H. Ince, The occurrence and fate of anti-inflammatory and analgesic pharmaceuticals in sewage and fresh water: Treatability by conventional and non-conventional processes, *J. Hazard. Mater.* 187 (2011) 24–36.
- [14] S.K. Khetan, T.J. Collins, Human pharmaceuticals in the aquatic environment: A challenge to green chemistry, *Chem. Rev.* 107 (2007) 2319–2364.
- [15] B. Halling-Sørensen, S. Nors Nielsen, P.F. Lanzky, F. Ingerslev, H.C. Holten Lützhøft, S.E. Jørgensen, Occurrence, fate and effects of pharmaceutical substances in the environment- A review, *Chemosphere.* 36 (1998) 357–393.
- [16] H. Sanderson, R.A. Brain, D.J. Johnson, C.J. Wilson, K.R. Solomon, Toxicity classification and evaluation of four pharmaceuticals classes: antibiotics, antineoplastics, cardiovascular, and sex hormones, *Toxicology.* 203 (2004) 27–40.
- [17] J.P. Bound, N. Voulvoulis, Pharmaceuticals in the aquatic environment—a comparison of risk assessment strategies, *Chemosphere.* 56 (2004) 1143–1155.
- [18] B.I. Escher, R. Baumgartner, M. Koller, K. Treyer, J. Lienert, C.S. McArdell, Environmental toxicology and risk assessment of pharmaceuticals from hospital wastewater, *Water Res.* 45 (2011) 75–92.
- [19] D.W. Kolpin, E.T. Furlong, M.T. Meyer, E.M. Thurman, S.D. Zaugg, L.B. Barber, H.T. Buxton, Pharmaceuticals, hormones, and other organic wastewater contaminants in U.S. streams, 1999–2000: A national reconnaissance, *Environ. Sci. Technol.* 36 (2002) 1202–1211.
- [20] J. Maszkowska, S. Stolte, J. Kumirska, P. Łukaszewicz, K. Mioduszevska, A. Puckowski, M. Caban, M. Wagil, P. Stepnowski, A. Białk-Bielińska, Beta-blockers in the environment: Part II. Ecotoxicity study, *Sci. Total Environ.* 493 (2014) 1122–1126.
- [21] P. Vazquez-Roig, V. Andreu, C. Blasco, Y. Picó, Risk assessment on the presence of pharmaceuticals in sediments, soils and waters of the Pego–Oliva Marshlands (Valencia, eastern Spain), *Sci. Total Environ.* 440 (2012) 24–32.
- [22] M. Cleuvers, Initial risk assessment for three  $\beta$ -blockers found in the aquatic environment, *Chemosphere.* 59 (2005) 199–205.
- [23] L.J. Schulman, E.V. Sargent, B.D. Naumann, E.C. Faria, D.G. Dolan, J.P. Wargo, A Human health risk assessment of pharmaceuticals in the aquatic environment, *Hum. Ecol. Risk Assess.* 8 (2002) 657–680.

- [24] R. Andreozzi, V. Caprio, C. Ciniglia, M. de Champdoré, R. Lo Giudice, R. Marotta, E. Zuccato, Antibiotics in the environment: Occurrence in Italian STPs, fate, and preliminary assessment on algal toxicity of amoxicillin, *Environ. Sci. Technol.* 39 (2005) 8112–8112.
- [25] I. Sirés, E. Brillas, Remediation of water pollution caused by pharmaceutical residues based on electrochemical separation and degradation technologies: A review, *Environ. Int.* 40 (2012) 212–229.
- [26] P. Wang, Y.-L. He, C.-H. Huang, Reactions of tetracycline antibiotics with chlorine dioxide and free chlorine, *Water Res.* 45 (2011) 1838–1846.
- [27] M.A. Oturan, J.-J. Aaron, Advanced oxidation processes in water/wastewater treatment: Principles and applications. A review, *Crit. Rev. Environ. Sci. Technol.* 44 (2014) 2577–2641.
- [28] J.J. Pignatello, E. Oliveros, A. MacKay, Advanced oxidation processes for organic contaminant destruction based on the Fenton reaction and related chemistry, *Crit. Rev. Environ. Sci. Technol.* 36 (2006) 1–84.
- [29] K. Ikehata, N. Jodeiri Naghashkar, M. Gamal El-Din, Degradation of aqueous pharmaceuticals by ozonation and advanced oxidation processes: A review, *Ozone Sci. Eng.* 28 (2006) 353–414.
- [30] S. Vasudevan, M.A. Oturan, Electrochemistry: as cause and cure in water pollution—an overview, *Environ. Chem. Lett.* 12 (2014) 97–108.
- [31] G. Chen, Electrochemical technologies in wastewater treatment, *Sep. Purif. Technol.* 38 (2004) 11–41.
- [32] M.A. Rodrigo, N. Oturan, M.A. Oturan, Electrochemically assisted remediation of pesticides in soils and water: A review, *Chem. Rev.* 114 (2014) 8720–8745.
- [33] E. Brillas, I. Sires, M.A. Oturan, Electro-Fenton process and related electrochemical technologies based on Fenton’s reaction chemistry, *Chem. Rev.* 109 (2009) 6570–6631.
- [34] C.A. Martínez-Huitle, M.A. Rodrigo, I. Sirés, O. Scialdone, Single and coupled electrochemical processes and reactors for the abatement of organic water pollutants: A critical review, *Chem. Rev.* 115 (2015) 13362–13407.
- [35] I. Sirés, E. Brillas, M.A. Oturan, M.A. Rodrigo, M. Panizza, Electrochemical advanced oxidation processes: today and tomorrow. A review, *Environ. Sci. Pollut. Res.* 21 (2014) 8336–8367.

- [36] M.A. Oturan, Electrochemical advanced oxidation technologies for removal of organic pollutants from water, *Environ. Sci. Pollut. Res.* 21 (2014) 8333–8335.
- [37] M. Panizza, G. Cerisola, Direct and mediated anodic oxidation of organic pollutants, *Chem. Rev.* 109 (2009) 6541–6569.
- [38] C.A. Martínez-Huitle, E. Brillas, Decontamination of wastewaters containing synthetic organic dyes by electrochemical methods: A general review, *Appl. Catal. B Environ.* 87 (2009) 105–145.
- [39] B.P. Chaplin, Critical review of electrochemical advanced oxidation processes for water treatment applications, *Environ. Sci. Process. Impacts.* 16 (2014) 1182. doi:10.1039/c3em00679d.
- [40] M.A. Rodrigo, P. Cañizares, A. Sánchez-Carretero, C. Sáez, Use of conductive-diamond electrochemical oxidation for wastewater treatment, *Catal. Today.* 151 (2010) 173–177.
- [41] Y. Samet, S.C. Elaoud, S. Ammar, R. Abdelhedi, Electrochemical degradation of 4-chloroguaiacol for wastewater treatment using PbO<sub>2</sub> anodes, *J. Hazard. Mater.* 138 (2006) 614–619.
- [42] B. Correa-Lozano, C. Comninellis, A. De Battisti, Service life of Ti/SnO<sub>2</sub>-Sb<sub>2</sub>O<sub>5</sub> anodes, *J. Appl. Electrochem.* 27 (1997) 970–974.
- [43] H. Lin, J. Niu, J. Xu, Y. Li, Y. Pan, Electrochemical mineralization of sulfamethoxazole by Ti/SnO<sub>2</sub>-Sb/Ce-PbO<sub>2</sub> anode: Kinetics, reaction pathways, and energy cost evolution, *Electrochimica Acta.* 97 (2013) 167–174.
- [44] F. Sopaj, M.A. Rodrigo, N. Oturan, F.I. Podvorica, J. Pinson, M.A. Oturan, Influence of the anode materials on the electrochemical oxidation efficiency. Application to oxidative degradation of the pharmaceutical amoxicillin, *Chem. Eng. J.* 262 (2015) 286–294.
- [45] J.R. Smith, F.C. Walsh, R.L. Clarke, [No Title], *J. Appl. Electrochem.* 28 (1998) 1021–1033.
- [46] F.C. Walsh, Electrochemical technology for environmental treatment and clean energy conversion, *Pure Appl. Chem.* 73 (2001).
- [47] P. Geng, J. Su, C. Miles, C. Comninellis, G. Chen, Highly-Ordered Magnéli Ti<sub>4</sub>O<sub>7</sub> Nanotube Arrays as Effective Anodic Material for Electro-oxidation, *Electrochimica Acta.* 153 (2015) 316–324.

- [48] D. Bejan, J.D. Malcolm, L. Morrison, N.J. Bunce, Mechanistic investigation of the conductive ceramic Ebonex® as an anode material, *Electrochimica Acta*. 54 (2009) 5548–5556.
- [49] A.M. Zaky, B.P. Chaplin, Mechanism of p-substituted phenol oxidation at a Ti<sub>4</sub>O<sub>7</sub> reactive electrochemical membrane, *Environ. Sci. Technol.* 48 (2014) 5857–5867.
- [50] A.M. Zaky, B.P. Chaplin, Porous substoichiometric TiO<sub>2</sub> anodes as reactive electrochemical membranes for water treatment, *Environ. Sci. Technol.* 47 (2013) 6554–6563.
- [51] J. Li, Z. Ai, L. Zhang, Design of a neutral electro-Fenton system with Fe@Fe<sub>2</sub>O<sub>3</sub>/ACF composite cathode for wastewater treatment, *J. Hazard. Mater.* 164 (2009) 18–25.
- [52] Y. Wang, G. Zhao, S. Chai, H. Zhao, Y. Wang, Three-dimensional homogeneous ferrite-carbon aerogel: One pot fabrication and enhanced electro-Fenton reactivity, *ACS Appl. Mater. Interfaces*. 5 (2013) 842–852.
- [53] S. Ammar, M.A. Oturan, L. Labiadh, A. Guersalli, R. Abdelhedi, N. Oturan, E. Brillas, Degradation of tyrosol by a novel electro-Fenton process using pyrite as heterogeneous source of iron catalyst, *Water Res.* 74 (2015) 77–87.
- [54] N. Barhoumi, N. Oturan, H. Olvera-Vargas, E. Brillas, A. Gadri, S. Ammar, M.A. Oturan, Pyrite as a sustainable catalyst in electro-Fenton process for improving oxidation of sulfamethazine. Kinetics, mechanism and toxicity assessment, *Water Res.* 94 (2016) 52–61.

# Literature Review

Part of this chapter has been published as: Coupling of Membrane Filtration and Advanced Oxidation Processes for Removal of Pharmaceutical Residues: A Critical Review. *Separation and Purification Technology*, 156 (2015) 891–914. DOI: 10.1016/j.seppur.2015.09.059.

## Chapter 2

A comprehensive literature review is required prior to the research work described from chapter 3–6

In this chapter we reviewed previous works on EAOPs for removal of pharmaceuticals from wastewater with the focus on electrode materials for electrochemical wastewater treatment and heterogeneous electro-Fenton process. This review is important in order to understand the origins of pharmaceuticals in environment, their contamination level and mobility in different environmental compartments, natural ways of attenuating their contamination level and the analytical procedures/techniques available for their quantification in aquatic environment. It will also enable us to understand the subtle and chronicle effect as well as long term toxicology of this class of (emergent) pollutants on both aquatic and terrestrial ecosystem and why it is essential prevent their inputs into the environment. Several techniques that have been utilized for the removal of the pharmaceuticals from environment will be known and why the EAOPs are most efficient for their complete destruction and majority of other techniques are either not technical or economical efficient.

An extensive overview is also necessary to understand the different varieties of EAOPs and some of the most efficient among them in terms of efficiency, without neglecting the economic and environmental compatibility based on previous studies. The advantages and disadvantages of some prominent among them as well as the operating parameters that controls the efficiency of some of EAOPs must be understood in order to give us clue on where and how to improve the efficiency, reduce the operation cost and ensure a wide applicability of these processes. Based on our preliminary literature survey, a critical review was carried out on AO and EF processes with much focus on the role of electrode materials on the efficiency of both processes, since both are among the most widely studied EAOPs. Extensive review was also carried out on the pH window (pH is a crucial operating parameter in EF process) at which EF can be performs since majority of wastewater effluents are not in acidic pH at which process efficiency is optimal.

**Electrochemical Advanced Oxidation Processes for Removal of Organic pollutants from Water: Performance Studies for Sub-stoichiometric Titanium Oxide Anode and Hierarchical Layered Double Hydroxide Modified Carbon Felt Cathode: A Review****Abstract**

Pharmaceuticals and dyes as emerging pollutants became a major concern not only because of the threat posed to health and safety of the aquatic life but also due to their continuous accumulation in aquatic environment and development of antibiotic-resistant microbial strains. EAOPs such as AO and EF processes are some of prominent and efficient technique for the removal of these pollutants from aquatic environment. The efficiency of AO and EF processes in terms of performance, environmental compatibility and cost can be greatly enhanced by proper selection of electrode materials. While some electrodes such as BDD, doped SnO<sub>2</sub>, PbO<sub>2</sub> and substoichiometric TiO<sub>2</sub> allow complete mineralization of organic pollutants, others such as Pt, DSA and carbon can only oxidize pollutants to more stable intermediates. Doped SnO<sub>2</sub> and PbO<sub>2</sub> are relatively less expensive but have low stability and possible lead contamination in case of PbO<sub>2</sub> electrode due to leaching. BDD is the best electrode for electrochemical wastewater treatment but highly expensive. Substoichiometric TiO<sub>2</sub> is a less expensive and highly stable electrode with good oxidation potential. However, this electrode has not been extensively investigated and no study on the use of this electrode in EF process is available in the literature. On the other hand, the use of heterogeneous catalyst in EF system can enhance the efficiency of the process, extend the working pH range and allow the recyclability and reusability of the catalyst. This could be of great importance in the removal of pharmaceuticals from aquatic environment.



## 2.1 Introduction

For the past decades, there is astronomic increase in the demand for the earth's supply of drinking water due to continuous exponential growth in human population. As such, the protection of the integrity of water resources has become one of the crucial environmental issues of this century [1]. Although water bodies constitute majority of earth crust, only few (less than 3%) are available for human use due to high salinity of the others. In addition this few fresh water bodies are under continuous contamination by effluents of WWTPs, hospital, municipal sewage systems, industries, run-off water from agricultural land and others, thus constituting a great threat to the health and safety of both human and aquatic life.

Pharmaceuticals active compounds (PhACs) (human and veterinary) as emerging pollutants have received a lot of attention in the last decade not only because of the persistence and potential toxicity of these substances and their active metabolites but also due to their accumulation as a result of continuous introduction into receiving water bodies via WWTPs effluents [2]. Several investigations and reviews have reported the occurrence, fate and ecotoxicology of both human and veterinary PhACs in different environmental compartments [3–7]. It has been established that, the primary source through which PhACs enter into aquatic environment is effluents of WWTPs, although this is aggravated by indiscriminate disposal of unused drugs in drains and household garbage [8–12]. Other sources include; hospital wastewater effluents, direct discharge of untreated wastewater, aqua farming and livestock impoundments [13,14]. The poor volatility of these chemical substances implies that aqueous transport mechanisms remain the primary mode of their distribution in compartments of the environment [12].

On the other hand, textile factories discharge large volume of wastewater containing a high concentration of dyes that required to be treated. The wastewater from textile industries is very complex in constituent and difficult to remove completely by conventional physicochemical treatment technique []. Many dyes are highly soluble in water and resistant to biotic conversion (oxidation by organisms). They are a major threat to ecosystems, both aquatic and terrestrial because they are toxic and also consist of toxic auxiliary components [].

Consequently, there is need for complete elimination of PhACs, its active metabolites and azo dyes from aquatic compartments in order to avoid their health hazard and potential

ecotoxicity. The conventional wastewater treatment technique such as adsorption, bio-oxidation, coagulation, sedimentation and filtration applied in WWTPs cannot completely destroyed these pollutants, even with the combination of post treatment disinfection of the effluents by chlorination and/or ultra-violet radiation (UV) [2,15]. Chemical oxidation treatments such as chlorination and peroxidation usually leads to the formation of more stable and potential carcinogenic byproducts which are most time more toxic than the parent compounds [16,17]. AOPs are environmental friendly chemical, photochemical or electrochemical methods that utilized *in-situ* production of hydroxyl radical ( $\cdot\text{OH}$ ) as main oxidant [2,18,19]. The oxidant ( $\cdot\text{OH}$ ) is the second strongest oxidizing agent known after fluorine, with very high standard reduction potential ( $E^\circ(\cdot\text{OH}/\text{H}_2\text{O}) = 2.8 \text{ V vs SHE}$ ) and non-selectively react with most organics until their total mineralization [20]. Among AOPs, EAOPs have demonstrated greater ability to efficiently destroy a large variety of toxic and/or biorefractory pollutants [2,21–23]. These techniques are based on electrochemical production of  $\cdot\text{OH}$ , either directly from water oxidation at the anode or indirectly by total or partial *in-situ* generation of Fenton's reagent ( $\text{H}_2\text{O}_2 + \text{Fe}^{2+}$ ) [23–27]. Fenton-based EAOPs in particular is more efficient and has been successfully applied to the treatment of many pharmaceutical residues in recent years.

The efficiency of EAOPs processes, especially AO and EF is largely influenced by some operation parameters – most importantly selected electrode materials and nature of the catalyst used in Fenton's based EAOPs. The influence of electrode materials (i.e. anode material) on mineralization of organic pollutants by both AO and EF processes depends on the production of physisorbed (heterogeneous) hydroxyl radical ( $\text{M}(\cdot\text{OH})$ ) at the anode surface [27,28]. While some anode materials such as BDD,  $\text{SnO}_2\text{-Sb}$ ,  $\alpha\text{-PbO}_2$  and substoichiometric  $\text{TiO}_2$  can generate relatively high quantities of  $\text{M}(\cdot\text{OH})$  (non-active anodes), others like DSA, Pt and graphite has limited capacity for  $\text{M}(\cdot\text{OH})$  production [21,27]. The generated  $\text{M}(\cdot\text{OH})$  is highly efficient in mineralization of organic, thus enhance the performance of EAOPs. On the other hand, studies have shown that efficiency of EF process can be significantly enhanced by using heterogeneous rather than homogeneous Fenton catalyst.

In this review, the occurrence, fate and toxicity of the PhACs in the environment are discussed in the first part, while the basic principle of AO and EF are enumerated in the next two sections. In the fourth and fifth section, the selection of electrode materials and use of

heterogeneous EF for enhancing the removal of PhACs by electrochemical wastewater treatment are discussed.

## **2.2 Pharmaceuticals: Occurrence, fate and toxicity**

### *2.2.1 Occurrence of PhACs in aquatic environment*

Several thousand tons of both human and veterinary PhACs substances are produced per year across the globe. Majority of these medications administered by both human and livestock are excreted unmodified or partially modified via urine and feces and introduced directly into sewage system. The rate of metabolisms of each drugs in organism's system depends on the individual, nature of the drugs itself and dosage. While some are completely removed (diclofenac, carbamazepine), others are partially metabolized (amoxicillin) or not metabolized at all ( $\beta$ -blocker nadolol) [9,29]. Moreover, urine and feces of livestock are not treated like that of human, it may either remains on the pasture field or applied as manure which are eventually washed into aquatic environment by run-off water [29–32]. The presence of PhACs in surface and underground water has been reported by several authors and they attributed it to ineffective removal of these pollutants in WWTPs [3,5,8,31–42]. A schematic representation of the transport of PhACs in environment right from origin to the point where they cause serious hazardous effects is shown in Fig. 2-1.

Analyses of concentration of PhACs in aquatic environment are carried out by solid phase extraction followed by identification and quantification using either liquid chromatograph coupled with mass spectroscopy (LC-MS), high performance liquid chromatography (HPLC-MS), Reversed Phase-HPLC- electrospray tandem mass spectroscopy or Gas chromatography GC-MS [1,36,39,43–49]. Further, over 80 compounds, PhACs and several drugs metabolites have been detected in aquatic environment across the Europe, Australia, Brazil, US and Canada [3].

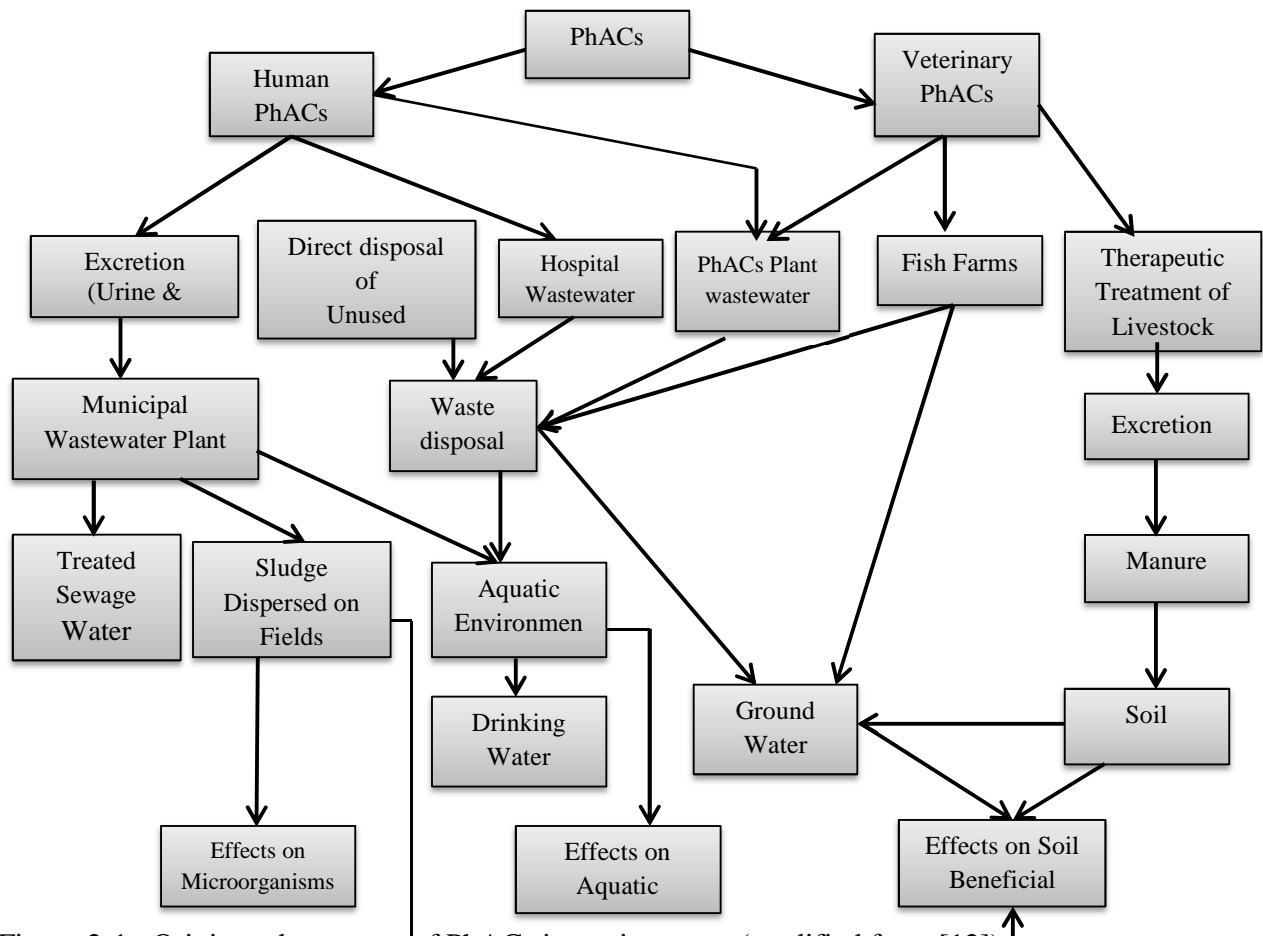


Figure 2-1– Origin and transport of PhACs in environment (modified from [12]).

Analytical studies of some receiving water in Romania indicates the presence of over 15 PhACs, metabolites, and intermediates belonging to various therapeutic groups with concentrations ranging from several  $\mu\text{g}$  to few  $\text{ng}$  [44]. About 29 PhACs and 12 drugs of abuse were detected in the intake of drinking water treatment plant in NE of Spain with concentrations up to several  $\text{ng}$  [50]. The analytical studies conducted by U.S. Geological Survey on water samples from network of 139 streams across several states show the presence of approximately 95 organic wastewater contaminants of which majority are PhACs [1]. Although the concentration measured were generally low and most time below drinking-water guidelines, health adversaries or aquatic-life criteria. More so, 13 PhACs from priority lists (UK Environment Agency and Oslo and Paris Commission) were detected from analytical survey of wastewater effluents and surface water of the lower river Tyne, UK [36]. The concentration of most of these PhACs in raw effluent range from 11 to  $67,570 \text{ ng L}^{-1}$ , whereas in surface water a much lower concentrations

(4 to 2370 ng L<sup>-1</sup>) were detected. PhACs such as clofibric acid, carbamazepine, codeine, fluoroquinolones, primidone or iodinated contrast agents have also been detected at µg L<sup>-1</sup> level in underground water and deeper soil horizon as a result of diffusion and infiltration of the drugs [3,51]. Also several PhACs have been detected in shallow underground water as a result of direct or indirect infiltration from livestock wastewater impoundments [46], manufacture spill accidents, underground leakage from sewage facilities and therapeutic treatment of livestock on fields [3,52].

### *2.2.2 Fate of PhACs in aquatic environment*

Investigations have shown that individual concentrations of most PhACs are higher in effluents of WWTPs/STPs than concentrations found in surface water due to dilution as well as partial remediation by natural pathways like hydrolysis, sorption onto colloids, biodegradation and photolysis/photo-transformation [12,32,53–56]. Partial transformation by abiotic reactions is much larger because most PhACs are bio-refractory. The speciation and concentration level of each PhACs are influenced by pH, natural organic matter (NOM) and ionic strength of the receiving water. Some PhACs at different pH become charged and can easily absorb onto colloids, trapped by NOM or associated with cations in the water and transferred to sediments [57,58].

### *2.2.3 Toxicity of PhACs in aquatic environment*

Although PhACs are synthesized to elicit a specific biological effect at low doses in human system but their presence in water bodies can adversely affect non-targeted organ in human or other life in ecosystem even at low concentration [44,48]. Studies have shown that the qualitative risk assessment ranking of PhACs relative to probability and potential severity for human and environmental health effects follows this trend: antibiotics > sex hormones > cardiovascular > antineoplastics. While the susceptibility of aquatic life to PhACs are in the following order daphnia > fish > algae, the predicted ranking order of relative toxicity is: sex hormones > cardiovascular = antibiotics > antineoplastics [10]. The presence of PhACs in

environment may result in unprecedented consequences such as proliferation and persistence of multi-resistant bacterial pathogenic strains in environment, ecotoxicological impacts and impairment of reproductive and endocrine system of aquatic organisms [31,46,59–65]. Further, abnormal physiological processes, increased incidences of cancer and potential increase in toxicity of chemical mixtures have also been reported [1,9]. Accumulation of diclofenac in different organs of fish as a result of long time exposure could cause severe health impairment such as histopathological and cytological effect in liver, kidney, gills and intestine of fish [66,67]. The effects of veterinary anti-bacterial and anti-parasitic compounds on zebrafish range from mortality, malformation and other sub-lethal responses [6]. Studies have also revealed that oxytetracycline and florfenicol commonly used in fish farming and livestock cause strong adverse effect on duckweed and algae but minimal effect on bacterial and crustaceans [7]. Ecotoxicology studies indicate that aquatic organisms show high sensitivity to beta-blockers [68,69]. It can affect cardiac rhythm; generate abnormalities or causes reproductive impairment in fish, Japanese medaka (*Oryzias latipes*) and had specific toxicity towards plankton and green algae [70,71]. Additionally, there are several evidences on the additive effects of pharmaceuticals, which means that even a low concentration, it might contribute to the global toxic potential of the total compounds in the aquatic environment [70].

### **2.3 Dyes Stuff in environment: Occurrence and Toxicity**

Dyes stuffs are complex aromatic molecular structures which are stable and refractory to degrade. Both synthetic and natural dyes have been applied in various industrial setups, however synthetic dyes are most preferred because they provided dyes with a wide range of fast colors and brighter shades [71]. However, due to the toxic nature and hazardous effects of synthetic dyes on both aquatic and terrestrial life, the interest in natural dyes has been revived in many developed countries [72]. Among the over 100,000 dyes available commercially at present, 70% is azo dyes. Over 1 million tons of dyes are produced annually, of which 50% are textile dyes [71, 73]. Textile industries consumed large volume of water and chemicals especially dyes during the wet processing stage and therefore large quantities of effluents/wastewater with varying constituents are delivered into environment. As such, the wastewater/effluents from

textile industries remain the major source of dye stuffs in both aquatic and terrestrial environments. The receiving water bodies and landfill are strongly affected and they are visible in water at concentrations as low as 1 ppm [71, 72]. One of the major reason for high dyes stuff in textile effluents/wastewater is improper dye up taken as well as fixation on the substrate during textile production and dyeing. Conventional treatment techniques rarely achieved satisfactory efficiency in treatment of textile industries effluents/wastewater because of its high composition variability and deep color intensity of the wastewater [72]. Other source of dye stuffs in environment including effluents from finishing industries, paints and pigment industries, cosmetic and pharmaceutical industries as well as wastewater from leather and printing industries.

Textile dyeing and finishing industry is the second largest pollution source (after agriculture) in fresh water because it is one of the most chemically intensive industries on earth [72, 74, 75]. The major problem of dye stuffs in environment is aesthetic pollutions in which the dyes change the color of both receiving water bodies as well as landfill. As said earlier, this pollutant is visible in environment even at a concentration as low as 1 ppm. The color change inhibits sunlight penetration, water transparency and water-gas solubility as well as oxygen distribution into water bodies and landfill, thus affecting the energy chain in the ecosystem. Indeed, the decrease in light penetration through water polluted with dye stuffs affect the photosynthetic activities, creating oxygen deficiencies and de-regulating the biological cycles of the aquatic biotic [76]. More importantly, the change in color of water bodies and landfill makes the environment irritating and dirty (Fig. 2).



Figure 2-1–Color change due to dyes contamination of surface water and landfill

Secondly, these effluents as a hazardous toxic waste consist aside from color, large volume of organic chemicals and heavy metals from dyeing and finishing salts. For instance, majority of the

dye stuffs contain sulphur, naphthol, nitrate, acetic acid, chromium compounds and heavy metals like Cu, Hg, Pb, Ni, Co, Cd, As and other auxiliary chemicals, all of which collectively makes the effluents highly toxic [72]. Besides, the effluents are usually at high temperature and pH, which is damaging.

Specific attention has been given to azo dyes because they pose very serious health risks to humans if they were used in particular textiles and if get to water bodies used for commercial and municipal usage. Azo dyes have been reported to show serious damage to ecosystems when discharged into water system without prior treatment, which is peculiar to developing countries. The major threat of azo dyes comes from the formation of highly dangerous, toxic, and carcinogenic aromatic amines which can be easily produced by azo group ( $\text{<math>-N=N-</math>}$ ) cleavage under certain conditions in the digestive tracts and other organs of animals as well as human [71]. Over 24 aromatic amines have been either confirmed or listed as carcinogenic and 5% of azo dyes can cleave to produce these hazardous compounds [77]. Based on this, in 2002 EU placed a ban on articles that may come in contact with skin which contains certain azo dyes that could break down to any of the 24 possible carcinogenic aromatic amines. In general, many azo dyes are highly toxic and contains auxiliary component that are toxic to ecosystem and mutagenic, and can have subtle to chronic effect on organisms depending on exposure time and concentration of the azo dye. The presence of azo dyes in surface water and landfill has been connected to growth reduction, neurosensory damage, metabolic stress and death in fish, and growth and productivity in plants. Therefore contamination by dye stuffs limits the downstream human water usage like recreation, drinking, fishing and irrigation [78].

## **2.4 Removal of organic pollutants from aqueous solution by EAOPs**

### *2.4.1 Electrooxidation/Anodic oxidation*

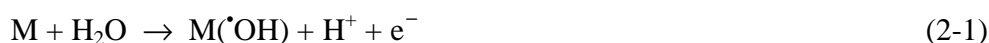
Electrooxidation is an emerging AOP, where pollutants are oxidized either directly by exchange of electrons between the anode and the pollutants or indirectly by strong reactive oxygen species (ROS) – most especially  $\text{<math>\cdot\text{OH}</math>}$  – generated on the anode surface [21,24,25,27]. The presence of chloride ions in the treated solution may facilitate indirect bulk oxidation by the



*in situ* electro-generation of active chlorines like hypochlorite, chlorine dioxide and chlorine, which could greatly enhance the overall electrochemical incineration of the organic pollutants [2,27]. The two types of electrooxidation oxidation processes (anodic oxidation and “mediated oxidation”- oxidation with active chlorine) have been widely employed in wastewater treatment predominantly on laboratory scale.

Electrooxidation or AO without active chlorine generation is the most prominent electrochemical technique for the remediation of wastewaters containing low contents of persistent organic pollutants (POPs) [26,79–82]. This technique was popularized and extensively developed by Comninellis research group. Oxidation of pollutants in electrolytic cell is achieved by either direct electron transfer to the anode or indirect or mediated oxidation with heterogeneous ROS formed from water discharge at the anode, such as physisorbed  $\cdot\text{OH}$  which are weakly attached to anode surface or chemisorbed “active oxygen” which are strongly attached to the surface of anode [27,83–85].

For wastewater treatment, high anodic potential is required to simultaneously oxidize the pollutants and discharge water for the production of adsorbed  $\cdot\text{OH}$  as well as the activation of the anode. Studies conducted by Comninellis research group [83,84,86] have shown that nature of electrode material has strong influence on both process selectivity and efficiency. For instance, several anodes favored partial and selected oxidation of organic pollutants (electrochemical conversion), while other produced complete mineralization of the compounds to  $\text{CO}_2$  (electrochemical combustion). Regardless of anode material, the first step in oxygen transfer reaction is the discharge of water molecules to form adsorbed  $\cdot\text{OH}$ :

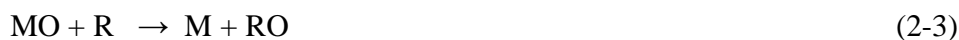


The nature of electrode material determines the next steps and two limiting classes of electrodes were established vis a vis “active” and “non-active” anodes:

(i) At “active” electrodes, the adsorbed radicals interact so strongly with the anode, forming chemisorbed “active oxygen” or higher oxide, provided that higher oxidation states are available on the electrode surface:



The surface redox pair MO/M (chemisorbed “active oxygen”) can act as a mediator in the selective oxidation or electrochemical conversion of organic compounds at surface of “active” electrodes:



Examples of active electrodes include DSA (RuO<sub>2</sub>, IrO<sub>2</sub>), Pt and doped Ti electrode.

(ii) At “non-active” electrodes, where the formation of a higher oxide is excluded, the surface of the anodes interact so weakly with the physisorbed hydroxyl radicals that these radicals indiscriminately oxidized the organics until complete combustion to CO<sub>2</sub>:



BDD, oxides of Sn and Pb are typical examples of non-active electrodes.

However, the quantities and versatility of both chemisorbed “active oxygen” and the physisorbed  $\cdot\text{OH}$  are affected by competitive side reactions that yield other oxidants (O<sub>2</sub>, H<sub>2</sub>O<sub>2</sub> and O<sub>3</sub>) which are less reactive compare to  $\cdot\text{OH}$ , resulting in decreased anodic process efficiency.

Electrooxidation with active chlorine on the other hand is predominant during treatment of wastewater containing high chloride ions concentration (i.e. reverse osmosis concentrates ROC) because large quantities of anodically generated active chlorine species such as Cl<sub>2</sub>, HClO/ClO<sup>-</sup> and ClO<sub>2</sub><sup>-</sup> are formed, which can oxidize the organics in competition with ROS [27,87].



The yielded soluble chlorine diffuses away from anode to be rapidly hydrolyzed and disproportionated to hypochlorous acid and chlorine ion in the bulk solution:



The chlorine-mediated electrolysis has been found particularly suitable and advantageous for the treatment of real wastewater with high sodium chloride concentrations such as ROC, olive oil wastewater, textile and tannery effluents since salinity could sufficiently lower the energy consumption because it increases the conductivity of the solution [88–90]. The most widely used electrode materials for *in situ* generation of active chlorine are based on platinum or mixed-metal-oxides (e.g. RuO<sub>2</sub>, IrO<sub>2</sub>, TiO<sub>2</sub>) [27]. Formation and accumulation of toxic

chlorinated organic compounds – chloro-derivatives, trihalomethanes and chloroamines – during the electrolysis is the major drawback of this process [16,87,89,91].

#### 2.4.2 Electro-Fenton Process

EF process involves the formation of  $\cdot\text{OH}$  radical in bulk via Fenton's reaction (Eq. 2-8) between continuously electrogenerated  $\text{H}_2\text{O}_2$  at a suitable cathode fed with air/ $\text{O}_2$  and iron catalyst added initially to the treated solution at catalytic amount [22,23,82]. The non-selective attacks of organics contaminants in the bulk solution by  $\cdot\text{OH}$  gives several intermediates which undergo further combustion to  $\text{CO}_2$ . Interestingly, only small quantity of catalytic  $\text{Fe}^{2+}/\text{Fe}^{3+}$  is required because the Fenton's reagent ( $\text{H}_2\text{O}_2 + \text{Fe}^{2+}$ ) is continuously electrogenerated (Eq. 2-9) and regenerated (Eq. 2-10) by cathodic reduction of  $\text{O}_2$  and  $\text{Fe}^{3+}$  respectively [21,92,93]. The fast regeneration of Fenton's reagents accelerates the production of  $\cdot\text{OH}$  radical by Fenton's reaction (Eq. 2-8), which enhances the removal of the organics from treated solution. Thus, the EF process possess high degradation efficiency than similar AO when both processes are applied separately [21,23].



#### ❖ Selection of Fenton's Catalyst

The selection of the iron source and regeneration of  $\text{Fe}^{2+}$  requires for Fenton's reaction strongly depend on the nature of cathode used. Studies have shown that  $\text{Fe}^{2+}$  is slowly regenerated in gas diffused electrodes (GDEs) because  $\text{O}_2$  reduction is predominant. As such  $\text{Fe}^{2+}$  is the preferred catalyst source for GDEs electrodes. In contrast, both  $\text{Fe}^{3+}$  and  $\text{Fe}^{2+}$  ions can be utilized as iron source with 3D-carbonaceous materials because of rapid regeneration of  $\text{Fe}^{2+}$  by cathodic reduction of  $\text{Fe}^{3+}$  [94–96]. More so, the cathodic regeneration of  $\text{Fe}^{2+}$  has also been found to depend on factors such as electrode potential and area, pH, temperature and the catalyst content [97]. Therefore, preliminary studies are usually conducted to establish optimum

conditions at which waste reaction such as iron sludge production and H<sub>2</sub>O<sub>2</sub> decomposition are minimal.

Some authors have demonstrated the possibility of utilizing other metallic ions such as Cu<sup>2+</sup>/Cu<sup>+</sup> [98–100], Co<sup>3+</sup>/Co<sup>2+</sup> [98,99] and Mn<sup>3+</sup>/Mn<sup>2+</sup> [100] couples instead of Fe<sup>3+</sup>/Fe<sup>2+</sup> pair as catalyst to electrogenerate <sup>•</sup>OH in the bulk from Fenton-like reactions. Other authors [101,102] have reported excellent co-catalyst effect of copper ions in Fenton systems as a result of the enhanced Fe<sup>2+</sup> regeneration from eq. 2-11.



#### ❖ Electrolysis System

The cell configurations utilized in EF technology are either undivided cell – reactor in which all the electrodes are in one compartment with the electrolyte or divided cell – where the anodic half-cell containing anolyte (wastewater) is separated from cathodic half-cell housing catholyte (supporting electrolyte) by either porous membrane or salt bridge. Nature of electrodes (anode and cathode) has a significant influence on the efficiency of EF process, as such proper selection of electrodes material is a prerequisite in EF process. Cathode materials such as graphite, carbon felt (CF), activated carbon fiber (ACF), reticulated vitreous carbon, carbon sponge, carbon nanotubes and GDEs have been successfully employed in EF processes whereas anode materials such as graphite, Pt, mixed metal oxides and BDD are usually preferred [23].

In EF process with undivided cell equipped with high oxidation power anode (i.e. BDD or Pt), the destruction of organics is achieved by simultaneous action of both homogeneously <sup>•</sup>OH formed in bulk by Fenton's reaction (Eq. 2-8) and heterogeneous physisorbed ROS mainly M(<sup>•</sup>OH), which is produced by water discharge reaction (Eq. 2-1) at a high O<sub>2</sub>-overpotential anode surface [21–23].

#### ❖ Operating Parameters

Several operating parameters have been enumerated to influence the degradation of organics in EF process. Such parameters include O<sub>2</sub>/air feeding, stirring rate or liquid flow rate,

temperature and pH of the solution, electrolyte composition, applied potential or current, iron catalyst and initial pollutant concentration. It is imperative to optimize these parameters during electrolysis to achieve the best current efficiency and lowest energy cost.

#### *2.4.3 Electrode materials for electrochemical oxidation*

The efficiency of electrochemical oxidation process greatly depends on the nature of anode material used. As explained in section 2.3.1, electrodes are grouped into two: “active” electrodes with low oxygen evolution overpotential (i.e. good catalyst for oxygen evolution reaction) and characterized with only partial oxidation of organics; and “non-active” electrodes with high oxygen evolution overpotential (poor catalyst for oxygen evolution reaction) and favors mineralization of organic to CO<sub>2</sub> [27,82,84]. However in practice, most electrodes exhibit a mixed behavior, because organic oxidation and oxygen evolution reactions occur via parallel reaction paths [85]. Some works have enumerate major electrodes - their properties, advantages and limitations [21,26,27,85,103] and are hereby summarized in the following section.

##### *2.4.3.1 Carbon and graphite electrodes*

Three dimensional electrodes (fluidized bed, pack bed, carbon particles, porous electrodes, carbon felt, carbon sponge, activated carbon fiber, reticulated vitreous carbon and carbon nanotubes) made of carbon and graphite have be widely used in electrochemical treatment of organics because they are cheap, have a large surface area, and can combine adsorption and electrochemical degradation of pollutants [27]. As an anode in electrooxidation, carbonaceous electrodes of different configurations such as carbon-felt [104,105], carbon pellet [106], carbon-fiber [107–109], glassy carbon [110] and graphite-particles [111–113] have been employed in the electrochemical treatment of organic pollutants. This class of electrode have been studied for the electrooxidation of phenols [106,110], dyes [109,113] and pharmaceuticals [28]. For instance, Sopaj et al., 2014 [28] investigated electrooxidation of amoxicillin using carbon-felt, carbon-graphite, carbon-fiber and some other known commercially available electrode materials in an undivided electrochemical cell. Relatively high oxidation of amoxicillin

was observed with commercial Pt electrode compared to carbon-fiber and carbon-graphite, which in turn performed better than DSA. However, it must be noted that the generation of strong oxidant such as physisorbed hydroxyl radical ( $\cdot\text{OH}$ ) can oxidize  $\text{sp}^2$ -carbon of the anode in the case of carbonaceous electrode which will affect the oxidation of organic pollutant. Besides, carbon-based anodes undergo surface corrosion and burnt that reduces their service life when utilized in electrooxidation at high potential [27].

Carbon based electrodes has been successfully used as electrodes in Fenton's based EAOPs, however majority of the studies have investigated these electrodes as cathode [21–23,114]. As anode materials in Fenton's based EAOPs, excellent degradation and relatively high mineralization of organics have been reported [21], since the degradation and mineralization of organics are mainly by homogeneously generated  $\cdot\text{OH}$  from Fenton's reaction in the bulk solution. High surface area carbonaceous materials such as carbon-felt, graphite-felt, carbon-sponge, carbon-fiber, activated and carbon-cloth has been the most widely studied cathode materials for Fenton-based EAOPs due to their high capacity for *in-situ* production of large quantities of hydrogen peroxide ( $\text{H}_2\text{O}_2$ ) [21].

#### 2.4.3.2 Ruthenium, Thallium and Iridium oxides – based electrodes

Highly conducting thin film mixed-metal oxides deposited on titanium alloys popularly called DSA have been studied over the past decade as a good catalysts for chlorine and oxygen evolution respectively [27]. These electrodes are classified as “active” electrodes and have strong interaction with the generated  $\cdot\text{OH}$ . As such, they have lower oxidizing power and promote selective oxidation (i.e. conversion) rather than mineralization of organic pollutants [115]. The thin-film are made of  $\text{RuO}_2$ ,  $\text{IrO}_2$ ,  $\text{Ta}_2\text{O}_5$  or mixed metal oxides majorly containing Ru, and Ir oxides with empirical formula  $\text{Ru}_x\text{Ir}_{1-x}\text{O}_2$  deposited on Ti substrate. They are highly robust, chemically and mechanically stable, and have been applied in electrochemical wastewater treatment for the removal of organic pollutants over the past two decades [116]. However, the major disadvantage of applying these electrodes in electrooxidation is that organic oxidation is expected to yield low current efficiency for complete combustion, because the secondary reaction of oxygen evolution is favored [27].

As an anode in electrooxidation, studies have compared the performance of RuO<sub>2</sub>-based electrode with other commercial electrodes such as Pt, PbO<sub>2</sub>, SnO<sub>2</sub>, BDD or even ebonex® (Ti<sub>4</sub>O<sub>7</sub>) for the degradation and mineralization of organic pollutants such phenol [117,118], 4-chlorophenol [119–121], real wastewater effluent [122], 1,4-benzoquinone [123–125], p-nitrosodimethylaniline [125], petrochemical industry wastewater [126], amoxicillin [28], methyl red [127] and cyanide aqueous wastes containing sulfate and chloride anions [128]. Electrooxidation of organics with electrode based on RuO<sub>2</sub> generally yield slow degradation rate with the formation of stable intermediates as well as several carboxylic acids with limited mineralization to CO<sub>2</sub> or TOC removal [27]. However, some authors have reported relatively high mineralization of organics in electrooxidation with Ir, Sn, Ti, or Ta doped RuO<sub>2</sub> electrodes [120,121].

As anode in Fenton's based EAOPs, DSA electrodes have been reported to show relatively high mineralization of organics since the oxidation of organics is predominantly performed by the large quantities of Fenton's reagent generated <sup>•</sup>OH in the bulk. However the performance of these class of electrodes are inferior to that of non-active anode like BDD or PbO<sub>2</sub>, as expected due to the contribution of the heterogeneous hydroxyl radicals generated at the anode surface. For instance, Wu et al. (2012) [129] studied the removal of antibiotic tetracycline from aqueous solution using CF cathode and DSA anode with focus on the influence of experimental variables such as current, initial pH and tetracycline concentration on the drug removal efficiency analyzed by Response Surface Methodology based on Box-Behnken statistical experiment design. Further studies compared the efficiency of Ti/RuO<sub>2</sub>-IrO<sub>2</sub>, Pt and BDD anodes and CF or stainless steel cathode for tetracycline removal by AO and EF [130]. The performance of Ti/RuO<sub>2</sub>-IrO<sub>2</sub> anode using either CF or stainless steel was found to be lower compared to either Pt or BDD anode. Similar results were reported for EF treatment of pharmaceutical ranitidine, with the mineralization efficiency obtained with Ti/RuO<sub>2</sub>-IrO<sub>2</sub> anode inferior to that of Pt or BDD anode [131].

### 2.4.3.3 Platinum electrodes

Pt electrodes have been used for decades as electrode materials in EAOPs because of their good conductivity and chemical stability even at high potentials [27]. They are classified as “active anode” because the  $\cdot\text{OH}$  generated at the surface of this anode is further oxidized to chemisorbed oxygen ( $\text{M}=\text{O}$ ), which are effective in electrochemical conversion rather than combustion of organic pollutants. Studies have shown that efficiency of Pt anode in terms of degradation and mineralization of organics in electrooxidation is relatively better than carbonaceous and  $\text{RuO}_2$ -based electrodes but far inferior to “non-active” anodes such as BDD or doped  $\text{SnO}_2$  and  $\text{PbO}_2$  [28]. These electrodes have been used in electrooxidation of varieties of organic pollutants, such as phenol [83,117,132], chlorophenols [133,134], synthetic dyes [135–137], herbicides [138], petrochemical industry wastewater [139] and pharmaceuticals [2,140–144].

Several studies have reported the use of Pt electrodes in Fenton based EAOPs for oxidation of different organic pollutants either as the lone anode or in comparison with other commercially available electrodes such as DSA or BDD. Organic pollutants such as textile dyes, pesticides, pharmaceuticals, real wastewater and other hydrocarbon contaminants have been remediated with electrochemically generated hydroxyl radicals using Pt and suitable cathode materials and have been summarized in several reviews in literature [2,21–23,81,82,95,144,145]. For instance, the degradation of azo dyes – azobenzene, p-methyl red and methyl orange in aqueous solution was investigated using a Pt anode and a CF cathode [146]. Excellent degradation of all the dyes and their intermediates byproducts was observed until their final oxidation to  $\text{CO}_2$  and water. Complete mineralization of direct orange 61 by EF using Pt anode and CF cathode was also reported by Hammami et al. [147]. Diagne et al. (2006) [148] reported excellent mineralization of methyl parathion by electrochemically generated Fenton’s reagent using Pt anode and CF cathode.



#### 2.4.3.4 Doped-Tin oxides ( $\text{SnO}_2$ ) based electrodes

Pure  $\text{SnO}_2$  has low conductivity at room temperature and thus cannot be used as electrode material in EAOPs. However, antimony (Sb) doped  $\text{SnO}_2$  has high conductivity with a potential for  $\text{O}_2$  evolution of  $\sim 1.9$  V versus SHE [27,103], thus makes it effective anode material for oxidation of organics. Several other dopants such as Ar, B, Bi, F, Cl and P have been investigated as an alternative to Sb, since the latter is a toxic substance with an US-EPA drinking water limit of  $6 \mu\text{g L}^{-1}$  [103]. A spin trap experiment using *N,N*-dimethyl-*p*-nitrosoaniline demonstrate the formation of  $\cdot\text{OH}$  at the  $\text{SnO}_2$  electrode surface [83] and in turn, the combustion/mineralization of substrates in aqueous solution [149,150]. Although several studies have investigated the used of doped- $\text{SnO}_2$  electrodes in oxidation of organics on laboratory scale [124,151,152], they have not been applied on commercial scale due to their short-service life [153–155]. The short-service life of this class of electrodes is attributed to two mechanisms: (i) the formation of non-conductive Sn-hydroxide layer on the outer surface of the anode and (ii) the passivation of the underlying Ti substrate that causes delamination of the doped- $\text{SnO}_2$  film [156–158]. The former (Sn-hydroxide) is believed to be caused by hydration of  $\text{SnO}_2$  surface and can be minimized by doping with Pt, while the latter (passivation of Ti substrate) can be mitigated by intercalation of an  $\text{IrO}_2$  interlayer between the Ti support and the  $\text{Sb}_2\text{O}_4$  doped  $\text{SnO}_2$  thin film coating, which has been proven to tremendously improve the service life of the electrode [154,159].

Several studies have reported the greater potential of doped  $\text{SnO}_2$  for electrochemical wastewater treatment. Early studies reported complete mineralization of wide range of organic compounds irrespective of pH, with the efficiency far greater than that of Pt anodes [156]. Subsequent studies have also obtained complete mineralization of organics such as phenol [118,149,160,161], pharmaceuticals [161,162], pesticides [163], azo dyes [161], humic acids and landfill leachate [164] with  $\text{Sb}_2\text{O}_4$  doped  $\text{SnO}_2$  anodes at moderate current density.

As anode in EF process, doped  $\text{SnO}_2$  electrode has attracted very limited attention, possibly due to the fact that it is not commercially available. In fact, there is no study available in literature concerning the application of this electrode in EF process to the best of our knowledge.

#### 2.4.3.5 Lead oxide ( $\alpha$ - $PbO_2$ ) based electrodes

Lead oxide anodes have been widely applied on industrial scale because they are inexpensive and easy to prepare [27]. They have good conductivity and large surface area and have been extensively studied for the oxidation of organics. Earlier studies have shown that  $PbO_2$  electrode has been utilized as pellets, however later research mainly explore  $PbO_2$  and doped  $PbO_2$  anodes deposited on a variety of substrate such as Ta, Ti, stainless steel and Exbonex® [165–168]. Spin trap experiments [123,168] have confirmed the production of  $\cdot OH$  on  $PbO_2$  and doped  $PbO_2$ , but the mechanism for the production of  $\cdot OH$  at the  $PbO_2$  electrode is still not well understood. Summary of the proposed mechanism of generation of  $\cdot OH$  on  $PbO_2$  based electrodes can be found in literature [27,103]. The generated  $\cdot OH$  are weakly adsorbed onto the surface of the  $PbO_2$  anode, thus make it readily available for substrate oxidation. The oxidation potential of  $PbO_2$  electrode for organic pollutants removal has been reported to be relatively closed to that of BDD [169].

Several studies have reported the application of  $PbO_2$  and doped  $PbO_2$  electrodes for oxidation of organics such as synthetic dyes [166,170,171], hydroquinone [139], 2,4-nitrophenol [172], chloranilic acid [123], *p*-nitrophenol [173], herbicides and pesticides [163], diethyl phthalate [174], real landfill leachate [164] and pharmaceuticals [28,175].

However, there are limited literatures on the application of this electrode in EF process for the treatment of wastewater.

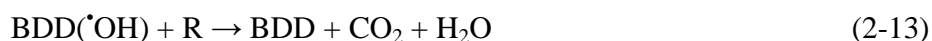
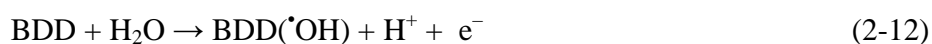
#### 2.4.3.6 Boron doped diamond electrodes

Synthetic boron-doped diamond (BDD) thin film deposited on suitable substrate is the most efficient and widely studied electrode for EAOPs remediation of wastewater [27]. Diamond films are grown on non-diamond substrates (e.g. silicon, tungsten, molybdenum, titanium, niobium, tantalum or glassy carbon) using chemical vapor deposition because this method is inexpensive and has been widely developed for commercial production of crystalline diamond films for industrial application [27,103,176]. The common dopant used in diamond electrode is boron, due to its low charge carrier activation energy (0.37 eV) [177]. The extent of boron

doping controls the behavior of the diamond electrode with low doping level ( $\sim 10^{17}$  atoms  $\text{cm}^{-3}$ ) diamond exhibits semiconductor properties, whereas high doping level ( $\sim 10^{20}$  atoms  $\text{cm}^{-3}$ ) diamond exhibits semi-metallic conductivity [176,178].

BDD electrodes possess several technologically important properties that distinguish them from other electrodes. For instance, they are known for their extreme stability under anodic polarization in aqueous and non-aqueous electrolytes due to C atoms being in  $\text{sp}^3$  hybridization [179]. They have excellent corrosion resistant in very aggressive media even during long-term cycling from hydrogen to oxygen evolution [180]. Further, they possess inert surface with low adsorption properties and strong tendency to resist deactivation [181]. However, BDD film electrodes are still subject to possible failure especially at high applied current density, majorly due to film delamination from the substrate [182] and wear at grain boundaries [183].

Due to their excellent properties, BDD electrodes promote the production of weakly adsorbed hydroxyl radicals during the electrolysis in the region of water discharge. The produced radical unselectively and completely mineralize organic pollutants with a high current efficiency [27] according to the equations (2-12) and (2-13):



This mechanism confirmed experimentally using 5,5-dimethyl-1-pyrroline-N-oxide and salicylic acid as spin trapping, showed that the oxidation process on the BDD electrodes involves hydroxyl radicals as electrogenerated intermediates [184].

In the last two decades, several laboratories have been investigating this material for wastewater treatment and the corresponding research papers have increased exponentially [27,103]. As anode in both AO and EF, many publications have reported that BDD electrodes allow complete mineralization (with very good current efficiencies) of different classes of organic pollutants, which have been summarized in several reviews [2,21–24,26,27,81,82,95,103,144,145].

#### 2.4.3.7 Doped and substoichiometric titanium oxides based electrode

Ceramic electrodes based on sub-stoichiometric  $\text{TiO}_2$ , and doped- $\text{TiO}_2$  have been developed and tested for potential application in electrochemical wastewater treatment [185–188]. Stoichiometric  $\text{TiO}_2$  is an insulator with an electrical conductivity of  $\sim 10^{-9} \Omega^{-1} \text{cm}^{-1}$  [189,190]. However, creating oxygen deficiencies in the  $\text{TiO}_2$  lattice structure can drastically change its electronic properties. Introduction of oxygen deficiencies in  $\text{TiO}_2$  lattice can be accomplished at temperature above  $900^\circ\text{C}$  under a  $\text{H}_2/\text{coke}$  reduced atmosphere, in the presence of reduced metals (e.g., Ti), or by doping with group five elements such as V, Nb or Ta [103]. In all case,  $\text{Ti}^{(\text{IV})}$  is converted to  $\text{Ti}^{(\text{III})}$  with n-type semiconductor behavior.

The Ti–O system belongs to a homologous series called “Magnéli phases” with the empirical formula  $\text{Ti}_n\text{O}_{2n-1}$ , ( $n \geq 3$ ) [191]. Several oxides in this series exhibit high electrical conductivity at room temperature [189,192,193], good corrosion resistant in aqueous electrolytes and high chemical stability, especially the first three oxides from the series, i.e.  $\text{Ti}_3\text{O}_5$ ,  $\text{Ti}_4\text{O}_7$  and  $\text{Ti}_5\text{O}_9$  [187,189,190]. For instance,  $\text{Ti}_4\text{O}_7$  has electrical conductivity of  $166 \Omega^{-1} \text{cm}^{-1}$ , which is many order of magnitude greater than the conductivity of  $\text{TiO}_2$  [189,194]. The oxygen deficiency of sub-oxides of  $\text{TiO}_2$  phases are due to edge sharing of  $\text{TiO}_6$  octahedral in the crystallographic shear plane [195]. Structurally, this electrode is considered to contain a layer of TiO sandwiched with three layers of  $\text{TiO}_2$  [189]. Several reduction technique have been investigated with the sole aim of synthesize materials consisting majorly  $\text{Ti}_4\text{O}_7$ , since it is the most conducting oxide in the series [189]. However, studies have shown that mixture of sub-oxides of  $\text{TiO}_2$  is usually produced from  $\text{TiO}_2$  irrespective of the reduction method employed. It is important to note that excessive reduction of  $\text{TiO}_2$  create a structure with significant oxygen-deficiencies, which is extremely brittle and less conductive than  $\text{Ti}_4\text{O}_7$  [186,188].

Ceramic sub-stoichiometric  $\text{TiO}_2$  electrodes consisting majorly  $\text{Ti}_4\text{O}_7$  are commercially available and sold under the trade name Ebonex® [125,196]. Studies have shown that Ebonex® ceramic electrodes behave as non-active anode with respect to water oxidation and hydroxyl radical generation [186,197]. However, the hydroxyl radical formed at its surface appears to be less abundant but more reactive compared with BDD anode at analogous condition [125]. Few studies have investigated the potential of Ebonex® and sub-stoichiometric  $\text{TiO}_2$  nanotube arrays

as suitable electrode in various laboratory scale electrochemical wastewater treatment [125,198–201]. However,  $\text{Ti}_4\text{O}_7$  electrodes are primarily used in cathodic protection of metallic structures [188]. In addition there is growing interest in the synthesis and application of these electrodes as supports for batteries, fuel cells, catalysts and electrocatalysts due to its corrosion resistance and electrical stability [186,189,195,202,203].

The major challenge of application of sub-stoichiometric  $\text{TiO}_2$  electrodes is the formation of thin layer of passivating  $\text{TiO}_2$  coating due to the oxygen deficient nature of sub-stoichiometric  $\text{TiO}_2$ , which allows the possibility of oxygen incorporation into the lattice structure during anodic polarization [195,202]. Conflict results have been reported concerning the reversibility of the passivation layer possibly due to the presence of different Magneli phases in the Ebonex® tested; while some studies have shown that the passivation was reversible upon cathodic polarization [195], other studies report that the passivation is not totally reversible [103]. However, recent work by Bejan et al. (2012) [197] with Ebonex® ( $\text{Ti}_4\text{O}_7$ ) has shown that periodic polarity reversals during the oxidation of sulfide were able to prevent electrode passivation. Further, soft-sand blasting has been found to partially restore the activity of the Ebonex® after reduction in oxidation potential due to passivation. Extensive studies are still need to understand the mechanism of passivation/reactivation of  $\text{Ti}_4\text{O}_7$  electrodes.

Some studies have also investigated the doping of  $\text{TiO}_2$  (rutile phase) with Nb which produces ceramic materials with very high electrical conductivity [204]. Niobium-doped rutile  $\text{TiO}_2$  (NDR) has been found to be highly conductive with proposed general formula of  $\text{Ti}_{1-x}\text{Nb}_x\text{O}_2$  and a typical oxide composition of  $\text{Ti}_{0.9}\text{Nb}_{0.1}\text{O}_2$  has electrical conductivity similar to that of  $\text{Ti}_4\text{O}_7$  [202,205]. The mechanism of doping in this case is by direct substitution of  $\text{Nb}^{5+}$  for  $\text{Ti}^{4+}$ , which is highly favored due to the similarity in crystal radii of both  $\text{Nb}^{5+}$  and  $\text{Ti}^{4+}$  when present in a 6-coordinate structure [206]. As such, doped oxides have much more resistant to oxidation than  $\text{Ti}_4\text{O}_7$  as they consist of negligible anion deficiencies [202,205]. Based on this unique feature, the NDR has been studied for application in regenerative fuel cells, fuel cell and battery supports, dye-sensitized solar cells and electrocatalysts for water oxidation [202,204,207–209]. However, only limited study could be found in literature that utilized doped- $\text{TiO}_2$  for EAOPs.

As stated earlier, both electrode materials can generate hydroxyl radical *via* water oxidation reaction [125,199,200] for organic pollutants oxidation. Some recent studies have also employed the formability of sub-oxides and doped TiO<sub>2</sub> to produce conductive porous reactive electrochemical membranes consisting of monolithic structures of Ti<sub>4</sub>O<sub>7</sub> electrodes for concurrent filtration and electrooxidation of organics [199,200]. Other studies have reported the excellent oxidation potential of sub-stoichiometric TiO<sub>2</sub> nanotube arrays compared to both Ti<sub>4</sub>O<sub>7</sub> particles electrode and BDD for phenol mineralization [201]. Although, electrochemical water treatment potential of both sub-stoichiometric and doped TiO<sub>2</sub> electrodes are very exciting, the durability and electrochemical stability of both still require extensive investigation. In fact, all studies that have been carried out on Ti<sub>4</sub>O<sub>7</sub> and doped-TiO<sub>2</sub> for electrochemical wastewater treatment were performed at low current densities (i.e. < 10 mA cm<sup>-1</sup>). Future research should also investigate these electrodes for oxidation of complex organic pollutants such as pharmaceuticals, pesticides and synthetic dyes. More importantly, these electrodes have not been used in Fenton's based EAOPs because of formation of yellowish Ti(H<sub>2</sub>O<sub>2</sub>)<sub>4</sub> complexes which inhibit Fenton's reaction.

#### 2.4.4 Heterogeneous electro-Fenton process

Heterogeneous EF uses solid catalyst sources for the generation of <sup>•</sup>OH. It has been investigated as a promising alternative to homogeneous EF to overcome necessities for catalyst quantity optimization as well as widening the pH range at which EF process can be performed [210,211]. As stated in section 2.3.2, all Fenton's based AOPs are optimum at pH 2.5 – 3.5, as such performing EF process outside this pH range results in lower efficiency of the process. For instance at pH ≤ 2, the formation of peroxonium ions (H<sub>3</sub>O<sub>2</sub><sup>+</sup>) which makes the electrogenerated H<sub>2</sub>O<sub>2</sub> electrophilic and reduces its reactivity towards Fe<sup>2+</sup> in addition to the preferential H<sub>2</sub> evolution at the cathode occurring at lower acidic pH, while at pH ≥ 4.0, there is both precipitation of Fe<sup>3+</sup> (elimination of the catalyst) as ferric hydroxide and the decomposition of generated H<sub>2</sub>O<sub>2</sub> into water and O<sub>2</sub>, thus hindering the production of <sup>•</sup>OH [21,25]. Heterogeneous EF has been developed to overcome the challenges of narrow pH window encountered in EF process. Additionally, heterogeneous EF offers added advantage of reusability of catalyst for several

cycles as well as its easy separation from the treated solution. The coagulation step used as post-treatment to remove the catalyst in EF usually results in generation of large quantities of ferric iron sludge which constitutes additional separation and disposal problem, and in turn increases the operational cost [210].

Generally catalyst/co-catalyst supported on substrate must possess some characteristics in order to achieve the required improvement in activity and overcome the challenges encounter in homogeneous Fenton's reaction. The most important characteristic is the catalytic activity and stability of the material [212]. Reusability in several runs is not a good criterion for determine stability of catalyst since substrate-to-catalyst ratio determined the reusability [213]. In essence large excessive quantities of solid catalyst should always allow reuse of materials in several consecutive reaction runs whereas; lesser amounts of solid catalyst would make reusability more difficult. The maximum productivity of solid catalyst can be measure by performing an experiment with a large excess of substrate for a prolong time until complete deactivation of the catalyst. Analysis of this experiment can also reveal the deactivation rate of the catalyst and its causes [212].

Other parameter closely related to stability is the leaching of the catalyst to the aqueous phase which must be minimized to avoid excess catalyst in the solution that can act as homogeneous catalyst [210]. In case there is leaching of catalyst into the solution, the overall catalytic activity maybe the combination of both activity of the leached species and the activity of the solid catalyst. Although leaching may enhance the overall catalytic activity performance but it usually leads to depletion of metal sites in the solids and may cause loss of solid catalytic activity in the long run [212].

Studies have shown that there are two main mechanisms of oxidation of organics in heterogeneous EF process: homogeneous catalyzed and surfaced catalyzed processes depending on the pH at which the EF process is being performed and the nature of the catalyst used [210,214]. Under low pH conditions the process appears to be controlled by both redox cycling of dissolved iron ( $\text{Fe}^{2+}/\text{Fe}^{3+}$ ) and the surface catalyzed mechanism, the former emanating from the dissolution of Fe catalyst. At circumneutral pH, the contribution of dissolved iron species to

the catalytic decomposition of  $\text{H}_2\text{O}_2$  should be negligible because Fe[III] is insoluble [214]. As such, catalytic decomposition of  $\text{H}_2\text{O}_2$  at higher pH is considered as a surface-catalyzed process.

Heterogeneous EF can be broadly divided into two groups – those with added solid catalyst and catalyst impregnated electrode. Both are vividly discussed in the next section.

#### *2.4.4.1 Heterogeneous electro-Fenton process using added catalyst*

Heterogeneous EF process using added solid catalyst utilized natural or synthetic relatively insoluble Fe or Fe compound supported on substrate. As stated earlier, the overall aim is to achieve reusability of the catalyst, easy separation after EF treatment and widening the pH window at which EF can be performed. Early studies investigated the viability of goethite ( $\text{FeO}(\text{OH})$ ) as an iron dosage source for aniline mineralization by a modified process termed goethite catalyzed EF [215]. Further works by the group [216] extended their studies to other iron oxides minerals such as wustite ( $\text{FeO}$ ), magnetite ( $\text{Fe}_3\text{O}_4$ ) and hematite ( $\alpha\text{-Fe}_2\text{O}_3$ ) for their use in both EF and photo-EF processes. The efficiency of EF process with wustite and magnetite was found to be greater than  $\text{Fe}^{2+}$ , whereas that of goethite and hematite is much lower. The difference in the performance was attributed to the ability of the minerals oxide to release  $\text{Fe}^{2+}$  to the bulk, which react with electrogenerated  $\text{H}_2\text{O}_2$  via Fenton reaction (eq. 2-8) so that the system could behave as pure homogeneous catalysts that act as self-regulatory iron source.

Since then several researchers and laboratory and in turn corresponding publications have been tailored towards this aspect of EF process, especially in the last 3 years. For instance Ramirez et al. (2010) [217] utilized Fe – supported on Naflon membrane and ion-exchange amberlite and purolite resin as a catalyst in photo-EF for degradation of aqueous orange-II dye solution. While up to 60% TOC removal was achieved under experimental condition employed, the Fe was relatively fixed on the supports with limited desorption. Iglesias et al., (2013) [218] studied the application of Fe-loaded sepiolite obtained by adsorption as an effective heterogeneous catalyst in EF for degradation of Reactive Black 5. Total decoloration of the dye was achieved in all numbers of batches tested with slight reduction in efficiency with increase in number of batches. At optimum conditions, total decolorization was obtained with a COD



reduction of 86.7 % and an energy consumption per decolorized dye mass of 12.76 kWh/kg. Some studies recently utilized pyrite as heterogeneous source of  $\text{Fe}^{2+}$  and pH regulator in EF treatment of pharmaceuticals such as sulfamethazine [219], levofloxacin [220], azo dye [221] and phenolic compound tyrosol [222]. In all cases, the oxidation/mineralization of the pollutants by pyrite catalyzed EF was found to be higher than corresponding classical EF process at similar experimental conditions with BDD or Pt anodes. Synthesized nano- $\text{Fe}_3\text{O}_4$  has also been utilized to catalyzed EF for the oxidation of catechol from aqueous solution [223]. Several operation parameters such as temperature, pH, catalyst loading and initial catechol concentration were found to affect the efficiency of the process with excellent mineralization and catalyst reusability obtained at optimum experimental conditions.

Other studies have utilized Fe-loaded and Mn-alginate as catalyst for heterogeneous EF treatment of malodorous compound, indole [224] and reactive black 5 respectively [225], with efficient mineralization and reusability obtained for Fe-loaded alginate, whereas poor degradation of the dye was achieved with Mn-loaded alginate due to deposition of  $\text{MnO}_2$  at the anode. In a related studies, Fe-supported Y-zeolite and Fe-Y zeolite loaded alginate was utilized for the heterogeneous EF removal of pesticide from ground water [226]. The reusability of Fe-supported Y-zeolite was found to be relatively low but was significantly improved when embedded in alginate. Similar studies reported the use of Fe-modified bentonite synthesized via green chemistry using green tea extract as reducing and capping agent as catalyst in heterogeneous EF degradation of orange II dye [227]. Some of the recent studies on heterogeneous EF with catalyst added are summarized in Table 2-1.

**Table 2-1**– Summary of some recent studies on heterogeneous EF treatment with added catalyst

Pollutants	Catalyst	Solution	Cathode/ anode	Efficiency	Current density/Ener gy	Ref.
Indole	Fe-alginate	20 mg L <sup>-1</sup> indole in Na <sub>2</sub> SO <sub>4</sub> at pH 3 and 7 h	CF/Pt	90 % TOC	0.53 mA cm <sup>-1</sup>	[224]

sulfamethazine	Pyrite (FeS <sub>2</sub> )	200 mL of 0.2 mM of the drug in 50 mM Na <sub>2</sub> SO <sub>4</sub> at pH 3	CF/Pt CF/BDD	87% TOC 95% TOC	20 mA cm <sup>-1</sup>	[219]
Amaranth food dye	Fe <sub>3-x</sub> Cu <sub>x</sub> O <sub>4</sub> 0 ≤ x ≤ 0.25	400 mL of 100 mg L <sup>-1</sup> of dye in 1M KOH at pH 13.4	GDE/Pt	70% TOC	483 kWh kg <sup>-1</sup>	[228]
Levofloxacin	Pyrite (FeS <sub>2</sub> )	200 mL of 0.23 mM drug in 50 mM Na <sub>2</sub> SO <sub>4</sub> at pH 3	CF/BDD	95% TOC	50 mA cm <sup>-1</sup>	[220]
p-nitrophenol (p-NP)	Clump steel wire	50 mg L <sup>-1</sup> of p-NP in 50 mM Na <sub>2</sub> SO <sub>4</sub> at pH 3	GDE/PbO <sub>2</sub>	79% TOC	3 mA cm <sup>-1</sup>	[229]
Orange II	Fe-bentonite	400 mL of 100 mg L <sup>-1</sup> of dye in 50 mM Na <sub>2</sub> SO <sub>4</sub> at pH 3	Graphite/graphite	76% COD	14.29 mA cm <sup>-1</sup>	[227]
2,4-DCP	Fe-C particle	300 mL of 120 mg L <sup>-1</sup> of 2,4-DCP in 50 mM Na <sub>2</sub> SO <sub>4</sub> at pH 6.7	GDE/Ti/Ir O <sub>2</sub> -RuO <sub>2</sub>	55% TOC	12.5 mA cm <sup>-1</sup>	[230]
Reactive Black 5	Mn-alginate	150 mL working volume at pH 2	Graphite/graphite paper	73% TOC	-	[225]
AHPS dye	Pyrite (FeS <sub>2</sub> )	250 mL of 175 mg L <sup>-1</sup> of AHPS dye in 50 mM	Graphite felt/BDD	90% TOC	75 mA cm <sup>-1</sup>	[221]

		Na <sub>2</sub> SO <sub>4</sub> at pH 3				
Imidacloprid and Chlorpiryfsol	Fe-Y zeolite Alginate-Fe-Y zeolite	150 mL of the pesticides in 100 mM Na <sub>2</sub> SO <sub>4</sub>	Graphite/BDD	-	-	[231]
Catechol	Nano-Fe <sub>3</sub> O <sub>4</sub>	200 mL of catechol solution at pH 3	ACF/Pt	73% TOC	10 mA cm <sup>-1</sup>	[223]
Reactive Black 5	Fe-sepiolite	150 mL of RB5 in 0.01 M Na <sub>2</sub> SO <sub>4</sub>	Graphite/BDD	-	-	[218]
Phenol	Fe-Cu nanoclay	100 mL phenol in 0.05 M Na <sub>2</sub> SO <sub>4</sub>	Glassy carbon/Pt	-	-	[232]
m-cresol	Fe-activated carbon	150 mL of m-cresol in 0.02 M Na <sub>2</sub> SO <sub>4</sub>	Nickel foam/BD D	83% TOC	-	[233]

#### 2.4.4.2 Heterogeneous electro-Fenton process using catalyst impregnated electrode

Modified carbonaceous electrodes (cathode) have been recently developed, which act as electrode as well as the catalyst in heterogeneous electron-Fenton system [210,214]. In many cases, the catalysts are impregnated or loaded on materials potent for H<sub>2</sub>O<sub>2</sub> generation such as active carbon fiber, carbon-felt, graphite felt and recently carbon aerogel. The catalytic performance in most cases is due to combination of both homogeneous oxidation in the bulk of the solution because of leaching of the catalyst and heterogeneous oxidation at the surface of the cathode at low pH value, whereas surfaced catalyzed process is predominant as pH increases [214]. The efficiency, stability and reusability of the catalyst impregnated electrodes are largely

affected by the technique by which the catalyst is grafted into the carbon matrix. The technique used controls the adhesion and mechanical wearing of the catalyst from cathode matrix.

Several studies have investigated various methods to obtain functionalized cathodic materials for applications in heterogeneous EF process for mineralization of organic pollutants. For instance, pyrrhotite ( $\text{Fe}_{1-x}\text{S}_x$ ) powder grafted on graphite sheets by conductive silver paste was utilized as cathodic heterogeneous Fenton catalyst to degrade biorefractory organics in landfill leachate [234]. Previous studies by Zhang and co-workers utilized  $\text{Fe}@\text{Fe}_2\text{O}_3$  nanowires as an iron source mixing with multi-walled carbon nanotubes and fixed to tetrafluoroethylene (PTFE) as cathode materials for degradation of rhodamine B at neutral pH [210]. The same authors [235] have investigated activated carbon-supported nano- $\text{FeOOH}$  cathode prepared by depositing iron oxide nanocrystals on the surface of activated carbon for the oxidative degradation of amaranth dye. The prepared electrode was able to achieve desirable reactivity but low stability due to mechanical wearing, dissolution and agglomeration of the catalyst during EF treatment. Some studies have also reported Fe-loaded activated carbon cathode prepared either by adsorption or electrochemical technique as an effective electrode and catalyst for the degradation of m-cresol and Orange II solution [233,236]. The use of carbon-aerogel loaded with different kinds of solid Fe- catalyst such as  $\text{Fe}@\text{Fe}_2\text{O}_3\text{C}$  and iron oxide-graphene/nanotubes have recently been investigated for the degradation of various organic pollutants on a wide pH range [214,237,238]. The Fe-loaded aerogel in most cases are highly stable and shows excellent reactivity towards organic pollutants over a wide pH range. However, some of the synthesis techniques seem more complex for commercial application.

## **2.5 Conclusions**

The occurrence, fate and toxicology of pharmaceutical residues in aquatic environment and their removal by EAOPs such as AO and EF are detailed in this chapter. The efficiency of EAOPs such as AO and EF for the removal of pharmaceutical residues could be significantly enhanced in terms of performance and cost by proper selection of electrode materials and in case of EF by heterogeneous catalyst system.

Active electrodes such as Pt, DSA and carbonaceous materials are generally not suitable for AO process because only electrochemical conversion can be achieved at their surface with limited mineralization of the pollutants. Non-active anode such as doped SnO<sub>2</sub>, PbO<sub>2</sub>, sub-stoichiometric TiO<sub>2</sub> and BDD on the other hand produces large quantities of  $\cdot\text{OH}$  at their surfaces which could achieve almost complete electrochemical combustion of organic pollutants to CO<sub>2</sub>. However, doped SnO<sub>2</sub> electrodes are relatively unstable and have short-service life, whereas PbO<sub>2</sub> presents post hazardous risk due to possible leaching, especially at basic pH. Although BDD remain the best anode for electrochemical water/wastewater treatment, the high cost of production has limited its application on industrial scale. Sub-stoichiometric TiO<sub>2</sub> represents a low cost alternative electrode because it is produce from TiO<sub>2</sub>, which is a highly abundant feedstock in universe. This electrode has relatively high potential for production of  $\cdot\text{OH}$  and mineralization of organic pollutants. However, this electrode has not been extensively studied for electrochemical AO and EF. Indeed, its performances were investigated in the following chapters.

On the other hand, heterogeneous EF system is an exciting alternative to homogeneous EF with the possibility of performing EF at a wide range of pH without necessarily reduce the efficiency of the process. This is possible because surface-catalyzed oxidation process controls the mineralization of the organic as the pH increases. Additionally heterogeneous EF proffer recyclability and reusability of the catalyst thus make the process efficient and economical for commercial application purposes.

**References**

- [1] D.W. Kolpin, E.T. Furlong, M.T. Meyer, E.M. Thurman, S.D. Zaugg, L.B. Barber, H.T. Buxton, Pharmaceuticals, hormones, and other organic wastewater contaminants in U.S. streams, 1999–2000: A national reconnaissance, *Environ. Sci. Technol.* 36 (2002) 1202–1211.
- [2] I. Sirés, E. Brillas, Remediation of water pollution caused by pharmaceutical residues based on electrochemical separation and degradation technologies: A review, *Environ. Int.* 40 (2012) 212–229.
- [3] T. Heberer, Occurrence, fate, and removal of pharmaceutical residues in the aquatic environment: a review of recent research data, *Toxicol. Lett.* 131 (2002) 5–17.
- [4] C. Carlsson, A.-K. Johansson, G. Alvan, K. Bergman, T. Kühler, Are pharmaceuticals potent environmental pollutants?, *Sci. Total Environ.* 364 (2006) 67–87.
- [5] T. Ternes, The occurrence of micropollutants in the aquatic environment: a new challenge for water management, *Water Sci. Technol.* 55 (2007) 327.
- [6] G. Carlsson, J. Patring, J. Kreuger, L. Norrgren, A. Oskarsson, Toxicity of 15 veterinary pharmaceuticals in zebrafish (*Danio rerio*) embryos, *Aquat. Toxicol.* 126 (2013) 30–41.
- [7] M. Kołodziejaska, J. Maszkowska, A. Białk-Bielińska, S. Steudte, J. Kumirska, P. Stepnowski, S. Stolte, Aquatic toxicity of four veterinary drugs commonly applied in fish farming and animal husbandry, *Chemosphere.* 92 (2013) 1253–1259.
- [8] C.G. Daughton, T.A. Ternes, Pharmaceuticals and personal care products in the environment: agents of subtle change?, *Environ. Health Perspect.* 107 (1999) 907–938.
- [9] O.A.H. Jones, N. Voulvoulis, J.N. Lester, Human Pharmaceuticals in the Aquatic Environment a Review, *Environ. Technol.* 22 (2001) 1383–1394.
- [10] H. Sanderson, Probabilistic hazard assessment of environmentally occurring pharmaceuticals toxicity to fish, daphnids and algae by ECOSAR screening, *Toxicol. Lett.* 144 (2003) 383–395.
- [11] L.H.M.L.M. Santos, M. Gros, S. Rodriguez-Mozaz, C. Delerue-Matos, A. Pena, D. Barceló, M.C.B.S.M. Montenegro, Contribution of hospital effluents to the load of pharmaceuticals in urban wastewaters: Identification of ecologically relevant pharmaceuticals, *Sci. Total Environ.* 461-462 (2013) 302–316..

- [12] A. Ziyilan, N.H. Ince, The occurrence and fate of anti-inflammatory and analgesic pharmaceuticals in sewage and fresh water: Treatability by conventional and non-conventional processes, *J. Hazard. Mater.* 187 (2011) 24–36.
- [13] B. Halling-Sørensen, S. Nors Nielsen, P.F. Lanzky, F. Ingerslev, H.C. Holten Lützhøft, S.E. Jørgensen, Occurrence, fate and effects of pharmaceutical substances in the environment- A review, *Chemosphere.* 36 (1998) 357–393.
- [14] H. Sanderson, R.A. Brain, D.J. Johnson, C.J. Wilson, K.R. Solomon, Toxicity classification and evaluation of four pharmaceuticals classes: antibiotics, antineoplastics, cardiovascular, and sex hormones, *Toxicology.* 203 (2004) 27–40.
- [15] O.A. H. Jones, N. Voulvoulis, J.N. Lester, Human pharmaceuticals in wastewater treatment processes, *Crit. Rev. Environ. Sci. Technol.* 35 (2005) 401–427.
- [16] G. Hua, D.A. Reckhow, Comparison of disinfection byproduct formation from chlorine and alternative disinfectants, *Water Res.* 41 (2007) 1667–1678.
- [17] P. Wang, Y.L. He, C.H. Huang, Reactions of tetracycline antibiotics with chlorine dioxide and free chlorine, *Water Res.* 45 (2011) 1838–1846.
- [18] K. Ikehata, N. Jodeiri Naghashkar, M. Gamal El-Din, Degradation of aqueous pharmaceuticals by ozonation and advanced oxidation processes: A review, *Ozone Sci. Eng.* 28 (2006) 353–414.
- [19] R. Andreozzi, M. Canterino, R. Marotta, N. Paxeus, Antibiotic removal from wastewaters: The ozonation of amoxicillin, *J. Hazard. Mater.* 122 (2005) 243–250.
- [20] G.V. Buxton, N.D. Wood, S. Dyster, Ionisation constants of  $\cdot\text{OH}$  and  $\text{HO}\cdot_2$  in aqueous solution up to 200 °C. A pulse radiolysis study, *J. Chem. Soc. Faraday Trans. 1 Phys. Chem. Condens. Phases.* 84 (1988) 1113.
- [21] M.A. Oturan, J.-J. Aaron, Advanced oxidation processes in water/wastewater treatment: Principles and applications. A review, *Crit. Rev. Environ. Sci. Technol.* 44 (2014) 2577–2641.
- [22] I. Sirés, E. Brillas, M.A. Oturan, M.A. Rodrigo, M. Panizza, Electrochemical advanced oxidation processes: today and tomorrow. A review, *Environ. Sci. Pollut. Res.* 21 (2014) 8336–8367.
- [23] E. Brillas, I. Sires, M.A. Oturan, Electro-Fenton process and related electrochemical technologies based on Fenton’s reaction chemistry, *Chem. Rev.* 109 (2009) 6570–6631.

- [24] C.A. Martínez-Huitle, E. Brillas, Decontamination of wastewaters containing synthetic organic dyes by electrochemical methods: A general review, *Appl. Catal. B Environ.* 87 (2009) 105–145.
- [25] I. Sirés, E. Brillas, M.A. Oturan, M.A. Rodrigo, M. Panizza, Electrochemical advanced oxidation processes: today and tomorrow. A review, *Environ. Sci. Pollut. Res.* 21 (2014) 8336–8367.
- [26] C.A. Martínez-Huitle, M.A. Rodrigo, I. Sirés, O. Scialdone, Single and coupled electrochemical processes and reactors for the abatement of organic water pollutants: A critical review, *Chem. Rev.* 115 (2015) 13362–13407.
- [27] M. Panizza, G. Cerisola, Direct and mediated anodic oxidation of organic pollutants, *Chem. Rev.* 109 (2009) 6541–6569.
- [28] F. Sopaj, M.A. Rodrigo, N. Oturan, F.I. Podvorica, J. Pinson, M.A. Oturan, Influence of the anode materials on the electrochemical oxidation efficiency. Application to oxidative degradation of the pharmaceutical amoxicillin, *Chem. Eng. J.* 262 (2015) 286–294.
- [29] J.P. Bound, N. Voulvoulis, Pharmaceuticals in the aquatic environment—a comparison of risk assessment strategies, *Chemosphere.* 56 (2004) 1143–1155.
- [30] L.J. Schulman, E.V. Sargent, B.D. Naumann, E.C. Faria, D.G. Dolan, J.P. Wargo, A Human health risk assessment of pharmaceuticals in the aquatic environment, *Hum. Ecol. Risk Assess.* 8 (2002) 657–680.
- [31] R. Andreozzi, V. Caprio, C. Ciniglia, M. de Champdoré, R. Lo Giudice, R. Marotta, E. Zuccato, Antibiotics in the environment: Occurrence in Italian STPs, fate, and preliminary assessment on algal toxicity of amoxicillin, *Environ. Sci. Technol.* 39 (2005) 8112–8112.
- [32] C. Miège, J.M. Choubert, L. Ribeiro, M. Eusèbe, M. Coquery, Fate of pharmaceuticals and personal care products in wastewater treatment plants – Conception of a database and first results, *Environ. Pollut.* 157 (2009) 1721–1726.
- [33] R. Hirsch, T. Ternes, K. Haberer, K.L. Kratz, Occurrence of antibiotics in the aquatic environment, *Sci. Total Environ.* 225 (1999) 109–118.
- [34] T.A. Ternes, Occurrence of drugs in German sewage treatment plants and rivers: Dedicated to Professor Dr. Klaus Haberer on the occasion of his 70th birthday.1, *Water Res.* 32 (1998) 3245–3260.



- [35] K. Kümmerer, Antibiotics in the aquatic environment – A review – Part I, *Chemosphere*. 75 (2009) 417–434.
- [36] P. Roberts, K. Thomas, The occurrence of selected pharmaceuticals in wastewater effluent and surface waters of the lower Tyne catchment, *Sci. Total Environ.* 356 (2006) 143–153.
- [37] K. Kümmerer, Drugs in the environment: emission of drugs, diagnostic aids and disinfectants into wastewater by hospitals in relation to other sources – a review, *Chemosphere*. 45 (2001) 957–969.
- [38] K. Kümmerer, The presence of pharmaceuticals in the environment due to human use – present knowledge and future challenges, *J. Environ. Manage.* 90 (2009) 2354–2366.
- [39] S.D. Kim, J. Cho, I.S. Kim, B.J. Vanderford, S.A. Snyder, Occurrence and removal of pharmaceuticals and endocrine disruptors in South Korean surface, drinking, and waste waters, *Water Res.* 41 (2007) 1013–1021.
- [40] J.H. Al-Rifai, C.L. Gabelish, A.I. Schäfer, Occurrence of pharmaceutically active and non-steroidal estrogenic compounds in three different wastewater recycling schemes in Australia, *Chemosphere*. 69 (2007) 803–815.
- [41] D. Bendz, N.A. Paxéus, T.R. Ginn, F.J. Loge, Occurrence and fate of pharmaceutically active compounds in the environment, a case study: Höje River in Sweden, *J. Hazard. Mater.* 122 (2005) 195–204.
- [42] S.K. Khetan, T.J. Collins, Human pharmaceuticals in the aquatic environment: A challenge to green chemistry, *Chem. Rev.* 107 (2007) 2319–2364.
- [43] S. Marchese, D. Perret, A. Gentili, R. Curini, F. Pastori, Determination of non-steroidal anti-inflammatory drugs in surface water and wastewater by Liquid Chromatography-Tandem Mass Spectrometry, *Chromatographia*. 58 (n.d.) 263–269.
- [44] Z. Moldovan, Occurrences of pharmaceutical and personal care products as micropollutants in rivers from Romania, *Chemosphere*. 64 (2006) 1808–1817.
- [45] H. Kim, Y. Hong, J. Park, V.K. Sharma, S. Cho, Sulfonamides and tetracyclines in livestock wastewater, *Chemosphere*. 91 (2013) 888–894.
- [46] S. Bartelt-Hunt, D.D. Snow, T. Damon-Powell, D. Miesbach, Occurrence of steroid hormones and antibiotics in shallow groundwater impacted by livestock waste control facilities, *J. Contam. Hydrol.* 123 (2011) 94–103.

- [47] S. Öllers, H.P. Singer, P. Fässler, S.R. Müller, Simultaneous quantification of neutral and acidic pharmaceuticals and pesticides at the low-ng/l level in surface and waste water, *J. Chromatogr. A.* 911 (2001) 225–234.
- [48] L. Patrolecco, N. Ademollo, P. Grenni, A. Tolomei, A. Barra Caracciolo, S. Capri, Simultaneous determination of human pharmaceuticals in water samples by solid phase extraction and HPLC with UV-fluorescence detection, *Microchem. J.* 107 (2013) 165–171.
- [49] F. Benvenuto, J.M. Marín, J.V. Sancho, S. Canobbio, V. Mezzanotte, F. Hernández, Simultaneous determination of triazines and their main transformation products in surface and urban wastewater by ultra-high-pressure liquid chromatography–tandem mass spectrometry, *Anal. Bioanal. Chem.* 397 (2010) 2791–2805.
- [50] M.R. Boleda, M.T. Galceran, F. Ventura, Behavior of pharmaceuticals and drugs of abuse in a drinking water treatment plant (DWTP) using combined conventional and ultrafiltration and reverse osmosis (UF/RO) treatments, *Environ. Pollut.* 159 (2011) 1584–1591.
- [51] P. Vazquez-Roig, V. Andreu, C. Blasco, Y. Picó, Risk assessment on the presence of pharmaceuticals in sediments, soils and waters of the Pego–Oliva Marshlands (Valencia, eastern Spain), *Sci. Total Environ.* 440 (2012) 24–32.
- [52] S. Mompelat, B. Le Bot, O. Thomas, Occurrence and fate of pharmaceutical products and by-products, from resource to drinking water, *Environ. Int.* 35 (2009) 803–814.
- [53] M. Ramil, T. El Aref, G. Fink, M. Scheurer, T.A. Ternes, Fate of beta blockers in aquatic-sediment systems: Sorption and biotransformation, *Environ. Sci. Technol.* 44 (2010) 962–970.
- [54] A.C. Alder, C. Schaffner, M. Majewsky, J. Klasmeier, K. Fenner, Fate of  $\beta$ -blocker human pharmaceuticals in surface water: Comparison of measured and simulated concentrations in the Glatt Valley Watershed, Switzerland, *Water Res.* 44 (2010) 936–948.
- [55] J. Maszkowska, S. Stolte, J. Kumirska, P. Łukaszewicz, K. Mioduszevska, A. Puckowski, M. Caban, M. Wagil, P. Stepnowski, A. Białk-Bielińska, Beta-blockers in the environment: Part I. Mobility and hydrolysis study, *Sci. Total Environ.* 493 (2014) 1112–1121.

- [56] T.J. Scheytt, P. Mersmann, T. Heberer, Mobility of pharmaceuticals carbamazepine, diclofenac, ibuprofen, and propyphenazone in miscible-displacement experiments, *J. Contam. Hydrol.* 83 (2006) 53–69.
- [57] J. Ke, K.Y.H. Gin, L.H. Tan, M. Reinhard, Fate of endocrine-disrupting and pharmaceutically active substances in sand columns fed with secondary effluent, *J. Environ. Eng.* 138 (2012) 1067–1076.
- [58] C. Tixier, H.P. Singer, S. Oellers, S.R. Müller, Occurrence and fate of carbamazepine, clofibrac acid, diclofenac, ibuprofen, ketoprofen, and naproxen in Surface Waters, *Environ. Sci. Technol.* 37 (2003) 1061–1068.
- [59] A. Pruden, Balancing water sustainability and public health goals in the face of growing concerns about antibiotic resistance, *Environ. Sci. Technol.* 48 (2014) 5–14. doi:10.1021/es403883p.
- [60] K. Fent, A. Weston, D. Caminada, Ecotoxicology of human pharmaceuticals, *Aquat. Toxicol.* 76 (2006) 122–159.
- [61] K.A. Kidd, P.J. Blanchfield, K.H. Mills, V.P. Palace, R.E. Evans, J.M. Lazorchak, R.W. Flick, Collapse of a fish population after exposure to a synthetic estrogen, *Proc. Natl. Acad. Sci.* 104 (2007) 8897–8901.
- [62] S. Mompelat, O. Thomas, B. Le Bot, Contamination levels of human pharmaceutical compounds in French surface and drinking water, *J. Environ. Monit.* 13 (2011) 2929.
- [63] J. Maszkowska, S. Stolte, J. Kumirska, P. Łukaszewicz, K. Mioduszevska, A. Puckowski, M. Caban, M. Wagil, P. Stepnowski, A. Białk-Bielińska, Beta-blockers in the environment: Part II. Ecotoxicity study, *Sci. Total Environ.* 493 (2014) 1122–1126.
- [64] N. Pounds, S. Maclean, M. Webley, D. Pascoe, T. Hutchinson, Acute and chronic effects of ibuprofen in the mollusc *Planorbis carinatus* (Gastropoda: Planorbidae), *Ecotoxicol. Environ. Saf.* 70 (2008) 47–52.
- [65] S. Ghosh, T.M. LaPara, The effects of sub-therapeutic antibiotic use in farm animals on the proliferation and persistence of antibiotic resistance among soil bacteria, *ISME J.* 1 (2007) 191–203.
- [66] J. Schwaiger, H. Ferling, U. Mallow, H. Wintermayr, R.D. Negele, Toxic effects of the non-steroidal anti-inflammatory drug diclofenac, *Aquat. Toxicol.* 68 (2004) 141–150.

- [67] R. Triebkorn, H. Casper, A. Heyd, R. Eikemper, H.-R. Köhler, J. Schwaiger, Toxic effects of the non-steroidal anti-inflammatory drug diclofenac, *Aquat. Toxicol.* 68 (2004) 151–166.
- [68] D.B. Huggett, B.W. Brooks, B. Peterson, C.M. Foran, D. Schlenk, Toxicity of select beta adrenergic receptor-blocking pharmaceuticals ( $\beta$ -blockers) on aquatic organisms, *Arch. Environ. Contam. Toxicol.* 43 (2002) 229–235.
- [69] D. Huggett, I. Khan, C. Foran, D. Schlenk, Determination of beta-adrenergic receptor blocking pharmaceuticals in United States wastewater effluent, *Environ. Pollut.* 121 (2003) 199–205.
- [70] M. Cleuvers, Initial risk assessment for three  $\beta$ -blockers found in the aquatic environment, *Chemosphere.* 59 (2005) 199–205.
- [71] H.A. Boyter, *Environmental legislations USA, Environmental aspects of textile dyeing.* Woodhead, Cambridge, England (2007).
- [72] R. Kant, Textile dyeing industry an environmental hazard, *Natural Sci.* 4 (2012) 22–26.
- [73] K. Singh, S. Arora, Removal of synthetic textile dyes from wastewater: A critical review on present treatment technologies, *Crit Rev Environ Sci Technol* 41 (2011) 807–878.
- [74] Y. Anjaneyulu, N.S. Chary, D.S.S. Raj (2005) Decolorization of industrial effluents available methods and emerging technologies, *Rev. Environ. Sci. Biotechnol.* 4 (2005) 245–273.
- [75] S. Arora, Textile Dyes: It's Impact on Environment and its Treatment, *J. Bioremed. Biodeg.* 5 (2014) e146.
- [76] K.T. Chung, The significance of azo-reduction in the mutagenesis and carcinogenesis of azo dyes, *Mutat. Res.* 114 (1983) 269–281.
- [77] L.C. Apostol, L. Pereira, R. Pereira, M. Gavrilescu, M.M. Alves, Biological decolorization of Xanthene dyes by anaerobic granular biomass. *Biodegradation* 23 (2012) 725–37
- [78] A. Puntener, C. Page, European Ban on Certain Azo Dyes, *Quality and Environment, TFL* (2004)
- [79] M. Panizza, G. Cerisola, Application of diamond electrodes to electrochemical processes, *Electrochimica Acta.* 51 (2005) 191–199.

- [80] P. Canizares, J. Lobato, R. Paz, M. Rodrigo, C. Saez, Electrochemical oxidation of phenolic wastes with boron-doped diamond anodes, *Water Res.* 39 (2005) 2687–2703.
- [81] S. Vasudevan, M.A. Oturan, Electrochemistry: as cause and cure in water pollution—an overview, *Environ. Chem. Lett.* 12 (2014) 97–108.
- [82] M.A. Rodrigo, N. Oturan, M.A. Oturan, Electrochemically assisted remediation of pesticides in soils and water: A review, *Chem. Rev.* 114 (2014) 8720–8745.
- [83] C. Comninellis, Electrocatalysis in the electrochemical conversion/combustion of organic pollutants for waste water treatment, *Electrochimica Acta.* 39 (1994) 1857–1862.
- [84] B. Marselli, J. Garcia-Gomez, P.-A. Michaud, M.A. Rodrigo, C. Comninellis, Electrogeneration of hydroxyl radicals on boron-doped diamond electrodes, *J. Electrochem. Soc.* 150 (2003) D79.
- [85] C.A. Martínez-Huitle, S. Ferro, Electrochemical oxidation of organic pollutants for the wastewater treatment: direct and indirect processes, *Chem. Soc. Rev.* 35 (2006) 1324.
- [86] B. Boye, E. Brillas, B. Marselli, P.-A. Michaud, C. Comninellis, G. Farnia, G. Sandonà, Electrochemical incineration of chloromethylphenoxy herbicides in acid medium by anodic oxidation with boron-doped diamond electrode, *Electrochimica Acta.* 51 (2006) 2872–2880.
- [87] A.Y. Bagastyo, D.J. Batstone, I. Kristiana, W. Gernjak, C. Joll, J. Radjenovic, Electrochemical oxidation of reverse osmosis concentrate on boron-doped diamond anodes at circumneutral and acidic pH, *Water Res.* 46 (2012) 6104–6112.
- [88] M. Panizza, Electrochemical treatment of wastewater containing polyaromatic organic pollutants, *Water Res.* 34 (2000) 2601–2605.
- [89] M. Panizza, G. Cerisola, Influence of anode material on the electrochemical oxidation of 2-naphthol, *Electrochimica Acta.* 49 (2004) 3221–3226.
- [90] M. Zhou, L. Liu, Y. Jiao, Q. Wang, Q. Tan, Treatment of high-salinity reverse osmosis concentrate by electrochemical oxidation on BDD and DSA electrodes, *Desalination.* 277 (2011) 201–206.
- [91] G. Pérez, A.R. Fernández-Alba, A.M. Urtiaga, I. Ortiz, Electro-oxidation of reverse osmosis concentrates generated in tertiary water treatment, *Water Res.* 44 (2010) 2763–2772.

- [92] A. Özcan, Y. Şahin, A.S. Koparal, M.A. Oturan, A comparative study on the efficiency of electro-Fenton process in the removal of protham from water, *Appl. Catal. B Environ.* 89 (2009) 620–626.
- [93] N. Oturan, M.A. Oturan, Degradation of three pesticides used in viticulture by electrogenerated Fenton's reagent, *Agron. Sustain. Dev.* 25 (2005) 267–270.
- [94] I. Sirés, J.A. Garrido, R.M. Rodríguez, E. Brillas, N. Oturan, M.A. Oturan, Catalytic behavior of the  $\text{Fe}^{3+}/\text{Fe}^{2+}$  system in the electro-Fenton degradation of the antimicrobial chlorophene, *Appl. Catal. B Environ.* 72 (2007) 382–394.
- [95] M.A. Oturan, Electrochemical advanced oxidation technologies for removal of organic pollutants from water, *Environ. Sci. Pollut. Res.* 21 (2014) 8333–8335.
- [96] M.A. Oturan, M.C. Edelahe, N. Oturan, K. El kacemi, J.-J. Aaron, Kinetics of oxidative degradation/mineralization pathways of the phenylurea herbicides diuron, monuron and fenuron in water during application of the electro-Fenton process, *Appl. Catal. B Environ.* 97 (2010) 82–89.
- [97] Z. Qiang, J.-H. Chang, C.-P. Huang, Electrochemical regeneration of  $\text{Fe}^{2+}$  in Fenton oxidation processes, *Water Res.* 37 (2003) 1308–1319.
- [98] N. Oturan, M. Zhou, M.A. Oturan, Metomyl Degradation by electro-Fenton and electro-Fenton-like processes: A kinetics study of the effect of the nature and concentration of some transition metal ions as catalyst, *J. Phys. Chem. A.* 114 (2010) 10605–10611.
- [99] M. Pimentel, N. Oturan, M. Dezotti, M.A. Oturan, Phenol degradation by advanced electrochemical oxidation process electro-Fenton using a carbon felt cathode, *Appl. Catal. B Environ.* 83 (2008) 140–149.
- [100] R. Salazar, E. Brillas, I. Sirés, Finding the best  $\text{Fe}^{2+}/\text{Cu}^{2+}$  combination for the solar photoelectro-Fenton treatment of simulated wastewater containing the industrial textile dye Disperse Blue 3, *Appl. Catal. B Environ.* 115-116 (2012) 107–116.
- [101] E. Brillas, M.A. Baños, S. Camps, C. Arias, P.-L. Cabot, J.A. Garrido, R.M. Rodríguez, Catalytic effect of  $\text{Fe}^{2+}$ ,  $\text{Cu}^{2+}$  and UVA light on the electrochemical degradation of nitrobenzene using an oxygen-diffusion cathode, *New J Chem.* 28 (2004) 314–322.
- [102] C. Flox, S. Ammar, C. Arias, E. Brillas, A.V. Vargas-Zavala, R. Abdelhedi, Electro-Fenton and photoelectro-Fenton degradation of indigo carmine in acidic aqueous medium, *Appl. Catal. B Environ.* 67 (2006) 93–104.

- [103] B.P. Chaplin, Critical review of electrochemical advanced oxidation processes for water treatment applications, *Environ. Sci. Process. Impacts*. 16 (2014) 1182.
- [104] A.M. Polcaro, S. Palmas, Electrochemical oxidation of chlorophenols, *Ind. Eng. Chem. Res.* 36 (1997) 1791–1798.
- [105] P. Canizares, J.A. Dominguez, M.A. Rodrigo, J. Villasenor, J. Rodriguez, Effect of the current intensity in the electrochemical oxidation of aqueous phenol wastes at an activated carbon and steel anode, *Ind. Eng. Chem. Res.* 38 (1999) 3779–3785.
- [106] A.M. Polcaro, S. Palmas, F. Renoldi, M. Mascia, Three-dimensional electrodes for the electrochemical combustion of organic pollutants, *Electrochim. Acta*. 46 (2000) 389–394.
- [107] J. Yang, J.P. Jia, J. Liao, Y.L. Wang, Removal of fulvic acid from water electrochemically using active carbon fiber electrode, *Water Res.* 38 (2004) 4353–4360.
- [108] Z.M. Shen, W.H. Wang, J.P. Jia, J.C. Ye, X. Feng, A. Peng, Degradation of dye solution by an activated carbon fiber electrode electrolysis system, *J. Hazard. Mater.* 84 (2001) 107–116.
- [109] F. Yi, S. Chen, C. Yuan, Effect of activated carbon fiber anode structure and electrolysis conditions on electrochemical degradation of dye wastewater, *J. Hazard. Mater.* 157 (2008) 79–87.
- [110] M. Gattrell, D. Kirk, The electrochemical oxidation of aqueous phenol at a glassy-carbon electrode, *Can. J. Chem. Eng.* 68 (1990) 997–1003.
- [111] Y.M. Awad, N.S. Abuzaid, Electrochemical oxidation of phenol using graphite anodes, *Sep. Sci. Technol.* 34 (1999) 699–708.
- [112] Y.M. Awad, N.S. Abuzaid, The influence of residence time on the anodic oxidation of phenol, *Sep. Purif. Technol.* 18 (2000) 227–236.
- [113] L. Fan, F.L. Yang, W.S. Yang, Performance of the decolorization of an azo dye with bipolar packed bed cell, *Sep. Purif. Technol.* 34 (2004) 89–96.
- [114] M.A. Oturan, Electrochemical advanced oxidation technologies for removal of organic pollutants from water, *Environ. Sci. Pollut. Res.* 21 (2014) 8333–8335.
- [115] J. Radjenovic, B.I. Escher, K. Rabaey, Electrochemical degradation of the  $\beta$ -blocker metoprolol by  $\text{Ti/Ru}_{0.7}\text{Ir}_{0.3}\text{O}_2$  and  $\text{Ti/SnO}_2\text{-Sb}$  electrodes, *Water Res.* 45 (2011) 3205–3214.

- [116] A.Y. Bagastyo, J. Radjenovic, Y. Mu, R.A. Rozendal, D.J. Batstone, K. Rabaey, Electrochemical oxidation of reverse osmosis concentrate on mixed metal oxide (MMO) titanium coated electrodes, *Water Res.* 45 (2011) 4951–4959.
- [117] Y.J. Feng, X.Y. Li, Electro-catalytic oxidation of phenol on several metal-oxide electrodes in aqueous solution, *Water Res.* 37 (2003) 2399–2407.
- [118] X.Y. Li, Y.H. Cui, Y.J. Feng, Z.M. Xie, J.D. Gu, Reaction pathways and mechanisms of the electrochemical degradation of phenol on different electrodes, *Water Res.* 39 (2005) 1972–1981. doi:10.1016/j.watres.2005.02.021.
- [119] A. Polcaro, S. Palmas, F. Renoldi, M. Mascia, Three-dimensional electrodes for the electrochemical combustion of organic pollutants, *Electrochimica Acta.* 46 (2000) 389–394.
- [120] R.D. Coteiro, A.R. De Andrade, Electrochemical oxidation of 4-chlorophenol and its by-products using  $\text{Ti/Ru}_{0.3}\text{M}_{0.7}\text{O}_2$  ( $\text{M} = \text{Ti}$  or  $\text{Sn}$ ) anodes: preparation route versus degradation efficiency, *J. Appl. Electrochem.* 37 (2007) 691–698.
- [121] M.O. Azzam, M. Al-Tarazi, Y. Tahboub, Anodic destruction of 4-chlorophenol solution, *J. Hazard. Mater.* 75 (2000) 99–113.
- [122] D.C. de Moura, C.K.C. de Araújo, C.L.P.S. Zanta, R. Salazar, C.A. Martínez-Huitle, Active chlorine species electrogenerated on  $\text{Ti/Ru}_{0.3}\text{Ti}_{0.7}\text{O}_2$  surface: Electrochemical behavior, concentration determination and their application, *J. Electroanal. Chem.* 731 (2014) 145–152.
- [123] C.A. Martínez-Huitle, M.A. Quiroz, C. Comninellis, S. Ferro, A. De Battisti, Electrochemical incineration of chloranilic acid using  $\text{Ti/IrO}_2$ ,  $\text{Pb/PbO}_2$  and  $\text{Si/BDD}$  electrodes, *Electrochim. Acta.* 50 (2004) 949–956.
- [124] C. Pulgarin, N. Adler, P. Peringer, C. Comninellis, Electrochemical Detoxification of a 1,4-Benzoquinone Solution in Waste-Water Treatment, *Water Res.* 28 (1994) 887–893. doi:10.1016/0043-1354(94)90095-7.
- [125] D. Bejan, J.D. Malcolm, L. Morrison, N.J. Bunce, Mechanistic investigation of the conductive ceramic Ebonex® as an anode material, *Electrochimica Acta.* 54 (2009) 5548–5556.
- [126] A.J.C. da Silva, E.V. dos Santos, C.C. de Oliveira Morais, C.A. Martínez-Huitle, S.S.L. Castro, Electrochemical treatment of fresh, brine and saline produced water generated by



- petrochemical industry using Ti/IrO<sub>2</sub>-Ta<sub>2</sub>O<sub>5</sub> and BDD in flow reactor, *Chem. Eng. J.* 233 (2013) 47–55.
- [127] M.G. Tavares, L.V.A. da Silva, A.M. Sales Solano, J. Tonholo, C.A. Martínez-Huitle, C.L.P.S. Zanta, Electrochemical oxidation of Methyl Red using Ti/Ru<sub>0.3</sub>Ti<sub>0.7</sub>O<sub>2</sub> and Ti/Pt anodes, *Chem. Eng. J.* 204-206 (2012) 141–150.
- [128] P. Cañizares, M. Díaz, J.A. Domínguez, J. Lobato, M.A. Rodrigo, Electrochemical treatment of diluted cyanide aqueous wastes: Electrochemical treatment of diluted cyanide aqueous wastes, *J. Chem. Technol. Biotechnol.* 80 (2005) 565–573.
- [129] J. Wu, H. Zhang, N. Oturan, Y. Wang, L. Chen, M.A. Oturan, Application of response surface methodology to the removal of the antibiotic tetracycline by electrochemical process using carbon-felt cathode and DSA (Ti/RuO<sub>2</sub>-IrO<sub>2</sub>) anode, *Chemosphere.* 87 (2012) 614–620.
- [130] N. Oturan, J. Wu, H. Zhang, V.K. Sharma, M.A. Oturan, Electrocatalytic destruction of the antibiotic tetracycline in aqueous medium by electrochemical advanced oxidation processes: Effect of electrode materials, *Appl. Catal. B Environ.* 140-141 (2013) 92–97.
- [131] H. Olvera-Vargas, N. Oturan, E. Brillas, D. Buisson, G. Esposito, M.A. Oturan, Electrochemical advanced oxidation for cold incineration of the pharmaceutical ranitidine: Mineralization pathway and toxicity evolution, *Chemosphere.* 117 (2014) 644–651.
- [132] M. Gattrell, D. Kirk, A study of the oxidation of phenol at platinum and preoxidized platinum surfaces, *J. Electrochem. Soc.* 140 (1993) 1534–1540.
- [133] J.D. Rodgers, W. Jedral, N.I. Bunce, Electrochemical oxidation of chlorinated phenols, *Environ. Sci. Technol.* 33 (1999) 1453–1457.
- [134] S.K. Johnson, L.L. Houk, J.R. Feng, R.S. Houk, D.C. Johnson, Electrochemical incineration of 4-chlorophenol and the identification of products and intermediates by mass spectrometry, *Environ. Sci. Technol.* 33 (1999) 2638–2644.
- [135] M. Panizza, G. Cerisola, Electrocatalytic materials for the electrochemical oxidation of synthetic dyes, *Appl. Catal. B Environ.* 75 (2007) 95–101.
- [136] M. Hamza, R. Abdelhedi, E. Brillas, I. Sirés, Comparative electrochemical degradation of the triphenylmethane dye Methyl Violet with boron-doped diamond and Pt anodes, *J. Electroanal. Chem.* 627 (2009) 41–50.

- [137] C.K.C. Araújo, G.R. Oliveira, N.S. Fernandes, C.L.P.S. Zanta, S.S.L. Castro, D.R. da Silva, C.A. Martínez-Huitle, Electrochemical removal of synthetic textile dyes from aqueous solutions using Ti/Pt anode: role of dye structure, *Environ. Sci. Pollut. Res.* 21 (2014) 9777–9784.
- [138] E. Brillas, M.Á. Baños, J.A. Garrido, Mineralization of herbicide 3,6-dichloro-2-methoxybenzoic acid in aqueous medium by anodic oxidation, electro-Fenton and photoelectro-Fenton, *Electrochimica Acta.* 48 (2003) 1697–1705.
- [139] E.V. dos Santos, S.F.M. Sena, D.R. da Silva, S. Ferro, A. De Battisti, C.A. Martínez-Huitle, Scale-up of electrochemical oxidation system for treatment of produced water generated by Brazilian petrochemical industry, *Environ. Sci. Pollut. Res.* 21 (2014) 8466–8475.
- [140] E. Guinea, J.A. Garrido, R.M. Rodríguez, P.-L. Cabot, C. Arias, F. Centellas, E. Brillas, Degradation of the fluoroquinolone enrofloxacin by electrochemical advanced oxidation processes based on hydrogen peroxide electrogeneration, *Electrochimica Acta.* 55 (2010) 2101–2115.
- [141] E. Brillas, S. Garcia-Segura, M. Skoumal, C. Arias, Electrochemical incineration of diclofenac in neutral aqueous medium by anodic oxidation using Pt and boron-doped diamond anodes, *Chemosphere.* 79 (2010) 605–612.
- [142] E.B. Cavalcanti, S.G. -Segura, F. Centellas, E. Brillas, Electrochemical incineration of omeprazole in neutral aqueous medium using a platinum or boron-doped diamond anode: Degradation kinetics and oxidation products, *Water Res.* 47 (2013) 1803–1815.
- [143] S.L. Ambuludi, M. Panizza, N. Oturan, A. Özcan, M.A. Oturan, Kinetic behavior of anti-inflammatory drug ibuprofen in aqueous medium during its degradation by electrochemical advanced oxidation, *Environ. Sci. Pollut. Res.* 20 (2012) 2381–2389.
- [144] L. Feng, E.D. van Hullebusch, M.A. Rodrigo, G. Esposito, M.A. Oturan, Removal of residual anti-inflammatory and analgesic pharmaceuticals from aqueous systems by electrochemical advanced oxidation processes. A review, *Chem. Eng. J.* 228 (2013) 944–964.
- [145] O. Ganzenko, D. Huguenot, E.D. van Hullebusch, G. Esposito, M.A. Oturan, Electrochemical advanced oxidation and biological processes for wastewater treatment: A review of the combined approaches, *Environ. Sci. Pollut. Res.* 21 (2014) 8493–8524.

- [146] E. Guivarch, S. Trevin, C. Lahitte, M.A. Oturan, Degradation of azo dyes in water by Electro-Fenton process, *Environ. Chem. Lett.* 1 (2003) 38–44.
- [147] S. Hammami, N. Oturan, N. Bellakhal, M. Dachraoui, M.A. Oturan, Oxidative degradation of direct orange 61 by electro-Fenton process using a carbon felt electrode: Application of the experimental design methodology, *J. Electroanal. Chem.* 610 (2007) 75–84. d
- [148] M. Diagne, N. Oturan, M.A. Oturan, Removal of methyl parathion from water by electrochemically generated Fenton's reagent, *Chemosphere.* 66 (2007) 841–848.
- [149] C. Comninellis, C. Pulgarin, Electrochemical Oxidation of Phenol for Waste-Water Treatment Using SnO<sub>2</sub> Anodes, *J. Appl. Electrochem.* 23 (1993) 108–112.
- [150] S. Stucki, R. Kotz, B. Carcer, W. Suter, Electrochemical waste-water treatment using high overvoltage anodes 2: Anode performance and applications, *J. Appl. Electrochem.* 21 (1991) 99–104.
- [151] B. Wang, W. Kong, H. Ma, Electrochemical treatment of paper mill wastewater using three-dimensional electrodes with Ti/Co/SnO<sub>2</sub>-Sb<sub>2</sub>O<sub>5</sub> anode, *J. Hazard. Mater.* 146 (2007) 295–301. doi:10.1016/j.jhazmat.2006.12.031.
- [152] X.M. Chen, F.R. Gao, G.H. Chen, Comparison of Ti/BDD and Ti/SnO<sub>2</sub>-Sb<sub>2</sub>O<sub>5</sub> electrodes for pollutant oxidation, *J. Appl. Electrochem.* 35 (2005) 185–191.
- [153] P. Lipp, F. Sacher, G. Baldauf, Removal of organic micro-pollutants during drinking water treatment by nanofiltration and reverse osmosis, *Desalination Water Treat.* 13 (2010) 226–237.
- [154] B. Correa-Lozano, C. Comninellis, A. De Battisti, Service life of Ti/SnO<sub>2</sub>-Sb<sub>2</sub>O<sub>5</sub> anodes, *J. Appl. Electrochem.* 27 (1997) 970–974.
- [155] Y. Samet, S.C. Elaoud, S. Ammar, R. Abdelhedi, Electrochemical degradation of 4-chloroguaiacol for wastewater treatment using PbO<sub>2</sub> anodes, *J. Hazard. Mater.* 138 (2006) 614–619.
- [156] R. Kotz, S. Stucki, B. Carcer, Electrochemical waste-water treatment using high overvoltage anodes 1: Physical and electrochemical properties of SnO<sub>2</sub> anodes, *J. Appl. Electrochem.* 21 (1991) 14–20.

- [157] F. Montilla, E. Morallon, J.L. Vazquez, Evaluation of the electrocatalytic activity of antimony-doped tin dioxide anodes toward the oxidation of phenol in aqueous solutions, *J. Electrochem. Soc.* 152 (2005) B421–B427.
- [158] F. Montilla, E. Morallon, A. De Battisti, J.L. Vazquez, Preparation and characterization of antimony-doped tin dioxide electrodes. Part 1. Electrochemical characterization, *J. Phys. Chem. B.* 108 (2004) 5036–5043.
- [159] C. Zanta, P.A. Michaud, C. Comninellis, A.R. De Andrade, J.F.C. Boodts, Electrochemical oxidation of p-chlorophenol on SnO<sub>2</sub>-Sb<sub>2</sub>O<sub>5</sub> based anodes for wastewater treatment, *J. Appl. Electrochem.* 33 (2003) 1211–1215.
- [160] C. Comninellis, A. DeBattisti, Electrocatalysis in anodic oxidation of organics with simultaneous oxygen evolution, *J. Chim. Phys. Phys.-Chim. Biol.* 93 (1996) 673–679.
- [161] L. Ciríaco, D. Santos, M.J. Pacheco, A. Lopes, Anodic oxidation of organic pollutants on a Ti/SnO<sub>2</sub>-Sb<sub>2</sub>O<sub>4</sub> anode, *J. Appl. Electrochem.* 41 (2011) 577–587.
- [162] D. Santos, M.J. Pacheco, A. Gomes, A. Lopes, L. Ciríaco, Preparation of Ti/Pt/SnO<sub>2</sub>-Sb<sub>2</sub>O<sub>4</sub> electrodes for anodic oxidation of pharmaceutical drugs, *J. Appl. Electrochem.* 43 (2013) 407–416.
- [163] C.A. Martínez-Huitle, A. De Battisti, S. Ferro, S. Reyna, M. Cerro-López, M.A. Quiro, Removal of the pesticide methamidophos from aqueous solutions by electrooxidation using Pb/PbO<sub>2</sub>, Ti/SnO<sub>2</sub>, and Si/BDD electrodes, *Environ. Sci. Technol.* 42 (2008) 6929–6935.
- [164] M. Panizza, C.A. Martinez-Huitle, Role of electrode materials for the anodic oxidation of a real landfill leachate – Comparison between Ti–Ru–Sn ternary oxide, PbO<sub>2</sub> and boron-doped diamond anode, *Chemosphere.* 90 (2013) 1455–1460.
- [165] N.B. Tahar, A. Savall, A comparison of different lead dioxide coated electrodes for the electrochemical destruction of phenol, *J. New Mater. Electrochem. Syst.* 2 (1999) 19–26.
- [166] M. Panizza, G. Cerisola, Electrochemical degradation of methyl red using BDD and PbO<sub>2</sub> anodes, *Ind. Eng. Chem. Res.* 47 (2008) 6816–6820.
- [167] F. Bonfatti, S. Ferro, F. Lavezzo, M. Malacarne, G. Lodi, A. De Battisti, Electrochemical incineration of glucose as a model organic substrate I. Role of the electrode material, *J. Electrochem. Soc.* 146 (1999) 2175–2179.

- [168] Y. Song, G. Wei, R. Xiong, Structure and properties of  $\text{PbO}_2\text{-CeO}_2$  anodes on stainless steel, *Electrochim. Acta.* 52 (2007) 7022–7027.
- [169] L. Gherardini, P.A. Michaud, M. Panizza, C. Comninellis, N. Vatistas, Electrochemical oxidation of 4-chlorophenol for wastewater treatment - Definition of normalized current efficiency ( $\phi$ ), *J. Electrochem. Soc.* 148 (2001) D78–D82.
- [170] M. Panizza, G. Cerisola, Electrocatalytic materials for the electrochemical oxidation of synthetic dyes, *Appl. Catal. B-Environ.* 75 (2007) 95–101.
- [171] L.S. Andrade, L.A.M. Ruotolo, R.C. Rocha-Filho, N. Bocchi, S.R. Biaggio, J. Iniesta, V. Garcia-Garcia, V. Montiel, On the performance of Fe and Fe,F doped Ti-Pt/ $\text{PbO}_2$  electrodes in the electrooxidation of the Blue Reactive 19 dye in simulated textile wastewater, *Chemosphere.* 66 (2007) 2035–2043.
- [172] M.A. Quiroz, J.L. Sánchez-Salas, S. Reyna, E.R. Bandala, J.M. Peralta-Hernández, C.A. Martínez-Huitle, Degradation of 1-hydroxy-2,4-dinitrobenzene from aqueous solutions by electrochemical oxidation: Role of anodic material, *J. Hazard. Mater.* 268 (2014) 6–13.
- [173] M.A. Quiroz, S. Reyna, C.A. Martínez-Huitle, S. Ferro, A. De Battisti, Electrocatalytic oxidation of p-nitrophenol from aqueous solutions at Pb/ $\text{PbO}_2$  anodes, *Appl. Catal. B Environ.* 59 (2005) 259–266.
- [174] L. Vazquez-Gomez, A. de Battisti, S. Ferro, M. Cerro, S. Reyna, C.A. Martínez-Huitle, M.A. Quiroz, Anodic oxidation as green alternative for removing diethyl phthalate from wastewater using Pb/ $\text{PbO}_2$  and Ti/ $\text{SnO}_2$  Anodes, *CLEAN - Soil Air Water.* 40 (2012) 408–415.
- [175] H. Lin, J. Niu, J. Xu, Y. Li, Y. Pan, Electrochemical mineralization of sulfamethoxazole by Ti/ $\text{SnO}_2\text{-Sb/Ce-PbO}_2$  anode: Kinetics, reaction pathways, and energy cost evolution, *Electrochimica Acta.* 97 (2013) 167–174.
- [176] A. Kraft, Doped diamond: A compact review on a new, versatile electrode material, *Int. J. Electrochem. Sci.* 2 (2007) 355–385.
- [177] W. Haenni, P. Rychen, M. Fryda, C. Comninellis, Industrial applications of diamond electrodes, *Thin-Film Diam. II.* 77 (2004) 149–196.
- [178] J.S. Xu, M.C. Granger, Q.Y. Chen, J.W. Strojek, T.E. Lister, G.M. Swain, Boron-doped diamond thin-film electrodes, *Anal. Chem.* 69 (1997) A591–A597.

- [179] H.B. Martin, A. Argoitia, U. Landau, A.B. Anderson, J.C. Angus, Hydrogen and oxygen evolution on boron-doped diamond electrodes, *J. Electrochem. Soc.* 143 (1996) L133–L136.
- [180] R. Ramesham, M.F. Rose, Electrochemical characterization of doped and undoped CVD diamond deposited by microwave plasma, *Diam. Relat. Mater.* 6 (1997) 17–27.
- [181] G. Swain, R. Ramesham, The electrochemical activity of boron-doped polycrystalline diamond thin-film electrodes, *Anal. Chem.* 65 (1993) 345–351.
- [182] B.P. Chaplin, I. Wyle, H. Zeng, J.A. Carlisle, J. Farrell, Characterization of the performance and failure mechanisms of boron-doped ultrananocrystalline diamond electrodes, *J. Appl. Electrochem.* 41 (2011) 1329–1340.
- [183] B.P. Chaplin, D.K. Hubler, J. Farrell, Understanding anodic wear at boron doped diamond film electrodes, *Electrochimica Acta.* 89 (2013) 122–131.
- [184] B. Marselli, J. Garcia-Gomez, P.A. Michaud, M.A. Rodrigo, C. Comninellis, Electrogeneration of hydroxyl radicals on boron-doped diamond electrodes, *J. Electrochem. Soc.* 150 (2003) D79–D83.
- [185] R.J. Pollock, J.F. Houlihan, A.N. Bain, B.S. Coryea, Electrochemical properties of a new electrode material, Ti<sub>4</sub>O<sub>7</sub>, *Mater. Res. Bull.* 19 (1984) 17–24.
- [186] G. Chen, E.A. Betterton, R.G. Arnold, Electrolytic oxidation of trichloroethylene using a ceramic anode, *J. Appl. Electrochem.* 29 (1999) 961–970.
- [187] K. Kolbrecka, J. Przulski, Sub-stoichiometric titanium oxides as ceramic electrodes for oxygen evolution—structural aspects of the voltammetric behaviour of Ti<sub>n</sub>O<sub>2n-1</sub>, *Electrochimica Acta.* 39 (1994) 1591–1595.
- [188] J.R. Smith, F.C. Walsh, R.L. Clarke, Electrodes based on Magnéli phase titanium oxides: the properties and applications of Ebonex<sup>(R)</sup> materials. *J. Appl. Electrochem.* 28, 1021–1033, *J. Appl. Electrochem.* 28 (1998) 1021–1033.
- [189] F.C. Walsh, R.G.A. Wills, The continuing development of Magnéli phase titanium sub-oxides and Ebonex® electrodes, *Electrochimica Acta.* 55 (2010) 6342–6351.
- [190] J.E. Graves, D. Pletcher, R.L. Clarke, F.C. Walsh, The electrochemistry of Magnéli phase titanium oxide ceramic electrodes Part I. The deposition and properties of metal coatings, *J. Appl. Electrochem.* 21 (1991) 848–857.

- [191] S. Andersson, B. Collén, U. Kuylenstierna, A. Magnéli, A. Magnéli, H. Pestmalis, S. Åsbrink, Phase analysis studies on the titanium-oxygen system., *Acta Chem. Scand.* 11 (1957) 1641–1652.
- [192] A.A. Gusev, E.G. Avvakumov, A.Z. Medvedev, A.I. Masliy, Ceramic electrodes based on Magnéli phases of titanium oxides, *Sci. Sinter.* 39 (2007) 51–57.
- [193] Y. Le Page, P. Strobel, Structural chemistry of magnéli phases  $Ti_nO_{2n-1}$  ( $4 \leq n \leq 9$ ). I. Cell and structure comparisons, *J. Solid State Chem.* 43 (1982) 314–319.
- [194] J.E. Graves, D. Pletcher, R.L. Clarke, F.C. Walsh, The electrochemistry of Magnéli phase titanium oxide ceramic electrodes Part II: Ozone generation at Ebonex and Ebonex/lead dioxide anodes, *J. Appl. Electrochem.* 22 (1992) 200–203.
- [195] G. Chen, C.C. Waraksa, H. Cho, D.D. Macdonald, T.E. Mallouka, EIS Studies of porous oxygen electrodes with discrete particles, *J. Electrochem. Soc.* 150 (2003) E423.
- [196] K. Scott, H. Cheng, The anodic behaviour of Ebonex® in oxalic acid solutions, *J. Appl. Electrochem.* 32 (2002) 583–589.
- [197] D. Bejan, E. Guinea, N.J. Bunce, On the nature of the hydroxyl radicals produced at boron-doped diamond and Ebonex® anodes, *Electrochimica Acta.* 69 (2012) 275–281.
- [198] C.L.K. Tennakoon, R.C. Bhardwaji, J.O. Bockris, Electrochemical treatment of human wastes in a packed bed reactor, *J. Appl. Electrochem.* 26 (1996) 18–29.
- [199] A.M. Zaky, B.P. Chaplin, Mechanism of p-substituted phenol oxidation at a  $Ti_4O_7$  reactive electrochemical membrane, *Environ. Sci. Technol.* 48 (2014) 5857–5867.
- [200] A.M. Zaky, B.P. Chaplin, Porous substoichiometric  $TiO_2$  anodes as reactive electrochemical membranes for water treatment, *Environ. Sci. Technol.* 47 (2013) 6554–6563.
- [201] P. Geng, J. Su, C. Miles, C. Comninellis, G. Chen, Highly-ordered Magnéli  $Ti_4O_7$  nanotube arrays as effective anodic material for electro-oxidation, *Electrochimica Acta.* 153 (2015) 316–324.
- [202] G. Chen, S.R. Bare, T.E. Mallouk, Development of supported bi-functional electrocatalysts for unitized regenerative Fuel Cells, *J. Electrochem. Soc.* 149 (2002) A1092.
- [203] K. Ellis, A. Hill, J. Hill, A. Loyns, T. Partington, The performance of Ebonex® electrodes in bipolar lead-acid batteries, *J. Power Sources.* 136 (2004) 366–371.

- [204] M. Fehse, S. Cavaliere, P.E. Lippens, I. Savych, A. Iadecola, L. Monconduit, D.J. Jones, J. Rozière, F. Fischer, C. Tessier, L. Stievano, Nb-doped TiO<sub>2</sub> nanofibers for lithium ion batteries, *J. Phys. Chem. C*. 117 (2013) 13827–13835.
- [205] D. Morris, Y. Dou, J. Rebane, C.E.J. Mitchell, R.G. Egdell, D.S.L. Law, A. Vittadini, M. Casarin, Photoemission and STM study of the electronic structure of Nb-doped TiO<sub>2</sub>, *Phys. Rev. B*. 61 (2000) 13445–13457.
- [206] R.D. Shannon, Revised effective ionic radii and systematic studies of interatomic distances in halides and chalcogenides, *Acta Crystallogr. Sect. 32* (1976) 751–767. doi:10.1107/S0567739476001551.
- [207] S.G. Kim, M.J. Ju, I.T. Choi, W.S. Choi, H.-J. Choi, J.-B. Baek, H.K. Kim, Nb-doped TiO<sub>2</sub> nanoparticles for organic dye-sensitized solar cells, *RSC Adv.* 3 (2013) 16380.
- [208] M. Yang, D. Kim, H. Jha, K. Lee, J. Paul, P. Schmuki, Nb doping of TiO<sub>2</sub> nanotubes for an enhanced efficiency of dye-sensitized solar cells, *Chem Commun.* 47 (2011) 2032–2034.
- [209] A.M. Ruiz, A. Cornet, K. Shimano, J.R. Morante, N. Yamazoe, Effects of various metal additives on the gas sensing performances of TiO<sub>2</sub> nanocrystals obtained from hydrothermal treatments, *Sensors Actuators B Chem.* 108 (2005) 34–40.
- [210] J. Li, Z. Ai, L. Zhang, Design of a neutral electro-Fenton system with Fe@Fe<sub>2</sub>O<sub>3</sub>/ACF composite cathode for wastewater treatment, *J. Hazard. Mater.* 164 (2009) 18–25.
- [211] H.-H. Huang, M.-C. Lu, J.-N. Chen, Catalytic decomposition of hydrogen peroxide and 2-chlorophenol with iron oxides, *Water Res.* 35 (2001) 2291–2299.
- [212] S. Navalon, M. Alvaro, H. Garcia, Heterogeneous Fenton catalysts based on clays, silicas and zeolites, *Appl. Catal. B Environ.* 99 (2010) 1–26.
- [213] Q. Wang, S. Tian, J. Long, P. Ning, Use of Fe(II)Fe(III)-LDHs prepared by coprecipitation method in a heterogeneous-Fenton process for degradation of Methylene Blue, *Catal. Today.* 224 (2014) 41–48.
- [214] Y. Wang, G. Zhao, S. Chai, H. Zhao, Y. Wang, Three-dimensional homogeneous ferrite-carbon aerogel: One pot fabrication and enhanced electro-Fenton reactivity, *ACS Appl. Mater. Interfaces.* 5 (2013) 842–852.



- [215] C.M. Sánchez-Sánchez, E. Expósito, J. Casado, V. Montiel, Goethite as a more effective iron dosage source for mineralization of organic pollutants by electro-Fenton process, *Electrochem. Commun.* 9 (2007) 19–24.
- [216] E. Expósito, C.M. Sánchez-Sánchez, V. Montiel, Mineral iron oxides as iron source in electro-Fenton and photoelectro-Fenton mineralization processes, *J. Electrochem. Soc.* 154 (2007) E116.
- [217] J. Ramírez, L.A. Godínez, M. Méndez, Y. Meas, F.J. Rodríguez, Heterogeneous photoelectro-Fenton process using different iron supporting materials, *J. Appl. Electrochem.* 40 (2010) 1729–1736.
- [218] O. Iglesias, M.A. Fernández de Dios, M. Pazos, M.A. Sanromán, Using iron-loaded sepiolite obtained by adsorption as a catalyst in the electro-Fenton oxidation of Reactive Black 5, *Environ. Sci. Pollut. Res.* 20 (2013) 5983–5993.
- [219] N. Barhoumi, N. Oturan, H. Olvera-Vargas, E. Brillas, A. Gadri, S. Ammar, M.A. Oturan, Pyrite as a sustainable catalyst in electro-Fenton process for improving oxidation of sulfamethazine. Kinetics, mechanism and toxicity assessment, *Water Res.* 94 (2016) 52–61.
- [220] N. Barhoumi, L. Labiadh, M.A. Oturan, N. Oturan, A. Gadri, S. Ammar, E. Brillas, Electrochemical mineralization of the antibiotic levofloxacin by electro-Fenton-pyrite process, *Chemosphere.* 141 (2015) 250–257.
- [221] L. Labiadh, M.A. Oturan, M. Panizza, N.B. Hamadi, S. Ammar, Complete removal of AHPS synthetic dye from water using new electro-fenton oxidation catalyzed by natural pyrite as heterogeneous catalyst, *J. Hazard. Mater.* 297 (2015) 34–41.
- [222] S. Ammar, M.A. Oturan, L. Labiadh, A. Guersalli, R. Abdelhedi, N. Oturan, E. Brillas, Degradation of tyrosol by a novel electro-Fenton process using pyrite as heterogeneous source of iron catalyst, *Water Res.* 74 (2015) 77–87. doi:10.1016/j.watres.2015.02.006.
- [223] B. Hou, H. Han, S. Jia, H. Zhuang, P. Xu, D. Wang, Heterogeneous electro-Fenton oxidation of catechol catalyzed by nano-Fe<sub>3</sub>O<sub>4</sub>: kinetics with the Fermi's equation, *J. Taiwan Inst. Chem. Eng.* 56 (2015) 138–147.
- [224] S.B. Hammouda, F. Fourcade, A. Assadi, I. Soutrel, N. adhoum, A. Amrane, L. Monser, Effective heterogeneous electro-Fenton process for the degradation of a malodorous

- compound, indole, using iron loaded alginate beads as a reusable catalyst, *Appl. Catal. B Environ.* 182 (2016) 47–58.
- [225] M.Á. Fernández de Dios, E. Rosales, M. Fernández-Fernández, M. Pazos, M.Á. Sanromán, Degradation of organic pollutants by heterogeneous electro-Fenton process using Mn-alginate composite: Mn-alginate composite as catalyst in electro-Fenton process, *J. Chem. Technol. Biotechnol.* 90 (2015) 1439–1447.
- [226] O. Iglesias, M.A.F. de Dios, T. Tavares, M.A. Sanromán, M. Pazos, Heterogeneous electro-Fenton treatment: preparation, characterization and performance in groundwater pesticide removal, *J. Ind. Eng. Chem.* 27 (2015) 276–282.
- [227] N. Qiao, H. Ma, M. Hu, Design of a neutral three-dimensional electro-Fenton system with various bentonite-based Fe particle electrodes: A comparative study, *Mater. Res. Innov.* 19 (2015) S2–137–S2–141.
- [228] W.R.P. Barros, J.R. Steter, M.R.V. Lanza, A.C. Tavares, Catalytic activity of  $\text{Fe}_{3-x}\text{Cu}_x\text{O}_4$  ( $0 \leq x \leq 0.25$ ) nanoparticles for the degradation of Amaranth food dye by heterogeneous electro-Fenton process, *Appl. Catal. B Environ.* 180 (2016) 434–441.
- [229] Q. Tang, D. Wang, D. Yao, C. Yang, Y. Sun, Heterogeneous electro-Fenton oxidation of p-nitrophenol with a reusable fluffy clump steel wire, *Desalination Water Treat.* 57 (2016) 15475–15485.
- [230] C. Zhang, M. Zhou, G. Ren, X. Yu, L. Ma, J. Yang, F. Yu, Heterogeneous electro-Fenton using modified iron–carbon as catalyst for 2,4-dichlorophenol degradation: Influence factors, mechanism and degradation pathway, *Water Res.* 70 (2015) 414–424.
- [231] O. Iglesias, M.A.F. de Dios, T. Tavares, M.A. Sanromán, M. Pazos, Heterogeneous electro-Fenton treatment: preparation, characterization and performance in groundwater pesticide removal, *J. Ind. Eng. Chem.* 27 (2015) 276–282.
- [232] E.G. Garrido-Ramírez, M.L. Mora, J.F. Marco, M.S. Ureta-Zañartu, Characterization of nanostructured allophane clays and their use as support of iron species in a heterogeneous electro-Fenton system, *Appl. Clay Sci.* 86 (2013) 153–161.
- [233] L. Bounab, O. Iglesias, E. González-Romero, M. Pazos, M. Ángeles Sanromán, Effective heterogeneous electro-Fenton process of m-cresol with iron loaded activated carbon, *RSC Adv.* 5 (2015) 31049–31056.

- [234] Y. Li, A. Lu, H. Ding, X. Wang, C. Wang, C. Zeng, Y. Yan, Microbial fuel cells using natural pyrrhotite as the cathodic heterogeneous Fenton catalyst towards the degradation of biorefractory organics in landfill leachate, *Electrochem. Commun.* 12 (2010) 944–947.
- [235] G. Zhang, Y. Zhou, F. Yang, FeOOH-catalyzed heterogeneous electro-Fenton system upon anthraquinone@graphene nanohybrid cathode in a divided electrolytic cell: Catholyte-regulated catalytic oxidation performance and mechanism, *J. Electrochem. Soc.* 162 (2015) H357–H365.
- [236] J.A. Banuelos, O. Garcia-Rodriguez, F.J. Rodriguez-Valadez, L.A. Godinez, Electrochemically prepared iron-modified activated carbon electrodes for their application in electro-Fenton and photoelectro-Fenton processes, *J. Electrochem. Soc.* 162 (2015) E154–E159.
- [237] Y. Wang, H. Zhao, G. Zhao, Highly ordered mesoporous Fe<sub>3</sub>O<sub>4</sub>@carbon embedded composite: high catalytic activity, wide pH range and stability for heterogeneous electro-Fenton, *Electroanalysis*. 28 (2016) 169–176. doi:10.1002/elan.201500488.
- [238] S.D. Sklari, K.V. Plakas, P.N. Petsi, V.T. Zaspalis, A.J. Karabelas, Toward the development of a novel electro-fenton system for eliminating toxic organic substances from water. Part 2. Preparation, characterization, and evaluation of iron-impregnated carbon felts as cathodic electrodes, *Ind. Eng. Chem. Res.* 54 (2015) 2059–2073.

# Electrooxidation using Sub-stoichiometric Titanium Oxide ( $\text{Ti}_4\text{O}_7$ ) Anode

This chapter has been published as:

Soliu O. Ganiyu, Nihal Oturan, Stéphane Raffy, Marc Cretin, Roséline Esmilaire, Eric van Hullebusch, Giovanni Esposito, Mehmet A. Oturan (2016). Sub-stoichiometric Titanium Oxide ( $\text{Ti}_4\text{O}_7$ ) as a Suitable Ceramic Anode for Electrooxidation of Organic Pollutants: A Case Study of Kinetics, Mineralization and Toxicity Assessment of Amoxicillin, *Water Research* 106, 171-181. DOI:10.1016/j.watres.2016.09.056

## **CHAPTER 3**

Substoichiometric titanium oxide ( $\text{Ti}_4\text{O}_7$ ) as anode material for electrooxidation of complex organics is required as this material represents a low cost alternative to other commercially available anode materials. Only few studies with major focus on degradation efficiency without in-depth considerations of the behavior, have investigated this anode material according to literature. Further, simple molecules have been studied without focus on emerging and complex pollutants especially pharmaceuticals.

---

**Sub-stoichiometric Titanium Oxide (Ti<sub>4</sub>O<sub>7</sub>) as a Suitable Ceramic Anode for Electrooxidation of Organic Pollutants: A Case Study of Kinetics, Mineralization and Toxicity Assessment of Amoxicillin**

**Abstract**

Electrochemical degradation of aqueous solutions containing antibiotic amoxicillin (AMX) has been extensively studied in an undivided electrolytic cell using a sub-stoichiometric titanium oxide (Ti<sub>4</sub>O<sub>7</sub>) anode, elaborated by plasma deposition. Oxidative degradation of AMX by hydroxyl radicals was assessed as a function of applied current and was found to follow pseudo-first order kinetics. The use of carbon-felt cathode enhanced oxidation capacity of the process due to the generation of H<sub>2</sub>O<sub>2</sub>. Comparative studies at low current intensity using DSA and Pt anodes led to lower mineralization efficiencies compared to Ti<sub>4</sub>O<sub>7</sub> anode: 36 and 41% TOC removal for DSA and Pt respectively compared to 69% for Ti<sub>4</sub>O<sub>7</sub> anode. Besides, the use of BDD anode under similar operating conditions allowed reaching higher mineralization (94%) efficiency. Although Ti<sub>4</sub>O<sub>7</sub> anode provides a lesser mineralization rate compared to BDD, it exhibits better performance compared to the classical anodes (Pt and DSA) and can constitute an alternative to BDD anode for a cost effective electro-oxidation process. Moreover several aromatic and aliphatic oxidation reaction intermediates and inorganic end-products were identified and a plausible mineralization pathway of AMX involving these intermediates was proposed.

**Keywords:** Electro-oxidation; Amoxicillin; Ti<sub>4</sub>O<sub>7</sub> anode; Hydroxyl radicals; Plasma deposition; Mineralization

### 3.1 Introduction

AO (or electrooxidation) is one of the most popular EAOPs that able to oxidize efficiently, organic pollutants present in aqueous solution. It is based on the generation of hydroxyl radicals at surface of a high O<sub>2</sub>-overpotential anode M via water oxidation reaction (eq. 3-1) [1–3]. The sorbed hydroxyl radicals (M(•OH)) is non-selective highly oxidizing agent and very reactive species against organic contaminants. Therefore it is able to oxidize organic pollutants until ultimate oxidation state, i.e., mineralization [4]. This process has been studied as a possible treatment technique for the remediation of wastewater with low content of various recalcitrant organic pollutants [5–8].



Based on the interaction between the anode surface and M(•OH), anode materials are classified into two: “non-active” anodes (e.g. BDD, PbO<sub>2</sub> and Ti/SnO<sub>2</sub>) where the oxygen atom of M(•OH) is not covalently bound to the surface of the anode and “active” anodes (e.g., Pt, Ti/RuO<sub>2</sub>, Ti/RuO<sub>2</sub>-IrO<sub>2</sub> and Ti/IrO<sub>2</sub>-Ta<sub>2</sub>O<sub>5</sub>) in which M(•OH) is further oxidized to form chemisorbed active oxygen with the oxygen atom covalently bound to anode surface (M=O) [9]. The former (M(•OH)) usually leads to complete mineralization (electrochemical combustion) of the substrate [10–14], whereas significant mineralization of complex substrates rarely occur with the active anodes [15–17]. BDD thin-film electrodes are the best anode material known for electrooxidation due to their high chemical stability and generation of M(•OH) in large quantities that ensures complete mineralization of organic pollutants [18–24]. However, the high cost of BDD electrode and scarcity of suitable substrate limit its large-scale application [3]. Furthermore, relatively short service life of Ti/SnO<sub>2</sub>-Sb based electrodes and high risk of lead contamination by chemical leaching of PbO<sub>2</sub> electrodes have prevent their practical applications, even though both electrodes are relatively effective for electrooxidation of organic pollutants [25–29].

Recently, ceramic electrodes based on sub-stoichiometric titanium oxides, particularly Ti<sub>4</sub>O<sub>7</sub> has been developed and tested for potential application in electrochemical wastewater treatment [30–32]. The Ti–O system belongs to Magnéli phases homologous series with the empirical formula Ti<sub>n</sub>O<sub>2n-1</sub>, (*n* ≥ 3) [33]. Several oxides in this series exhibit high electrical

conductivity at room temperature, good corrosion resistant and high chemical stability, especially  $4 \leq n \leq 6$  oxides from the series, i.e., Ti<sub>4</sub>O<sub>7</sub>, Ti<sub>5</sub>O<sub>9</sub> and Ti<sub>6</sub>O<sub>11</sub> [30,34,35]. Studies have shown that Ti<sub>4</sub>O<sub>7</sub> ceramic electrode behave as non-active anode with respect to water oxidation and hydroxyl radical generation [30,36,37]. However, the M(<sup>•</sup>OH) formed at its surface appears to be less abundant when compared with BDD anode at analogous condition [36]. Although the potential of these oxides as suitable electrode in electrochemical wastewater treatment has been demonstrated in the last decade, only few studies are available in literature [30,37–40]. Furthermore, relatively simple organic substrates have been investigated with little attention given to emerging micropollutants such as pharmaceutical residues.

AMX, a  $\beta$ -lactam antibiotic is among the most commonly detected pharmaceuticals in sewage treatment plants, effluents and surface water [41–44]. It has low metabolism in both human and livestock body system; as such 80–90% is excreted and released into the environment as unmodified drug [45,46]. Like many of other antibiotics, it is widely and unrestricted used in both human and veterinary medicine, and of great concern due to their adverse environmental impacts such as proliferation of antibiotic resistant pathogens and ecotoxicology [44,47–49]. Different treatment techniques have been employed for the removal of AMX from aqueous solution, including AOPs such as Fenton's reagent [50–53], ozonation [54,55], heterogeneous photocatalysis [56,57] and EAOPs using different anode materials [58–60]. Electrochemical based technologies were found to achieve much high mineralization in most cases, whereas other AOPs treatments only achieve good degradation with the formation of more stable intermediates that were mineralized at a very lower rate.

This paper investigates the potential use of the sub-stoichiometric titanium oxide (Ti<sub>4</sub>O<sub>7</sub>) as ceramic electrode for degradation and mineralization of AMX in aqueous medium. The effects of applied current and AMX initial concentration on the decay kinetics of AMX were systematically studied. TOC decay was assessed to elucidate the mineralization of AMX. For comparison, similar studies were conducted with other known commercial anodes such as Pt, DSA and BDD. A possible reaction mechanism of the electrochemical mineralization of AMX was proposed by analyzing and quantifying the aromatic intermediates, short-chain carboxylic acids and released inorganic ions. Further, the evolution of solution toxicity during electrochemical treatment was examined.



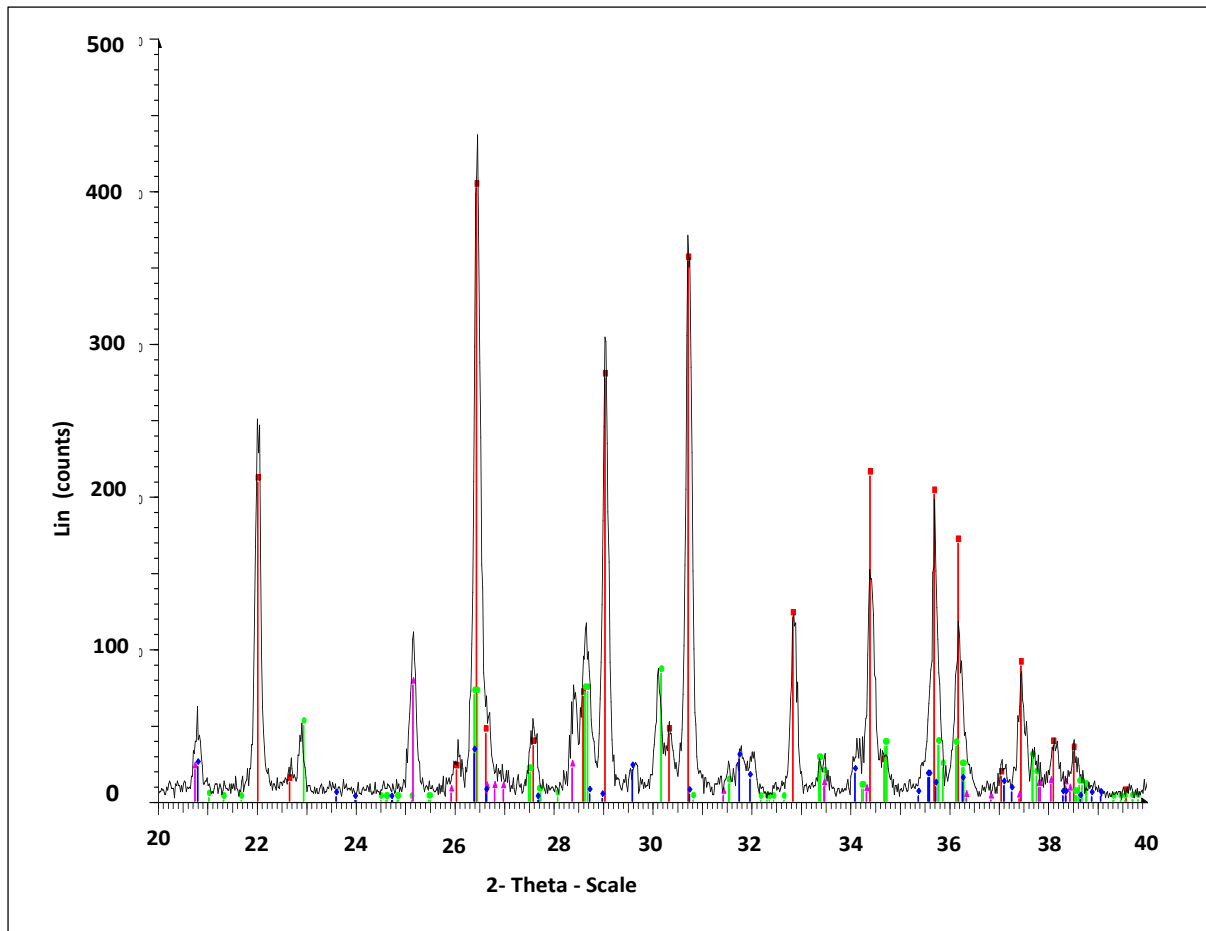
## 3.2 Materials and Methods

### 3.2.1 Chemicals

All chemicals used in this study were reagent grade or higher and were used as received without further purification. AMX- (C<sub>16</sub>H<sub>19</sub>N<sub>3</sub>O<sub>5</sub>S, with >90% purity) was obtained from Sigma-Aldrich. Sodium sulfate (Na<sub>2</sub>SO<sub>4</sub>), sodium chloride (NaCl), potassium sulfate (K<sub>2</sub>SO<sub>4</sub>), sulfuric acid (H<sub>2</sub>SO<sub>4</sub>) and phosphoric acid (H<sub>3</sub>PO<sub>4</sub>) were supplied by Sigma-Aldrich, Merck, and Acros. Oxalic (H<sub>2</sub>C<sub>2</sub>O<sub>4</sub>), oxamic (C<sub>2</sub>H<sub>3</sub>NO<sub>3</sub>), acetic (C<sub>2</sub>H<sub>4</sub>O<sub>2</sub>), maleic (C<sub>4</sub>H<sub>4</sub>O<sub>4</sub>), glyoxylic (C<sub>2</sub>H<sub>2</sub>O<sub>3</sub>) and malonic (C<sub>3</sub>H<sub>4</sub>O<sub>4</sub>) acids were obtained from Acros, Fluka and Alfa Aesar. Bioluminescence bacteria and the activation reagent LCK 487 LUMISTOX were supplied by Hach Lange France SAS. All solutions were prepared with Milli-Q ultra-pure water (> 18 MΩ at 25 °C). Organic solvents and other chemicals used were HPLC or analytic grade from Sigma-Aldrich, Fluka and Merck.

### 3.2.2 Preparation and characterization of Ti<sub>4</sub>O<sub>7</sub> electrode

TiO<sub>x</sub> particles were prepared by electro-fusion method. Briefly, a mixture of TiO<sub>2</sub> (ALTICHEM >98%) and coke (Coke de Brai AO151203 ALTICHEM 98%C) was fed into a Heroult-furnace and an electric arc was created between the two graphite electrodes. This electric arc was able to melt the fed mixture that was eventually poured into a graphite mold. The obtained ingot was jaw-crushed, milled and sieved to obtain powder with particle size smaller than 70 μm. The X-ray diffraction spectrum of the powder obtained shows a mixture of Ti<sub>3</sub>O<sub>5</sub>, Ti<sub>4</sub>O<sub>7</sub>, Ti<sub>5</sub>O<sub>9</sub>, and Ti<sub>6</sub>O<sub>11</sub> phases (Fig. 3-1).

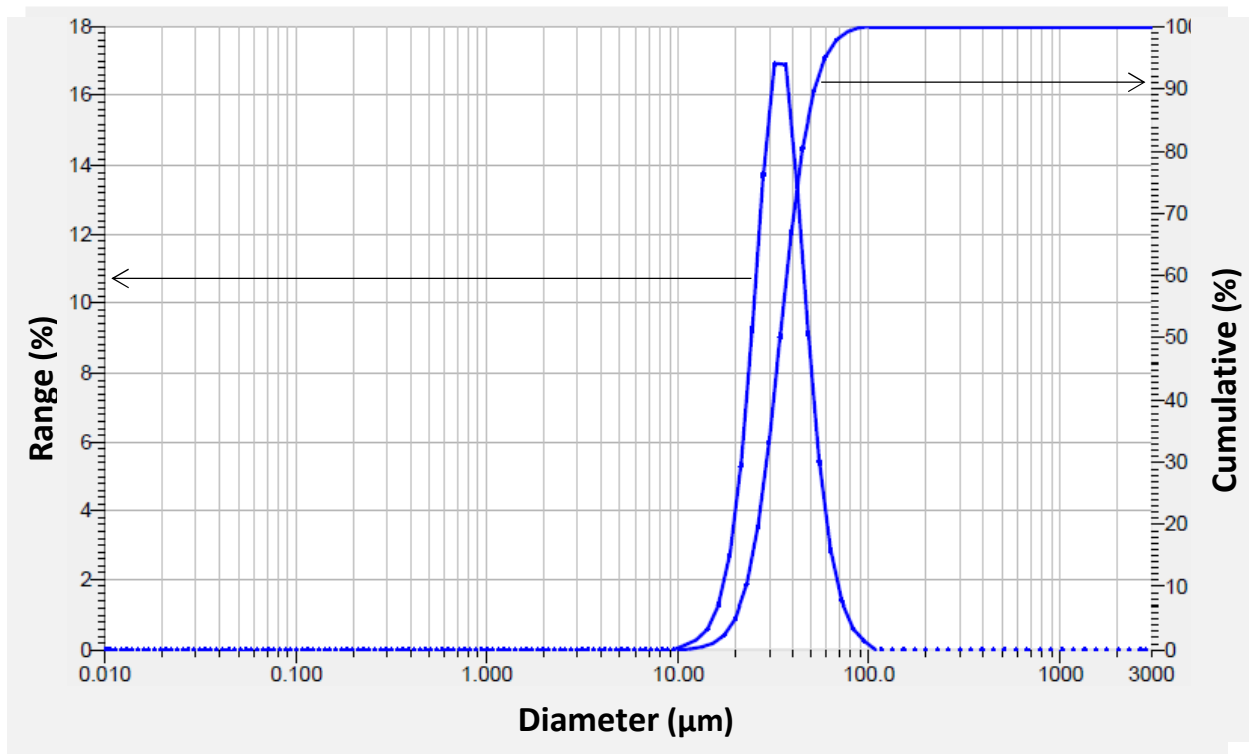


- 00-051-0641 (N) - Titanium Oxide - Ti<sub>5</sub>O<sub>9</sub> - Triclinic
- ◆ 01-077-1392 (\*) - Titanium Oxide - Ti<sub>4</sub>O<sub>7</sub> - Triclinic
- 01-076-1266 (\*) - Titanium Oxide - Ti<sub>6</sub>O<sub>11</sub> - Triclinic
- ▲ 01-082-1138 (\*) - Titanium Oxide - Ti<sub>3</sub>O<sub>5</sub> - Monoclinic

**Figure 3-1** – X-ray diffraction pattern of the powder used in preparing Ti<sub>4</sub>O<sub>7</sub> anode

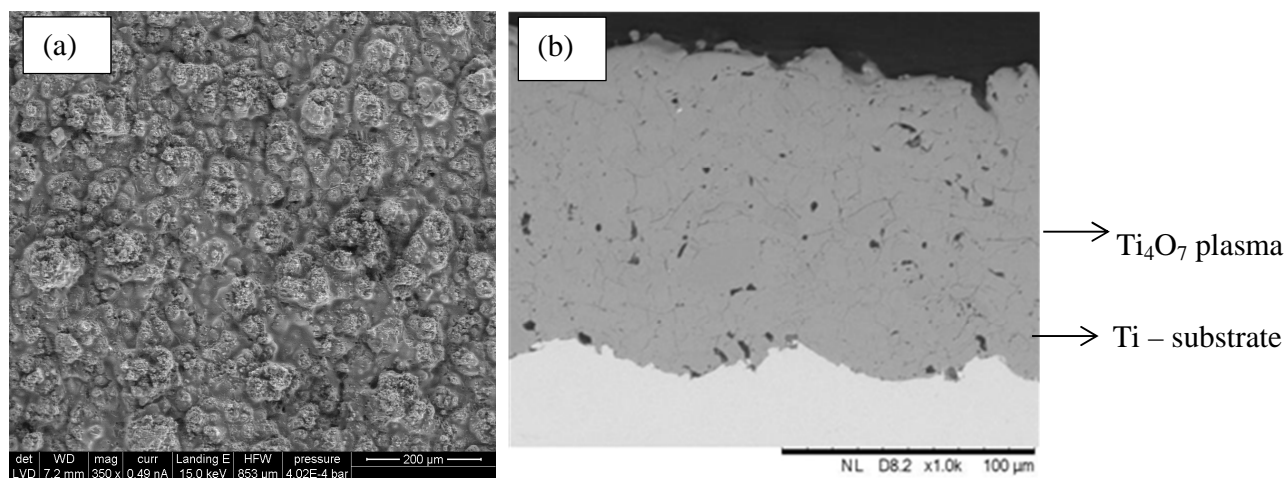
The fused TiO<sub>x</sub> particles were used to make a plasma-coating on a Ti substrate of 4 cm x 6 cm. The plasma torch (Saint-Gobain ProPlasma STD) consists of a tungsten cathode and a copper annular anode. Argon and hydrogen gas (19.6% H<sub>2</sub>) was introduced in the space between these two electrodes. A direct current (DC) potential is applied to the electrodes; leading to an electric arc (38 kW) which ionizes both argon and hydrogen and produces a “plasma plume” with inner temperature range of 10000 to 15000 °C. The TiO<sub>x</sub> particles were introduced into this

plasma plume using argon as carrier gas ( $30 \text{ g min}^{-1}$ ; injector diameter = 1.8 mm; injection angle =  $+10^\circ$ ). They are melted and accelerated by the plasma onto the Ti substrate that has been pretreated by sand-blasting to create a rough surface. The  $\text{TiO}_x$  particle size distribution (obtained from HORIBA Laser Scattering Particle Size Distribution Analyzer - PARTICA LA-950V2) is shown in Fig. 3-2 and indicate that 80% of the particles are in the range 20-60 $\mu\text{m}$ , which is critical for plasma spraying. Melted particles impact the substrate as “splats” that are quenched at the contact of the cold titanium plate. A homogenous and continuous lamellar coating (Fig. 3-3) was obtained by the motion of the torch versus the substrate (linear velocity =  $800 \text{ mm s}^{-1}$ ; step = 2 mm). X-ray diffraction of the prepared electrode shows that the main phase in this plasma-coating was  $\text{Ti}_4\text{O}_7$ .



D10 = 22.6 $\mu\text{m}$ ; D50 = 34.2 $\mu\text{m}$ ; D90 = 52 $\mu\text{m}$

Figure 3-2 –  $\text{TiO}_x$  particle size distribution used in preparation of  $\text{Ti}_4\text{O}_7$ .



### 3.2.3 Electrolytic system

Electrolytic experiments were performed in an open, undivided and cylindrical glass cell of 6 cm diameter and 250 mL capacity with the solution vigorously stirred by a magnetic PTFE bar during treatment to enhance the mass transport towards the electrodes. A constant current was supplied with a Hameg HM8040 triple power DC supply. Four electrodes, all of 24 cm<sup>2</sup> area were used as anode: Ti<sub>4</sub>O<sub>7</sub> (4 cm × 6 cm thin film deposited on Ti substrate, SAINT GOBAIN CREE, France), commercial pure Pt mesh, BDD (4 cm × 6 cm, CONDIAS, Germany), and commercial DSA (4 cm × 6 cm, Baoji Xinyu GuangJiDian Limited Liability Company, China). The cathode was either a tri-dimensional, large surface area CF (14 cm × 5 cm × 0.5 cm, Carbone-Lorraine, France) or stainless steel with 24 cm<sup>2</sup> surface area.

The anode was centered in the electrolytic cell, surrounded by the CF cathode which covers the inner wall of the cell. When using CF as cathode, compressed air was continuously bubbled into the cell through a silica frit at about 1 L min<sup>-1</sup>, starting 10 min prior to electrolysis to maintain the O<sub>2</sub> concentration in the solution. *In-situ* H<sub>2</sub>O<sub>2</sub> generation was attained by 2e<sup>-</sup> reduction of dissolved oxygen at the cathode (Brillas et al., 2009). To examine the influence of applied current (10 – 120 mA) on AMX degradation and mineralization, 230 mL aqueous solutions of 0.1 mM AMX (19.6 mg L<sup>-1</sup> TOC) containing 0.05 M Na<sub>2</sub>SO<sub>4</sub> as supporting electrolyte were used to conduct the electrochemical experiments at natural pH (~ 5.7) of the

solution. Besides, similar experiments were conducted under analogous conditions to investigate the effect of initial AMX concentrations (0.05 – 0.2 mM) on the degradation kinetics at applied current of 120 mA. The contribution of H<sub>2</sub>O<sub>2</sub> to the degradation and mineralization of AMX was examined by substituting CF with stainless steel as cathode. All trials were conducted at room temperature (23 ± 2 °C) in duplicate.

#### 3.2.4 Instruments and analytical procedures

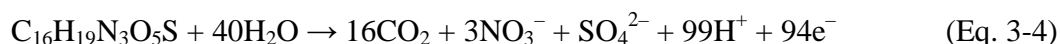
The mineralization of treated solutions was analyzed in terms of TOC abatement, which was measured on a Shimadzu VSCH TOC analyzer according to the thermal catalytic oxidation principle. Reproducible TOC values with ±2 % accuracy were found using the non-purgeable organic carbon method. The percentage TOC removal was calculated according to the following equation:

$$\text{TOC removal (\%)} = \frac{\Delta(\text{TOC})_{\text{exp}}}{\text{TOC}_0} \times 100 \quad (\text{Eq. 3-2})$$

where  $\Delta(\text{TOC})_{\text{exp}}$  is the experimental TOC decay at electrolysis time  $t$  (mg L<sup>-1</sup>) and  $\text{TOC}_0$  is the corresponding initial value before electrolysis. The mineralization current efficiency (MCE in %) was calculated from the following equation (Brillas et al., 2009):

$$\text{MCE (100\%)} = \frac{n F V_s \Delta(\text{TOC})_{\text{exp}}}{4.32 \times 10^7 m I t} \times 100 \quad (\text{Eq. 3-3})$$

where  $F$  is the Faraday constant (96487 C mol<sup>-1</sup>),  $V_s$  is the solution volume (L),  $4.32 \times 10^7$  is a conversion factor ( $=3,600 \text{ s h}^{-1} \times 12,000 \text{ mg of C mol}^{-1}$ ),  $m$  is the number of carbon atoms of AMX (16 C atoms) and  $I$  is the applied current (A) and  $n$  is the number of electron consumed per molecule of AMX; taken to be 70 assuming complete mineralization of AMX into CO<sub>2</sub>, NO<sub>3</sub><sup>-</sup> and SO<sub>4</sub><sup>2-</sup>:



The concentration decay of AMX during electrolysis was analyzed by injecting 20  $\mu\text{L}$  sample to the reversed-phase HPLC set-up, (Model L-7455 Lachrom, Merck Hitachi, Japan) equipped with a L-7100 pump and fitted with a Purospher RP-18, 5  $\mu\text{m}$ , 25 cm  $\times$  4.6 mm (i.d.) analytical column at 40  $^{\circ}\text{C}$  with the detection performed on L-7455 photodiode array detector at a selected wavelength of 232 nm. The AMX concentration was determined periodically using an isocratic solvent elution of methanol/water (pH  $\sim$  3 by  $\text{H}_3\text{PO}_4$ ) 10:90 (v/v) as a mobile phase at a flow rate of 0.4  $\text{mL min}^{-1}$ .

Generated aliphatic carboxylic acids during treatment were identified and quantified by ion-exclusion HPLC using Merck Lachrom liquid chromatograph equipped with an L-2130 pump, fitted with a C18 Acclaim OA (organic acids), 4 mm  $\times$  25 cm (i.d.) column at 40  $^{\circ}\text{C}$ , and coupled with a L-2400 UV detector selected at wavelength of 210 nm, using 1%  $\text{H}_2\text{SO}_4$  at 0.2  $\text{mL min}^{-1}$  as mobile phase. The concentrations of  $\text{NO}_3^-$ ,  $\text{NH}_4^+$  and  $\text{SO}_4^{2-}$  released to the treated solutions were assessed on ion chromatography by injecting 50  $\mu\text{L}$  samples into a Dionex ICS-1000 Basic Ion Chromatography set-up coupled with a Dionex DS6 conductivity detector containing a cell maintained at 35  $^{\circ}\text{C}$  through Chromeleon SE software. The  $\text{NO}_3^-$  and  $\text{SO}_4^{2-}$  content were determined with a Dionex AS4A-SC, 25 cm  $\times$  4 mm (i.d.) anion-exchange column using a mixture of 1.8 mM  $\text{Na}_2\text{CO}_3$  and 1.7 mM  $\text{NaHCO}_3$  solution at 2.0  $\text{mL min}^{-1}$  as mobile phase. For  $\text{NH}_4^+$  detection, a Dionex CS12A, 25 cm  $\times$  4 mm (i.d.) cation column and a mobile phase of 9 mM  $\text{H}_2\text{SO}_4$  at 1.0  $\text{mL min}^{-1}$  was used.

GC-MS analyses were performed using a Thermo Scientific GC-MS analyzer equipped with a TRACE 1300 gas chromatography coupled to an ISQ single quadrupole mass spectrophotometer operating in electron impact mode at 70 eV. Samples for GC-MS were obtained by solvent extraction of organic components of 10  $\text{cm}^3$  of electrolyzed solution with 45  $\text{cm}^3$  of dichloromethane (three extractions with 15  $\text{cm}^3$  each), followed by drying of the organic fraction over 2 g of  $\text{MgSO}_4$ , filtered and concentrated to a volume of 1  $\text{cm}^3$  with a rotary evaporator under vacuum. The samples were directly analyzed by GC-MS using a TG-5MS 0.25  $\mu\text{m}$ , 30 m  $\times$  0.25 mm (i.d.) column, with a temperature ramp of 50  $^{\circ}\text{C}$  for 3 min, 10  $^{\circ}\text{C min}^{-1}$  up to 250  $^{\circ}\text{C}$  and 4 min hold time. The temperature of the injector and detector were 200 and 250  $^{\circ}\text{C}$  respectively, and helium was used as carrier gas at a flow rate of 1.5  $\text{mL min}^{-1}$ . The mass spectra were identified by Xcalibur data library.

The evolution of toxicity of treated AMX solutions at different electrolysis times was performed by means of Microtox<sup>®</sup> method. Toxicity of the samples was evaluated based on the inhibition of the bio-luminescence of the bacteria *V. fischeri*. The pH of all the analyzed samples was adjusted to 6.5 – 7.5 with the aid of 0.01 – 0.1 mM NaOH, and the bioluminescence measurements were performed on both blank as well as electrolyzed AMX solutions after 5 and 15 min of exposure to *V. fischeri* bacteria using Microtox method.

### 3.3 Results and Discussion

#### 3.3.1. Kinetic studies of AMX degradation

The kinetics of the degradation of AMX by electrogenerated oxidants especially M(<sup>•</sup>OH) has been studied from the decay of its concentration monitored by reversed-phase HPLC. A well-defined absorption peak related to AMX was always displayed at a retention time ( $t_R$ ) of 10.8 min on the chromatograms. As shown in Fig. 3-4a and 3-4b, the decay of AMX concentration is dependent on the applied current and much rapid degradation was observed with increasing current with both Ti<sub>4</sub>O<sub>7</sub> and BDD anodes. The concentration of AMX reduced to 0.09 mM (~4.0 mg L<sup>-1</sup>) in both cases when a lower current of 10 mA was applied for 120 min, whereas it was completely degraded after 120 and 80 min at 30 and 60 mA respectively. However, a slightly faster decay in AMX concentration was observed with Ti<sub>4</sub>O<sub>7</sub> anode at 120 mA (Fig. 3-4a), with the drug disappeared after 40 min compared to 60 min observed with BDD anode (Fig. 3-4b). The increase in reaction rate of AMX with raising current is related to the production of larger quantities of electrogenerated active oxidant (M(<sup>•</sup>OH)) from water oxidation at anode surface (eq. 3-1), which rapidly oxidize AMX molecules. Comparative studies at 120 mA with DSA and Pt anodes and CF cathode show lower degradation rate as expected with active anodes, with AMX concentration drops to ~0.04 mM (1.5 mg L<sup>-1</sup>) after 120 min with DSA anode and disappeared from the solution after 80 min with Pt anode, due to smaller quantity of M(<sup>•</sup>OH) generated at their surfaces and high chemisorption of generated <sup>•</sup>OH to anode surface.

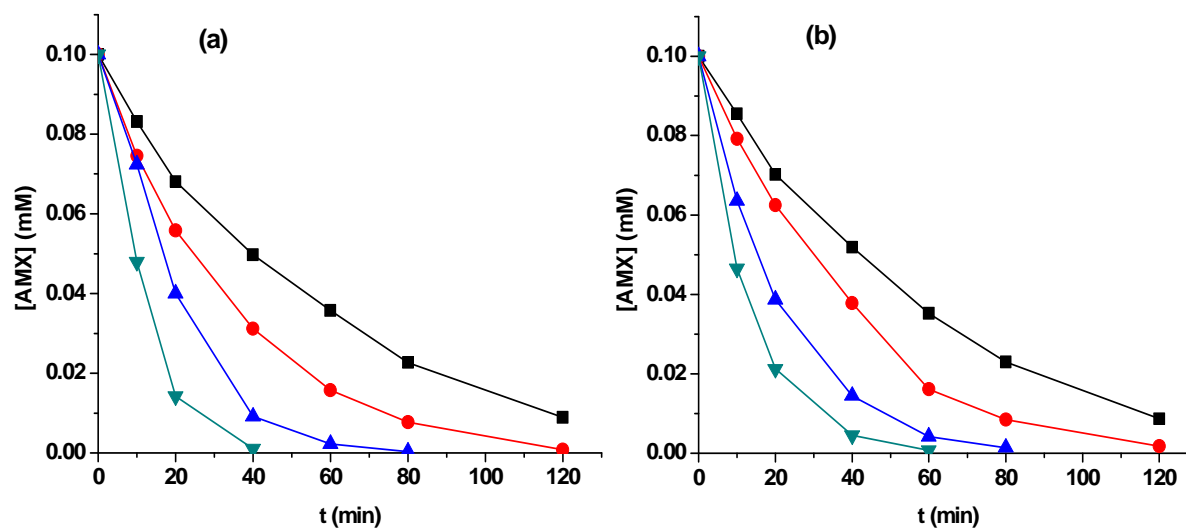


**Figure 3-4** – Effect of applied current: (-■-) 10 mA (-●-) 30 mA, (-▲-) 60 mA and (-▼-) 120 mA on AMX concentration decay vs. electrolysis time for the electrooxidation treatment of 0.1 mM AMX in 0.05 M Na<sub>2</sub>SO<sub>4</sub> using (a) Ti<sub>4</sub>O<sub>7</sub> and (b) BDD anode and CF cathode.

In all case, the oxidation of AMX by M(<sup>•</sup>OH) was fitted with pseudo first-order kinetic reaction assuming a quasi-stationary state for M(<sup>•</sup>OH) concentration, since it is very reactive and cannot be accumulated in the medium. This implies that a constant concentration of M(<sup>•</sup>OH) always reacts with AMX [61]. The analysis of the plots using linear regression yielded apparent rate constant ( $k_{app,AMX}$ ) values that are summarized in Table 3-1, with excellent linear correlations ( $R^2 \approx 0.99$ ). As shown in Table 3-1, the  $k_{app,AMX}$  values gradually increases as the current raises from 10 to 120 mA with both Ti<sub>4</sub>O<sub>7</sub> and BDD anodes. It is worthy to note that  $k_{app,AMX}$  values for both anodes are relatively close with slightly better values for Ti<sub>4</sub>O<sub>7</sub> anode at 60 and 120 mA.

The influence of AMX concentration (0.05, 0.1 and 0.2 mM) on its degradation kinetic, studied at applied current of 120 mA with both Ti<sub>4</sub>O<sub>7</sub> and BDD anodes shows that AMX was completely removed from the medium after short electrolysis times of 40, 60 and 80 min for 0.05, 0.1 and 0.2 mM concentrations, respectively, demonstrating the high potential of Ti<sub>4</sub>O<sub>7</sub> anode in electrooxidation of organics even at high concentration level. The  $k_{app,AMX}$  values (Table 3-1) diminished with increasing of initial AMX concentrations from 0.05 to 0.2 mM with



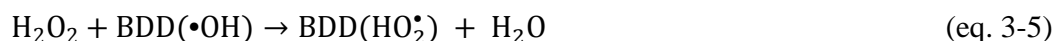
both anodes. This is logical because under analogous experimental conditions, identical concentration and nature of oxidants, especially M(<sup>•</sup>OH) are generated at the surface of anode. As such, high ratio of oxidants to AMX is expected at lower initial concentration, suggesting greater possibility of AMX oxidation that resulted into higher  $k_{app,AMX}$  values. Additionally, huge quantity of intermediates by-products is expected to be generated at higher initial concentration, thus limiting the reaction between AMX molecules and M(<sup>•</sup>OH) since the latter is a non-selective radical and will also react with formed intermediates species.

**Table 3-1** – Apparent rate constants ( $k_{app,AMX}$ ) for the electrooxidation of AMX by M(<sup>•</sup>OH), assuming pseudo first-order reaction.

Cell	[AMX] (mM)	$k_{app, AMX}$ (min <sup>-1</sup> )			
		10 mA	30 mA	60 mA	120 mA
<b>DSA/CF</b>	0.1				0.02
<b>Pt/CF</b>	0.1				0.05
<b>Ti<sub>4</sub>O<sub>7</sub>/CF</b>	0.05				0.12
	0.1	0.02	0.03	0.07	0.10
	0.2				0.05
<b>Ti<sub>4</sub>O<sub>7</sub>/SS</b>	0.1			0.02	0.03
<b>BDD/CF</b>	0.05				0.10
	0.1	0.02	0.03	0.05	0.08
	0.2				0.04
<b>BDD/SS</b>	0.1			0.03	0.05

To clarify the contribution of H<sub>2</sub>O<sub>2</sub> as a weak oxidant to AMX concentration decay with both Ti<sub>4</sub>O<sub>7</sub> and BDD anodes, experiments were carried out by replacing CF with stainless steel as cathode. CF is well known for H<sub>2</sub>O<sub>2</sub> generation potential, whereas stainless steel has a very limited capacity for H<sub>2</sub>O<sub>2</sub> generation [62]. Fig. 3-5a and 3-5b shows the contribution of H<sub>2</sub>O<sub>2</sub> to the AMX degradation assessed from experiment performed at 120 mA using Ti<sub>4</sub>O<sub>7</sub> and BDD anodes. It is obvious that the generated H<sub>2</sub>O<sub>2</sub> contributes significantly to the decay of AMX concentration in the treated solution. The decay rate of AMX tremendously decreased when CF

was replaced by stainless steel as cathode material. However, the decrease in degradation rate was more slightly pronounced with Ti<sub>4</sub>O<sub>7</sub> when compared with BDD. The generated H<sub>2</sub>O<sub>2</sub> contribution is either by direct oxidation as a weak oxidant or indirectly after its destructive reaction with M(<sup>•</sup>OH) to generate hydrogen peroxy radical M(HO<sub>2</sub><sup>•</sup>) (eq. 3-5) [63]:



It must be noted that the oxidation of AMX by either of these oxidants (H<sub>2</sub>O<sub>2</sub> or M(HO<sub>2</sub><sup>•</sup>)) mainly leads to the formation of stable intermediates with very limited mineralization as it is explained in section 3.3.2.

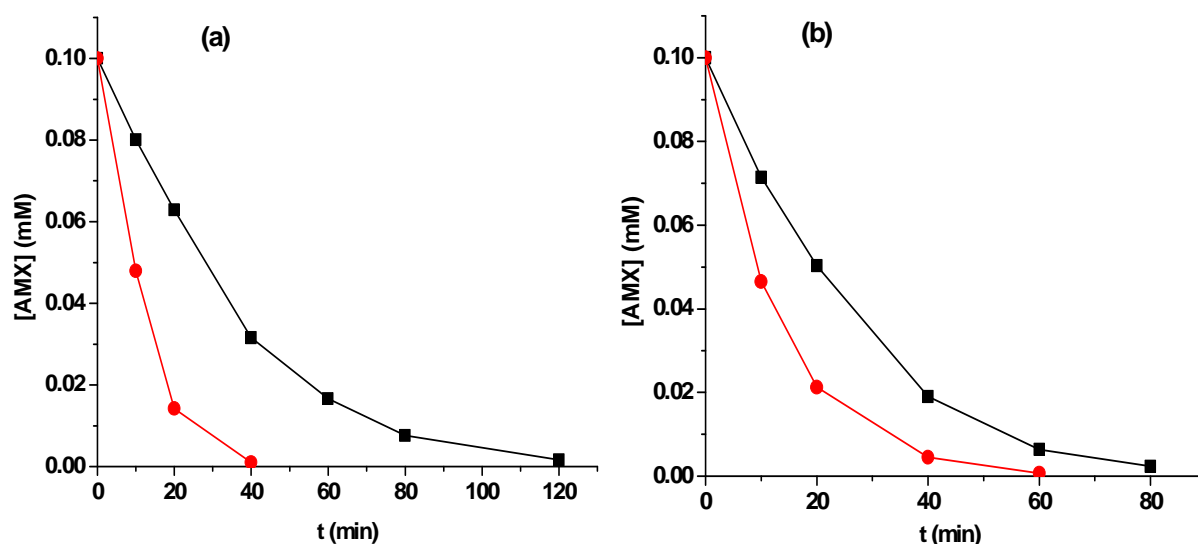


**Figure 3-5** – Contribution of in-situ generated H<sub>2</sub>O<sub>2</sub> to the decay of AMX concentration vs time with stainless steel cathode (-■-) and CF cathode (-●-) for the electrooxidation at 120 mA of 0.1 mM AMX in 0.05 M Na<sub>2</sub>SO<sub>4</sub> using (a) Ti<sub>4</sub>O<sub>7</sub> and (b) BDD anode.

### 3.3.2 Mineralization of AMX solution

The potential of Ti<sub>4</sub>O<sub>7</sub> as a suitable anode for electrochemical oxidation of AMX was assessed by studying the mineralization of 0.1 mM AMX solutions (corresponding to 19.6 mg L<sup>-1</sup> initial TOC) at varying applied current from 10 to 120 mA. Figure 3-6a depicts the decay of TOC vs electrolysis time at different applied current obtained for the experiments

performed with Ti<sub>4</sub>O<sub>7</sub> anode. An improved mineralization degree with rising in applied current and electrolysis time with final TOC removal being 20%, 33%, 45% and 69% at 10, 30, 60 and 120 mA, respectively, was obtained after 480 min of electrolysis. This behavior agrees with the generation of high quantity of M(<sup>•</sup>OH) from water oxidation (eq. 3-1), leading to quick oxidation of both AMX and its intermediates as explained in section 3.3.1. Relatively low mineralization was obtained at lower applied current (10 and 30 mA) due to lower anodic potential ( $\leq$  water discharge potential) which limits the generation of M(<sup>•</sup>OH) [40]. However, improved mineralization was obtained when applied current was increased from 30 to 120 mA. It should be noted that the partial mineralization of AMX solution (69% TOC removal) obtained in this study is clearly due to relatively low applied current studied (i.e.  $< 5 \text{ mA cm}^{-1}$  current density). A much better mineralization could be achieved at higher current density but may be detrimental to the stability of the anode.

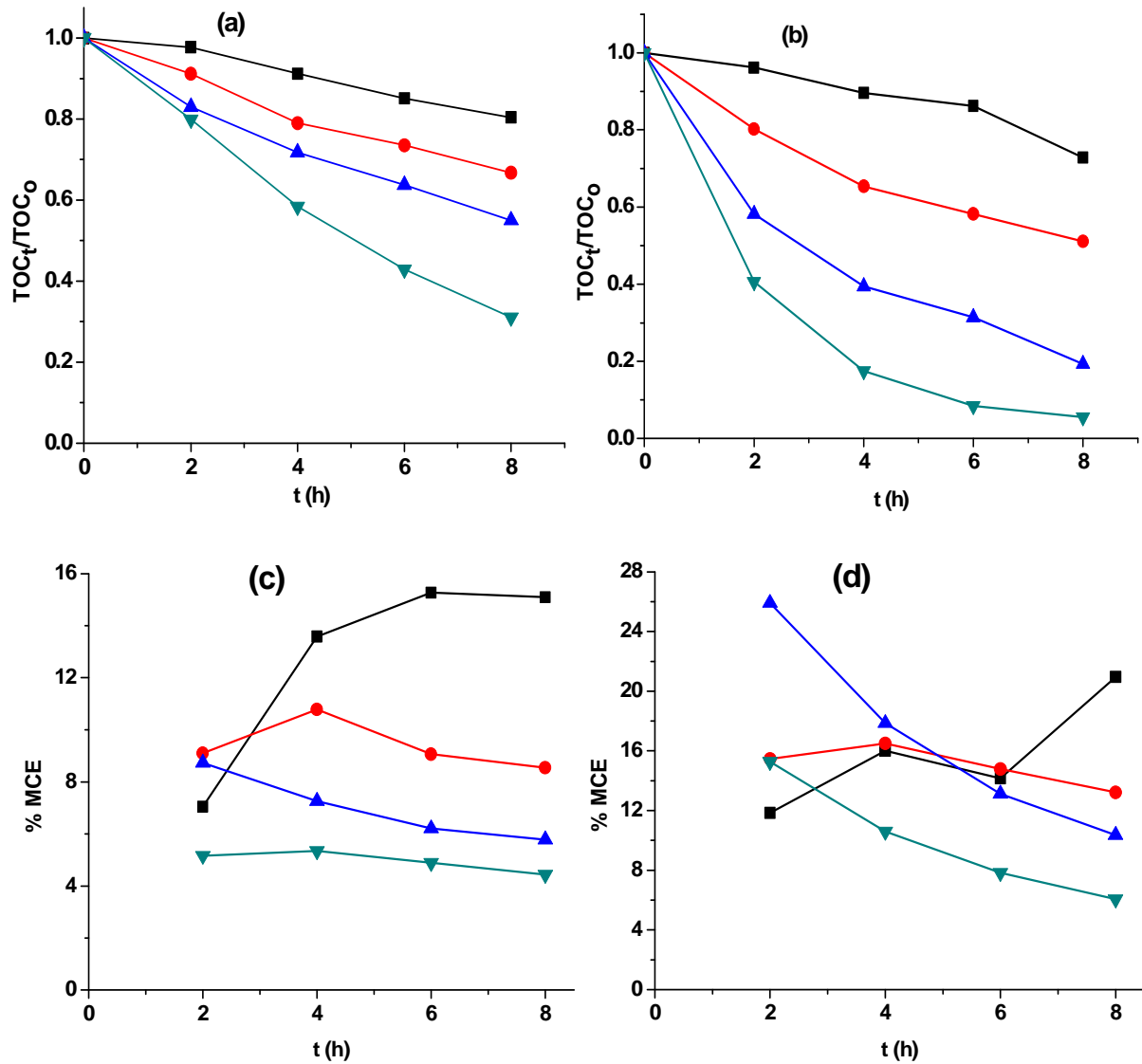
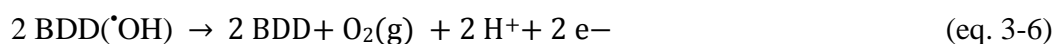


**Figure 3-6** – Effect of applied current: (-■-) 10 mA (-●-) 30 mA, (-▲-) 60 mA and (-▼-) 120 mA on TOC removal (a, b) and mineralization current efficiency(c, d) vs. electrolysis time during the electrooxidation of 0.1 mM (19.6 mg L<sup>-1</sup> initial TOC) AMX in 0.05 M Na<sub>2</sub>SO<sub>4</sub> using Ti<sub>4</sub>O<sub>7</sub>, (a, c) and BDD (b, d) anode and carbon-felt cathode.

A comparison study with other anode materials especially BDD, was made under same experimental conditions ( $I = 10 - 120$  mA) (Fig. 3-6b), while experiments were performed at a fixed current of 120 mA for DSA and Pt anodes. As expected, BDD anode shows superior TOC

removal compared to Ti<sub>4</sub>O<sub>7</sub> anode, especially at high applied current values (i.e. 60 and 120 mA) due to the larger power of BDD for the production of BDD(<sup>•</sup>OH) from the water oxidation reaction (eq. 3-1). After 480 min of electrolysis, a maximum of 94% TOC removal was achieved at 120 mA with BDD anode compared to 69% obtained at the same current with Ti<sub>4</sub>O<sub>7</sub> anode. A much smaller TOC removal of 36% and 41% was obtained with DSA and Pt anode, respectively, demonstrating that these latter anodes have limited mineralization ability for organic pollutants.

Further, increase in applied current from 30 to 60 mA causes a faster TOC decay with BDD (Fig. 3-6b) compared to Ti<sub>4</sub>O<sub>7</sub> anode (Fig. 3-6a), indicating the high potent of BDD for the production of BDD(<sup>•</sup>OH) at higher currents. However, increased applied current from 60 to 120 mA shows marginal TOC removal (Fig. 3-6b) compared to significant increment obtained with Ti<sub>4</sub>O<sub>7</sub> anode (Fig. 3-6a). The decrease in mineralization efficiency observed with BDD anode at higher applied current can be related to the gradual acceleration of parallel non-oxidative reactions consuming hydroxyl radicals, mainly the recombination reactions of BDD(<sup>•</sup>OH) (eq. 3-6 and 3-7) when they are generated at high concentration on the anode surface, in particular, with relatively lower concentrations of organic matter. This was clearly seen in (Fig. 3-6c and 3-6d) where the decay in MCE between 60 and 120 mA was much significant with BDD anode (Fig. 3-6d) compared to Ti<sub>4</sub>O<sub>7</sub> anode (Fig. 3-6c)



It should be noted that H<sub>2</sub>O<sub>2</sub> as an oxidant has minimal contribution to the mineralization of AMX with Ti<sub>4</sub>O<sub>7</sub> anode as shown in Fig. 3-7a, in contrast to oxidation experiments (Fig. 3-5a). Indeed it can oxidize some easily oxidizable organics but cannot mineralize hardly oxidizable reaction intermediates. Other studies [64,65] have shown that *in-situ* generated H<sub>2</sub>O<sub>2</sub> has negligible direct effect on the mineralization of organics. In fact, its excessive accumulation may inhibit organic oxidation via the destruction of Ti<sub>4</sub>O<sub>7</sub>(<sup>•</sup>OH) in a similar manner to that in eq. 3-5, as it was observed in this study after 240 min of electrolysis at 60 mA (Fig. 3-7a). For instance after 480 min of electrolysis, the mineralization efficiency obtained with and without H<sub>2</sub>O<sub>2</sub> generation (CF and stainless steel cathodes) were 45% and 48% respectively, indicating slight reduction in efficiency with the former.

The stability of the activity of Ti<sub>4</sub>O<sub>7</sub> anode was also assessed by comparing mineralization experiment after < 25 h and > 200 h of usage in electrooxidation process at 60 mA. Almost 17% loss in mineralization efficiency was observed after 200 h of utilization (Fig. 3-7b), with subsequent studies exhibited no significant reduction in mineralization. Such loss in activity of Ti<sub>4</sub>O<sub>7</sub> can be explained either by the formation of passivation layer on the surface of the anode or partial conversion of Ti<sub>4</sub>O<sub>7</sub> at the surface of the anode to less conducting TiO<sub>2</sub>, which can be removed by “soft” sand blasting of the anode surface or polarity inversion to partially restore its activity [38].

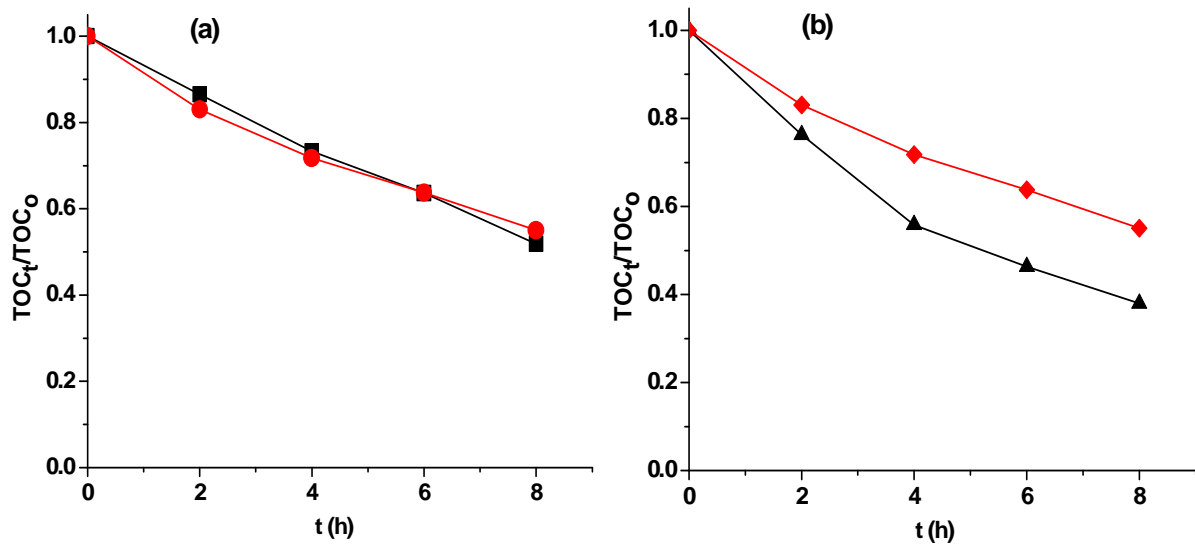


**Figure 3-7** – (a) Effect of in-situ generated H<sub>2</sub>O<sub>2</sub> on the mineralization of 0.1 mM AMX (19.6 mg L<sup>-1</sup> TOC) in 0.05 M Na<sub>2</sub>SO<sub>4</sub> medium at applied current of 60 mA, (-■-) without H<sub>2</sub>O<sub>2</sub> (stainless steel cathode) and (-●-) with H<sub>2</sub>O<sub>2</sub> generation using Ti<sub>4</sub>O<sub>7</sub> anode. (b) Stability of activity of Ti<sub>4</sub>O<sub>7</sub> with usage time for mineralization of 0.1 mM AMX (19.6 mg L<sup>-1</sup> TOC) in 0.05 M Na<sub>2</sub>SO<sub>4</sub> medium at applied current of 60 mA: (-▲-) < 25 h, (-◆-) > 200 h of usage.

### 3.3.3 Evolution of the oxidation byproducts of AMX and mineralization pathways

The oxidation of an organic compound containing heteroatoms on a non-active anode such as BDD or Ti<sub>4</sub>O<sub>7</sub> usually proceeds via the formation of aromatic by-products, short-chain aliphatic carboxylic acids and inorganic ions. It is important to note that the release of inorganic ions in the electrolyzed solution is a major signal of pollutant mineralization [22,28]. Upon covalent bonds cleavage of AMX molecules and oxidation of formed lower molecular weight species, organic N atom was released to the solution and quantified as NH<sub>4</sub><sup>+</sup> and NO<sub>3</sub><sup>-</sup> by ion chromatography without detecting NO<sub>2</sub><sup>-</sup>, while S atom was recovered as SO<sub>4</sub><sup>2-</sup> in the treated solutions containing 0.1 mM of AMX (Fig. 3-8a and 3-8b) at 120 mA constant current electrolysis. The amount of both NH<sub>4</sub><sup>+</sup> and NO<sub>3</sub><sup>-</sup> ions continuously accumulated in treated solution over 480 min of treatment with either Ti<sub>4</sub>O<sub>7</sub> or BDD anode as shown in Fig. 3-8a and 3-8b. Majority of N atom released was detected as NH<sub>4</sub><sup>+</sup>, with significant proportion as NO<sub>3</sub><sup>-</sup> in both cases, which could be explained by the partial reduction of small fraction of the formed NO<sub>3</sub><sup>-</sup> to NH<sub>4</sub><sup>+</sup> as it has been experimentally confirmed by previous studies [64,66], although Thiam et al., 2015 [66] did not observe reduction of NO<sub>3</sub><sup>-</sup> to NH<sub>4</sub><sup>+</sup> on carbon-PTFE air-diffusion cathode. Similarly, S atom is oxidized and gradually accumulated as SO<sub>4</sub><sup>2-</sup> over the treated time to reach overall 0.1 mM (100% of initial S) with both anodes. After 480 min of electrolysis, 0.141 mM NH<sub>4</sub><sup>+</sup> and 0.068 mM NO<sub>3</sub><sup>-</sup> representing 47 and 22% respectively of the initial N atom in 0.1 mM AMX solution (0.3 mM N) was found in the final solution treated with Ti<sub>4</sub>O<sub>7</sub> anode, whereas 0.186 mM NH<sub>4</sub><sup>+</sup> (62% of initial N) and 0.086 mM NO<sub>3</sub><sup>-</sup> (29% of initial N) was obtained with BDD anode, indicating much better mineralization with BDD anode as shown in Fig. 3-6b. While the organic S was totally recovered as SO<sub>4</sub><sup>2-</sup> in the treated solutions, the amount of inorganic N was far less than the total initial N content of 0.1 mM AMX solution (i.e. 69% and 91% for Ti<sub>4</sub>O<sub>7</sub> and BDD anodes respectively). In the case of BDD anode, the mass balance is almost complete since the rest of N (9%) is present in oxamic acid that was not mineralized (remained in the solution after treatment) (Fig. 3-9b). In contrast the mass balance for N is slightly deficient in the case of Ti<sub>4</sub>O<sub>7</sub> anode that can be explained by its relatively lower mineralization power (24% of N is present in non-mineralized oxamic acid) (Fig. 3-9a). The remaining 7% of non-detected N can be present in other non-identified N-containing organics remaining in the treated solution judging from the profiles of NH<sub>4</sub><sup>+</sup>, NO<sub>3</sub><sup>-</sup> and oxamic acid (Fig.

3-8a and 3-9a) which continuously accumulated without sign of reaching plateau after 480 min of treatment or may have been loss as volatile N-compounds (N<sub>x</sub>O<sub>y</sub>) [68,69].

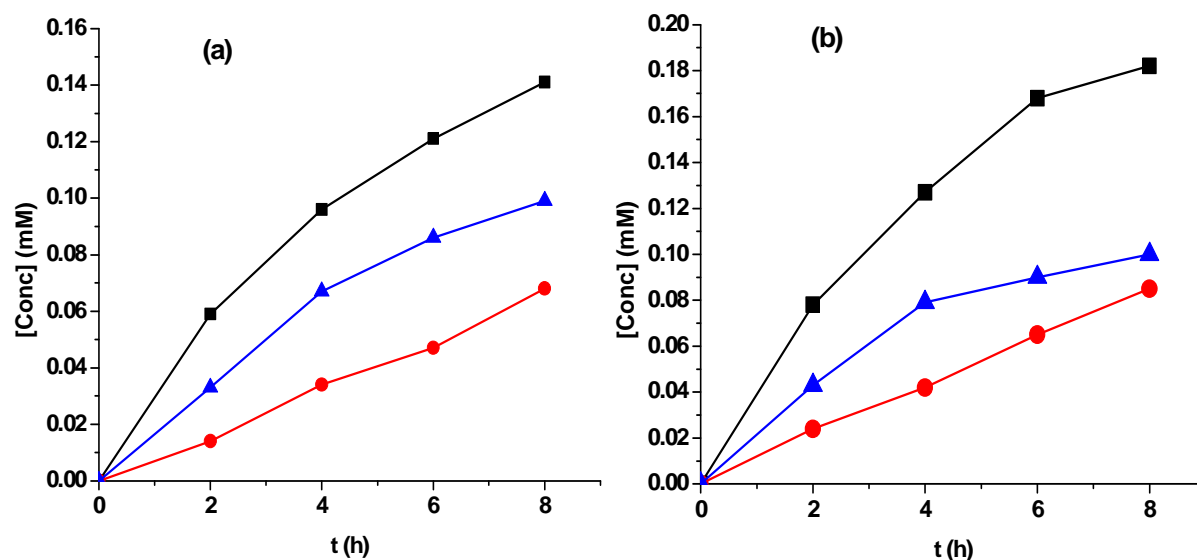


**Figure 3-8** – Time-course of the identified inorganic ions: (-■-) NH<sub>4</sub><sup>+</sup> (-●-) NO<sub>3</sub><sup>-</sup> and (-▲-) SO<sub>4</sub><sup>2-</sup> during the electrooxidation of 0.1 mM AMX in 0.05 M K<sub>2</sub>SO<sub>4</sub> (for NH<sub>4</sub><sup>+</sup>) and NaCl (for (SO<sub>4</sub><sup>2-</sup>) analyses during constant current electrolysis at 120 mA using (a) Ti<sub>4</sub>O<sub>7</sub> and (b) BDD anode and CF cathode.

Ion-exclusion chromatographs of the treated solution at different electrolysis time showed the formation of several carboxylic acids such as oxalic, oxamic, malonic, maleic, glyoxylic and acetic acids from the cleavage of both aromatics and non-aromatics intermediates by-products. The evolution of these carboxylic acids shown in Fig. 3-9a and 3-9b indicates high accumulation rate at the early stage of electrolyses, with further treatment caused decline in their concentrations especially with BDD anode. In both case, oxalic acid reaches the highest concentration (0.14 mM and 0.08 mM for Ti<sub>4</sub>O<sub>7</sub> and BDD anodes respectively) because it is the ultimate product of oxidative cleavage of benzenic moiety of aromatic intermediates [70,71] before mineralization. It must be noted that the persistence of these carboxylic acids after 480 min of electrolysis, specifically with Ti<sub>4</sub>O<sub>7</sub> anode accounts for the large residual TOC (Fig. 3-6a) observed in the treated solution.



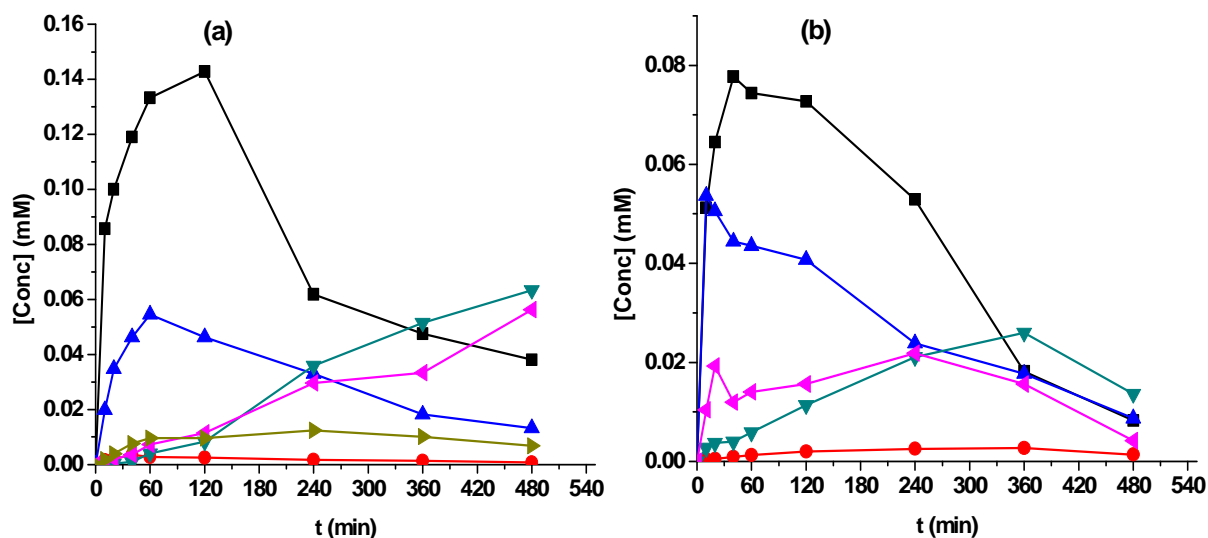


**Figure 3-9** – Time-course of the identified short-chain carboxylic acids: (-■-) oxalic; (-●-) maleic; (-▲-) malonic (-▼-) oxamic; (-◀-) acetic; (-▶-) glyoxylic during the electrooxidation of 0.1 mM AMX in 0.05 M Na<sub>2</sub>SO<sub>4</sub> solution at 120 mA using (a) Ti<sub>4</sub>O<sub>7</sub> and (b) BDD and CF cathode.

To elucidate the mechanism of AMX mineralization during the electrochemical treatment, the intermediates formed after 60 min of electrolysis of 230 mL solution containing 0.3 mM AMX in 0.05 M Na<sub>2</sub>SO<sub>4</sub> at 120 mA were identified by GC-MS. Based on the identified intermediate products; two oxidation pathways were proposed (Fig. 3-10). The first path (1) involves the cleavage of the peptide bond closed to phenyl group with the formation of 2-amino (4-hydroxyphenyl) acetic acid (**A**,  $m/z = 167.16$ ) and a bicyclic lactamic product (**B**,  $m/z = 231.20$ ), with the latter (**B**) further oxidized in several steps with the release of NH<sub>4</sub><sup>+</sup> and NO<sub>3</sub><sup>-</sup> to form an open-chain structure containing sulfonic group. The bicyclic lactamic product (**B**) and its oxidized products observed in this study were also reported for photocatalytic oxidation of AMX [57], which was formed in combination with p-hydroxybenzoic acid as a result of N-dealkylation of AMX at the secondary amine group. However in the present studies, p-hydroxybenzoic acid ( $m/z = 139.06$ ) was a product of subsequent hydroxylation and dehydrogenation of **A** at the primary amino group (release as NH<sub>4</sub><sup>+</sup>), followed by decarboxylation (elimination of CO<sub>2</sub>) reaction. Its further hydroxylation and dehydrogenation

forms characteristic intermediate products, hydroquinone ( $m/z = 110$ ) and benzoquinone ( $m/z = 108.01$ ), respectively. The second path (2) starts with Ti<sub>4</sub>O<sub>7</sub>(<sup>•</sup>OH) attack on the primary amino group leading to the formation of product C ( $m/z = 366$ ) which subsequently cleavage at both secondary amine and carbonyl group, forming oxamic acid, acetamide, p-hydrobenzoic acid, and a bicyclic lactamic product, that were further oxidized in similar manner to those formed in first path (1). The carbonyl intermediates was also reported by [57]. Further Ti<sub>4</sub>O<sub>7</sub>(<sup>•</sup>OH) attack on acetamide, benzoquinone and sulfonic contained structure produces several carboxylic acids such as oxalic, oxamic, malonic, maleic, glyoxylic and acetic acids, that are later oxidized to CO<sub>2</sub>, water and inorganic ions [72].

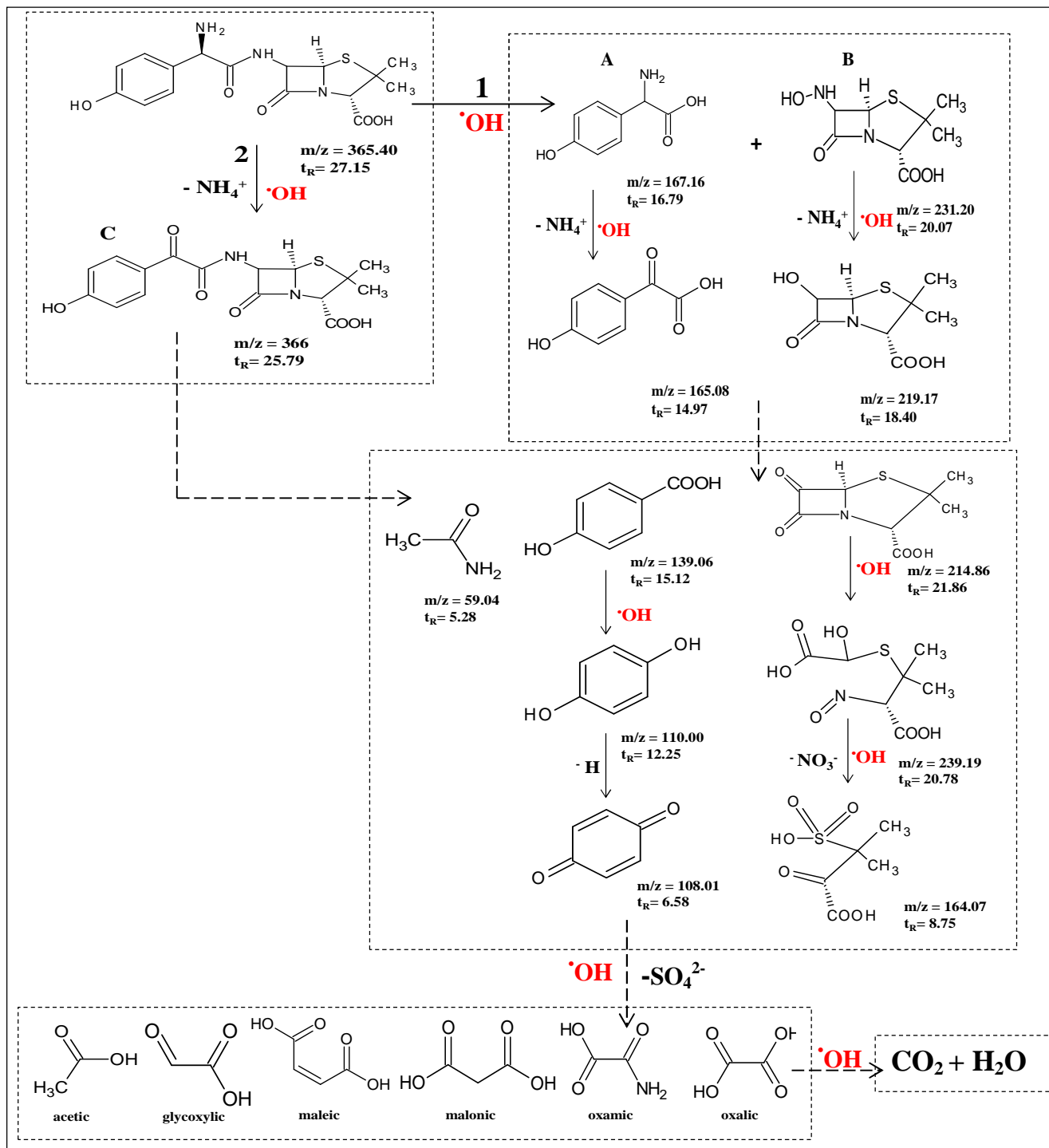
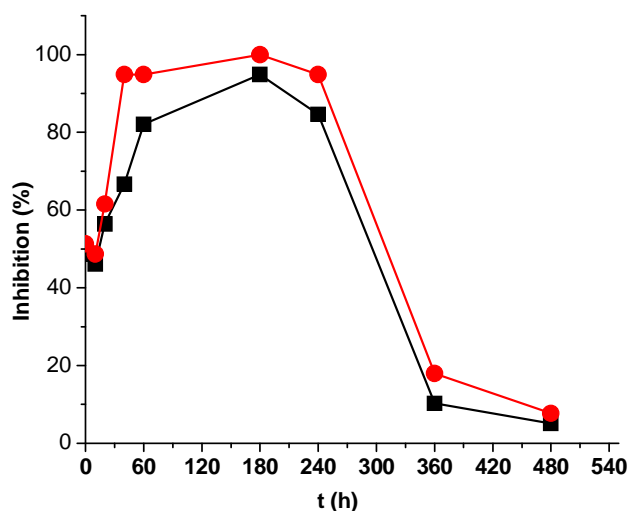


Figure 3-10 – Proposed reaction mechanism for the total mineralization of AMX by electrooxidation using Ti<sub>4</sub>O<sub>7</sub> anode.

### 3.3.5 Evolution of toxicity of AMX solution during electrooxidation treatment

The change in toxicity of 0.1 mM AMX solution over electrolysis time during electrooxidation treatment with Ti<sub>4</sub>O<sub>7</sub> anode at 120 mA was investigated by monitoring the bioluminescence inhibition of *V. fischeri* bacteria caused by the presence of AMX and its oxidation by-products. As depicted in Fig. 3-11, the bioluminescence inhibition increases at the early stages of electrolysis attaining maximum values of 100%, indicating the formation of aromatic/cyclic organics as the predominant oxidation intermediates which are more toxic than initial AMX molecule. The maximum inhibition persisted up to 240 min of electrolysis due to lower mineralization of these intermediates with Ti<sub>4</sub>O<sub>7</sub> anode, which is in agreement with the TOC decay reported in Fig. 3-6a. A sharp drop in bioluminescence inhibition follows, indicating drastic decay in toxicity owing to the further degradation of the toxic intermediates into less toxic compounds [73]. The bioluminescence inhibition attained its minimum value after 360 min of electrolysis, indicating the mineralization/degradation of both AMX and its oxidation reaction intermediates into less toxic and biodegradable short chain carboxylic acid.



**Figure 3-11**– Toxicity evolution of 0.1 mM AMX solution during electro-oxidation with Ti<sub>4</sub>O<sub>7</sub> anode at 120 mA in terms of Inhibition of luminescence of *V. fischeri* bacteria after (-■-) 5 min and (-●-) 15 min exposure time

### 3.4 Conclusions

From the above results and discussion, we can draw the following main conclusions:

- Ti<sub>4</sub>O<sub>7</sub> anode prepared by plasma deposition is an effective anode for electrooxidation of AMX solutions at its natural pH.
- The prepared anode consist only Ti<sub>4</sub>O<sub>7</sub> because all the other sub-oxides of TiO<sub>2</sub> formed during the reduction of TiO<sub>2</sub> with coke were transformed to Ti<sub>4</sub>O<sub>7</sub> during plasma deposition.
- Faster degradation and relatively high mineralization of AMX have been achieved by electrooxidation with Ti<sub>4</sub>O<sub>7</sub> anode compared to DSA and Pt anodes at similar experimental conditions. However it exhibits relatively lower performances compared to BDD anode.
- The decay of AMX always follow pseudo-first order kinetics and the apparent rate constant ( $k_{app, AMX}$ ) for oxidation of AMX increased with applied current; enhanced by *in-situ* H<sub>2</sub>O<sub>2</sub> generation and diminished with increased initial AMX concentration.
- There is a slight (10%) reduction in the activity of the prepared Ti<sub>4</sub>O<sub>7</sub> anode after 200 h of usage, possibly due to passivation.
- The major mineralization end-products after mineralization treatment at 120 mA are short-chain carboxylic and inorganic ions.
- Both aromatic intermediates and bicyclic lactamic products of AMX were identified by GC-MS. Using these data and analysis of released inorganic ions and carboxylic acid, a plausible mineralization pathway of AMX with Ti<sub>4</sub>O<sub>7</sub> anode was proposed.
- Initial AMX solution shows relatively high inhibition to *V. fischeri* bacteria, which further increased at the early stage of electrooxidation due to formation of cyclic intermediates but sharply decreased at the later stage of electrolysis.

Since the Ti<sub>4</sub>O<sub>7</sub> is produced mainly from TiO<sub>2</sub> which is very cheap and highly abundant material, this anode could be an interesting alternative in industrial wastewater treatment by electrooxidation.

**References**

- [1] B. Marselli, J. Garcia-Gomez, P.-A. Michaud, M.A. Rodrigo, C. Comninellis, Electrogeneration of hydroxyl radicals on boron-doped diamond electrodes, *J. Electrochem. Soc.* 150 (2003) D79.
- [2] C.A. Martínez-Huitle, S. Ferro, Electrochemical oxidation of organic pollutants for the wastewater treatment: direct and indirect processes, *Chem. Soc. Rev.* 35 (2006) 1324.
- [3] M. Panizza, G. Cerisola, Direct and mediated anodic oxidation of organic pollutants, *Chem. Rev.* 109 (2009) 6541–6569.
- [4] M.A. Oturan, J.-J. Aaron, Advanced oxidation processes in water/wastewater treatment: Principles and applications. A review, *Crit. Rev. Environ. Sci. Technol.* 44 (2014) 2577–2641.
- [5] P. Cañizares, A. Beteta, C. Sáez, L. Rodríguez, M.A. Rodrigo, Use of electrochemical technology to increase the quality of the effluents of bio-oxidation processes. A case studied, *Chemosphere.* 72 (2008) 1080–1085.
- [6] C.A. Martínez-Huitle, E. Brillas, Decontamination of wastewaters containing synthetic organic dyes by electrochemical methods: A general review, *Appl. Catal. B Environ.* 87 (2009) 105–145.
- [7] M. Panizza, G. Cerisola, Application of diamond electrodes to electrochemical processes, *Electrochimica Acta.* 51 (2005) 191–199.
- [8] M.A. Rodrigo, P. Cañizares, C. Buitrón, C. Sáez, Electrochemical technologies for the regeneration of urban wastewaters, *Electrochimica Acta.* 55 (2010) 8160–8164.
- [9] C. Comninellis, Electrocatalysis in the electrochemical conversion/combustion of organic pollutants for waste water treatment, *Electrochimica Acta.* 39 (1994) 1857–1862.
- [10] S. Ammar, R. Abdelhedi, C. Flox, C. Arias, E. Brillas, Electrochemical degradation of the dye indigo carmine at boron-doped diamond anode for wastewaters remediation, *Environ. Chem. Lett.* 4 (2006) 229–233.
- [11] L. Ciríaco, C. Anjo, J. Correia, M.J. Pacheco, A. Lopes, Electrochemical degradation of Ibuprofen on Ti/Pt/PbO<sub>2</sub> and Si/BDD electrodes, *Electrochimica Acta.* 54 (2009) 1464–1472.

- [12] C.A. Martínez-Huitle, A. De Battisti, S. Ferro, S. Reyna, M. Cerro-López, M.A. Quiro, Removal of the Pesticide Methamidophos from Aqueous Solutions by Electrooxidation using Pb/PbO<sub>2</sub>, Ti/SnO<sub>2</sub>, and Si/BDD Electrodes, *Environ. Sci. Technol.* 42 (2008) 6929–6935.
- [13] M.A. Quiroz, J.L. Sánchez-Salas, S. Reyna, E.R. Bandala, J.M. Peralta-Hernández, C.A. Martínez-Huitle, Degradation of 1-hydroxy-2,4-dinitrobenzene from aqueous solutions by electrochemical oxidation: Role of anodic material, *J. Hazard. Mater.* 268 (2014) 6–13.
- [14] I. Sirés, E. Brillas, G. Cerisola, M. Panizza, Comparative depollution of mecoprop aqueous solutions by electrochemical incineration using BDD and PbO<sub>2</sub> as high oxidation power anodes, *J. Electroanal. Chem.* 613 (2008) 151–159.
- [15] B. Boye, E. Brillas, B. Marselli, P.-A. Michaud, C. Comminellis, G. Farnia, G. Sandonà, Electrochemical incineration of chloromethylphenoxy herbicides in acid medium by anodic oxidation with boron-doped diamond electrode, *Electrochimica Acta.* 51 (2006) 2872–2880.
- [16] M.G. Tavares, L.V.A. da Silva, A.M. Sales Solano, J. Tonholo, C.A. Martínez-Huitle, C.L.P.S. Zanta, Electrochemical oxidation of Methyl Red using Ti/Ru<sub>0.3</sub>Ti<sub>0.7</sub>O<sub>2</sub> and Ti/Pt anodes, *Chem. Eng. J.* 204-206 (2012) 141–150.
- [17] K. Waterston, J.W. Wang, D. Bejan, N.J. Bunce, Electrochemical waste water treatment: Electrooxidation of acetaminophen, *J. Appl. Electrochem.* 36 (2006) 227–232.
- [18] A. El-Ghenymy, C. Arias, P.L. Cabot, F. Centellas, J.A. Garrido, R.M. Rodríguez, E. Brillas, Electrochemical incineration of sulfanilic acid at a boron-doped diamond anode, *Chemosphere.* 87 (2012) 1126–1133.
- [19] C. Flox, J.A. Garrido, R.M. Rodríguez, F. Centellas, P.-L. Cabot, C. Arias, E. Brillas, Degradation of 4,6-dinitro-o-cresol from water by anodic oxidation with a boron-doped diamond electrode, *Electrochimica Acta.* 50 (2005) 3685–3692.
- [20] M.F. García-Montoya, S. Gutiérrez-Granados, A. Alatorre-Ordaz, R. Galindo, R. Ornelas, J.M. Peralta-Hernández, Application of electrochemical/BDD process for the treatment wastewater effluents containing pharmaceutical compounds, *J. Ind. Eng. Chem.* 31 (2015) 238–243.

- [21] M. Muruganathan, S. Yoshihara, T. Rakuma, N. Uehara, T. Shirakashi, Electrochemical degradation of 17 $\beta$ -estradiol (E2) at boron-doped diamond (Si/BDD) thin film electrode, *Electrochimica Acta*. 52 (2007) 3242–3249.
- [22] A. Özcan, Y. Şahin, A.S. Koparal, M.A. Oturan, Protham mineralization in aqueous medium by anodic oxidation using boron-doped diamond anode: Influence of experimental parameters on degradation kinetics and mineralization efficiency, *Water Res.* 42 (2008) 2889–2898.
- [23] M.A. Rodrigo, P. Cañizares, A. Sánchez-Carretero, C. Sáez, Use of conductive-diamond electrochemical oxidation for wastewater treatment, *Catal. Today*. 151 (2010) 173–177.
- [24] X. Zhu, J. Ni, J. Wei, P. Chen, Scale-up of B-doped diamond anode system for electrochemical oxidation of phenol simulated wastewater in batch mode, *Electrochimica Acta*. 56 (2011) 9439–9447.
- [25] G. Chen, Electrochemical technologies in wastewater treatment, *Sep. Purif. Technol.* 38 (2004) 11–41.
- [26] L. Ciríaco, D. Santos, M.J. Pacheco, A. Lopes, Anodic oxidation of organic pollutants on a Ti/SnO<sub>2</sub>-Sb<sub>2</sub>O<sub>4</sub> anode, *J. Appl. Electrochem.* 41 (2011) 577–587.
- [27] B. Correa-Lozano, C. Comninellis, A. De Battisti, Service life of Ti/SnO<sub>2</sub>-Sb<sub>2</sub>O<sub>5</sub> anodes, *J. Appl. Electrochem.* 27 (1997) 970–974.
- [28] H. Lin, J. Niu, J. Xu, Y. Li, Y. Pan, Electrochemical mineralization of sulfamethoxazole by Ti/SnO<sub>2</sub>-Sb/Ce-PbO<sub>2</sub> anode: Kinetics, reaction pathways, and energy cost evolution, *Electrochimica Acta*. 97 (2013) 167–174.
- [29] Y. Samet, S.C. Elaoud, S. Ammar, R. Abdelhedi, Electrochemical degradation of 4-chloroguaiacol for wastewater treatment using PbO<sub>2</sub> anodes, *J. Hazard. Mater.* 138 (2006) 614–619.
- [30] G. Chen, E.A. Betterton, R.G. Arnold, Electrolytic oxidation of trichloroethylene using a ceramic anode, *J. Appl. Electrochem.* 29 (1999) 961–970.
- [31] K. Kolbrecka, J. Przulski, Sub-stoichiometric titanium oxides as ceramic electrodes for oxygen evolution—structural aspects of the voltammetric behaviour of Ti<sub>n</sub>O<sub>2n-1</sub>, *Electrochimica Acta*. 39 (1994) 1591–1595.
- [32] R.J. Pollock, J.F. Houlihan, A.N. Bain, B.S. Coryea, Electrochemical properties of a new electrode material, Ti<sub>4</sub>O<sub>7</sub>, *Mater. Res. Bull.* 19 (1984) 17–24.



- [33] J.R. Smith, F.C. Walsh, R.L. Clarke, [No Title], *J. Appl. Electrochem.* 28 (1998) 1021–1033.
- [34] A.A. Gusev, E.G. Avvakumov, A.Z. Medvedev, A.I. Masliy, Ceramic electrodes based on Magnéli phases of titanium oxides, *Sci. Sinter.* 39 (2007) 51–57.
- [35] F.C. Walsh, R.G.A. Wills, The continuing development of Magnéli phase titanium sub-oxides and Ebonex® electrodes, *Electrochimica Acta.* 55 (2010) 6342–6351.
- [36] D. Bejan, E. Guinea, N.J. Bunce, On the nature of the hydroxyl radicals produced at boron-doped diamond and Ebonex® anodes, *Electrochimica Acta.* 69 (2012) 275–281.
- [37] P. Geng, J. Su, C. Miles, C. Comninellis, G. Chen, Highly-ordered Magnéli Ti<sub>4</sub>O<sub>7</sub> nanotube arrays as effective anodic material for electro-oxidation, *Electrochimica Acta.* 153 (2015) 316–324.
- [38] D. Bejan, J.D. Malcolm, L. Morrison, N.J. Bunce, Mechanistic investigation of the conductive ceramic Ebonex® as an anode material, *Electrochimica Acta.* 54 (2009) 5548–5556.
- [39] A.M. Zaky, B.P. Chaplin, Mechanism of p-substituted phenol oxidation at a Ti<sub>4</sub>O<sub>7</sub> reactive electrochemical membrane, *Environ. Sci. Technol.* 48 (2014) 5857–5867.
- [40] A.M. Zaky, B.P. Chaplin, Porous substoichiometric TiO<sub>2</sub> anodes as reactive electrochemical membranes for water treatment, *Environ. Sci. Technol.* 47 (2013) 6554–6563.
- [41] T. Heberer, Occurrence, fate, and removal of pharmaceutical residues in the aquatic environment: a review of recent research data, *Toxicol. Lett.* 131 (2002) 5–17.
- [42] O.A.H. Jones, N. Voulvoulis, J.N. Lester, Human pharmaceuticals in the aquatic environment: A review, *Environ. Technol.* 22 (2001) 1383–1394.
- [43] D.W. Kolpin, E.T. Furlong, M.T. Meyer, E.M. Thurman, S.D. Zaugg, L.B. Barber, H.T. Buxton, Pharmaceuticals, hormones, and other organic wastewater contaminants in U.S. Streams, 1999–2000: A national reconnaissance, *Environ. Sci. Technol.* 36 (2002) 1202–1211.
- [44] K. Kümmerer, Antibiotics in the aquatic environment – A review – Part I, *Chemosphere.* 75 (2009) 417–434.
- [45] E. Benito-Peña, A.I. Partal-Rodera, M.E. León-González, M.C. Moreno-Bondi, Evaluation of mixed mode solid phase extraction cartridges for the preconcentration of beta-lactam

- antibiotics in wastewater using liquid chromatography with UV-DAD detection, *Anal. Chim. Acta.* 556 (2006) 415–422.
- [46] J.P. Bound, N. Voulvoulis, Pharmaceuticals in the aquatic environment—a comparison of risk assessment strategies, *Chemosphere.* 56 (2004) 1143–1155.
- [47] S.D. Costanzo, J. Murby, J. Bates, Ecosystem response to antibiotics entering the aquatic environment, *Mar. Pollut. Bull.* 51 (2005) 218–223.
- [48] R. Hirsch, T. Ternes, K. Haberer, K.-L. Kratz, Occurrence of antibiotics in the aquatic environment, *Sci. Total Environ.* 225 (1999) 109–118.
- [49] A. Pruden, Balancing water sustainability and public health goals in the face of growing concerns about antibiotic resistance, *Environ. Sci. Technol.* 48 (2014) 5–14.
- [50] E.S. Elmolla, M. Chaudhuri, Degradation of the antibiotics amoxicillin, ampicillin and cloxacillin in aqueous solution by the photo-Fenton process, *J. Hazard. Mater.* 172 (2009) 1476–1481.
- [51] C. Mavronikola, M. Demetriou, E. Hapeshi, D. Partassides, C. Michael, D. Mantzavinos, D. Kassinos, Mineralisation of the antibiotic amoxicillin in pure and surface waters by artificial UVA- and sunlight-induced Fenton oxidation, *J. Chem. Technol. Biotechnol.* 84 (2009) 1211–1217.
- [52] J.J. Pignatello, E. Oliveros, A. MacKay, Advanced oxidation processes for organic contaminant destruction based on the Fenton reaction and related chemistry, *Crit. Rev. Environ. Sci. Technol.* 36 (2006) 1–84.
- [53] A.G. Trovó, R.F. Pupo Nogueira, A. Agüera, A.R. Fernandez-Alba, S. Malato, Degradation of the antibiotic amoxicillin by photo-Fenton process – Chemical and toxicological assessment, *Water Res.* 45 (2011) 1394–1402.
- [54] R. Andreozzi, M. Canterino, R. Marotta, N. Paxeus, Antibiotic removal from wastewaters: The ozonation of amoxicillin, *J. Hazard. Mater.* 122 (2005) 243–250.
- [55] F. Javier Benitez, J.L. Acero, F.J. Real, G. Roldán, Ozonation of pharmaceutical compounds: Rate constants and elimination in various water matrices, *Chemosphere.* 77 (2009) 53–59.
- [56] E.S. Elmolla, M. Chaudhuri, Photocatalytic degradation of amoxicillin, ampicillin and cloxacillin antibiotics in aqueous solution using UV/TiO<sub>2</sub> and UV/H<sub>2</sub>O<sub>2</sub>/TiO<sub>2</sub> photocatalysis, *Desalination.* 252 (2010) 46–52.

- [57] D. Klauson, J. Babkina, K. Stepanova, M. Krichevskaya, S. Preis, Aqueous photocatalytic oxidation of amoxicillin, *Catal. Today*. 151 (2010) 39–45.
- [58] M. Panizza, A. Dirany, I. Sirés, M. Haidar, N. Oturan, M.A. Oturan, Complete mineralization of the antibiotic amoxicillin by electro-Fenton with a BDD anode, *J. Appl. Electrochem.* 44 (2014) 1327–1335.
- [59] D. Santos, M.J. Pacheco, A. Gomes, A. Lopes, L. Ciriaco, Preparation of Ti/Pt/SnO<sub>2</sub>–Sb<sub>2</sub>O<sub>4</sub> electrodes for anodic oxidation of pharmaceutical drugs, *J. Appl. Electrochem.* 43 (2013) 407–416.
- [60] F. Sopaj, M.A. Rodrigo, N. Oturan, F.I. Podvorica, J. Pinson, M.A. Oturan, Influence of the anode materials on the electrochemical oxidation efficiency. Application to oxidative degradation of the pharmaceutical amoxicillin, *Chem. Eng. J.* 262 (2015) 286–294.
- [61] I. Sirés, N. Oturan, M.A. Oturan, Electrochemical degradation of  $\beta$ -blockers. Studies on single and multicomponent synthetic aqueous solutions, *Water Res.* 44 (2010) 3109–3120.
- [62] A. Özcan, Y. Şahin, A. Savaş Kopal, M.A. Oturan, Carbon sponge as a new cathode material for the electro-Fenton process: Comparison with carbon felt cathode and application to degradation of synthetic dye basic blue 3 in aqueous medium, *J. Electroanal. Chem.* 616 (2008) 71–78.
- [63] E. Brillas, I. Sires, M.A. Oturan, Electro-Fenton process and related electrochemical technologies based on Fenton's reaction chemistry, *Chem. Rev.* 109 (2009) 6570–6631.
- [64] I. Sirés, N. Oturan, M.A. Oturan, Electrochemical degradation of  $\beta$ -blockers. Studies on single and multicomponent synthetic aqueous solutions, *Water Res.* 44 (2010) 3109–3120.
- [65] I. Sirés, N. Oturan, M.A. Oturan, R.M. Rodríguez, J.A. Garrido, E. Brillas, Electro-Fenton degradation of antimicrobials triclosan and triclocarban, *Electrochimica Acta.* 52 (2007) 5493–5503.
- [66] M.J. Martin de Vidales, M. Millán, C. Sáez, P. Cañizares, M.A. Rodrigo, What happens to inorganic nitrogen species during conductive diamond electrochemical oxidation of real wastewater?, *Electrochem. Commun.* 67 (2016) 65–68.
- [67] A. Thiam, E. Brillas, F. Centellas, P.L. Cabot, I. Sirés, Electrochemical reactivity of Ponceau 4R (food additive E124) in different electrolytes and batch cells, *Electrochimica Acta.* 173 (2015) 523–533.

- [68] E. Brillas, S. Garcia-Segura, M. Skoumal, C. Arias, Electrochemical incineration of diclofenac in neutral aqueous medium by anodic oxidation using Pt and boron-doped diamond anodes, *Chemosphere*. 79 (2010) 605–612.
- [69] A. El-Ghenmy, P.L. Cabot, F. Centellas, J.A. Garrido, R.M. Rodríguez, C. Arias, E. Brillas, Electrochemical incineration of the antimicrobial sulfamethazine at a boron-doped diamond anode, *Electrochimica Acta*. 90 (2013) 254–264.
- [70] M.A. Oturan, M. Pimentel, N. Oturan, I. Sirés, Reaction sequence for the mineralization of the short-chain carboxylic acids usually formed upon cleavage of aromatics during electrochemical Fenton treatment, *Electrochimica Acta*. 54 (2008) 173–182.
- [71] E. Brillas, S. Garcia-Segura, M. Skoumal, C. Arias, Electrochemical incineration of diclofenac in neutral aqueous medium by anodic oxidation using Pt and boron-doped diamond anodes, *Chemosphere*. 79 (2010) 605–612.
- [72] S. Garcia-Segura, E. Brillas, Mineralization of the recalcitrant oxalic and oxamic acids by electrochemical advanced oxidation processes using a boron-doped diamond anode, *Water Res.* 45 (2011) 2975–2984.
- [73] A. Dirany, I. Sirés, N. Oturan, A. Özcan, M.A. Oturan, Electrochemical treatment of the antibiotic sulfachloropyridazine: Kinetics, reaction pathways, and toxicity evolution, *Environ. Sci. Technol.* 46 (2012) 4074–4082.

## **Chapter 4**

---

# **Substoichiometric Titanium oxide ( $\text{Ti}_4\text{O}_7$ ): A New Electrode in EF Process**

This chapter has been submitted to *Electrochimica Acta* for consideration as:

Soliu O. Ganiyu, Nihal Oturan, Stéphane Raffy, Marc Cretin, Eric van Hullebusch, Giovanni Esposito, Mehmet A. Oturan (2016). Use of Sub-stoichiometric Titanium Oxide as a Ceramic Electrode in Anodic Oxidation and Electro-Fenton Degradation of the Beta-blocker Propranolol: Degradation Kinetics and Mineralization Pathway

## **CHAPTER 4**

The use of substoichiometric titanium oxide as anode material has not been reported for EF process. Studies are required to understanding the behavior and performance of this anode material in comparison with other commercially available electrode in EF process.

**Use of Sub-stoichiometric Titanium Oxide as a Ceramic Electrode in Anodic Oxidation and Electro-Fenton Degradation of the Beta-blocker Propranolol: Degradation Kinetics and Mineralization Pathway**

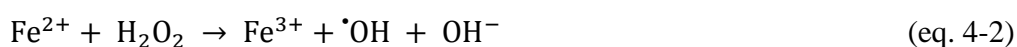
**Abstract**

Oxidative degradation of aqueous acidic solutions of the beta-blocker propranolol (PPN) has been studied by AO and for the first time by EF process using sub-stoichiometric titanium oxide ( $\text{Ti}_4\text{O}_7$ ) anode elaborated by plasma deposition. The oxidative degradation of the PPN by  $\text{Ti}_4\text{O}_7(\cdot\text{OH})$  formed at the surface of the  $\text{Ti}_4\text{O}_7$  anode and  $\cdot\text{OH}$  generated via electrochemically assisted Fenton's reaction was investigated. Decay of PPN concentration followed pseudo-first order reaction kinetics with degradation rates influenced by both applied current and initial PPN concentration. The absolute rate constant of the reaction between PPN and  $\cdot\text{OH}/\text{Ti}_4\text{O}_7(\cdot\text{OH})$  was determined by competition kinetics and found to be  $(2.99 \pm 0.02) \times 10^9 \text{ L mol}^{-1} \text{ s}^{-1}$ . Relatively high mineralization efficiency of PPN solution (82% TOC removal) was achieved by AO with  $\text{Ti}_4\text{O}_7$  anode at 120 mA after 480 min of treatment, whereas almost complete mineralization (96% TOC removal) was reached at similar conditions in EF process. Analogous EF treatment with DSA anode showed lower mineralization (89% TOC removal) compared to  $\text{Ti}_4\text{O}_7$  anode. The initial N content of PPN was mainly released as  $\text{NH}_4^+$ , with smaller proportion of  $\text{NO}_3^-$ . Aromatic intermediates such as 1-naphtol; hydroxylated 1-naphtol and phthalic acid were identified by both reversed-phase HPLC and GC-MS analyses. Oxalic, oxamic, maleic and glyoxylic acids were the main short-chain carboxylic acid detected. Based on the identified intermediates, carboxylic acids and inorganic end-products as well as TOC removal results, a plausible reaction sequence for mineralization of PPN by electrogenerated hydroxyl radicals was proposed.

**Keywords:** Propranolol; Degradation kinetics; Sub-stoichiometric titanium oxide; Plasma deposition; Anodic oxidation; Electro-Fenton; Mineralization

#### 4.1 Introduction

EAOPs are eco-friendly  $\cdot\text{OH}$ -mediated electrochemical treatments in which organic pollutants are non-selectively destroyed by *in-situ* electrochemically generated hydroxyl radical ( $\cdot\text{OH}$ ). These radicals are formed either at the anode surface from water discharge reaction (eq. 4-1) [1–4], or in the bulk of the solution *via* Fenton's reaction (eq. 4-2) between externally added catalyst ( $\text{Fe}^{2+}$ ) and *in situ* electrogenerated  $\text{H}_2\text{O}_2$  [5–9].



In the absence of ferrous iron in the solution, the process is called AO. This process is effective with high  $\text{O}_2$  evolution overpotential anodes (M) such as  $\text{PbO}_2$  or BDD. When using cathodes such as CF that promotes generation of  $\text{H}_2\text{O}_2$ , it is named AO- $\text{H}_2\text{O}_2$  [10–12].

In EF process, homogeneous  $\cdot\text{OH}$  are generated from electrochemically assisted Fenton's reaction (eq. 4-2). The Fenton's reagent (*i.e.*  $\text{H}_2\text{O}_2 + \text{Fe}^{2+}$ ) is continuously electro-generated/regenerated in the solution by 2-electron reduction of dissolved oxygen (eq. 4-3) and 1-electron reduction of  $\text{Fe}^{3+}$  (eq. 4-4) formed by Fenton's reaction, respectively, at the cathode [13–15]. As such only small quantity of  $\text{Fe}^{2+}$  is required to catalyze the Fenton's reaction.



Hydroxyl radical is the second strongest oxidant after fluorine with very high standard redox potential ( $E^{\circ}_{(\cdot\text{OH}/\text{H}_2\text{O})} = 2.80 \text{ V/SHE}$ ) [16]. Therefore  $\cdot\text{OH}/\text{M}(\cdot\text{OH})$  are able to oxidize organics efficiently, till complete mineralization (*i.e.* transformation to  $\text{CO}_2$ ) [6,17].

EF process is considered more efficient compared to AO because oxidation of organics may occur at the anode surface in addition to the homogeneously generated  $\cdot\text{OH}$  in bulk, depending on the nature of anode material used [18–20]. In fact, when a high  $\text{O}_2$  over



potential anode such as BDD, doped SnO<sub>2</sub> or β-PbO<sub>2</sub> is used, heterogeneous hydroxyl radicals (M(•OH)) are formed at the surface of anode, which have been found to be more effective in mineralization of Fe-carboxylic complexes formed during the EF process, which are highly resistant to oxidation by homogeneous •OH in the bulk [6,21]. On the other hand, the use of “active anode” materials such as DSA, Pt and carbon based anodes, usually results in partial mineralization of organic pollutants due to the limited generation of M(•OH) at these anode surfaces [20,22]. However, BDD is highly expensive compared to DSA and carbon based anodes, while the use of β-PbO<sub>2</sub> poses high risk of lead contamination *via* chemical leaching and Ti/SnO<sub>2</sub> based electrodes has relatively short service life, even when doped with antimony or cerium [2,23].

Sub-stoichiometric titanium oxides ceramic electrodes, developed in late 80's, could represent a cost effective and efficient alternative anode materials for electrochemical wastewater treatment applications due to their promising characteristic and inexpensive production route [24]. In fact, these electrodes are relatively robust in aggressive media, exhibit high electrical conductivity at room temperature and excellent stability with respect to water oxidation and reduction under anodic (> 2 V *vs* SCE) and cathodic (~ -1.4 V *vs* SCE), swept respectively, especially Ti<sub>4</sub>O<sub>7</sub> [25,26]. They are solely prepared from TiO<sub>2</sub>, one of the most abundant feed-stocks available on planet, thus they are less expensive materials compared to BDD, Pt or DSA [24,27]. Ti<sub>4</sub>O<sub>7</sub> electrode is a “non-active” electrode like BDD which generates M(•OH) *via* water oxidation (Eq. 4-1) [28,29]. Therefore, the mineralization of refractory carboxylic acid complex by Ti<sub>4</sub>O<sub>7</sub>(•OH) is possible when this electrode is used in EF process. Few studies have reported the potential of this material as electrode in electrooxidation of organic pollutants [27,30–32], but it has not been tested in EF process. This is understandable because EF process is carried out at acidic pH (pH~3) which can be detrimental to the stability of this material. More so, the formation of yellowish Ti(H<sub>2</sub>O<sub>2</sub>)<sub>4</sub> complex is paramount at this pH due to partial dissolution of titanium oxides, with titanium reacts with H<sub>2</sub>O<sub>2</sub> and thus inhibiting the Fenton's reaction (eq. 4-2).

However, our previous study [33] have shown that plasma deposited Ti<sub>4</sub>O<sub>7</sub> is highly stable and does not form complex with H<sub>2</sub>O<sub>2</sub> at circumneutral pH (5.8) when tested in anodic oxidation with *in-situ* H<sub>2</sub>O<sub>2</sub> generation (*i.e.* AO-H<sub>2</sub>O<sub>2</sub>) because of high adhesion of

the thin coated on the Ti substrate. The high temperature of the “plasma plume” (10 000 – 15 000 °C) *via* which Ti<sub>4</sub>O<sub>7</sub> was deposited ensures deep fusion/penetration into substrate surface and enhance its sealing and stability.

PPN is one of the common beta adrenergic antagonists (beta-blockers) pharmaceutical used in treatment of cardiac arrhythmias, hypertension, anxiety therapies, angina, as well as in veterinary medicine; and sometimes used illegally as doping agent in many sports [34,35]. It is also among most frequently detected beta-blockers in aquatic environment [36]. The major source of PPN in wastewater includes private household, pharmaceutical plant wastewater, livestock impoundments as well as effluents from hospitals and retirement homes [37]. Natural remediation paths such as sorption, biodegradation, hydrolysis and photodegradation may attenuate the concentration of PPN in aquatic environment, but studies have shown that it has high degree of persistence and bioaccumulation in water bodies [39,40]. Ecotoxicology studies indicate that aquatic organisms show high sensitivity to PPN [41]. It can affect cardiac rhythm, generate abnormalities or causes reproductive impairment in fish, Japanese medaka (*Oryzias latipes*) and had specific toxicity towards plankton and green algae [42–44]. Additionally, there are several evidences on the additive effects of PPN, which means that even at low concentration, it might contribute to the global toxic potential of the total compounds in the aquatic environment [42].

Advanced oxidation processes (AOPs) such as ozonation or ozone/Fe<sup>2+</sup> [45,46], pulse and  $\gamma$  radiolysis [47], ferrate (VI) oxidation [48], solar or UV photolysis [49] and solar or UV TiO<sub>2</sub> photocatalysis [50,51] have been reported to achieve good degradation but relatively poor mineralization of PPN in aqueous solution. On the other hand, better mineralization of PPN was obtained with EAOPs treatments [17,52].

In this study, we investigated for the first time the potential of Ti<sub>4</sub>O<sub>7</sub> as a suitable anode in EF degradation of aqueous solutions of PPN using CF cathode. The effect of applied current and initial concentration on the degradation rate and mineralization of PPN solution were carefully studied. Comparative studies under anodic oxidation and EF using Ti<sub>4</sub>O<sub>7</sub> and DSA anodes were investigated on both degradation of PPN and mineralization of

its aqueous solution. Aromatic intermediates, short-chain carboxylic acids as well as inorganic ions formed during the treatment were detected and quantified by chromatographic techniques and based on these intermediates and end-products, a plausible mineralization pathway was proposed.

## 4.2 Experimental

### 4.2.1 Chemicals

Analytical grade (>99% purity) propranolol hydrochloride,  $C_{16}H_{21}NO_2$ , was purchased from Aldrich and used without further purification. Para-hydroxybenzoic acid (pHBA) (99.5%), anhydrous sodium sulfate (99%), potassium sulfate (99%) and iron II sulfate heptahydrate (99.5%) were supplied by Aldrich, Acros organics and Chimie-Plus. Methanol (HPLC grade, Aldrich), sulfuric (98%, Acros organics), phosphoric (85%, Aldrich) and acetic acids (glacial p.a., Acros organic) were obtained as reagent grade. Ammonium oxalate (99%) and sodium nitrate (99.5%) were obtained from Merck and Aldrich. Oxalic, oxamic, glyoxylic, and maleic acids were analytic grade supplied by Acros organics, Fluka and Alfa Aesar. All solutions were prepared with ultra-pure water obtained from a Millipore Milli-Q system with resistivity > 18 M $\Omega$  cm at 25 °C.

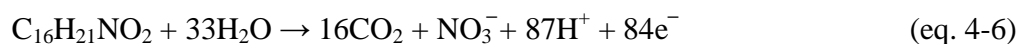
### 4.2.2 Instruments and analytical procedures

The solution pH was measured with a CyberScan pH 1500 pH-meter from Eutech Instruments. Electrolyses were performed with a Hameg HM7042-5 triple power supply at constant current. The decay of dissolved organic carbon, which is considered as TOC was used in assessing the mineralization of the PPN solutions. This analytical parameter was measured with a Shimadzu VCSH TOC analyzer. Reproducible TOC values with an accuracy of  $\pm 2\%$  were determined using the non-purgeable organic carbon method.

The TOC data obtained were then used to estimate the MCE (%) for each treated solution at a given electrolyses time  $t$  (h) using the following equation [6]:

$$\text{MCE (\%)} = \frac{n F V_s \Delta(\text{TOC})_{\text{exp}}}{4.32 \times 10^7 m I t} \cdot 100 \quad (\text{eq. 4-5})$$

where  $F$  is the Faraday constant ( $96\,487 \text{ C mol}^{-1}$ ),  $V_s$  is the solution volume (L),  $\Delta(\text{TOC})_{\text{exp}}$  is the experimental TOC decay ( $\text{mg L}^{-1}$ ),  $4.32 \times 10^7$  is a conversion factor ( $=3,600 \text{ s h}^{-1} \times 12,000 \text{ mg of C mol}^{-1}$ ),  $m$  is the number of carbon atoms of PPN (16 C atoms) and  $I$  is the applied current (A). The number of electrons ( $n$ ) consumed per each molecule of PPN was taken as 84 assuming that PPN completely mineralized into  $\text{CO}_2$  and  $\text{NO}_3^-$  as primary and main inorganic ions (eq. 4-6). The overall reaction can be written as follows:



The decay kinetics of PPN and the evolution of its aromatic intermediates were followed by reversed-phase HPLC using a Merck Lachrom liquid chromatograph, equipped with a L-7100 pump, fitted with a Purospher RP-18,  $5 \mu\text{m}$ ,  $25 \text{ cm} \times 4.6 \text{ mm}$  (i.d) column at  $40 \text{ }^\circ\text{C}$  and a L-7455 photodiode array detector selected at a wavelength of  $232 \text{ nm}$ .  $20 \mu\text{L}$  aliquots were injected into the HPLC setup with isocratic elution of the column by a mixture of methanol (pH 3) – water (pH 3) (both adjusted by  $1 \text{ M H}_3\text{PO}_4$ ) at 40:60 (v/v) as the mobile phase at  $0.4 \text{ mL min}^{-1}$  for PPN decay kinetics, aromatic intermediates and the determination of the absolute rate constant ( $k_{\text{abs}}$ ) of oxidation of PPN by hydroxyl radicals. Short-chain carboxylic acids were identified and quantified by ion-exclusion HPLC using  $1.0 \text{ mM H}_2\text{SO}_4$  as mobile phase at  $0.2 \text{ mL min}^{-1}$  and detection wavelength of  $210 \text{ nm}$ .

The ammonium and nitrate ions released during the electrolyses were detected and quantified by ion chromatography (IC) (Dionex-100) system coupled with a conductimetric detector (Dionex- DS6) operating at  $35 \text{ }^\circ\text{C}$ . A cation (IonPac<sup>®</sup> CS12A- Dionex ( $25 \text{ cm} \times 4 \text{ mm}$ )) and an anion (IonPac<sup>®</sup> AS14-Dionex ( $25 \text{ cm} \times 4 \text{ mm}$ )) exchanger column were used for ammonium and nitrate analyses, respectively. In both cases,  $50 \mu\text{L}$  samples were injected into IC. The mobile phase was composed of  $1.8 \text{ mM Na}_2\text{CO}_3$  and  $1.7 \text{ mM NaHCO}_3$  at  $2.0 \text{ mL min}^{-1}$ , and  $9.0 \text{ mM H}_2\text{SO}_4$  at  $1.0 \text{ mL min}^{-1}$  for anionic and cationic column, respectively.

Aromatic intermediates formed after 20 min of EF treatment of 0.3 mM PPN solution at 60 mA were identified by Thermo Scientific GC-MS analyzer equipped with a Trace-1300 series GC coupled to an ISQ-Single Quadrupole MS operating in electron impact mode at 70 eV. To obtain samples for GC-MS, organic components of 10 cm<sup>3</sup> of electrolyzed solution were solvent extracted by 45 cm<sup>3</sup> of ethylacetate (three extractions with 15 cm<sup>3</sup> each), followed by drying of the organic fraction over 2 g of MgSO<sub>4</sub>, filtered and concentrated to a volume of 1 cm<sup>3</sup> with a rotary evaporator under vacuum. The samples were directly analyzed using a TG-5MS 0.25 μm, 30 cm × 0.25 mm (i.d.) column, with a temperature of 50 °C for 3 min and a temperature ramp of 10 °C min<sup>-1</sup> up to 250 °C and 4 min hold time. The injector and detector temperatures were 200 and 250 °C, respectively, and helium was used as carrier gas at a flow rate of 1.5 mL min<sup>-1</sup>. The mass spectra were identified by Xcalibur data library.

#### 4.2.3 Electrolytic systems

Experiments were performed in a 250 mL undivided cylindrical glass cell (6 cm diameter) equipped with two electrodes and vigorously stirred with PTFE magnetic bar during treatment to ensure homogenization of the solution and mass transport of the reactants towards the electrodes. Two anode materials both of 24 cm<sup>2</sup> surface area: Ti<sub>4</sub>O<sub>7</sub> (4 cm × 6 cm thin film plasma deposited on Ti alloy, Saint Gobain, France), and commercial DSA (4 cm × 6 cm mixed metal oxide Ti/RuO<sub>2</sub>-IrO<sub>2</sub>) from Baoji Xinyu GuangJiDian Limited Liability Company, China) were studied. The cathode was a tri-dimensional, large surface area CF (14 cm × 5 cm × 0.5 cm, Carbone-Lorraine, France). In all cases, the anode was centered in the electrolytic cell and was surrounded by the cathode, which covered the inner wall of the cell. The solution was continuously saturated with O<sub>2</sub> by bubbling compressed air at atmospheric pressure through a frit at about 1 L min<sup>-1</sup>, starting 10 min before electrolyses to attain a steady O<sub>2</sub> concentration. In-situ production of H<sub>2</sub>O<sub>2</sub> was ensured in all the experiments by 2e<sup>-</sup> reduction of dissolved O<sub>2</sub> in the solution (eq. 4-3).

For EF experiments, 0.1 mM  $\text{Fe}^{2+}$  in form of solid  $\text{FeSO}_4 \cdot 7\text{H}_2\text{O}$  was added into the solution as catalyst. Electrolyses were performed at room temperature ( $23 \pm 2$ ) °C with 230 mL synthetic aqueous acidic solutions (pH 3) containing 0.1 mM of propranolol in 0.05 M  $\text{Na}_2\text{SO}_4$  as a supporting electrolyte, under the application of a constant current in the range of 10 – 120 mA. All experiments were performed in duplicate and the medium values (with standard deviation less than 10%) were used for building figures.

### 4.3 Results and discussion

#### 4.3.1 Comparative mineralization of PPN solution by AO and EF processes

The effectiveness of  $\text{Ti}_4\text{O}_7$  as a suitable ceramic anode was tested in AO and EF processes by electrolyzing a 0.1 mM ( $19.2 \text{ mg L}^{-1}$  TOC) PPN solution at pH 3. Fig. 4-1 shows the decay of TOC over electrolysis time. The AO experiment performed at 60 mA with the commercial DSA anode shows poor mineralization of PPN (curve a) solution, which only attained 46% TOC removal after 480 min of electrolysis, whereas study with  $\text{Ti}_4\text{O}_7$  anode led to a relatively high mineralization of PPN solution (curve b) with approximately 72% TOC removal at analogous experimental conditions, indicating its higher oxidation power compared to DSA anode. As a non-active anode, it has much greater potential for the generation of large quantities of  $\text{M}(\cdot\text{OH})$  compared to active anodes such as DSA [30]. A further increase in applied current to 120 mA yielded much better mineralization with  $\text{Ti}_4\text{O}_7$  anode (curve c), attaining 82% TOC removal after 480 min of electrolysis. This can be explained by the concomitant production of greater amount of  $\text{Ti}_4\text{O}_7(\cdot\text{OH})$  from water oxidation reaction (eq. 4-1), which can quickly oxidize both PPN and its organic intermediates when using a non-active anode [53]. The superiority of EF process compared to AO can be seen in curve d; the experiment performed at 60 mA using  $\text{Ti}_4\text{O}_7$  anode showed an excellent mineralization rate ( $> 93\%$  TOC removal) compared to AO using either  $\text{Ti}_4\text{O}_7$  or DSA anode at the same current. The accelerated TOC decay observed in EF process using  $\text{Ti}_4\text{O}_7$  anode can be explained by the production of higher amount of homogeneous  $\cdot\text{OH}$  in the bulk solution from the electrocatalytically induced

Fenton's reaction (eq. 4-2) in addition to  $\text{Ti}_4\text{O}_7$  ( $\cdot\text{OH}$ ) generated at the  $\text{Ti}_4\text{O}_7$  surface. Additionally, the presence of  $\cdot\text{OH}$  generated in the bulk ensure easy interaction between the PPN molecules and the oxidants, thus minimizing the influence of mass transport of pollutant towards anode since the oxidants are produced in the bulk of solution and not affected by mass transfer to the anode surface or its vicinity as in the case of AO treatment [18,52,54]. Further comprehensive studies with  $\text{Ti}_4\text{O}_7$  and DSA anode were performed under EF condition since the efficiency of EF process in terms of TOC removal was far better than AO counterpart.

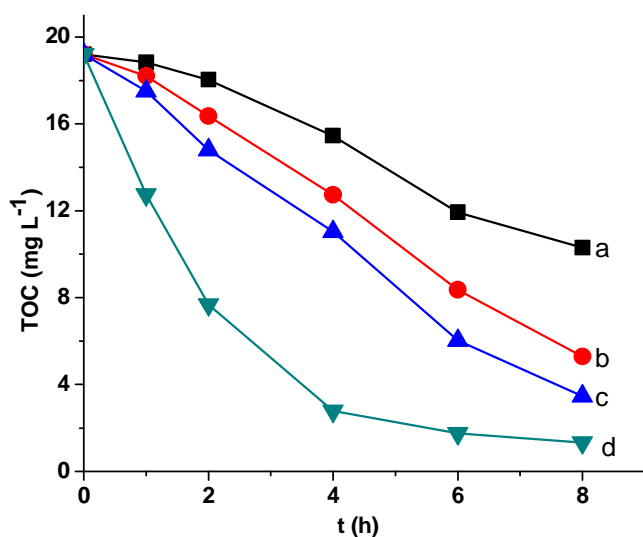


**Figure 4-1**– Decay of the TOC vs electrolysis time during the degradation of 0.1 mM PPN (corresponding to  $19.2 \text{ mg L}^{-1}$  initial TOC) in  $0.05 \text{ M Na}_2\text{SO}_4$  solution at pH 3 by anodic oxidation (a-c) and electro-Fenton (d) using (a) DSA and (b-d)  $\text{Ti}_4\text{O}_7$  anode. Current: (a, b, and d) 60 mA, and (c) 120 mA.

The effect of applied current on the mineralization of PPN during EF treatment with either  $\text{Ti}_4\text{O}_7$  or DSA anode is shown in Fig. 4-2. It was apparent from Fig. 4-2 that a high current led to a quicker mineralization of PPN regardless of the anode material used. For instance after 480 min of electrolysis using  $\text{Ti}_4\text{O}_7$  anode, the percentage TOC removal increases from 46% to 83% when the applied current was increased from 10 to 30 mA (Fig. 4-2a). Almost complete mineralization ( $\sim 93\%$  TOC removal) was obtained when the

current was raised to 60 mA, indicating the potential of EF for complete decontamination of PPN solution. The increase in applied current accelerates the formation of Ti<sub>4</sub>O<sub>7</sub>(<sup>•</sup>OH) (eq. 4-1) and ensures faster electrogeneration of H<sub>2</sub>O<sub>2</sub> (eq. 4-3) and regeneration of Fe<sup>2+</sup> (eq. 4-4) which in turn accelerates <sup>•</sup>OH production as main oxidant [53,55]. However, further increase in current to 120 mA showed only marginal enhancement (*i.e.* 96% TOC removal at 120 mA), suggesting that mass transport of oxygen and iron ions towards the cathode determines the oxidation rate at high current [52]. Comparative studies with DSA anode shows similar trends (Fig. 4-2b) but with lower mineralization rate compared to trial performed with Ti<sub>4</sub>O<sub>7</sub> anode. For example, after 480 min of electrolysis, TOC removal of 43, 74, 83 and 89% were obtained for 10, 30, 60 and 120 mA respectively. Since similar amount of homogeneous <sup>•</sup>OH is expected to be generated from Fenton's reaction (eq. 4-2) in the bulk solution at analogous conditions, the greater TOC removal observed at all current studied with Ti<sub>4</sub>O<sub>7</sub> anode indicates the contribution and effectiveness of Ti<sub>4</sub>O<sub>7</sub>(<sup>•</sup>OH) in mineralizing the by-products compared to DSA(<sup>•</sup>OH). Fig. 4-2c and 4-2d depicted corresponding mineralization current efficiency (MCE) calculated from eq. 4-5 obtained for the above trials. For all trials, a progressive fall in MCE with time and applied current was observed for both Ti<sub>4</sub>O<sub>7</sub> and DSA anodes, indicating a gradual loss of the oxidation ability of the EF process. This phenomenon can be explained by the formation of highly resistant short-chain organic by-products such as carboxylic acids that are hardly oxidized and the depletion in organic matter concentration in the electrolytic cell which limit mass transport and enhance the parasitic reactions [56,57].



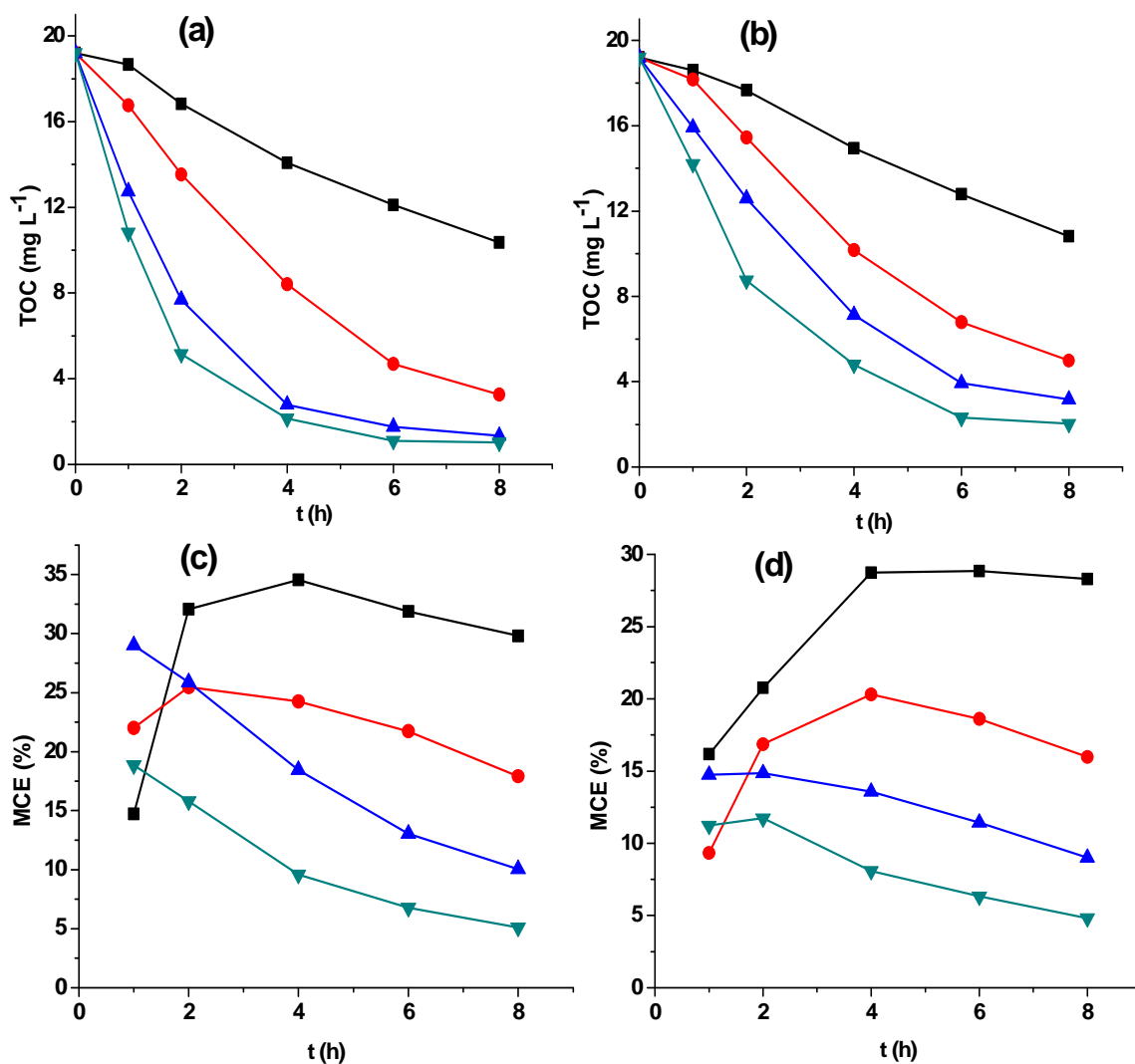


**Figure 4-2** – Effect of applied current on the decay of TOC (a, b) and mineralization current efficiency (MCE) (c, d) vs electrolysis time for the mineralization of 0.1 mM PPN (19.2 mg L<sup>-1</sup> initial TOC) in 0.05 M Na<sub>2</sub>SO<sub>4</sub> with 0.1 mM Fe<sup>2+</sup> at pH 3 using (a, c) Ti<sub>4</sub>O<sub>7</sub> and (b, d) DSA anodes at applied current of (■) 10 mA, (●) 30 mA, (▲) 60 mA, and (▼) 120 mA.

Fig. 4-3 shows the influence of initial concentration on PPN mineralization studied at 60 mA for 0.05, 0.1 and 0.2 mM PPN solutions using Ti<sub>4</sub>O<sub>7</sub> anode. Almost similar mineralization rates were observed at lower PPN concentrations (0.05 and 0.1 mM) (Fig. 4-3a), whereas the rate slightly diminishes at high concentration (0.2 mM) even though larger amount of TOC (~34 mg L<sup>-1</sup>) was removed as shown in the inset panel (Fig 4-3a). This

implies that EF with Ti<sub>4</sub>O<sub>7</sub> anode can be effectively used even for high organic content wastewater. It must be noted that at higher pollutant concentration, there is limited enhancement of parasitic reactions which usually consumes  $\cdot\text{OH}$  because the larger number of organic molecules that are available ensure maximum interaction with the oxidizing species. For this reason, a more efficient process is usually obtained when treating solutions with higher amount of organic pollutants as depicted by the calculated MCE (Fig. 4-3b) [52].

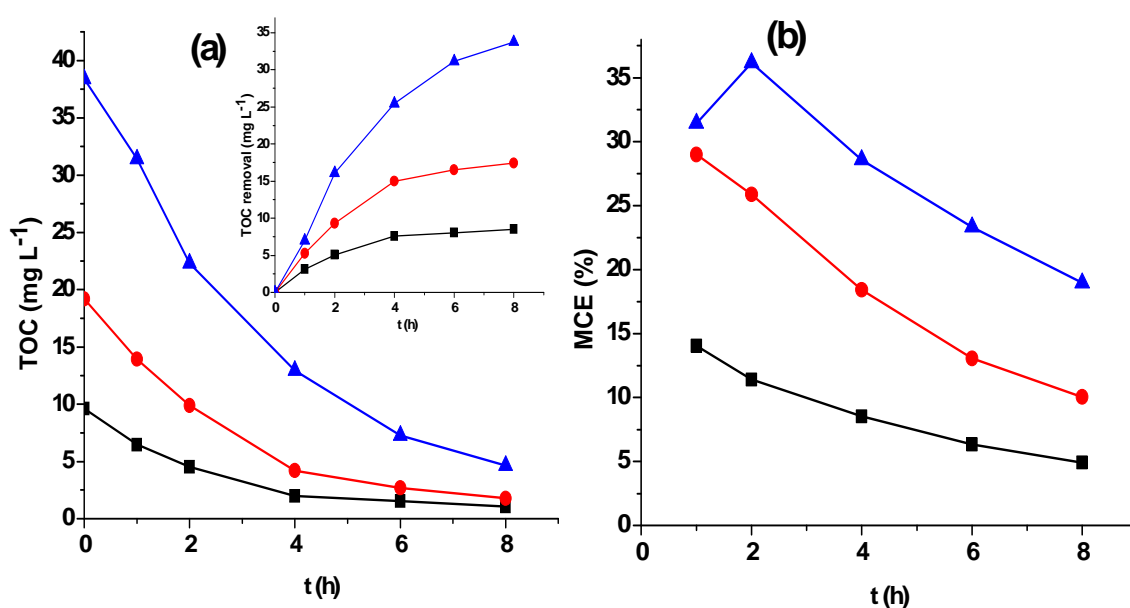


**Figure 4-3** – Effect of initial PPN concentration on the decay of TOC (a) and mineralization current efficiency (MCE) (b) vs electrolysis time for the mineralization of PPN in 0.05 M Na<sub>2</sub>SO<sub>4</sub> with 0.1 mM Fe<sup>2+</sup> using Ti<sub>4</sub>O<sub>7</sub> anode and applied current of 60 mA; (■) 0.05 mM (9.6 mg L<sup>-1</sup> TOC), (●) 0.1 mM (19.2 mg L<sup>-1</sup> TOC), and (▲) 0.2 mM (38.4 mg L<sup>-1</sup> TOC).

#### 4.3.2 Degradation kinetics of PPN

The decay of the PPN concentration over electrolysis time studied at different conditions was followed by reversed phase HPLC, which displayed a well-defined symmetric peak corresponding to PPN at  $t_R = 9.5$  min. Fig. 4-4 shows the effect of some

operation parameters on the PPN concentration decay during electrochemical treatment using CF cathode and either Ti<sub>4</sub>O<sub>7</sub> or DSA anode. Firstly, the effect of type of applied EAOPs (*i.e.* AO-H<sub>2</sub>O<sub>2</sub> vs EF) was assessed by electrolyzing 0.1 mM (29.6 mg L<sup>-1</sup>) PPN solution containing 0.05 M Na<sub>2</sub>SO<sub>4</sub> at pH 3 without Fe<sup>2+</sup> (AO – H<sub>2</sub>O<sub>2</sub>) or with 0.1 mM Fe<sup>2+</sup> as catalyst (EF) using Ti<sub>4</sub>O<sub>7</sub> anode at 60 mA. As shown in Fig. 4-4a, a slow decay in PPN concentration was observed in AO-H<sub>2</sub>O<sub>2</sub> with total destruction of PPN achieved after 60 min of electrolysis, whereas much quicker degradation rate was obtained in EF process with just 10 min required for total disappearance of PPN. As explained in section 4.3.1, the concurrent generation of <sup>•</sup>OH both at the surface of Ti<sub>4</sub>O<sub>7</sub> anode and in bulk ensures faster degradation in EF process compared to AO-H<sub>2</sub>O<sub>2</sub> where the oxidant is only generated and confined at the anode surface.

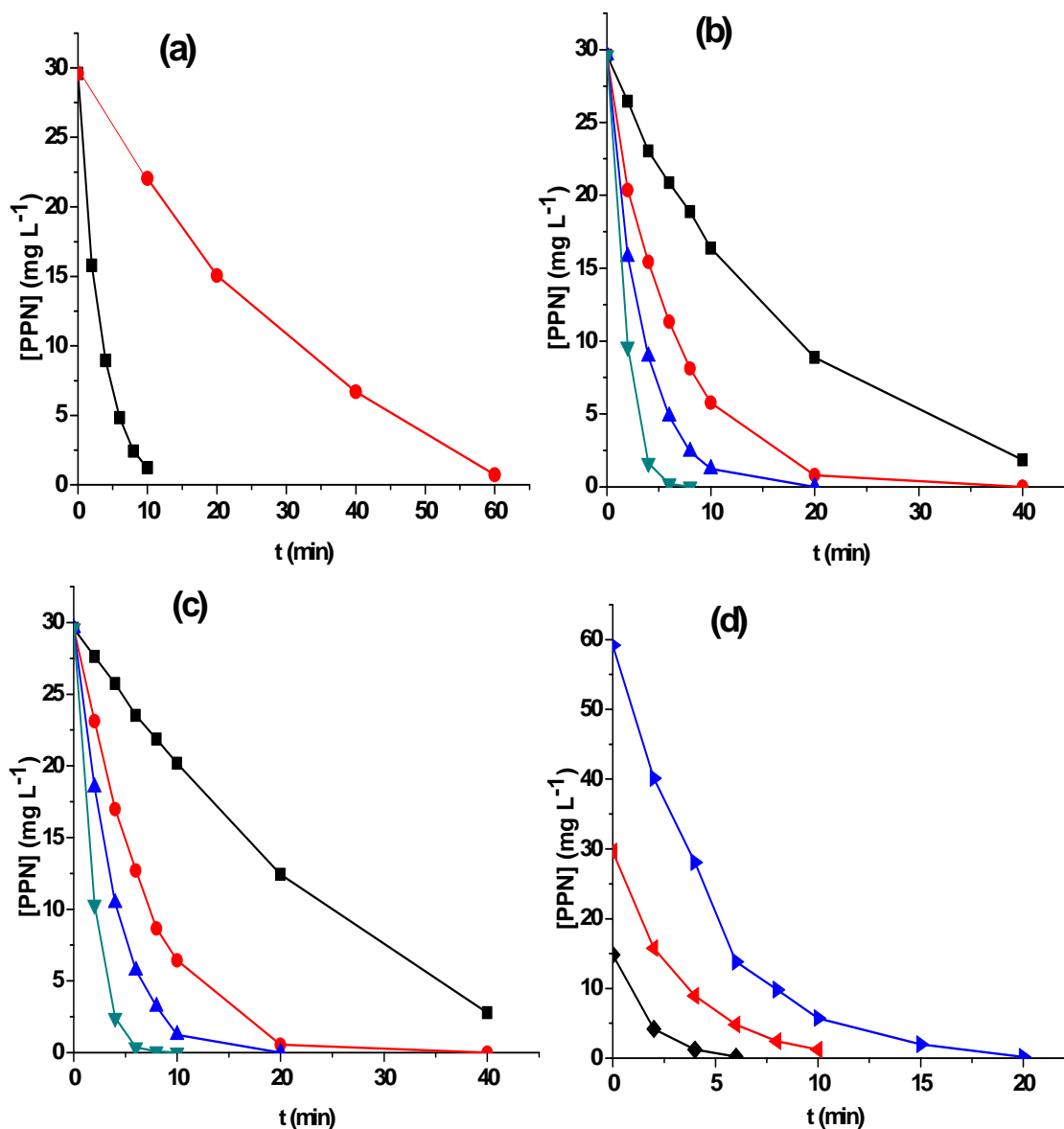


**Figure 4-4** – (a) Decay of PPN concentration vs electrolysis time for the treatment of 0.1 mM PPN at 60 mA and pH 3 using Ti<sub>4</sub>O<sub>7</sub> anode, (■) EF and (●) AO-H<sub>2</sub>O<sub>2</sub>; (b, c) effect of current and (d) effect of initial PPN concentration on the decay of PPN concentration vs electrolysis time for the EF treatment at pH 3 using (b) Ti<sub>4</sub>O<sub>7</sub>, (c) DSA anodes at initial concentration of 0.1 mM and applied current of (■) 10 mA, (●) 30 mA, (▲) 60 mA, and (▼) 120 mA; and (d) Ti<sub>4</sub>O<sub>7</sub> anode at applied current of 60 mA and initial concentration of (◆) 0.05 mM, (◄) 0.1 mM and (►) 0.2 mM.

The influence of applied current on the degradation of 0.1 mM PPN solution by EF process is shown in Fig. 4-4b and 4-4c for Ti<sub>4</sub>O<sub>7</sub> and DSA anodes respectively. Oxidative degradation kinetics of PPN is significantly enhanced by increasing the applied current from 10 mA to 120 mA and a shorter time was required for the complete destruction of PPN at high current in all treatment as expected from the accelerating rate of water oxidation and Fenton's reactions (eq. 4-1 and 4-2), generating greater quantities of Ti<sub>4</sub>O<sub>7</sub>(<sup>•</sup>OH) and <sup>•</sup>OH. Almost similar electrolysis time of 60, 20, and 10 min was required for complete oxidation of PPN when working at 10, 30 and 60 mA for treatment with both Ti<sub>4</sub>O<sub>7</sub> and DSA anodes. However, oxidation of PPN was slightly faster with Ti<sub>4</sub>O<sub>7</sub> compared with DSA anode at 120 mA with total PPN disappearance attained after 6 and 8 min respectively for Ti<sub>4</sub>O<sub>7</sub> and DSA anodes. This implies that the oxidation of PPN in EF process was predominantly by homogeneously generated <sup>•</sup>OH in the bulk (eq. 4-2), which results in similar decay rate observed with both anodes at lower applied current because at analogous conditions similar quantity of <sup>•</sup>OH is generated in EF process regardless of the anode materials used as stated in section 4.3.1. Further, at high applied current values, the rise in current did not yield proportional increase in degradation rate. This can be explained by the progressive enhancement of parasitic reactions like H<sub>2</sub> evolution at the cathode, H<sub>2</sub>O<sub>2</sub> decomposition and M(<sup>•</sup>OH) self-destruction at the anode [54,58], which reduces the oxidation rate during the treatment.

Fig. 4-4d shows the effect of initial concentration on PPN decay assessed by electrolyzing 0.05, 0.1 and 0.2 mM PPN solutions at 60 mA using EF process with 0.1 mM Fe<sup>2+</sup> and Ti<sub>4</sub>O<sub>7</sub> anode. A faster degradation was obtained for the treatment of 0.05 mM (14.8 mg L<sup>-1</sup>), with complete disappearance after just 6 min compared to 10 min required for 0.1 mM. In contrast, a longer time (20 min) was required for higher concentration of 0.2 mM (59.2 mg L<sup>-1</sup>), indicating reduction in degradation rate at higher concentration. This is expected since similar quantity of oxidants are generated in all cases and the oxidants interact with more PPN molecules as well as its generated organic intermediates at higher initial concentration due to non-selectivity of hydroxyl radicals [52].

For all trials, the oxidation of PPN with hydroxyl radicals was fitted by pseudo first-order kinetics assuming a quasi-stationary state for  $\cdot\text{OH}$  concentration.

$$v = -\frac{d[\text{PPN}]}{dt} = k_{abs,PPN}[\cdot\text{OH}][\text{PPN}] \quad (\text{eq. 4-7})$$

The kinetic analysis of the corresponding semi-logarithm plots by linear regression gives the apparent rate constants ( $k_{app,PPN}$ ) with excellent correlation coefficients ( $R^2 \approx 0.99$ ), which is summarized in Table 4-1. As can be seen in Table 4-1, the  $k_{app,PPN}$  values were enhanced at high current, lower initial PPN concentration as well as the presence of  $\text{Fe}^{2+}$  catalyst in the case of EF process. The contribution of  $\text{Ti}_4\text{O}_7(\cdot\text{OH})$  to the PPN degradation during EF process is also obvious with  $\text{Ti}_4\text{O}_7$  anode, in which the  $k_{app,PPN}$  values are slightly higher compared to DSA anode for all current studied. As mentioned earlier, the gradual enhancement of parasitic reactions at higher currents results in non-proportional increase in  $k_{app,PPN}$  observed as current increases.

**Table 4-1** –Apparent rate constants ( $k_{app,PPN}$ ) for the electrochemical degradation of PPN by  $\cdot\text{OH}$  assuming pseudo first-order reaction.

Electrolytic cell	[PPN] (mM)	[Fe <sup>2+</sup> ] (mM)	I (mA)	$k_{app,PPN} \times 10^1$
Ti <sub>4</sub> O <sub>7</sub> /CF	0.5	0.1	60	6.70
	0.1	0.1	10	0.60
	0.1	0.1	30	1.74
	0.1	0.1	60	3.08
	0.1	0.1	120	7.76
	0.1	–	10	0.07
	0.1	–	30	0.21
	0.1	–	60	0.36
	0.1	–	120	0.65
	0.2	0.1	60	2.27
DSA/CF	0.1	0.1	10	0.41
	0.1	0.1	30	1.49
	0.1	0.1	60	2.93
	0.1	0.1	120	7.10

The absolute rate constant for the oxidation of PPN by hydroxyl radicals ( $k_{abs,PPN}$ ) was determined by competition kinetics experiments performed at 30 and 60 mA with a solutions containing equimolar concentrations of PPN and pHBA (0.1 mM) as the standard competitor. The values of  $k_{abs,PPN}$  at 30 and 60 mA were determined to be  $2.96 \times 10^9$  and  $3.01 \times 10^9 \text{ L mol}^{-1} \text{ s}^{-1}$  respectively according to the eq. 4-7, and the average value of  $2.99 \times 10^9 \text{ L mol}^{-1} \text{ s}^{-1}$  was obtained. This value is close to the value ( $3.36 \times 10^9 \text{ L mol}^{-1} \text{ s}^{-1}$ ) recently reported for the reaction of PPN with hydroxyl radicals [52].

#### 4.3.3 Identification and evolution of the oxidation by-products

Generally all  $\beta$ -blockers contain two types of reactive sites, *i.e.*, the aromatic moiety and the lateral chain. The reaction between  $\cdot\text{OH}/\text{M}(\cdot\text{OH})$  and any member of this group is initiated by the formation of corresponding aromatic group with the release of the lateral chain. PPN degradation was not an exception case and the cleavage of the C-O bond of the molecule yields 1-naphtol which further oxidized to phthalic acid [17]. The reversed-phase HPLC analysis of electrolyzed solutions using similar condition reported for Fig. 4-3b shows two peaks at 6.3 and 14.4 min that is related to aromatic byproducts and suspected to be phthalic acid and 1-naphtol based on previous studies [17]. Both intermediate products were unequivocally confirmed using photodiode array detector by measuring and comparing their retention times and UV-vis spectra with those of corresponding standard compounds. Fig. 4-5 shows the time course of the two by-products obtained at applied current between 10 – 120 mA. In all cases, a typical accumulation – destruction profile was obtained thanks to greater formation of the intermediates from PPN degradation at the early stages, followed by predominant oxidation by  $\cdot\text{OH}/\text{Ti}_4\text{O}_7(\cdot\text{OH})$  in the later stages. As reported in the case of PPN, a rapid disappearance of both by-products was achieved at higher current. For instance, phthalic acid was totally destroyed after 20, 8 and 6 min (Fig. 4-5a), whereas 1-naphtol destruction requires just 10, 8 and 4 min (Fig. 4-5b) at 30, 60 and 120 mA, respectively. Maximum concentration of 0.35 and 0.25 mg L<sup>-1</sup> were attained for phthalic acid and 1-naphtol at 10 and 120 mA, respectively.



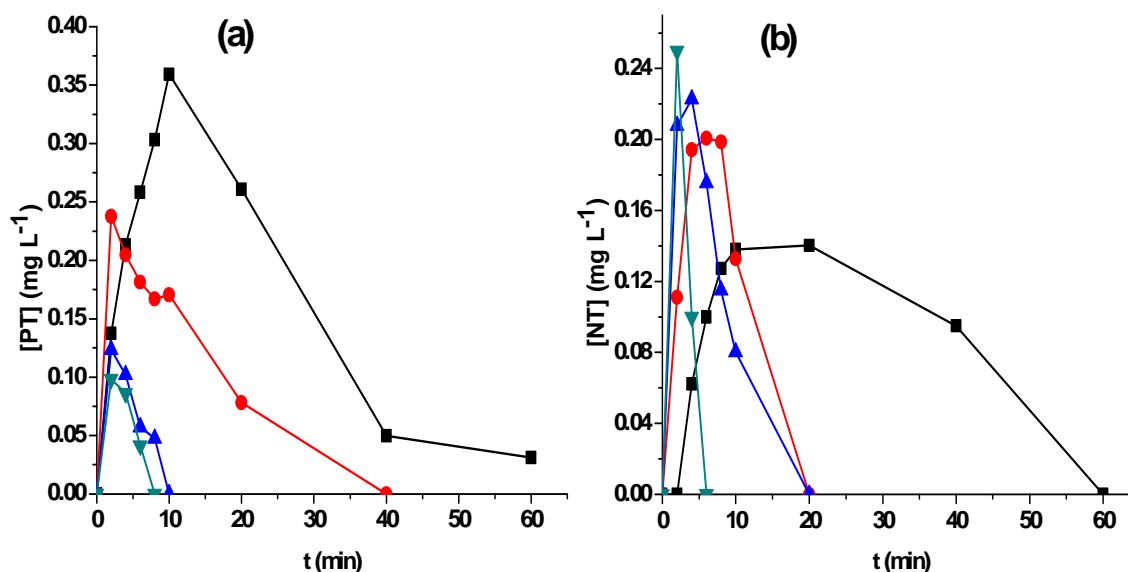


**Figure 4-5** – Time course of the concentration of main aromatic intermediates: (a) phthalic acid and (b) 1-naphthol accumulated during the EF treatment with Ti<sub>4</sub>O<sub>7</sub> anode of 0.1 mM PPN in 0.05 M Na<sub>2</sub>SO<sub>4</sub> with 0.1 mM Fe<sup>2+</sup> at pH 3 and applied current of (■) 10 mA, (●) 30 mA, (▲) 60 mA, and (▼) 120 mA.

The oxidative cleavage of the aromatic/cyclic intermediates as well as the oxidation of aliphatic intermediates with <sup>•</sup>OH/Ti<sub>4</sub>O<sub>7</sub>(<sup>•</sup>OH) leads to the formation of short-chain (C-4) carboxylic acids, which are less easily reactive and account for the residual TOC during the treatment [56,59,60]. Analysis of an electrolyzed 0.1 mM PPN solution under the conditions of Fig. 4-3b and 4-3c, at 60 mA with ion-exclusion HPLC gives chromatograms that displayed four well defined peaks corresponding to oxalic, oxamic, maleic and glyoxylic acid at retention time of 8.69, 12.97, 13.80 and 17.02 min, respectively. Their evolution during EF treatment with both anodes is shown in Fig. 4-6. A typical accumulation – destruction cycle was observed in both cases, with their formation started right from the beginning of electrolysis. The concentration profiles and maximum values were quite similar for both anodes, but a slower degradation was observed with DSA (Fig. 4-6a), confirming the earlier-mentioned lower oxidation ability of this anode compared to Ti<sub>4</sub>O<sub>7</sub> anode. While the cleavage of cyclic intermediates may lead to the formation of

oxalic, glyoxylic and maleic acids, oxamic acid can be formed from the oxidation of the lateral chain of the propranolol [17,56].

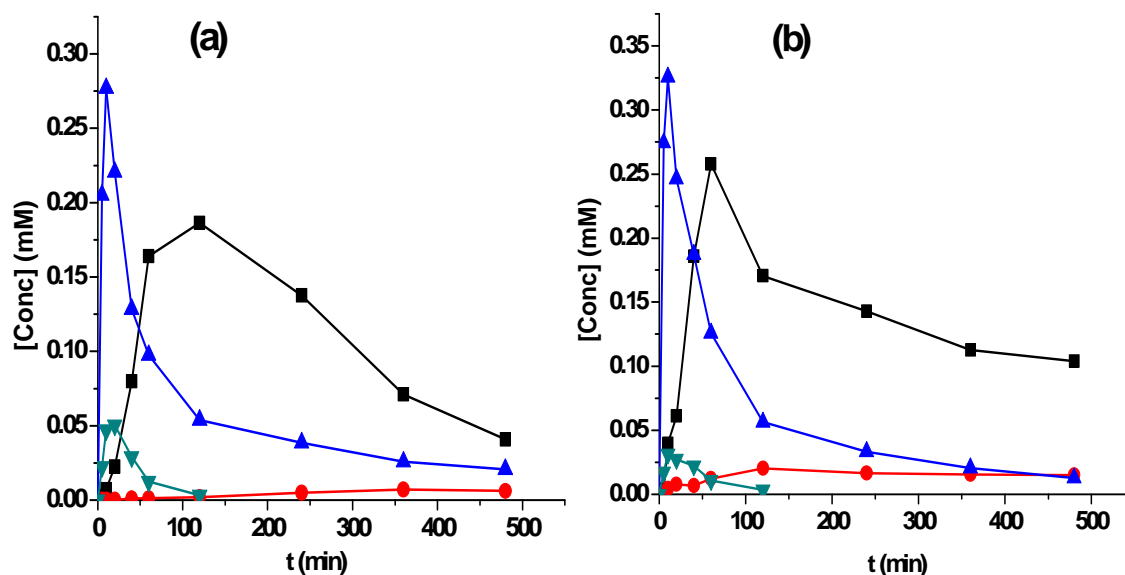


**Figure 4-6** – Time course of the concentration of the short-chain carboxylic acids: (■) oxalic, (●) oxamic, (▲) glyoxylic, and (▼) maleic acids accumulated during the treatment of 0.1 mM PPN in 0.05 M Na<sub>2</sub>SO<sub>4</sub> with 0.1 mM Fe<sup>2+</sup> at pH 3 and applied current of 60 mA using (a) Ti<sub>4</sub>O<sub>7</sub> and (b) DSA anodes.

The initial nitrogen content of PPN released in the treated solution in form of inorganic ions such as NH<sub>4</sub><sup>+</sup>, NO<sub>2</sub><sup>-</sup> and NO<sub>3</sub><sup>-</sup>, was analyzed and quantified by ion chromatography. No NO<sub>2</sub><sup>-</sup> was detected. The evolution of NH<sub>4</sub><sup>+</sup> and NO<sub>3</sub><sup>-</sup> in the treated solutions containing 0.1 mM PPN (0.1 mM initial N) at 60 mA with Ti<sub>4</sub>O<sub>7</sub> and DSA anodes is shown in Fig. 4-7. As can be seen in this figure, the initial N is predominantly recovered as NH<sub>4</sub><sup>+</sup> in the solution, which gradually and continuously accumulated during the electrolysis because the N-heteroatom was located in the lateral chain which is less easily oxidized. Appreciable amount of NO<sub>3</sub><sup>-</sup> ions were formed in treatment with Ti<sub>4</sub>O<sub>7</sub>, whereas only marginal quantity was recovered in the treatment with DSA anode. The high amount of NH<sub>4</sub><sup>+</sup> is probably due to the reduction of NO<sub>3</sub><sup>-</sup> at the large surface carbon-felt cathode. After 480 min of electrolysis, 0.066 mM NH<sub>4</sub><sup>+</sup> (66% of initial N) and 0.026 mM NO<sub>3</sub><sup>-</sup>

(26% of initial N) was obtained with Ti<sub>4</sub>O<sub>7</sub> anode, whereas 0.062 mM NH<sub>4</sub><sup>+</sup> (62% of initial N) and 0.019 mM NO<sub>3</sub><sup>-</sup> (19% of initial N) was released in treatment with DSA anode. The higher content of inorganic ions (92%) observed with Ti<sub>4</sub>O<sub>7</sub> compared to 81% obtained with DSA anode is in agreement with superior mineralization potential of the former anode as reported in Fig. 4-2. It must be noted that, the total nitrogenous inorganic ions released into the solution after 480 min of electrolysis (*i.e.* 92% and 81% for Ti<sub>4</sub>O<sub>7</sub> and DSA anodes, respectively) is less than 100%, indicating the presence of N-derivative organics remaining in the solution, especially oxamic acid with the concentration of 0.006 mM (6% N) and 0.014 mM (14% N) for Ti<sub>4</sub>O<sub>7</sub> and DSA anode, respectively, as shown in Fig. 4-6a and 4-6b. This implies that small fraction of initial N (2 and 5% for Ti<sub>4</sub>O<sub>7</sub> and DSA anodes, respectively) may have been lost as volatile N<sub>x</sub>O<sub>y</sub> during treatment [18,22].

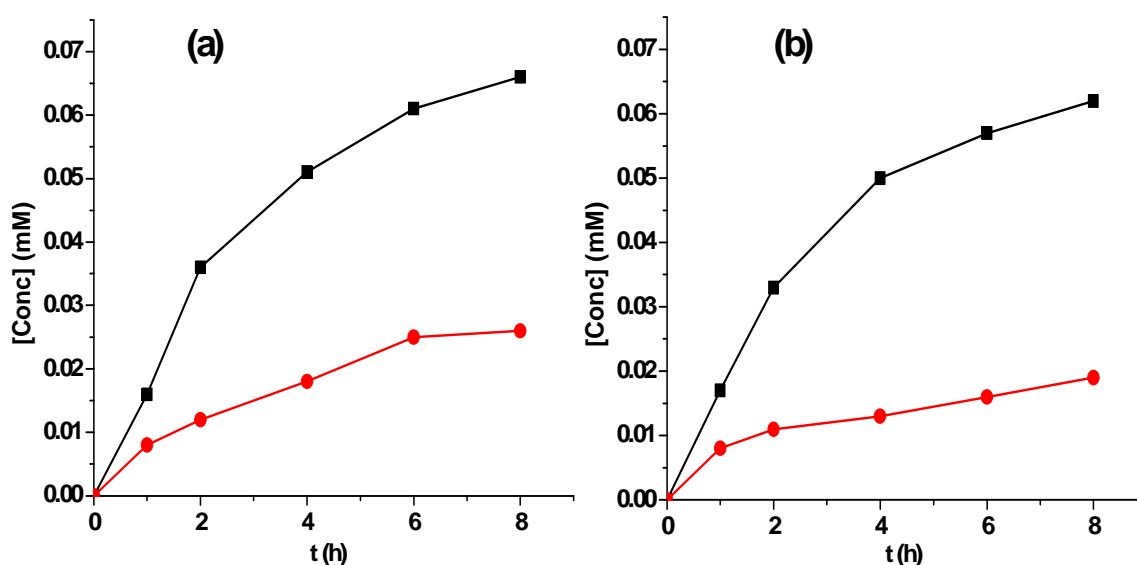


**Figure 4-7**– Time-course of concentration of nitrogenated inorganic ions: (■) NH<sub>4</sub><sup>+</sup> and (●) NO<sub>3</sub><sup>-</sup>, during the treatment of 0.1 mM PPN in 0.05 M Na<sub>2</sub>SO<sub>4</sub> (K<sub>2</sub>SO<sub>4</sub> for NH<sub>4</sub><sup>+</sup>) with 0.1 mM Fe<sup>2+</sup> at pH 3 and applied current of 60 mA using (a) Ti<sub>4</sub>O<sub>7</sub> and (b) DSA anodes.

#### 4.3.4 Reaction sequence for PPN mineralization

A plausible reaction sequence for the oxidation of PPN by  $\cdot\text{OH}/\text{Ti}_4\text{O}_7(\cdot\text{OH})$  was proposed based on the identified intermediate products obtained with the help of GC-MS, HPLC and IC analyses. Two reaction pathways were proposed as seen in Fig. 4-8. The first path (1) involves O-dealkylation by C–O bond cleavage between naphthalene ring and lateral chain with the formation of 1-naphthol and hydroxylated amine, which further undergoes  $\cdot\text{OH}/\text{Ti}_4\text{O}_7(\cdot\text{OH})$  attack at the secondary amine group to yield glycerol and propylamine. Acetone was formed from the hydroxylation of isopropylamine with the release of  $\text{NH}_4^+$ . The second pathway started by  $\cdot\text{OH}/\text{Ti}_4\text{O}_7(\cdot\text{OH})$  attack at the secondary amine group, leading to the formation of di-hydroxyl propoxyl naphthalene and propylamine which subsequently yielded acetone by hydroxylation. Further O-dealkylation between the naphthalene ring and di-hydroxyl propoxyl leads to the formation of 1-naphthol and glycerol. The 1-naphthol formed *via* both pathways is a characteristic intermediate product of PPN oxidation [17] and undergoes hydroxylation to form hydroxylated naphthol. This was followed by oxidative ring opening reaction, and further decarboxylation to form *p*-hydroxy di-ketone. Further hydroxylation of this compound at its both ketone functional groups yielded another characteristic oxidation product of PPN, phthalic acid [17]. Subsequent  $\cdot\text{OH}/\text{Ti}_4\text{O}_7(\cdot\text{OH})$  attack on phthalic acid, glycerol and acetone lead to the formation of short-chain carboxylic acid such as oxalic, glyoxylic, maleic and oxamic acids that are later oxidized to  $\text{CO}_2$  with the release of  $\text{H}_2\text{O}$  and  $\text{NH}_4^+$ .

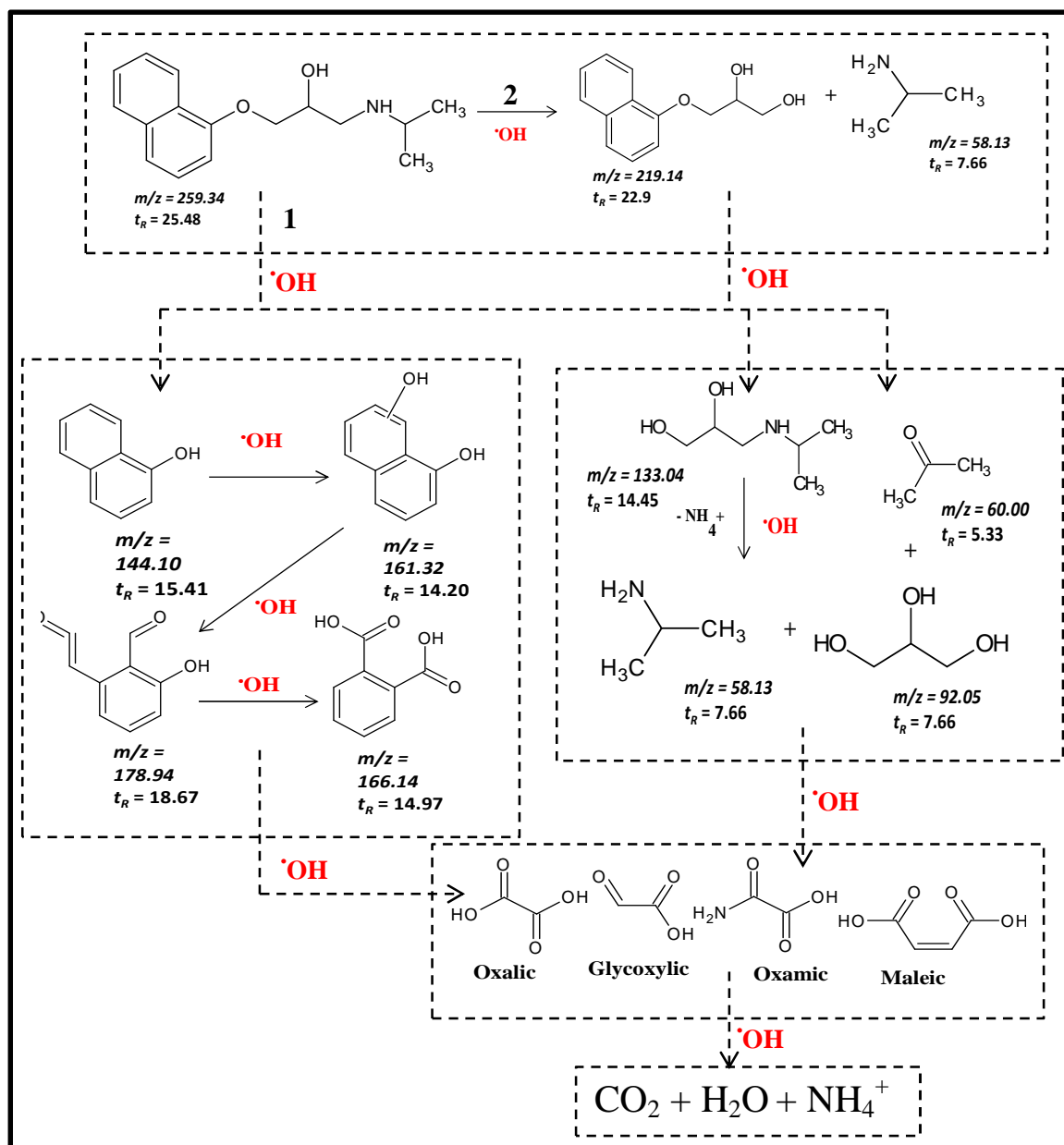


Figure 4-8 – Proposed reaction sequence for complete mineralization of PPN by EF process assuming  $\cdot\text{OH}$  as the main oxidizing agent.

#### 4.4 Conclusions

Plasma deposited Ti<sub>4</sub>O<sub>7</sub> ceramic electrode was studied as a suitable and cost-effective anode material for electrochemical degradation of aqueous solutions of PPN at acidic pH. Efficient degradation and mineralization of PPN was achieved with Ti<sub>4</sub>O<sub>7</sub> anode and CF cathode under AO and EF processes. Comparative AO and EF studies with DSA anode showed lower mineralization compared to Ti<sub>4</sub>O<sub>7</sub>, suggesting significantly high oxidation ability of Ti<sub>4</sub>O<sub>7</sub>(<sup>•</sup>OH) than DSA(<sup>•</sup>OH). The PPN concentration decay followed pseudo-first order reaction kinetics and the apparent rate constant increased with applied current but decreased with PPN concentration. The absolute rate constant for the reaction between hydroxyl radicals and PPN was determined as  $(2.99 \pm 0.02) \times 10^9 \text{ L mol}^{-1} \text{ s}^{-1}$  by using the competition kinetics method with *p*-HBA as the standard competitor. Characteristic aromatic intermediates of PPN oxidation such as 1-naphthol; hydroxylated 1-naphthol and phthalic acid were detected and quantified. Generated carboxylic acids such as oxalic, oxamic and glyoxylic were detected by ion-exclusion HPLC as final oxidation products that were further oxidized to CO<sub>2</sub>. The initial N was mainly released as NH<sub>4</sub><sup>+</sup> ion, along with relatively small proportion of NO<sub>3</sub><sup>-</sup> as measured by ionic chromatography. A plausible reaction sequence for the mineralization of PPN was proposed based on all the detected intermediates and assuming <sup>•</sup>OH as main oxidants. Finally, this study has demonstrated that Ti<sub>4</sub>O<sub>7</sub> is a very promising electrode for electrochemical treatment of PPN solutions by electrochemical advanced oxidation processes.

**References**

- [1] B. Marselli, J. Garcia-Gomez, P.A. Michaud, M.A. Rodrigo, C. Comninellis, Electrogeneration of hydroxyl radicals on boron-doped diamond electrodes, *J. Electrochem. Soc.* 150 (2003)
- [2] M. Panizza, G. Cerisola, Direct and mediated anodic oxidation of organic pollutants, *Chem. Rev.* 109 (2009) 6541–6569.
- [3] C.A. Martínez-Huitle, S. Ferro, Electrochemical oxidation of organic pollutants for the wastewater treatment: direct and indirect processes, *Chem. Soc. Rev.* 35 (2006) 1324.
- [4] M.A. Rodrigo, P. Cañizares, A. Sánchez-Carretero, C. Sáez, Use of conductive-diamond electrochemical oxidation for wastewater treatment, *Catal. Today.* 151 (2010) 173–177.
- [5] M.A. Oturan, J. Peiroten, P. Chartrin, A.J. Acher, Complete destruction of *p* - nitrophenol in aqueous medium by electro-Fenton method, *Environ. Sci. Technol.* 34 (2000) 3474–3479.
- [6] E. Brillas, I. Sires, M.A. Oturan, Electro-Fenton process and related electrochemical technologies based on Fenton's reaction chemistry, *Chem. Rev.* 109 (2009) 6570–6631.
- [7] J.M. Peralta-Hernández, Y. Meas-Vong, F.J. Rodríguez, T.W. Chapman, M.I. Maldonado, L.A. Godínez, In situ electrochemical and photo-electrochemical generation of the Fenton reagent: A potentially important new water treatment technology, *Water Res.* 40 (2006) 1754–1762.
- [8] M.A. Oturan, J.J. Aaron, Advanced oxidation processes in water/wastewater treatment: Principles and applications. A review, *Crit. Rev. Environ. Sci. Technol.* 44 (2014) 2577–2641.
- [9] C.A. Martínez-Huitle, M.A. Rodrigo, I. Sirés, O. Scialdone, Single and coupled electrochemical processes and reactors for the abatement of organic water pollutants: A critical review, *Chem. Rev.* 115 (2015) 13362–13407.
- [10] S. Vasudevan, M.A. Oturan, Electrochemistry: as cause and cure in water pollution— an overview, *Environ. Chem. Lett.* 12 (2014) 97–108.

- [11] I. Sirés, E. Brillas, M.A. Oturan, M.A. Rodrigo, M. Panizza, Electrochemical advanced oxidation processes: today and tomorrow. A review, *Environ. Sci. Pollut. Res.* 21 (2014) 8336–8367.
- [12] S.O. Ganiyu, E.D. van Hullebusch, M. Cretin, G. Esposito, M.A. Oturan, Coupling of membrane filtration and advanced oxidation processes for removal of pharmaceutical residues: A critical review, *Sep. Purif. Technol.* 156 (2015) 891–914.
- [13] I. Sirés, J.A. Garrido, R.M. Rodríguez, E. Brillas, N. Oturan, M.A. Oturan, Catalytic behavior of the  $\text{Fe}^{3+}/\text{Fe}^{2+}$  system in the electro-Fenton degradation of the antimicrobial chlorophene, *Appl. Catal. B Environ.* 72 (2007) 382–394.
- [14] H. Zhang, C. Fei, D. Zhang, F. Tang, Degradation of 4-nitrophenol in aqueous medium by electro-Fenton method, *J. Hazard. Mater.* 145 (2007) 227–232.
- [15] M.A. Oturan, M.C. Edelahe, N. Oturan, K. El kacemi, J.J. Aaron, Kinetics of oxidative degradation/mineralization pathways of the phenylurea herbicides diuron, monuron and fenuron in water during application of the electro-Fenton process, *Appl. Catal. B Environ.* 97 (2010) 82–89.
- [16] G.V. Buxton, N.D. Wood, S. Dyster, Ionisation constants of  $\cdot\text{OH}$  and  $\text{HO}\cdot_2$  in aqueous solution up to 200 °C. A pulse radiolysis study, *J. Chem. Soc. Faraday Trans. 1 Phys. Chem. Condens. Phases.* 84 (1988) 1113.
- [17] E. Isarain-Chávez, R.M. Rodríguez, J.A. Garrido, C. Arias, F. Centellas, P.L. Cabot, E. Brillas, Degradation of the beta-blocker propranolol by electrochemical advanced oxidation processes based on Fenton's reaction chemistry using a boron-doped diamond anode, *Electrochimica Acta.* 56 (2010) 215–221.
- [18] A. Dirany, I. Sirés, N. Oturan, M.A. Oturan, Electrochemical abatement of the antibiotic sulfamethoxazole from water, *Chemosphere.* 81 (2010) 594–602.
- [19] A. Mhemdi, M.A. Oturan, N. Oturan, R. Abdelhedi, S. Ammar, Electrochemical advanced oxidation of 2-chlorobenzoic acid using BDD or Pt anode and carbon felt cathode, *J. Electroanal. Chem.* 709 (2013) 111–117.
- [20] N. Oturan, J. Wu, H. Zhang, V.K. Sharma, M.A. Oturan, Electrocatalytic destruction of the antibiotic tetracycline in aqueous medium by electrochemical advanced oxidation processes: Effect of electrode materials, *Appl. Catal. B Environ.* 140-141 (2013) 92–97.



- [21] M.A. Rodrigo, N. Oturan, M.A. Oturan, Electrochemically assisted remediation of pesticides in soils and water: A review, *Chem. Rev.* 114 (2014) 8720–8745.
- [22] M. Panizza, A. Dirany, I. Sirés, M. Haidar, N. Oturan, M.A. Oturan, Complete mineralization of the antibiotic amoxicillin by electro-Fenton with a BDD anode, *J. Appl. Electrochem.* 44 (2014) 1327–1335.
- [23] G. Chen, Electrochemical technologies in wastewater treatment, *Sep. Purif. Technol.* 38 (2004) 11–41.
- [24] J.R. Smith, F.C. Walsh, R.L. Clarke, Electrodes based on Magnéli phase titanium oxides: The properties and applications of Ebonex<sup>(R)</sup> materials, *J. Appl. Electrochem.* 28 (1998) 1021–1033.
- [25] K. Scott, H. Cheng, The anodic behaviour of Ebonex® in oxalic acid solutions, *J. Appl. Electrochem.* 32 (2002) 583–589.
- [26] F.C. Walsh, R.G.A. Wills, The continuing development of Magnéli phase titanium sub-oxides and Ebonex® electrodes, *Electrochimica Acta.* 55 (2010) 6342–6351.
- [27] P. Geng, J. Su, C. Miles, C. Comninellis, G. Chen, Highly-ordered Magnéli Ti<sub>4</sub>O<sub>7</sub> Nanotube arrays as effective anodic material for electro-oxidation, *Electrochimica Acta.* 153 (2015) 316–324.
- [28] D. Bejan, E. Guinea, N.J. Bunce, On the nature of the hydroxyl radicals produced at boron-doped diamond and Ebonex® anodes, *Electrochimica Acta.* 69 (2012) 275–281.
- [29] G. Chen, E.A. Betterton, R.G. Arnold, Electrolytic oxidation of trichloroethylene using a ceramic anode, *J. Appl. Electrochem.* 29 (1999) 961–970.
- [30] D. Bejan, J.D. Malcolm, L. Morrison, N.J. Bunce, Mechanistic investigation of the conductive ceramic Ebonex® as an anode material, *Electrochimica Acta.* 54 (2009) 5548–5556.
- [31] A.M. Zaky, B.P. Chaplin, Mechanism of p-substituted phenol oxidation at a Ti<sub>4</sub>O<sub>7</sub> reactive electrochemical membrane, *Environ. Sci. Technol.* 48 (2014) 5857–5867.
- [32] A.M. Zaky, B.P. Chaplin, Porous substoichiometric TiO<sub>2</sub> anodes as reactive electrochemical membranes for water treatment, *Environ. Sci. Technol.* 47 (2013) 6554–6563.

- [33] S.O. Ganiyu, N. Oturan, S. Raffy, M. Cretin, R. Esmilaire, E. van Hullebusch, G. Esposito, M.A. Oturan, Sub-stoichiometric titanium oxide (Ti<sub>4</sub>O<sub>7</sub>) as a suitable ceramic anode for electrooxidation of organic pollutants: A case study of kinetics, mineralization and toxicity assessment of amoxicillin, *Water Res.* 106, 171–181.
- [34] S.K. Khetan, T.J. Collins, Human pharmaceuticals in the aquatic environment: A challenge to green chemistry, *Chem. Rev.* 107 (2007) 2319–2364.
- [35] L. Amendola, F. Molaioni, F. Botrè, Detection of beta-blockers in human urine by GC-MS-MS-EI: perspectives for the antidoping control, *J. Pharm. Biomed. Anal.* 23 (2000) 211–221.
- [36] J. Maszkowska, S. Stolte, J. Kumirska, P. Łukaszewicz, K. Mioduszevska, A. Puckowski, M. Caban, M. Wagil, P. Stepnowski, A. Białk-Bielińska, Beta-blockers in the environment: Part I. Mobility and hydrolysis study, *Sci. Total Environ.* 493 (2014) 1112–1121.
- [37] K. Kümmerer, Drugs in the environment: emission of drugs, diagnostic aids and disinfectants into wastewater by hospitals in relation to other sources – a review, *Chemosphere.* 45 (2001) 957–969.
- [38] C. Miège, M. Favier, C. Brosse, J.-P. Canler, M. Coquery, Occurrence of beta-blockers in effluents of wastewater treatment plants from the Lyon area (France) and risk assessment for the downstream rivers, *Talanta.* 70 (2006) 739–744.
- [39] M. Ramil, T. El Aref, G. Fink, M. Scheurer, T.A. Ternes, Fate of beta blockers in aquatic-sediment systems: Sorption and biotransformation, *Environ. Sci. Technol.* 44 (2010) 962–970.
- [40] L. Wang, H. Xu, W.J. Cooper, W. Song, Photochemical fate of beta-blockers in NOM enriched waters, *Sci. Total Environ.* 426 (2012) 289–295.
- [41] D.B. Huggett, B.W. Brooks, B. Peterson, C.M. Foran, D. Schlenk, Toxicity of select beta adrenergic receptor-blocking pharmaceuticals (β-blockers) on aquatic organisms, *Arch. Environ. Contam. Toxicol.* 43 (2002) 229–235.
- [42] M. Cleuvers, Initial risk assessment for three β-blockers found in the aquatic environment, *Chemosphere.* 59 (2005) 199–205.

- [43] E.M. Dzialowski, P.K. Turner, B.W. Brooks, Physiological and reproductive effects of beta adrenergic receptor antagonists in daphnia magna, *Arch. Environ. Contam. Toxicol.* 50 (2006) 503–510.
- [44] B.I. Escher, N. Bramaz, M. Richter, J. Lienert, Comparative ecotoxicological hazard assessment of beta-blockers and their human metabolites using a Mode-of-Action-Based Test Battery and a QSAR Approach <sup>†</sup>, *Environ. Sci. Technol.* 40 (2006) 7402–7408.
- [45] K. Ikehata, N. Jodeiri Naghashkar, M. Gamal El-Din, Degradation of aqueous pharmaceuticals by ozonation and advanced oxidation processes: A review, *Ozone Sci. Eng.* 28 (2006) 353–414.
- [46] M.L. Wilde, S. Montipó, A.F. Martins, Degradation of  $\beta$ -blockers in hospital wastewater by means of ozonation and Fe<sup>2+</sup>/ozonation, *Water Res.* 48 (2014) 280–295.
- [47] W. Song, W.J. Cooper, S.P. Mezyk, J. Greaves, B.M. Peake, Free radical destruction of  $\beta$ -blockers in aqueous solution, *Environ. Sci. Technol.* 42 (2008) 1256–1261.
- [48] G.A.K. Anquandah, V.K. Sharma, V.R. Panditi, P.R. Gardinali, H. Kim, M.A. Oturan, Ferrate(VI) oxidation of propranolol: Kinetics and products, *Chemosphere.* 91 (2013) 105–109.
- [49] I.H. Kim, N. Yamashita, Y. Kato, H. Tanaka, Discussion on the application of UV/H<sub>2</sub>O<sub>2</sub>, O<sub>3</sub> and O<sub>3</sub> /UV processes as technologies for sewage reuse considering the removal of pharmaceuticals and personal care products, *Water Sci. Technol.* 59 (2009) 945.
- [50] H. Yang, T. An, G. Li, W. Song, W.J. Cooper, H. Luo, X. Guo, Photocatalytic degradation kinetics and mechanism of environmental pharmaceuticals in aqueous suspension of TiO<sub>2</sub>: A case of  $\beta$ -blockers, *J. Hazard. Mater.* 179 (2010) 834–839.
- [51] J. Santiago-Morales, A. Agüera, M. del M. Gómez, A.R. Fernández-Alba, J. Giménez, S. Esplugas, R. Rosal, Transformation products and reaction kinetics in simulated solar light photocatalytic degradation of propranolol using Ce-doped TiO<sub>2</sub>, *Appl. Catal. B Environ.* 129 (2013) 13–29.

- [52] I. Sirés, N. Oturan, M.A. Oturan, Electrochemical degradation of  $\beta$ -blockers. Studies on single and multicomponent synthetic aqueous solutions, *Water Res.* 44 (2010) 3109–3120.
- [53] M. Muruganathan, S. Yoshihara, T. Rakuma, N. Uehara, T. Shirakashi, Electrochemical degradation of 17 $\beta$ -estradiol (E2) at boron-doped diamond (Si/BDD) thin film electrode, *Electrochimica Acta.* 52 (2007) 3242–3249.
- [54] M.A. Oturan, N. Oturan, M.C. Edelahi, F.I. Podvorica, K.E. Kacemi, Oxidative degradation of herbicide diuron in aqueous medium by Fenton's reaction based advanced oxidation processes, *Chem. Eng. J.* 171 (2011) 127–135.
- [55] A. El-Ghenymy, R.M. Rodríguez, E. Brillas, N. Oturan, M.A. Oturan, Electro-Fenton degradation of the antibiotic sulfanilamide with Pt/carbon-felt and BDD/carbon-felt cells. Kinetics, reaction intermediates, and toxicity assessment, *Environ. Sci. Pollut. Res.* 21 (2014) 8368–8378.
- [56] M.A. Oturan, M. Pimentel, N. Oturan, I. Sirés, Reaction sequence for the mineralization of the short-chain carboxylic acids usually formed upon cleavage of aromatics during electrochemical Fenton treatment, *Electrochimica Acta.* 54 (2008) 173–182.
- [57] A. Dirany, I. Sirés, N. Oturan, A. Özcan, M.A. Oturan, Electrochemical treatment of the antibiotic sulfachloropyridazine: Kinetics, reaction pathways, and toxicity evolution, *Environ. Sci. Technol.* 46 (2012) 4074–4082.
- [58] F. Sopaj, M.A. Rodrigo, N. Oturan, F.I. Podvorica, J. Pinson, M.A. Oturan, Influence of the anode materials on the electrochemical oxidation efficiency. Application to oxidative degradation of the pharmaceutical amoxicillin, *Chem. Eng. J.* 262 (2015) 286–294.
- [59] A. Özcan, Y. Şahin, A.S. Kopalal, M.A. Oturan, A comparative study on the efficiency of electro-Fenton process in the removal of prophan from water, *Appl. Catal. B Environ.* 89 (2009) 620–626.
- [60] E. Brillas, M.Á. Baños, J.A. Garrido, Mineralization of herbicide 3,6-dichloro-2-methoxybenzoic acid in aqueous medium by anodic oxidation, electro-Fenton and photoelectro-Fenton, *Electrochimica Acta.* 48 (2003) 1697–1705.

## **CHAPTER 5**

---

# **Heterogeneous Electro-Fenton Degradation of Organic Pollutants at circumneutral pH**

This chapter has been accepted in Journal of Material Chemistry A for publication as:

Soliu O. Ganiyu, Thi Xuan Huong Le, Mikhael Bechelany, Giovanni Esposito, Eric D. van Hullebusch, Mehmet A. Oturan, Marc Cretin (2016). Hierarchical CoFe-Layered Double Hydroxide Modified Carbon-felt Cathode for Heterogeneous Electro-Fenton. DOI: 10.1039/C6TA09100H

## **CHAPTER 5**

Narrow pH window and reusability of the catalyst has been major challenges of traditional/homogeneous EF process. Heterogeneous EF process using solid Fe-containing catalysts has been developed to overcome these challenges. Several Fe-containing natural minerals, Fe- modified carbonaceous cathode and transition metal – carbon aerogel have been investigated as suitable catalysts in heterogeneous EF, but no studies available on use of layered double hydroxide.

**Hierarchical CoFe-Layered Double Hydroxide Modified Carbon-felt Cathode: Synthesis, Characterization and Application in Heterogeneous Electro-Fenton Degradation of Organic Pollutants at circumneutral pH****ABSTRACT**

Hierarchical CoFe-Layered Double Hydroxide (CoFe-LDH) was grown on carbon felt (CF) as heterogeneous catalyst by *in-situ* solvothermal growth. The CoFe-LDH/CF serves as cathode as well as  $\text{Fe}^{2+}$  (catalyst) source in EF process. A combined structural and electrochemical characterization revealed highly ordered and well crystallized CoFe-LDH anisotropically grown on CF substrate with highly dense urchin-like structures that were highly stable at circumneutral pH. EF experiments with CoFe-LDH/CF cathode showed excellent mineralization of Acid Orange II (AO7) over a wide pH range (2 – 7.1). The mineralization of AO7 with CoFe-LDH/CF was by both homogeneous and surfaced catalyzed process at low acidic pH, whereas only surface catalyzed process occurs at circumneutral pH due to stability of the LDH as well as precipitation of the catalyst. Higher mineralization was achieved with CoFe-LDH/CF compared to homogeneous EF with raw CF using  $\text{Fe}^{2+}/\text{Co}^{2+}$  catalyst at all pH studied and the TOC removal with CoFe-LDH/CF cathode was at least 1.7 and 3.5 times higher than homogeneous system with  $\text{Fe}^{2+}/\text{Co}^{2+}$  at pH 5.83 and 7.1 respectively. The enhanced performance observed with CoFe-LDH/CF was ascribed to (i) surface-catalyzed reaction occurring at the surface of the cathode which can expand the working pH window and avoiding the precipitation of iron sludge as pH increases, (ii) enhanced generation of  $\text{H}_2\text{O}_2$  due to improved electroactive surface area of the cathode and (iii) co-catalyst effect of the  $\text{Co}^{2+}$  in the LDH that can promote regeneration and additional production of  $\text{Fe}^{2+}$  and hydroxyl radical, respectively. The CoFe-LDH/CF cathode exhibited relatively good reusability as the TOC removal after 2 h was still above 50% after 8 cycles of degradation, indicating that the prepared CoFe-LDH/CF is a promising cathode for the removal of organic pollutants by EF technology.

**Keywords:** Layered double hydroxide, Carbon felt, Heterogeneous catalyst, Solvothermal growth, Electro-Fenton, Hydroxyl radicals



## 5.1 Introduction

EF is an eco-friendly EAOP based on classical Fenton's reaction chemistry in which organic contaminants are destroyed by *in-situ* homogeneously generated hydroxyl radical ( $\bullet\text{OH}$ ) from the Fenton's reaction (eq. 5-1) between  $\text{Fe}^{2+}$  ion and hydrogen peroxide ( $\text{H}_2\text{O}_2$ ) [1–4].



The *in-situ* production of  $\text{H}_2\text{O}_2$  by  $2\text{e}^-$  reduction of dissolved oxygen (eq. 5-2) at the cathode has great influence on the efficiency of the EF process and the production rate depends on the nature of cathode materials [5–7].



An interesting characteristic of EF process is that only catalytic quantity of  $\text{Fe}^{2+}$  is required because it can be regenerated at the cathode by  $\text{e}^-$  reduction of  $\text{Fe}^{3+}$  (eq. 5-3) formed from Fenton's reaction (eq. 5-1) [1,8–10].



The *in situ* electrogeneration of  $\text{H}_2\text{O}_2$  (eq. 5-2) and the electro-regeneration of  $\text{Fe}^{2+}$  from  $\text{Fe}^{3+}$  allow continuous formation of  $\bullet\text{OH}$  that is able to destroy any organic pollutant [1,11].

The major challenges of homogeneous EF with  $\text{Fe}^{2+}$  are the narrow working pH window and non-reusability of the catalyst in several runs [12–14]. Optimization of the quantity of  $\text{Fe}^{2+}$  is another problem because excessive quantities of  $\text{Fe}^{2+}$  in the solution may promote the wasting reaction (eq. 5-4) that consumes the generated  $\bullet\text{OH}$ , thus reduce the efficiency of the process [15,16].



To avoid these problems, heterogeneous EF with Fe containing solid catalyst or modified electrodes has been developed for the effective oxidation of organic pollutants over a wide range of pH with excellent stability and reusability of the catalyst. Heterogeneous catalyst such as pyrite [17,18], magnetite [19] goethite [20], Fe/Mn-loaded alginate [21] and Fe-carbon PTFE [22] have been studied in EF treatment of organic pollutants. Fe@Fe-oxides functionalized

cathodic materials such as pyrrhotite grafted on graphite by conductive silver paste [23], Fe@Fe<sub>2</sub>O<sub>3</sub> nanowires mixed with carbon nanotubes and fixed on PTFE [12], activated carbon-supported nano-goethite (FeOOH) [20], Fe-modified activated carbon [24,25] and Fe-impregnated carbon-felt [26] electrodes have been investigated as catalyst source as well as cathode for EF oxidation at a wider pH range. Recently, Ferrite-carbon [14], FeCuC [27] and Fe<sub>3</sub>O<sub>4</sub>-C [28,29] aerogel have been synthesized in either one pot or more complex method and studied as efficient cathode materials to enhance electro-Fenton reactivity at acidic and neutral pHs.

The development of new electrodes that incorporate electrochemically active second phase containing transition metal oxides/hydroxides coated on carbon based matrixes for pseudo-capacitors used in energy conversion/storage devices [30,31] may be of great application in Fenton based EAOPs. The transition metals in the carbon based matrix electrode can act as heterogeneous catalyst which reacts with *in-situ* generated H<sub>2</sub>O<sub>2</sub> in a Fenton or Fenton-like reaction. LDHs are anionic clay materials that contain a brucite sheets of metallic cations (M<sup>II</sup> and M<sup>III</sup>) octahedrally coordinated by hydroxyl groups, forming M<sup>II</sup>(OH)<sub>6</sub>/M<sup>III</sup>(OH)<sub>6</sub> octahedral with charge-compensating anions positioned within the interlayer space [32,33]. Transition metal based LDHs possess tunable compositions and high dispersion of cations in their octahedral sheets which sometimes gives them astonishing electrochemical properties and have found several applications such as biosensors, alkaline secondary batteries, supercapacitors and recently used as electrocatalyst in water splitting/oxidation reaction [34,35]. These properties can also be harnessed for electrochemical wastewater treatment; with the transition metals catalyzed the process in a heterogeneous EF process. The possibility of using other transition metals such as copper, cobalt, and manganese [36–38] that have been tested as co-Fenton catalyst with Fe to improve the efficiency of EF process will be an added advantage of using LDH incorporated carbon based matrix cathode.

Additionally, the modification of carbon based matrix electrodes with LDH may also enhance the generation of H<sub>2</sub>O<sub>2</sub> due to increased electroactive surface area [39]. In fact, *Le et al.* [40] have shown that graphene modified carbon-felt cathode achieved better mineralization of azo-dye Acid Orang II (AO7) compared to raw carbon-felt due to the increase in electroactive surface area, which in turn enhance *in-situ* generation of H<sub>2</sub>O<sub>2</sub>. Therefore, this present study

investigates for the first time, the use of hierarchical CoFe-LDH grown on carbon-felt cathode for efficient degradation and mineralization of a model organic pollutant. The modified cathode was prepared by *in-situ* solvothermal process. The structural and electrochemical properties of the prepared cathode were examined by XRD, SEM-EDX, FTIR, XPS and cyclic voltammetry and electrochemical impedance spectroscopy. AO7, a common azo-dye found in high concentration in wastewater and effluent discharge from textile industries [41,42] was used as model pollutant. Besides, the influence of hydrothermal treatment parameters such as temperature, initial concentration of growth solution and treatment time on the performance of the prepared cathode was extensively studied. More importantly, the mineralization of AO7 solution by heterogeneous EF over a wide pH range as well as the leaching of the Co/Fe in the treated solution was systematically examined. For comparison, analogous studies were made with raw CF using externally added 0.2 mM Fe<sup>2+</sup>, Co<sup>2+</sup> or Co<sup>2+</sup>/Fe<sup>2+</sup> (1:1 and 2:1) as this value was reported in literature as the optimum concentration of Fe<sup>2+</sup> for EF process [43]

## 5.2 Experimental Procedures

### 5.2.1 Reagents and Materials

Carbon felt was obtained from Alfa Aesar. Cobalt II nitrate tetrahydrate, Co(NO<sub>3</sub>)<sub>2</sub>·4H<sub>2</sub>O (> 99% purity); iron III nitrate nonahydrate, Fe(NO<sub>3</sub>)<sub>3</sub>·9H<sub>2</sub>O (98% purity); iron II sulfate heptahydrate, FeSO<sub>4</sub>·7H<sub>2</sub>O (> 99% purity); urea, CO(NH<sub>2</sub>)<sub>2</sub> and ammonium fluoride, NH<sub>4</sub>F (99% purity) were purchased from Sigma Aldrich and used in the synthesis of LDH coated on the CF without further purification. AO7, C<sub>16</sub>H<sub>11</sub>N<sub>2</sub>NaO<sub>4</sub>S (Orange II sodium salt) and sodium sulfate, NaSO<sub>4</sub> (anhydrous, 99-100%) were also supplied by Sigma Aldrich. All solutions were prepared with ultra-pure water obtained from a Millipore Mill-Q system with resistivity > 18 MΩ cm at room temperature.

### 5.2.2 Electrode preparation

The CoFe-LDH modified CF (CoFe-LDH/CF) cathode was prepared by *in-situ* solvothermal process [44,45] in which CoFe-LDH was grown on CF substrate. The growth solution contains  $\text{Co}(\text{NO}_3)_2 \cdot 6\text{H}_2\text{O}$ ,  $\text{Fe}(\text{NO}_3)_3 \cdot 9\text{H}_2\text{O}$ ,  $\text{NH}_4\text{F}$  (0.125 M) and  $\text{CO}(\text{NH}_2)_2$  (0.5 M) dissolved in 100 mL of Milli-Q water with molar ratio of  $\text{Co}/\text{Fe} = 2:1$  ( $n/n$ ). The homogeneous solution was vigorously stirred for 30 min before transferred into a Teflon-lined stainless steel autoclave. Raw CF substrate (6.0 cm length  $\times$  1.0 cm width  $\times$  1.27 cm thickness) was pretreated with concentrated  $\text{HNO}_3$  and then washed in turn in ultrasonic bath with deionized water, acetone, ethanol and deionized water for 15 min each. The clean CF was immersed into the growth solution in Teflon autoclave for hydrothermal treatment at predetermined temperature and period. Subsequently, both the substrate coated with LDH and the solid LDH suspension were separated from the solution, washed extensively with distilled water followed by Milli-Q water and oven dried at 40 °C. The sample used for studying leaching of catalyst and reusability were dried at 80°C

### 5.2.3 Characterization

The surface morphology of the as-prepared cathode was analyzed by SEM (Hitachi S-4800), with an accelerating voltage of 10 kV, combined with EDX. TEM images were taken with a PHILLIP-CM 20. XRD were recorded on a BRUKER S5000 diffractometer, using  $\text{Cu-K}\alpha$  radiation (0.15418 nm) at 40 kV and 20 mA. FTIR pattern of the powder LDH was performed on NEXUS FTIR (ThermoFisher). The surface chemistry of the prepared sample was analyzed by XPS (ESCALAB 250 Thermal Electron) with  $\text{AlK}\alpha$  (1486.6 eV). Cyclic voltammetry (CV) experiments were carried out in solution of 50 mM  $\text{Na}_2\text{SO}_4$  using  $\mu\text{3AUT70466}$  Autolab System (Eco Chemie BV, Netherlands) without external addition  $\text{Fe}^{2+}$  source. A three-electrodes cell consisting of CoFe-LDH/CF as a working electrode, Pt foil and Saturated Calomel Electrode (SCE) as a counter and reference electrodes respectively was used to conduct the CV experiments. The electrical conductivity of the prepared cathode was determined by measuring electrode interfacial-charge transfer resistance using electrochemical impedance spectroscopy

(EIS). The EIS was performed at an open circuit voltage with voltage amplitude of 10 mV in a frequency range of 50 kHz to 100 MHz.

#### 5.2.4 EF experiment

The EF experiments were performed in an open, undivided cylindrical glass cell of diameter 4 cm and 300 mL capacity equipped with Pt gauze anode, placed in parallel to the cathode (4.5 cm × 1 cm × 1.27 cm) made of CoFe-LDH/CF at a distance of 2 cm. All experiments with CoFe-LDH/CF cathode were performed with 150 mL AO7 solutions (0.1 mM) containing 0.05 M Na<sub>2</sub>SO<sub>4</sub> as supporting electrolyte. The solution was constantly stirred by PTFE magnetic bar to ensure mass transfer towards the electrodes. Compressed air was continuously bubbled into the solution at about 1 L min<sup>-1</sup>, starting at 10 min prior to electrolysis to maintain a stationary O<sub>2</sub> level.

#### 5.2.5 Instrument and analytic procedure

All electrolyses experiments were performed with Lambda single power supply (Lambda Electronics, USA) at constant applied current of -40 mA. AO7 solution pH was adjusted with 1 M H<sub>2</sub>SO<sub>4</sub> or 0.1 mM NaOH and was measured with a pH 209 pH-meter from HANNA Instruments (Romania). The mineralization of the AO7 solutions was assessed from the decay of dissolved organic carbon, which can be considered as the TOC for highly water soluble organic compounds. The TOC of initial and electrolyzed samples were measured on a Shimadzu TOC-L CSH/CSN analyzer. Reproducible TOC values with ± 2% accuracy were obtained using the non-purgeable organic carbon method. Calibration curves for total organic and inorganic carbon analysis were built up by automatic dilution of standards solutions containing potassium hydrogen phthalate and sodium hydrogen carbonate for TOC and inorganic carbon, respectively. Percentage of TOC removal was calculated from to the following equation:

$$\text{TOC removal (\%)} = \frac{\Delta(\text{TOC})_{\text{exp}}}{\text{TOC}_0} \times 100 \quad (\text{eq. 5-5})$$

where  $\Delta(\text{TOC})_{\text{exp}}$  is the experimental TOC decay at electrolysis time  $t$  (mg L<sup>-1</sup>) and  $\text{TOC}_0$  is the corresponding initial value prior to electrolysis.

The leaching of both Co and Fe from as-prepared CoFe-LDH/CF cathode into the treated solution was monitored by Optima 8300 Optical Emission Spectrometer with Inductively Coupled Plasma (ICP-OES) (Perkin Elmer) at absorption wavelength of 230 and 239 nm for Co and Fe respectively. Standard solutions of different concentrations were prepared with Perkin Elmer IV (1000 ppm) by dilution with acidified Milli-Q water. The organic intermediate formed after 20 min of electrolysis were identified by GC-MS.

### 5.3 Results and Discussion

#### 5.3.1 Preparation of CoFe-LDH/CF electrode

CF, a well-known carbonaceous cathode for Fenton based EAOPs was used as a substrate for *in-situ* growth of CoFe-LDH multiwall, which serves as heterogeneous catalyst/co-catalyst for EF process. The reactions at hydrothermal temperature mainly involve progressive hydrolysis of  $\text{NH}_4\text{F}$  and decomposition of  $\text{CO}(\text{NH}_2)_2$  to  $\text{NH}_4\text{OH}$  (eq. 5-6 and 5-7). The resulting alkaline solution induces homogeneous nucleation, crystallization and growth of metallic hydroxides on the substrate (eq. 5-8) [45,46]:



The CF immersed in the growth solution acts as high energy sites for the nucleation and growth of the LDH on its surface compared to other sites in the growth solution.

#### 5.3.2 Structural and morphological properties of the CoFe-LDH/CF

SEM image of pretreated CF shows that it is clean, without organic and inorganic impurities that may have inherited during production process (Fig. 5-1a). After solvothermal synthesis, there was anisotropic growth of hierarchical CoFe-LDH onto the CF as shown in Fig.

5-1b-h, with the density/quantity of coating on the CF substrate closely related to the hydrothermal treatment temperature, time and initial concentration of the growth solution. In fact, treatment at 70 °C and 25:12.5 (*n/n*) initial Co<sup>2+</sup>/Fe<sup>3+</sup> concentration yielded a growth of fine but low dense LDH wall on the CF (Fig. 5-1b), indicating only nucleation of the LDH particles with limited crystal growth. The quantity of CoFe-LDH deposited on the CF at this temperature was not sufficient enough as it showed little enhancement of mineralization of organic pollutant (as demonstrated in section 5.3.4.2). Synthesis made at higher temperature of 90 °C with similar concentration for period of 4 h produced a highly dense and extensive growth of LDH on the CF substrate with formation of few urchin-like structures (Fig. 5-1c). These urchin-like structures extensively grown and increased in quantity for synthesis at 90 °C but longer period of time (7 h) (Fig 5-1d). For these synthesis conditions, it can be observed that the CF strands were entirely coated with CoFe-LDH, which are adhesively grafted on the CF. The magnified image (Fig. 5-1e) revealed that the CoFe-LDH wall and urchin-like structures are distributed across the entire surface of each CF strand, interconnected with each other, highly rough and porous which can enhance the diffusion of substance within the electrode. Further increase in hydrothermal treatment period to 21 h (Fig. 5-1f) as well as temperature (120 °C) (Fig. 5-1g) at this concentration shows little or no change in the morphology of the CoFe-LDH coated on CF substrate. Additionally, as shown in Fig. 5-1h, the increase in the initial concentration of the growth solution (i.e. 50:25) does not enhance the quantity of CoFe-LDH deposited on the CF substrate. The surface compositions of the LDH coated CF were analyzed by EDX and the elemental peaks of C, O, Fe and Co were obtained. Interestingly, the molar ratio of Co to Fe was found to be 2.17, consistent with the initial and normal molar ratio of M<sup>II</sup>/M<sup>III</sup> in LDH. Besides, elemental peak of F was detected, which may be one of the interlayer anions that neutralized the excess positive charge of LDH layers. The O peak emanates mainly from octahedral -OH and interlayer water.

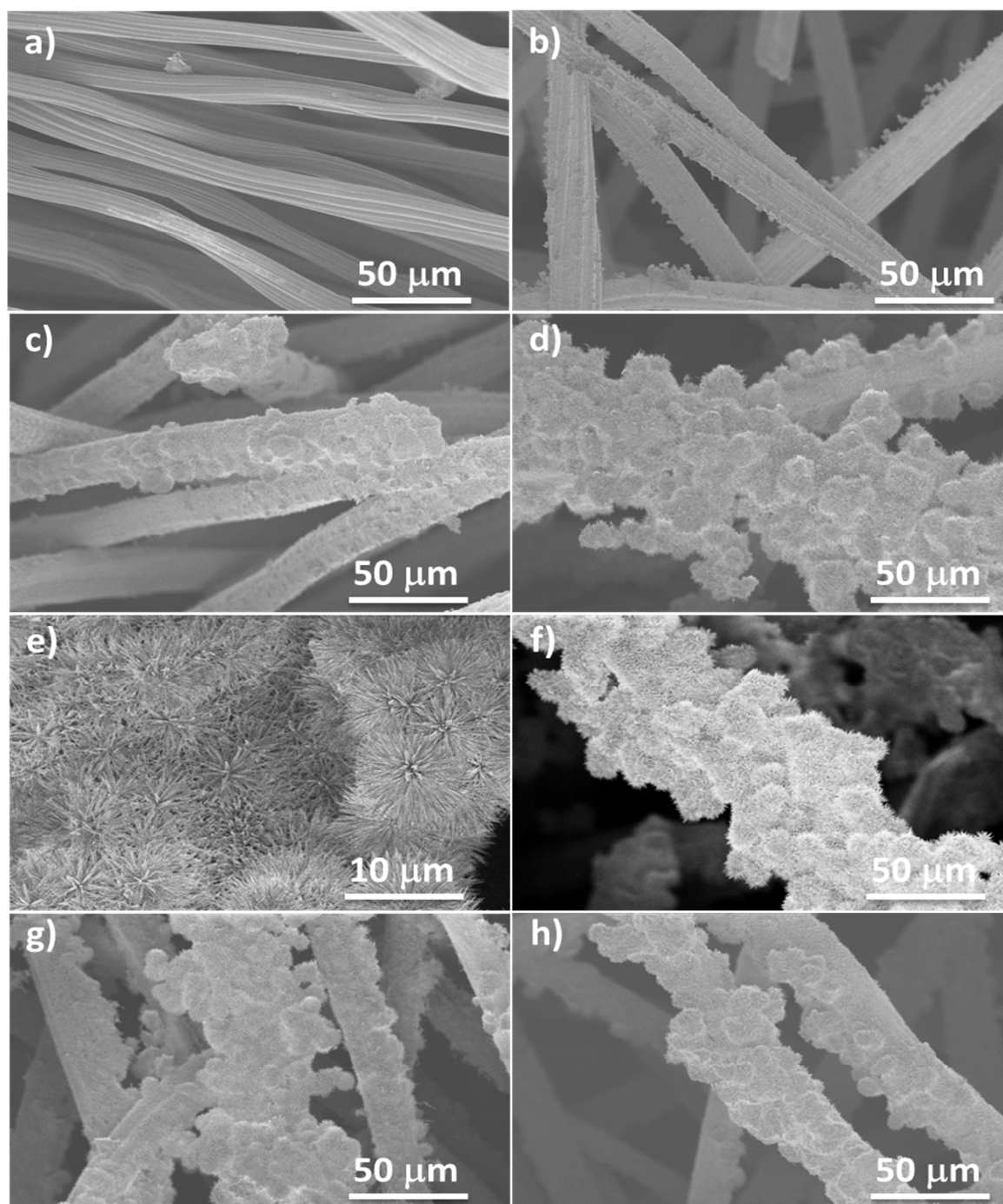


**Figure 5-1**– SEM images of (a) raw CF, (b) CoFe-LDH/CF – 70 °C for 7 h (c) CoFe-LDH/CF – 90 °C for 4 h (d) CoFe-LDH/CF – 90 °C for 7 h (e) magnified image of (d), (f) CoFe-LDH/CF – 90 °C for 21 h (g) CoFe-LDH/CF – 120 °C for 7 h and (h) CoFe-LDH/CF – 90 °C for 7 h. Note: (a-f) – 25:12.5 and (h) – 50: 25 ( $\text{Co}^{2+}/\text{Fe}^{3+}$ )



The TEM images (Figure 5-2) of CoFe-LDH deposited on CF showed rod-like structures with average width of 30–40 nm and lengths up to 400 nm. The CoFe-LDH plates were intercalated with each other to form a hierarchical network, which provide both high specific surface area and fast diffusion of substance within the structure for excellent electrochemical reactions.

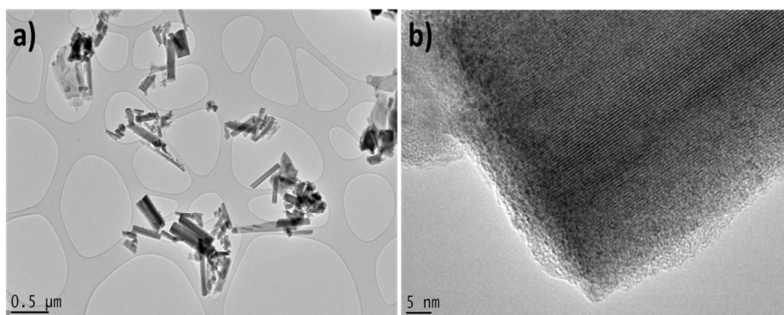


**Figure 5-2**– TEM images of CoFe-LDH.

The XRD patterns of the CoFe-LDH powder (Fig. 5-3a, upper diffractogram) and CoFe-LDH/CF cathode (Fig. 5-3a, lower diffractogram) showed characteristic reflections corresponding to the crystal planes (003), (006), (009), (012), (015), and (018), of a typical layered hydroxide-like phase. A good symmetry was obtained in the as-prepared LDH and LDH/CF as shown by the weak peaks at  $2\theta = 54.9^\circ$  and  $57^\circ$ , assigned to (110) and (113) crystal planes [47,48]. The broad peak at  $2\theta = 23.4^\circ$  and  $43.7^\circ$  in lower diffractogram of Fig. 5-3a was characteristic of carbon substrate on which the LDH was grown. It is important to note that no other crystalline phase was detected, indicating the high purity of the LDH phase grown on the CF substrate. The functional groups present in the as-prepared LDH/CF were examined from ATR FT-IR spectrum (Fig. 5-3b) of the powder CoFe-LDH using diamond indenter. The FT-IR spectrum was recorded in the wavelength range of  $400 - 4000 \text{ cm}^{-1}$ . As could be seen from the FTIR spectrum, a narrow band observed at around  $3690 \text{ cm}^{-1}$  was associated to the stretching vibration of non-hydrogen bonded O–H groups (OH in the brucite sheet). The second band located at  $3470 \text{ cm}^{-1}$  could be ascribed to the stretching vibration mode of hydrogen bonded O–H groups (interlayer water) in the CoFe-LDH [48,49]. The bands between  $2400 - 1900 \text{ cm}^{-1}$  were due to diamond indenter of the FT-IR. A small absorption band located at  $1610 \text{ cm}^{-1}$  was assigned to the bending vibration of absorbed water molecules onto the CoFe-LDH via hydrogen

bonding. The strong absorption band at  $1420\text{ cm}^{-1}$  is characteristic of N–O stretching mode of the surface adsorbed and interlayer nitrate species, which is predominantly from the starting reactants in growth solution (i.e.  $\text{Co}(\text{NO}_3)_2 \cdot 6\text{H}_2\text{O}$  and  $\text{Fe}(\text{NO}_3)_3 \cdot 9\text{H}_2\text{O}$ ). Additionally,  $\text{CO}_3^{2-}$  may also be identified as adsorbed or interlayer anions as shown by small band at  $1050\text{ cm}^{-1}$ , which may come from adsorption of  $\text{CO}_2$  either from the atmosphere or during the synthesis from the decomposition of urea [47]. Other bands observed in the lower wavelength region ( $856$  and  $735\text{ cm}^{-1}$ ) can be associated with stretching vibration of M–OH and M–O bondings (M = Co and Fe) in the brucite sheet of the LDH [50].

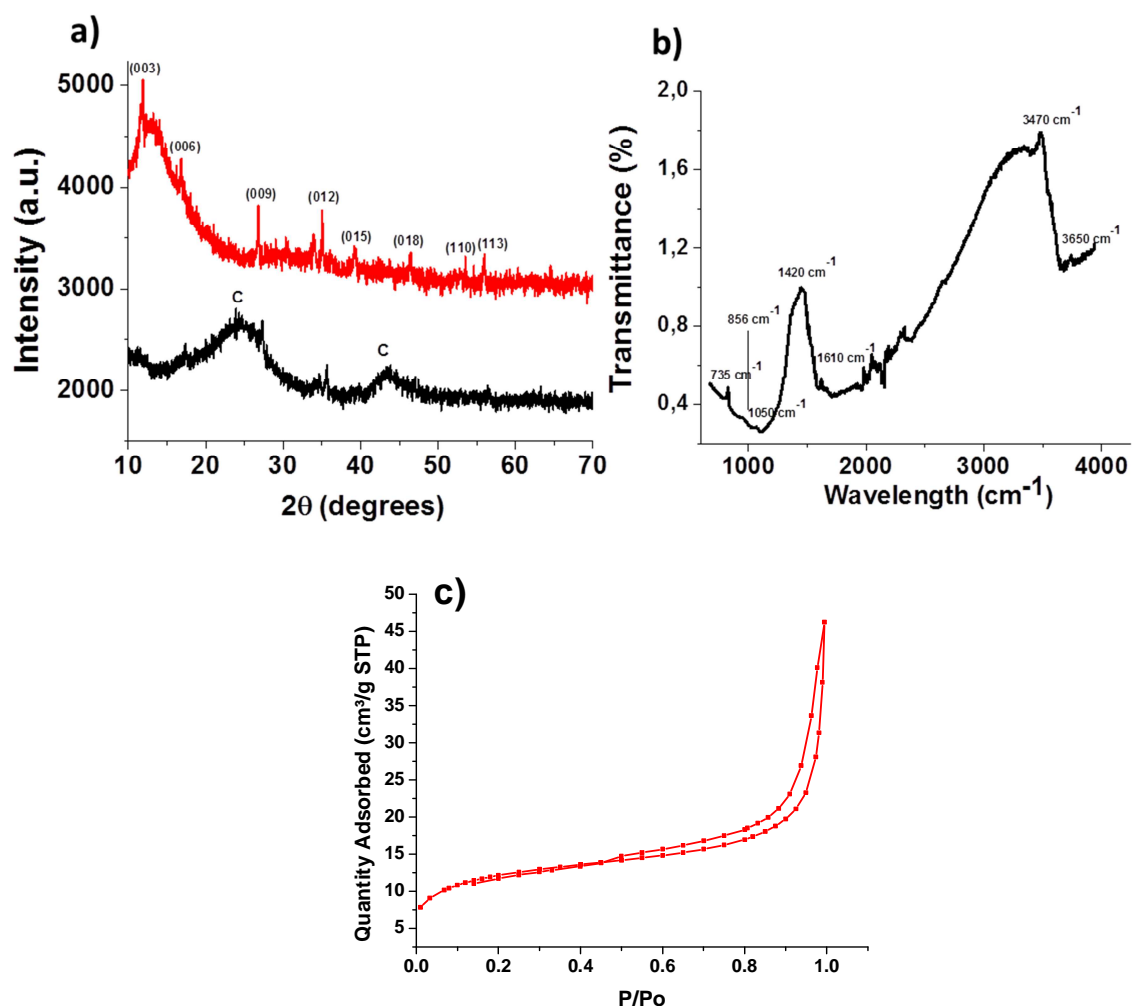


**Figure 5-3**– (a) XRD pattern of the powder CoFe-LDH (red curve) and CoFe-LDH/CF electrode (black curve), (b) FTIR – spectrum of the powder CoFe-LDH and (c) N<sub>2</sub> adsorption isotherm CoFe-LDH.

The N<sub>2</sub> adsorption-desorption result for CoFe-LDH showed type IV isotherm (Figure 3c) with hysteresis loop typical of mesoporous material. The BET surface area was 42.9 m<sup>2</sup> g<sup>-1</sup> and the total pore volume 0.18 cm<sup>3</sup> g<sup>-1</sup>.

The chemical composition and electronic states at the surface of the as-prepared CoFe-LDH on CF were analyzed by XPS, as shown in Fig. 5-4a and b, the Co 2p core lines split into Co 2p<sub>3/2</sub> (782.5 eV) and Co 2p<sub>1/2</sub> (798.2 eV) peaks with the later accompanied by a satellite band at 803.4 eV (Fig. 5-4a), demonstrative of a high-spin Co<sup>II</sup> state in the LDH material [48,51]. Similarly, the peaks of Fe 2p<sub>3/2</sub> and Fe 2p<sub>1/2</sub> emanates from the splitting of Fe 2p lines are located at 711.3 and 724.8 eV (Fig. 5-4b) respectively, having a spin energy separation of 13.5 eV [52]. The XPS spectra showed C1s core line at 287.5 eV, confirming the existence of carbon (Figure 4c). Existential state of other elements such as N, O and F in the CoFe-LDH/CF were confirmed by XPS as shown in Figure 4d.

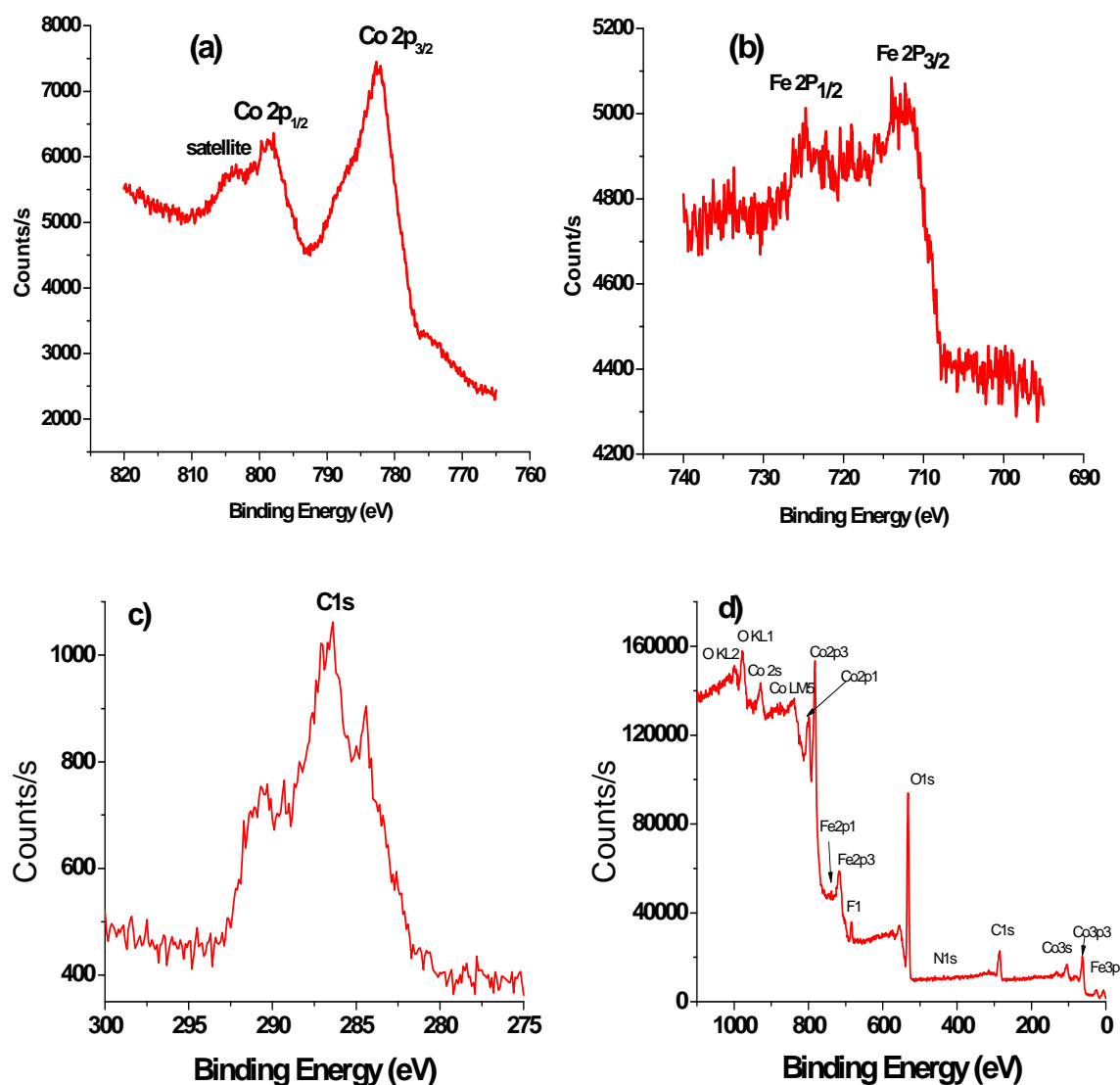


**Figure 5-4**– XPS spectra for (a) Co 2p, (b) Fe 2p of CoFe-LDH/CF, (c) C1s and (d) existential state of Co, Fe, C, O and N of CoFe-LDH/CF

### 5.3.3 Electrochemical behavior of the CoFe-LDH/CF

CV of the CoFe-LDH/CF (25:12.5, 90 °C and 7 h treatment) in 50 mM Na<sub>2</sub>SO<sub>4</sub> aqueous electrolyte at different pHs were shown in Fig. 5-5a. This study was essential in order to determine the contribution of the homogeneous Fenton's oxidation to the overall mineralization of the pollutants and the stability of the prepared cathode with pH. A slow reversible system at ~

0.25 V vs. SCE and  $\sim 0.56$  V vs. SCE during the anodic and cathodic sweeps were clearly observed at pH 2 and 3, indicating iron reduction and oxidation respectively ( $\text{Fe}^{3+}/\text{Fe}^{2+}$  redox couple). This implies that  $\text{Fe}^{\text{III}}$  was leached into the solution. The peak current increased with the decrease of pH, revealing the gradual leaching of Fe and Co into the solution since LDH became less stable as the solution was becoming more acidic. The presence of Co in the solution could lead to extra reversible conversion redox processes via reduction of  $\text{Fe}^{3+}$  by  $\text{Co}^{2+}$  [50]. No redox peak was observed at pH 5.83, indicating high stability of the CoFe-LDH coat on CF with negligible leaching of the metal ions into the solution.

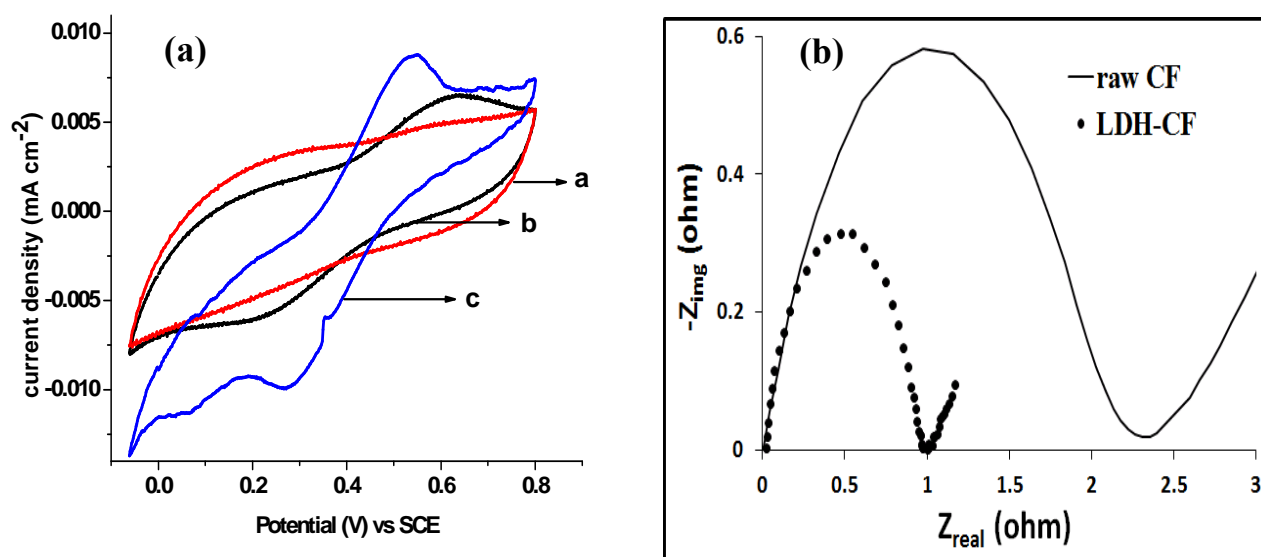


**Figure 5-5**– (a) CVs of CoFe-LDH/CF (synthesized at 90 °C for 7 h), in 50 mM  $\text{Na}_2\text{SO}_4$  at scan rate  $50 \text{ mVs}^{-1}$ : Curves at (a) pH 5.83, (b) pH 3 and (c) pH 2; and (b) EIS of raw and CoFe-LDH modified CF

Generally in EF process, excellent electrochemical properties (i.e. conductivity) of the electrode are as essential as the Fenton catalytic activity. The interface properties and potential of electron transfer between the electroactive substance and the prepared electrode was investigated by EIS. Fig. 5-5b shows the electrochemical impedance spectra of raw and CoFe-LDH modified CF electrodes. The Nyquist plots presents suppressing semicircle arcs corresponding to the interfacial charge-transfer resistance ( $R_{\text{ct}}$ ) with the intercepts on the real axis provides the actual value of  $R_{\text{ct}}$  (i.e. the diameter of the semicircle). As can be seen in Fig. 5-5b, There was

increase of interfacial resistance and in turn, decrease of electrical conductivity of the CF cathode after the modification with CoFe-LDH as shown by increase of the intercept of the Nyquist plot. However, the  $R_{ct}$  obtained was 0.97 and 2.3  $\Omega$  for raw CF and CoFe-LDH/CF respectively, indicating that the CF still maintains excellent conductivity after modified with CoFe-LDH. The increase in  $R_{ct}$  of CF from 0.97 to 2.3  $\Omega$  after modification with CoFe-LDH was expected since the LDH coating is non-conducting solid.

#### 5.3.4 Mineralization of AO7 by EF process using CoFe-LDH/CF cathode over wide pH range

The performance of the as-prepared CoFe-LDH/CF as a suitable cathode as well as catalyst source for heterogeneous EF process was evaluated by studying the mineralization of AO7 as a model pollutant at pH 2, 3, 5.83 and 7.1. As shown in Fig. 5-6a, high level of mineralization of AO7 was achieved in a wide pH range from 2 to 7.1 in heterogeneous EF oxidation with CoFe-LDH/CF cathode. For instance, TOC removal of 90, 97, 80, and 66% were obtained at pH 2, 3, 5.83 and 7.1 respectively, after 8 h of electrolysis. Based on literature [12,14], the heterogeneous EF reaction occurs on the surface of the CoFe LDH catalyst, thus expanding the working pH range of the EF process without the precipitation of the Fe/Co sludge. It is important to note that at lower pH (i.e. pH 2 and 3) the overall mineralization of the AO7 is a combination of both heterogeneous oxidation at the surface of the cathode and homogeneous oxidation in the bulk solution due to the leaching of the  $Fe^{III}/Co^{II}$  from the brucite sheet of the LDH. The ICP analysis of the treated solutions (Table 5-1) after 8 h shows significant leaching of the  $Fe^{III}/Co^{II}$  in the LDH at pH 2 and 3 (Table 5-1), confirmed the participation of the homogeneous EF in the mineralization of the AO7. The CoFe-LDH catalyst was highly stable as the pH increases toward basic region as shown by CV results (Fig. 5-5a), where the mineralization was major by heterogeneous EF reaction at the surface of the catalyst. This is apparent from the amount of Fe and Co found in the final solution, which is less than 0.08 mg L<sup>-1</sup> at pH 5.83 and 7.1 during the whole EF process (Table 5-1). The higher performance observed at pH 3 compared to pH 2 was primarily due to contribution of homogeneous electro-Fenton's reaction since it is optimum at pH ~ 3 [1]. The lower efficiency of EF at pH < 3 could be explained by (i) the preferential formation of peroxonium ions ( $H_3O_2^+$ ) which makes the

electrogenerated  $\text{H}_2\text{O}_2$  electrophilic and reduces its reactivity towards  $\text{Fe}^{2+}$  at such low pH [11,43], and (ii) huge quantities of the  $\text{Fe}^{\text{III}}/\text{Co}^{\text{II}}$  leached into the solution at pH 2, which may provoke wasting reactions (eq. 5-4) that consumed the generated hydroxyl radicals.

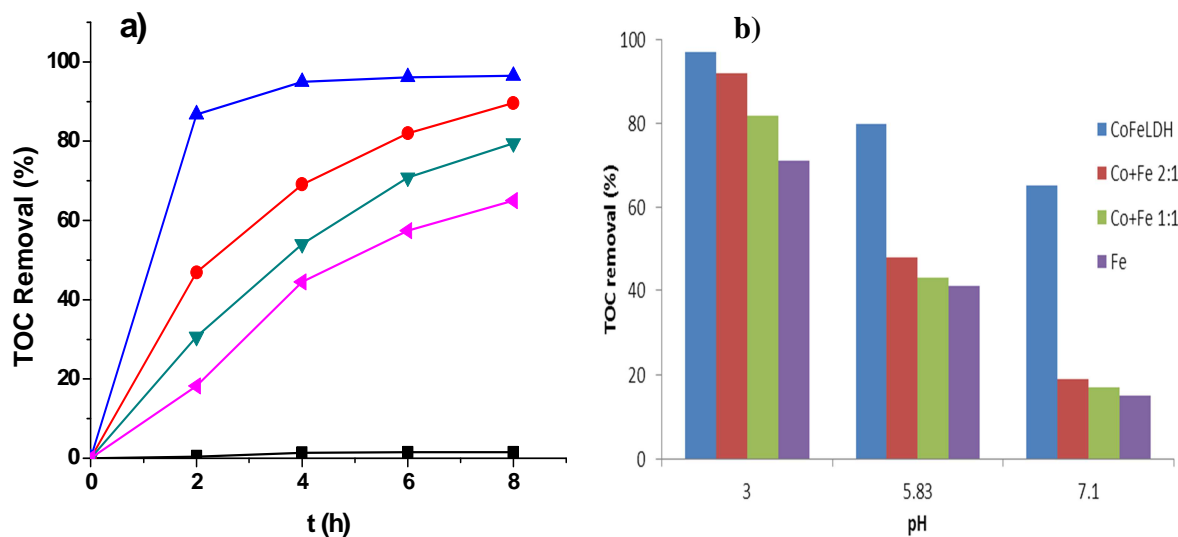


**Figure 5-6**– (a) Effect of initial solution pH on the mineralization of AO7 using CoFe-LDH/CF synthesized at 90 °C, for 7 h and 25:12.5 molar concentration, (■) pH 2, (●) pH 3, (▲) pH 5.83, and (▼) pH 7.1, (b) Comparison between heterogeneous EF with CoFe-LDH/CF cathode and homogeneous EF with raw CF cathode and  $\text{Fe}^{2+}/\text{Co}^{2+}$  at different pH. (RSD: 2%)

Comparison studies with traditional homogeneous EF process using 0.2 mM  $\text{Fe}^{2+}$ ,  $\text{Co}^{2+}$  or  $\text{Fe}^{2+}/\text{Co}^{2+}$  (1:1 or 1:2 n/n) and raw CF cathode, showed inferior mineralization compared to heterogeneous EF with CoFe-LDH at all pH studied (Fig. 6b). There was drastic reduction in mineralization efficiency in homogeneous EF system as the pH increases. After 8 h, TOC removal of 80% was attained at pH 5.83 in heterogeneous catalysis with CoFe-LDH/CF cathode, which is at least 1.7 times that of homogeneous system with  $\text{Fe}^{2+}/\text{Co}^{2+}$  at the same pH. Further increase in pH to 7.1 causes more drastic reduction in efficiency of homogeneous system with the TOC removal less than one-third of that of heterogeneous system with CoFe-LDH/CF cathode. This reduction was mainly due to  $\text{Fe}^{3+}/\text{Co}^{3+}$  precipitation which reduce the Fenton's reaction rate.

**Table 5-1**– Concentration of Co and Fe after 8h during EF treatment at different pHs

<b>pH</b>	<b>Co (mg L<sup>-1</sup>) RSD =1%</b>	<b>Fe (mg L<sup>-1</sup>) RSD =1%</b>
<b>2</b>	13.69	4.58
<b>3</b>	2.02	0.63
<b>5.83</b>	0.075	0.061
<b>7.1</b>	0.041	0.009

The mineralization of AO7 by  $\cdot\text{OH}$  generated by catalytic activity of CoFe-LDH/CF cathode proceeds via the formation of several aromatic/cyclic intermediates such as 4-aminophenol, hydroquinone, 1,4- benzoquinone, 1,2-naphthaquinone, 4-aminobenzosulphonic acid, 4-hydroxybenzosulphonic acid, 2-hydroxy-1,4-naphthalenedione and its derivatives, 2-formyl benzoic acid, and salicylic acid which have also been reported by previous studies [53,54]. Further oxidation of these intermediates by  $\cdot\text{OH}$  leads to cleavage of their cyclic rings to form several short-chain carboxylic acids which were later oxidized to  $\text{CO}_2$  and  $\text{H}_2\text{O}_2$ .

The corresponding AO7 conversion/degradation at pH 3 for the comparison studies showed in Figure 5-6b is given in Figure 5-7. Slightly faster degradation of AO7 was observed for homogeneous compared to heterogeneous EF process at the early stage of treatment as expected because the latter was much diffusion dependent compared to the former due to prevailing surfaced-catalyzed process that controlled the oxidation



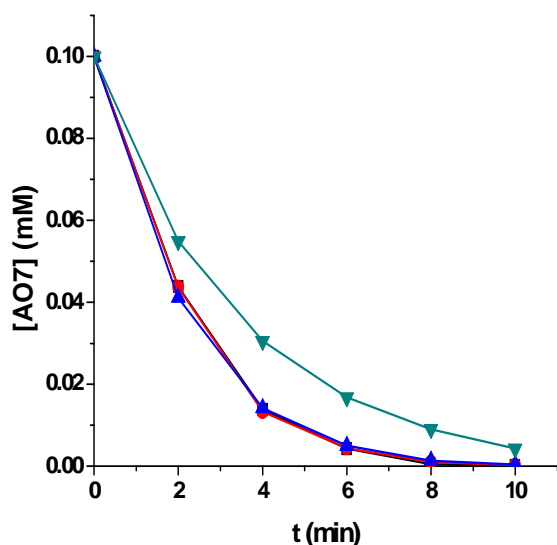


**Figure 5-7**– Degradation of AO7 at pH 3 (■) Fe<sup>2+</sup>, (●) Co + Fe (1:1), (▲) Co + Fe (2:1) (▼) CoFe-LDH/CF.

### 5.3.5 Effect of hydrothermal treatment parameters on mineralization of AO7

The influence of hydrothermal treatment parameters such as temperature, time and initial concentration on the mineralization of AO7 solution was investigated and the results were presented in Fig. 5-8. Overall, the hydrothermal treatment parameters control the loading and the morphology of the CoFe-LDH wall on the CF substrate which in turn affects the mineralization of AO7 because of difference in quantity of catalyst loaded on the CF. Among studied parameters, hydrothermal treatment temperature has the greatest effect on the mineralization of AO7 (Fig. 5-8a) with the highest TOC removal obtained with CoFe-LDH/CF synthesized at 90 °C. It is important to state that the effect of hydrothermal treatment temperature was investigated at initial molar concentration of 25:12.5 (Co<sup>2+</sup>:Fe<sup>3+</sup>) and treatment time of 7 h. The CoFe-LDH/CF synthesized at 70 °C has lower loading of CoFe-LDH compared to those synthesized at 90 or 120 °C. In fact, the loading of CoFe-LDH was found to be 0.540 (± 0.002), 7.2 (± 0.3) and 7.0 (± 0.3) mg cm<sup>-2</sup> for synthesis made at 70, 90 and 120 °C, respectively. At 70 °C, the decomposition of urea and NH<sub>4</sub>F into aqueous NH<sub>3</sub>, which initiated the concurrent precipitation of Co<sup>II</sup>/Fe<sup>III</sup> hydroxides into LDH, was relatively low. As such, very scanty nuclei of CoFe-LDH were formed on the CF substrate with limited growth (Fig. 5-1b). Optimum loading obtained at

90 °C could be attributed to excellent decomposition of both urea and  $\text{NH}_4\text{F}$  at this temperature which ensured high alkalinity of the growth solution, and in turn efficient nucleation and growth of CoFe-LDH on the CF substrate as shown in Fig. 5-1c,d. Although high loading was expected at 120 °C, but the latter was slightly lower compared to the one obtained at 90 °C. This could be explained by excessive growth of the LDH particles into heavy conglomerates which stripped them off from the substrate surface. After 8 h of electrolysis, the TOC removal was 73, 97 and 94% for 70, 90 and 120 °C, respectively.

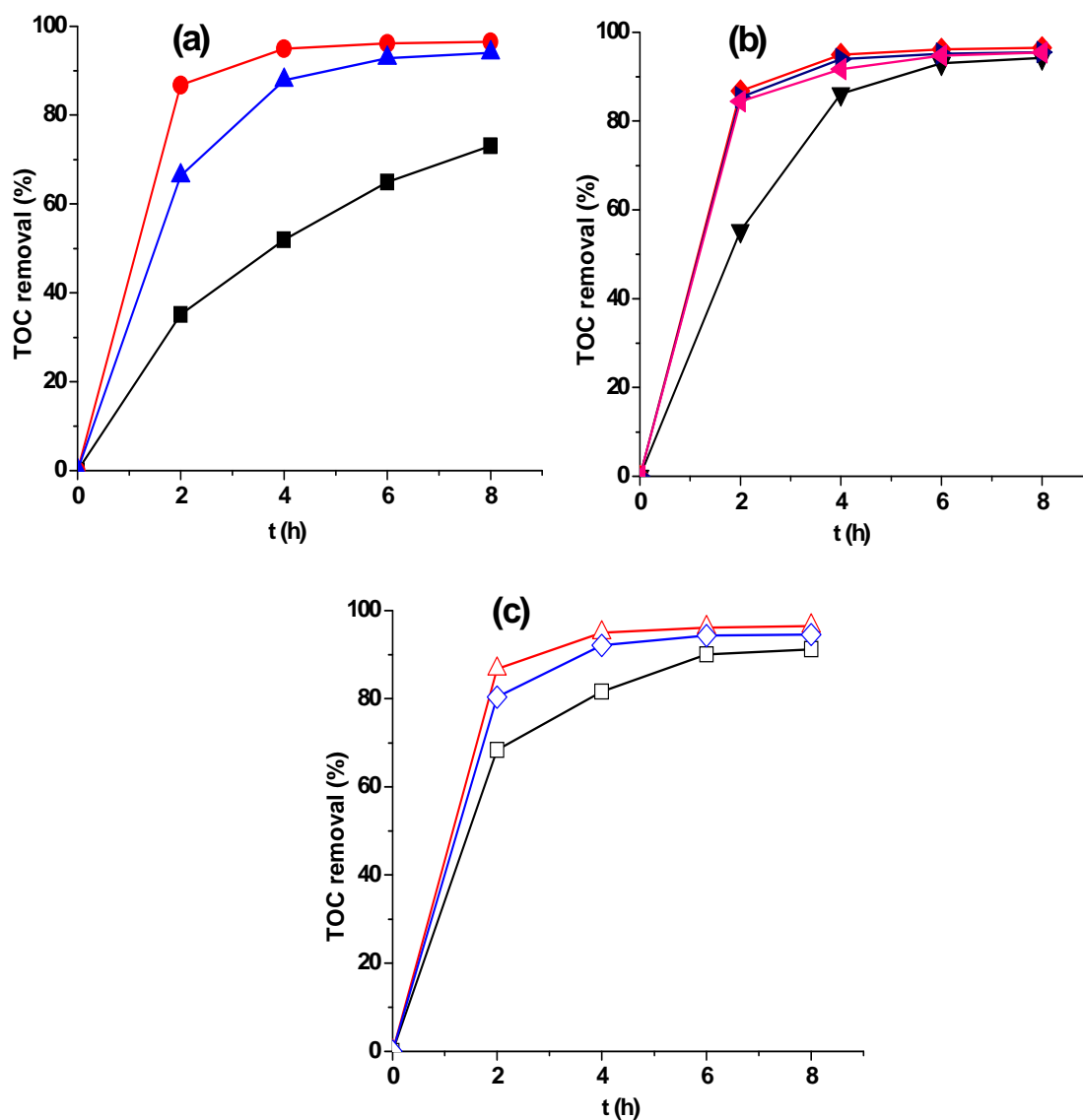


**Figure 6-8**– Effect of hydrothermal treatment parameters on the mineralization of AO7 at pH 3: (a) temperature (■) 70 °C, (●) 90 °C and (▲) 120 °C; (b) time (▼) 4 h, (◆) 7 h, (◀) 14 h and (▶) 21 h; and (c) initial molar concentration of growth solution (Co<sup>2+</sup>:Fe<sup>3+</sup>) (□) 10:5, (△) 25:12.5 and (◇) 50:25 (Co<sup>2+</sup>:Fe<sup>3+</sup>). (RSD: 2%)

Similar effect was observed with hydrothermal treatment time and initial concentration with optimum loading of CoFe-LDH on CF at 7h and initial molar ratio of 25:12.5 (Co<sup>2+</sup>:Fe<sup>3+</sup>). Synthesis made at lower and longer treatment time than 7 h or initial molar ration other than 25:12.5 (Co<sup>2+</sup>:Fe<sup>3+</sup>) shows less loading, which in turn reduced the efficiency of the heterogeneous EF system

### 5.3.6 Catalyst leaching and reusability of the CoFe-LDH/CF

The leaching of Co<sup>II</sup> and Fe<sup>III</sup> from CoFe-LDH/CF cathode investigated by studying EF treatment of AO7 at pH 3 was shown in Fig. 5-9a. Catalytic activity and stability are important features of a good catalyst, which determine its reusability for several cycles [52]. As a heterogeneous catalyst, metal species leaching from solid to the bulk solution was one key issue, and must be minimized to limit the contribution of homogeneous EF and enhance the reusability of the electrode. The concentrations of both Co and Fe gradually accumulated in the treated solution with electrolysis time and 0.63 and 2.02 mg L<sup>-1</sup> of Fe and Co, respectively, were found in the final solution after 8 h of electrolysis (Fig. 5-9a). This implies that the mineralization of the AO7 was mostly due to surface-catalyzed process, even at pH 3. The evidence of leaching at this pH is obvious in the SEM image and XPS analysis of the used CoFe-LDH/CF after 8 h of electrolysis which indicates significant removal of the needlelike structure of the LDH and reduction in XPS spectral of both Co and Fe respectively (Fig. 5-10a-c). The stability of the catalytic activity of prepared CoFe-LDH/CF was even much better at circumneutral pH as the leaching of metal ions from the LDH was less than 0.08 mg L<sup>-1</sup> during the whole EF process as shown in Table 5-1.

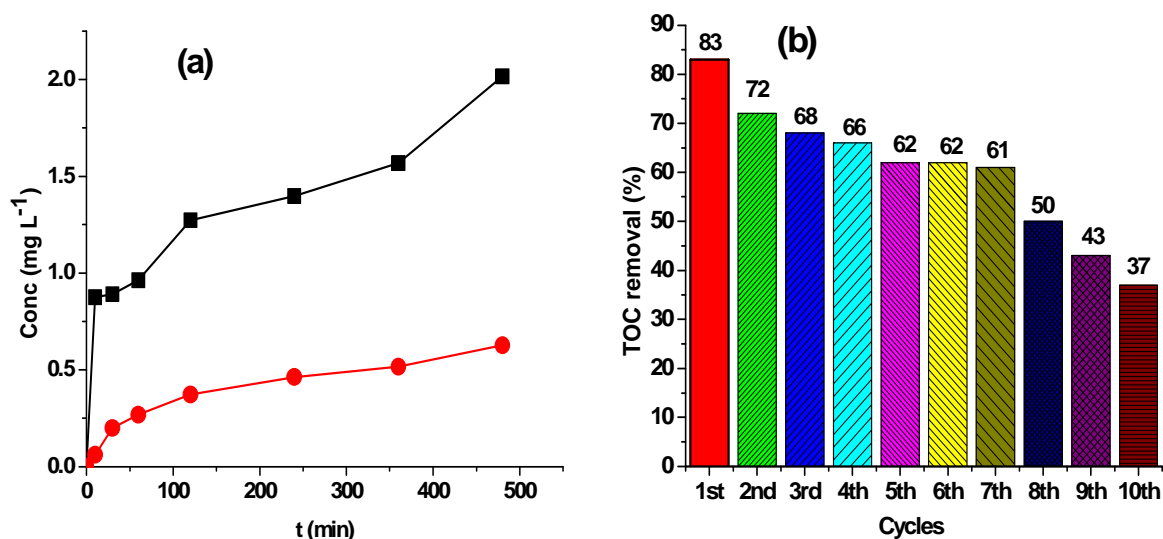


**Figure 5-9**– (a) Evolution of the concentration of Fenton's catalyst/co-catalyst in the treated solution (**RSD: 1%**); (■) Co and (●) Fe and (b) TOC removal (**RSD: 2%**) after 2 h vs number of cycles for the EF treatment using CoFe-LDH/CF synthesis at optimal conditions.

For practical environmental application and scale up, reusability of the prepared cathode was studied at pH 3 using CoFe-LDH/CF (90 °C; 7h and 25:12.5) dried at 80 °C after solvothermal treatment. Preliminary studies (result not reported) showed that drying as-prepared CoFe-LDH/CF at high temperature after solvothermal treatment enhanced the adhesion and stability of the catalytic activity of CoFe-LDH to the CF substrate but with slight reduction in mineralization efficiency of AO7. Indeed 6% and 10% reduction in mineralization efficiency were observed for sample dried at 80 and 100 °C respectively. This is attributed to the gradual collapse of the porous structure of the LDH into more compacted and less porous structure which hindered the diffusion of substance towards and from the carbon-felt matrix cathode. The production of hydrogen peroxide (H<sub>2</sub>O<sub>2</sub>) and reduction of leached Fe<sup>3+</sup> to Fe<sup>2+</sup> occur in the matrix of the carbon-felt substrate on which the LDH was deposited. As such, compacted LDH structure reduces the diffusion of substance. The reusability of CoFe-LDH/CF with number of cycles is shown in Fig. 5-9b. After the first cycle there was sharp reduction in TOC removal

(11%) largely due to mechanical wearing of the loosely bounded CoFe-LDH on CF substrate by the highly stirred treated solution. The TOC removal was almost stable afterward up till seventh (7<sup>th</sup>) cycle with approximately 10% reduction in TOC removal (Fig. 5-9b). Subsequent cycles showed lower mineralization of AO7 with TOC removal of 50, 43 and 37% for 8<sup>th</sup>, 9<sup>th</sup> and 10<sup>th</sup> cycle respectively, indicating the depletion of the catalyst (Co<sup>II</sup> and Fe<sup>III</sup>) from the cathode. The lost in catalyst was due to leaching at lower pH because LDH are relatively unstable at strong acidic pH. A much better reusability and stability is possible at circumneutral because of limited leaching of the metal ions from the LDH as explained earlier (Table 5-1).

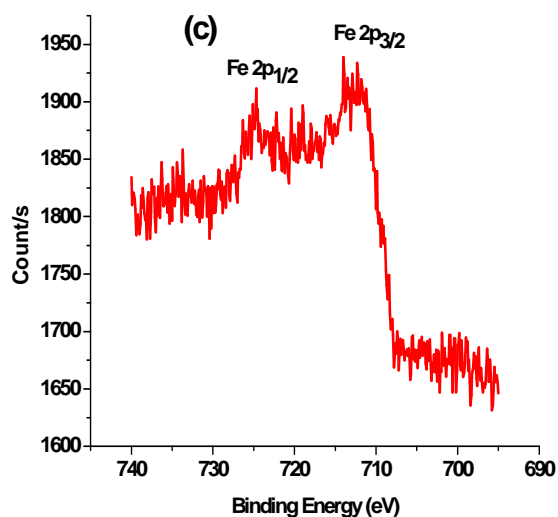
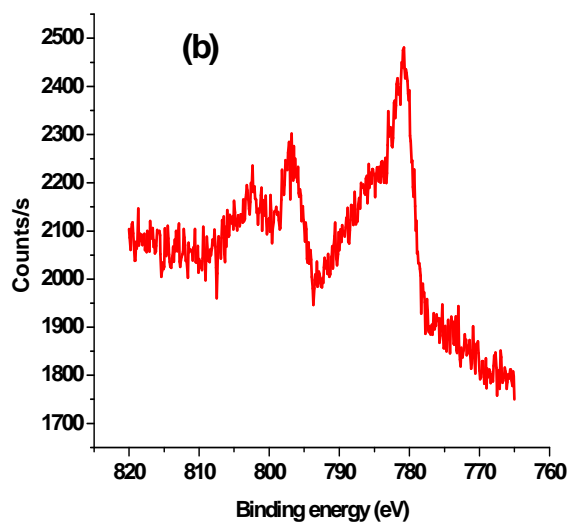
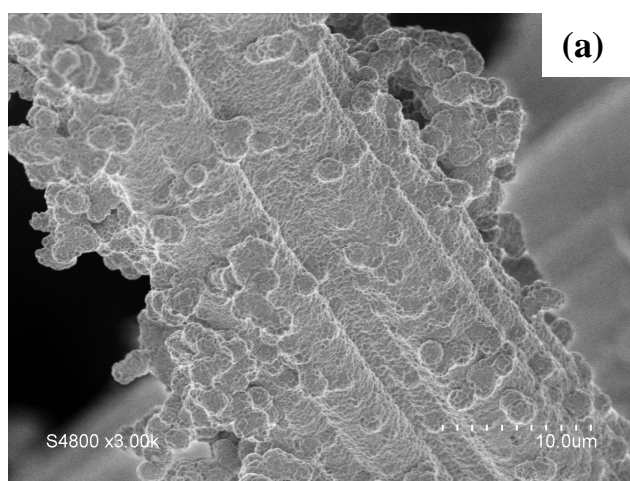


**Figure 5-10**– (a) SEM image of CoFe-LDH/CF; XPS spectra for (b) Co 2p and (d) Fe 2p of CoFe-LDH/CF after used in EF degradation of AO7 at pH 3 for 8 h.

### 5.3.7 Mechanism of Efficient removal of AO7 with CoFe-LDH/CF cathode in EF oxidation

Previous studies [12,14] have shown that mechanisms of Fenton's catalytic decomposition of  $\text{H}_2\text{O}_2$  by heterogeneous catalyst can be in two ways, depending on the working pH. Under low acidic pH conditions, the process is controlled by redox cycling of  $\text{Fe}^{2+}/\text{Fe}^{3+}$  in the solution and surface catalyzed process by  $\equiv\text{Fe}[\text{III}]\text{—OH}$  at the surface of the catalyst, with the Fe ions in the bulk comes from the dissolution of the catalyst due to acidic pH. However at circumneutral pH, the catalysis of the  $\text{H}_2\text{O}_2$  should mainly occur at the catalyst surface with negligible contribution of dissolved Fe – species since  $\text{Fe}^{3+}$  is insoluble at this pH.

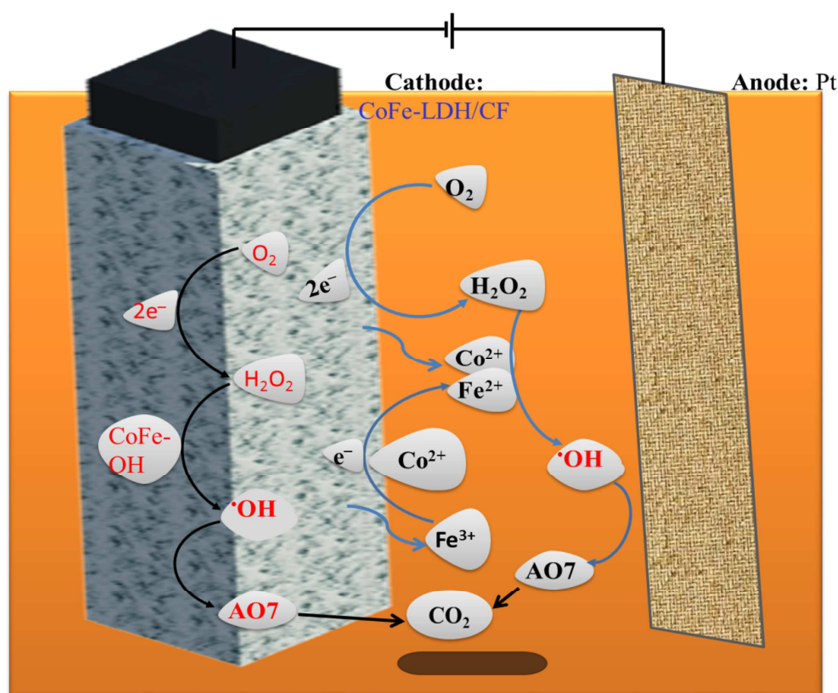
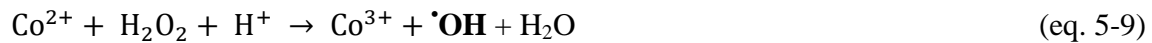


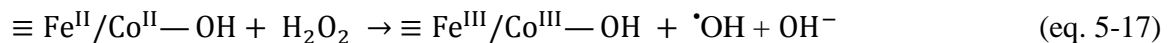
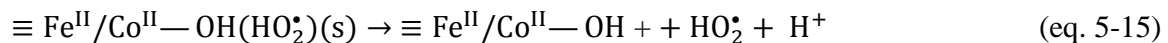
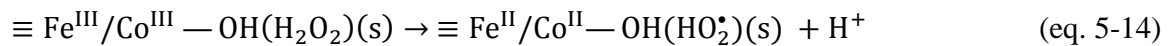
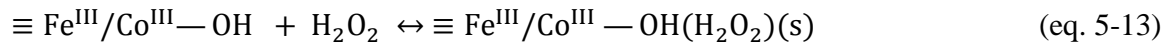
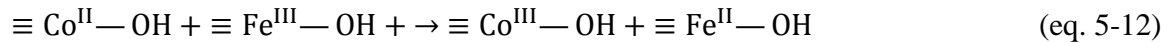
**Figure 5-11**– Schematic illustration of AO7 degradation in heterogeneous EF system with CoFe-LDH/CF cathode

The mineralization of AO7 by CoFe-LDH/CF cathode was proposed based on these two mechanisms as shown in Fig. 5-11. Firstly,  $\text{H}_2\text{O}_2$  is electrogeneration by  $2\text{e}^-$  reduction of oxygen adsorbed onto the surface of CoFe-LDH/CF cathode, and when working at lower pH 2 or 3,

concurrent partial leaching of  $\text{Co}^{\text{II}}/\text{Fe}^{\text{III}}$  occurs. At this pH, both mechanism controls the oxidation of the organics. In the bulk, the leached  $\text{Fe}^{3+}$  is first reduced to  $\text{Fe}^{2+}$  by obtaining electron at the cathode, diffused into the solution and, in conjunction with  $\text{Co}^{2+}$  catalyzed the decomposition of  $\text{H}_2\text{O}_2$  to produce  $\cdot\text{OH}$  in Fenton's (eq. 5-1) and Fenton-like reactions (eq. 5-9). The catalysis of  $\text{H}_2\text{O}_2$  is further accelerated by regeneration of  $\text{Fe}^{2+}$  from reduction of  $\text{Fe}^{3+}$  by  $\text{Co}^{2+}$  (eq. 5-10) in the bulk, as previously reported for homogeneous EF system [36].



The surface catalysis of  $\text{H}_2\text{O}_2$ , which occurs at the surface of CoFe-LDH/CF cathode and the predominant mechanism of mineralization of AO7 at circumneutral pH, also started in similar manner to homogeneous system with the production of  $\text{H}_2\text{O}_2$  in the carbon matrix of the cathode. The production of  $\cdot\text{OH}$  from catalytic decomposition of  $\text{H}_2\text{O}_2$  is strongly correlated to the production rate of  $\text{H}_2\text{O}_2$  and the catalyst properties. The surface-catalyzed mechanism for the production of  $\cdot\text{OH}$  at the surface of CoFe-LDH/CF is proposed as follow:



Under circumneutral pH conditions (pH 5.83 and 7.1), the application of applied current to the electrolytic cell immediately resulted in generation of large quantities of  $\text{H}_2\text{O}_2$  (eq. 5-2), and  $\equiv\text{Fe}^{\text{III}}-\text{OH}$  in the LDH obtained an electron to partial reduced to  $\equiv\text{Fe}^{\text{II}}-\text{OH}$  (eq. 5-11) [14,20] or via redox reduction by  $\equiv\text{Co}^{\text{II}}-\text{OH}$  (eq. 5-12) in a similar manner obtained in homogeneous EF system. The generated  $\text{H}_2\text{O}_2$  is adsorbed onto the surface of alkaline  $\equiv\text{Fe}^{\text{III}}/\text{Co}^{\text{III}}$  to generate  $\equiv\text{Fe}^{\text{III}}/\text{Co}^{\text{III}}-\text{OH}(\text{H}_2\text{O}_2)$  surface complex as presented in eq. 5-13, which later undergoes ground-state electron-transfer to form hydrogen peroxy radical complex (eq. 5-14). The generated  $\text{Fe}^{\text{II}}/\text{Co}^{\text{II}}-\text{OH}(\text{HO}_2^\bullet)$  at surface of the brucite sheet of the LDH can activated itself to form  $\text{Fe}^{\text{II}}/\text{Co}^{\text{II}}-\text{OH}$  and  $\text{HO}_2^\bullet$  (eq. 5-15) with the former catalyzes the decomposition of the  $\text{H}_2\text{O}_2$  generated in the carbon matrix to produced  $^\bullet\text{OH}$ . The AO7 molecules which are diffused towards and in the cathode rapidly oxidized by the generated  $^\bullet\text{OH}$ . Two parallel reaction pathways are possible for the produced  $^\bullet\text{OH}$ : (i) direct oxidation of organic pollutants and (ii) destructive reaction with  $\text{H}_2\text{O}_2$  to form  $\text{HO}_2^\bullet$  (eq. 5-20). However, the high diffusion rate of the AO7 to the cathode ensure the direct oxidation reaction is predominant and prevent the  $^\bullet\text{OH}$  quenching, thus improving the mineralization of the pollutant. Obviously, the  $\equiv\text{Co}^{\text{II}}-\text{OH}$  in the LDH enhanced the production of  $^\bullet\text{OH}$  via the Fenton-like reaction and regeneration of  $\text{Fe}^{\text{II}}-\text{OH}$  (eq. 5-13).

## 5.4 Conclusions

This study has investigated a facile and simple two-steps synthesis route to produce CoFe-LDH on the surface of CF substrate for application as suitable cathode as well as heterogeneous Fenton catalyst source for electrochemical wastewater treatment over a wide range of pH. The structure, morphology and loading of the CoFe-LDH on the CF substrate largely depended on the hydrothermal treatment temperature and time and the best synthesis was obtained at 90 °C for 7 h using initial Co/Fe molar concentration ratio of 25:12.5.

The as-deposited CoFe-LDH/CF cathode exhibited high performance catalytic activity in EF treatment of AO7 over a wide pH range, with superior TOC removal at all pH studied compared to analogous homogeneous treatment with  $\text{Fe}^{2+}$  and/or  $\text{Co}^{2+}$  using raw CF cathode.



The TOC removal with CoFe-LDH/CF cathode was at least 1.7 and 3.5 times higher than homogeneous system with  $\text{Fe}^{2+}/\text{Co}^{2+}$  at pH 5.83 and 7.1 respectively.

The mineralization of AO7 was majorly by surfaced-catalyzed process at circumneutral pH, whereas there is significant contribution of homogeneous EF oxidation when working at low acidic pH of 3 and 2. At circumneutral pH, the CoFe-LDH was very stable and the quantity of Fe and Co leached into the solution was negligible, thus minimized the anxiety of Co toxicity. Furthermore, the as-prepared CoFe-LDH/CF showed relatively good reusability at pH 3 with more than 50% TOC removal after 8 cycles of 2 h treatment. Based on the results obtained in this work, the CoFe-LDH/CF is a good cathode material for efficient mineralization of organic pollutants at circumneutral pH.

**Reference**

- [1] E. Brillas, I. Sires, M.A. Oturan, Electro-Fenton process and related electrochemical technologies based on Fenton's reaction chemistry, *Chem. Rev.* 109 (2009) 6570–6631.
- [2] J.M. Peralta-Hernández, Y. Meas-Vong, F.J. Rodríguez, T.W. Chapman, M.I. Maldonado, L.A. Godínez, In situ electrochemical and photo-electrochemical generation of the fenton reagent: A potentially important new water treatment technology, *Water Res.* 40 (2006) 1754–1762.
- [3] M.A. Oturan, J. Peirotten, P. Chartrin, A.J. Acher, Complete destruction of *p*-nitrophenol in aqueous medium by electro-Fenton method, *Environ. Sci. Technol.* 34 (2000) 3474–3479.
- [4] M.A. Oturan, N. Oturan, C. Lahitte, S. Trevin, Production of hydroxyl radicals by electrochemically assisted Fenton's reagent, *J. Electroanal. Chem.* 507 (2001) 96–102.
- [5] M.A. Oturan, N. Oturan, M.C. Edelahi, F.I. Podvorica, K.E. Kacemi, Oxidative degradation of herbicide diuron in aqueous medium by Fenton's reaction based advanced oxidation processes, *Chem. Eng. J.* 171 (2011) 127–135.
- [6] I. Sirés, F. Centellas, J.A. Garrido, R.M. Rodríguez, C. Arias, P.-L. Cabot, E. Brillas, Mineralization of clofibric acid by electrochemical advanced oxidation processes using a boron-doped diamond anode and  $\text{Fe}^{2+}$  and UVA light as catalysts, *Appl. Catal. B Environ.* 72 (2007) 373–381.
- [7] A. Özcan, Y. Şahin, A.S. Koparal, M.A. Oturan, A comparative study on the efficiency of electro-Fenton process in the removal of protham from water, *Appl. Catal. B Environ.* 89 (2009) 620–626.
- [8] M.A. Rodrigo, N. Oturan, M.A. Oturan, Electrochemically assisted remediation of pesticides in soils and water: A Review, *Chem. Rev.* 114 (2014) 8720–8745.
- [9] H. Zhang, C. Fei, D. Zhang, F. Tang, Degradation of 4-nitrophenol in aqueous medium by electro-Fenton method, *J. Hazard. Mater.* 145 (2007) 227–232.
- [10] C.A. Martínez-Huitle, M.A. Rodrigo, I. Sirés, O. Scialdone, Single and coupled electrochemical processes and reactors for the abatement of organic water pollutants: A critical review, *Chem. Rev.* 115 (2015) 13362–13407.

- [11] M.A. Oturan, J.-J. Aaron, Advanced oxidation processes in water/wastewater treatment: Principles and applications. A review, *Crit. Rev. Environ. Sci. Technol.* 44 (2014) 2577–2641.
- [12] J. Li, Z. Ai, L. Zhang, Design of a neutral electro-Fenton system with Fe@Fe<sub>2</sub>O<sub>3</sub>/ACF composite cathode for wastewater treatment, *J. Hazard. Mater.* 164 (2009) 18–25.
- [13] N. Qiao, H. Ma, M. Hu, Design of a neutral three-dimensional electro-Fenton system with various bentonite-based Fe particle electrodes: A comparative study, *Mater. Res. Innov.* 19 (2015) S2–137–S2–141.
- [14] Y. Wang, G. Zhao, S. Chai, H. Zhao, Y. Wang, Three-dimensional homogeneous ferrite-carbon aerogel: One pot fabrication and enhanced electro-Fenton reactivity, *ACS Appl. Mater. Interfaces.* 5 (2013) 842–852.
- [15] A. Dirany, I. Sirés, N. Oturan, M.A. Oturan, Electrochemical abatement of the antibiotic sulfamethoxazole from water, *Chemosphere.* 81 (2010) 594–602.
- [16] I. Sirés, J.A. Garrido, R.M. Rodríguez, E. Brillas, N. Oturan, M.A. Oturan, Catalytic behavior of the Fe<sup>3+</sup>/Fe<sup>2+</sup> system in the electro-Fenton degradation of the antimicrobial chlorophene, *Appl. Catal. B Environ.* 72 (2007) 382–394.
- [17] N. Barhoumi, L. Labiadh, M.A. Oturan, N. Oturan, A. Gadri, S. Ammar, E. Brillas, Electrochemical mineralization of the antibiotic levofloxacin by electro-Fenton-pyrite process, *Chemosphere.* 141 (2015) 250–257.
- [18] L. Labiadh, M.A. Oturan, M. Panizza, N.B. Hamadi, S. Ammar, Complete removal of AHPS synthetic dye from water using new electro-fenton oxidation catalyzed by natural pyrite as heterogeneous catalyst, *J. Hazard. Mater.* 297 (2015) 34–41.
- [19] B. Hou, H. Han, S. Jia, H. Zhuang, P. Xu, D. Wang, Heterogeneous electro-Fenton oxidation of catechol catalyzed by nano-Fe<sub>3</sub>O<sub>4</sub>: kinetics with the Fermi's equation, *J. Taiwan Inst. Chem. Eng.* 56 (2015) 138–147.
- [20] G. Zhang, Y. Zhou, F. Yang, FeOOH-Catalyzed Heterogeneous Electro-Fenton System upon Anthraquinone@Graphene Nanohybrid Cathode in a Divided Electrolytic Cell: Catholyte-Regulated Catalytic Oxidation Performance and Mechanism, *J. Electrochem. Soc.* 162 (2015) H357–H365. doi:10.1149/2.0691506jes.
- [21] S.B. Hammouda, F. Fourcade, A. Assadi, I. Soutrel, N. adhoum, A. Amrane, L. Monser, Effective heterogeneous electro-Fenton process for the degradation of a malodorous

- compound, indole, using iron loaded alginate beads as a reusable catalyst, *Appl. Catal. B Environ.* 182 (2016) 47–58.
- [22] C. Zhang, M. Zhou, G. Ren, X. Yu, L. Ma, J. Yang, F. Yu, Heterogeneous electro-Fenton using modified iron–carbon as catalyst for 2,4-dichlorophenol degradation: Influence factors, mechanism and degradation pathway, *Water Res.* 70 (2015) 414–424.
- [23] Y. Li, A. Lu, H. Ding, X. Wang, C. Wang, C. Zeng, Y. Yan, Microbial fuel cells using natural pyrrhotite as the cathodic heterogeneous Fenton catalyst towards the degradation of biorefractory organics in landfill leachate, *Electrochem. Commun.* 12 (2010) 944–947.
- [24] J.A. Banuelos, O. Garcia-Rodriguez, F.J. Rodriguez-Valadez, L.A. Godinez, Electrochemically prepared iron-modified activated carbon electrodes for their application in electro-Fenton and photoelectro-Fenton processes, *J. Electrochem. Soc.* 162 (2015) E154–E159.
- [25] L. Bounab, O. Iglesias, E. González-Romero, M. Pazos, M. Ángeles Sanromán, Effective heterogeneous electro-Fenton process of m-cresol with iron loaded activated carbon, *RSC Adv.* 5 (2015) 31049–31056.
- [26] S.D. Sklari, K.V. Plakas, P.N. Petsi, V.T. Zaspalis, A.J. Karabelas, Toward the development of a novel electro-Fenton system for eliminating toxic organic substances from water. Part 2. Preparation, characterization, and evaluation of iron-impregnated carbon felts as cathodic electrodes, *Ind. Eng. Chem. Res.* 54 (2015) 2059–2073.
- [27] H. Zhao, L. Qian, X. Guan, D. Wu, G. Zhao, Continuous Bulk FeCuC aerogel with ultradispersed metal nanoparticles: An efficient 3D heterogeneous electro-Fenton cathode over a wide range of pH 3–9, *Environ. Sci. Technol.* 50 (2016) 5225–5233.
- [28] Y. Wang, H. Zhao, G. Zhao, Highly ordered mesoporous Fe<sub>3</sub>O<sub>4</sub>@Carbon embedded composite: High catalytic activity, wide pH range and stability for heterogeneous electro-Fenton, *Electroanalysis.* 28 (2016) 169–176.
- [29] W. Chen, X. Yang, J. Huang, Y. Zhu, Y. Zhou, Y. Yao, C. Li, Iron oxide containing graphene/carbon nanotube based carbon aerogel as an efficient E-Fenton cathode for the degradation of methyl blue, *Electrochimica Acta.* 200 (2016) 75–83.
- [30] D.G. Evans, R.C.T. Slade, *Structural Aspects of Layered Double Hydroxides*, in: Springer-Verlag, Berlin/Heidelberg, 2005.

- [31] X. Long, Z. Wang, S. Xiao, Y. An, S. Yang, Transition metal based layered double hydroxides tailored for energy conversion and storage, *Mater. Today*. 19 (2016) 213–226.
- [32] Q. Wang, D. O'Hare, Recent Advances in the Synthesis and Application of Layered Double Hydroxide (LDH) Nanosheets, *Chem. Rev.* 112 (2012) 4124–4155.
- [33] L. Indira, M. Dixit, P.V. Kamath, Electrosynthesis of layered double hydroxides of nickel with trivalent cations, *J. Power Sources*. 52 (1994) 93–97.
- [34] A.M. Fogg, V.M. Green, H.G. Harvey, D. O'Hare, New separation science using shape-selective ion exchange intercalation chemistry, *Adv. Mater.* 11 (1999) 1466–1469.
- [35] X. Duan, D.G. Evans, eds., *Layered Double Hydroxides*, Springer-Verlag, Berlin/Heidelberg, 2006.
- [36] M. Pimentel, N. Oturan, M. Dezotti, M.A. Oturan, Phenol degradation by advanced electrochemical oxidation process electro-Fenton using a carbon felt cathode, *Appl. Catal. B Environ.* 83 (2008) 140–149.
- [37] R. Salazar, E. Brillas, I. Sirés, Finding the best  $\text{Fe}^{2+}/\text{Cu}^{2+}$  combination for the solar photoelectro-Fenton treatment of simulated wastewater containing the industrial textile dye Disperse Blue 3, *Appl. Catal. B Environ.* 115-116 (2012) 107–116.
- [38] N. Oturan, M. Zhou, M.A. Oturan, Metomyl degradation by electro-Fenton and electro-Fenton-like processes: A kinetics study of the effect of the nature and concentration of some transition metal ions as catalyst, *J. Phys. Chem. A*. 114 (2010) 10605–10611.
- [39] L. Zhou, Z. Hu, C. Zhang, Z. Bi, T. Jin, M. Zhou, Electrogenation of hydrogen peroxide for electro-Fenton system by oxygen reduction using chemically modified graphite felt cathode, *Sep. Purif. Technol.* 111 (2013) 131–136.
- [40] T.X.H. Le, M. Bechelany, S. Lacour, N. Oturan, M.A. Oturan, M. Cretin, High removal efficiency of dye pollutants by electron-Fenton process using a graphene based cathode, *Carbon*. 94 (2015) 1003–1011.
- [41] W. Hajjaji, S.O. Ganiyu, D.M. Tobaldi, S. Andrejkovičová, R.C. Pullar, F. Rocha, J.A. Labrincha, Natural Portuguese clayey materials and derived  $\text{TiO}_2$ -containing composites used for decolouring methylene blue (MB) and orange II (OII) solutions, *Appl. Clay Sci.* 83-84 (2013) 91–98.
- [42] Y.M. Slokar, A. Majcen Le Marechal, Methods of decoloration of textile wastewaters, *Dyes Pigments*. 37 (1998) 335–356.

- [43] I. Sirés, E. Brillas, M.A. Oturan, M.A. Rodrigo, M. Panizza, Electrochemical advanced oxidation processes: today and tomorrow. A review, *Environ. Sci. Pollut. Res.* 21 (2014) 8336–8367. doi:10.1007/s11356-014-2783-1.
- [44] X. Cai, X. Shen, L. Ma, Z. Ji, C. Xu, A. Yuan, Solvothermal synthesis of NiCo-layered double hydroxide nanosheets decorated on RGO sheets for high performance supercapacitor, *Chem. Eng. J.* 268 (2015) 251–259.
- [45] Y. Han, Z.-H. Liu, Z. Yang, Z. Wang, X. Tang, T. Wang, L. Fan, K. Ooi, Preparation of Ni<sup>2+</sup>–Fe<sup>3+</sup> layered double hydroxide material with high crystallinity and well-defined hexagonal shapes, *Chem. Mater.* 20 (2008) 360–363.
- [46] M. Gong, Y. Li, H. Wang, Y. Liang, J.Z. Wu, J. Zhou, J. Wang, T. Regier, F. Wei, H. Dai, An advanced Ni–Fe layered double hydroxide electrocatalyst for water oxidation, *J. Am. Chem. Soc.* 135 (2013) 8452–8455.
- [47] Y. Li, L. Zhang, X. Xiang, D. Yan, F. Li, Engineering of ZnCo-layered double hydroxide nanowalls toward high-efficiency electrochemical water oxidation, *J. Mater. Chem.* 2 (2014) 13250.
- [48] G. Nagaraju, G.S.R. Raju, Y.H. Ko, J.S. Yu, Hierarchical Ni–Co layered double hydroxide nanosheets entrapped on conductive textile fibers: a cost-effective and flexible electrode for high-performance pseudocapacitors, *Nanoscale.* 8 (2016) 812–825.
- [49] Y. Tang, Y. Liu, S. Yu, W. Guo, S. Mu, H. Wang, Y. Zhao, L. Hou, Y. Fan, F. Gao, Template-free hydrothermal synthesis of nickel cobalt hydroxide nanoflowers with high performance for asymmetric supercapacitor, *Electrochimica Acta.* 161 (2015) 279–289.
- [50] J. Zhao, J. Chen, S. Xu, M. Shao, D. Yan, M. Wei, D.G. Evans, X. Duan, CoMn-layered double hydroxide nanowalls supported on carbon fibers for high-performance flexible energy storage devices, *J. Mater. Chem.* 1 (2013) 8836.
- [51] T.J. Chuang, C.R. Brundle, D.W. Rice, Interpretation of the x-ray photoemission spectra of cobalt oxides and cobalt oxide surfaces, *Surf. Sci.* 59 (1976) 413–429.
- [52] Q. Wang, S. Tian, J. Long, P. Ning, Use of Fe(II)Fe(III)-LDHs prepared by co-precipitation method in a heterogeneous-Fenton process for degradation of Methylene Blue, *Catal. Today.* 224 (2014) 41–48.
- [53] A. Özcan, M.A. Oturan, N. Oturan, Y. Şahin, Removal of Acid Orange 7 from water by electrochemically generated Fenton’s reagent, *J. Hazard. Mater.* 163 (2009) 1213–1220.

- [54] T.X.H. Le, T.V. Nguyen, Z.A. Yacouba, L. Zoungrana, F. Avril, E. Petit, J. Mendret, V. Bonniol, M. Bechelany, S. Lacour, G. Lesage, M. Cretin, Toxicity removal assessments related to degradation pathways of azo dyes: Toward an optimization of Electro-Fenton treatment, *Chemosphere*. 161 (2016) 308–318.

## **CHAPTER 6**

---

### **General Conclusions and Future Perspectives**



## CHAPTER 6

### 6.1 General conclusions

The environmental and health challenges posed by the wide spread of pharmaceuticals and their active metabolites in aquatic environments has considerably increased the interest of researcher in developing effective, efficient, economical and environmental compatible technologies for their complete destruction to avoid their release to the environment. Electrochemical technologies constitute a response to such requirements due to the high efficiency they have shown for the mineralization of persistent organic pollutants and their degradation by-products. This work has investigated the performance of substoichiometric titanium oxide as a suitable ceramic anode material for electrochemical degradation of pharmaceuticals and the use of CoFe-LDH modified carbon-felt cathode in heterogeneous electro-Fenton mineralization of organic pollutant. The  $Ti_4O_7$  electrode was prepared by reducing commercial stoichiometric  $TiO_2$  – a highly abundant and cheap feedstock, with coke (carbon) followed by plasma deposition on sandblasted Ti-alloy substrate. The final electrode containing mainly  $Ti_4O_7$  is firmly coated on Ti substrate as shown by XRD and SEM analysis (Fig. 3 a, and 3b; chapter 3). The performance of the  $Ti_4O_7$  anode in electrochemical wastewater was compared with other commercially available electrode such as DSA, Pt and even BDD. On the other hand, CoFe-LDH was grown by solvothermal process on carbon-felt as heterogeneous catalyst for application in EF at circumneutral pH to overcome the challenges of narrow working pH window and reusability encounter in tradition electro-Fenton system. The efficiency of the heterogeneous system was compared with that of homogeneous system using soluble catalyst and raw carbon-felt cathode.

#### *6.1.1 Electrooxidation of pharmaceutical residues using sub-stoichiometric titanium oxides*

Substoichiometric  $TiO_2$  has demonstrated to be a suitable and effective electrode in electrooxidation of pharmaceutical AMX as these studies have shown (chapter 3). The main results are listed as follows:

- excellent degradation and relatively high mineralization of AMX was obtained with  $\text{Ti}_4\text{O}_7$  anode, with the mineralization much higher compared to DSA and Pt anode but inferior to BDD anode
- in-situ generated  $\text{H}_2\text{O}_2$  was found to significantly enhanced the AMX decay but have limited contribution to the mineralization of the drug.
- the decay of AMX concentrations always follow pseudo-first order kinetics with the apparent rate constant ( $k_{\text{app, AMX}}$ ) for oxidation of AMX increased with applied current; enhanced by *in-situ*  $\text{H}_2\text{O}_2$  generation and diminished with increased initial AMX concentration.
- there is a slight (17%) reduction in the activity of the prepared  $\text{Ti}_4\text{O}_7$  anode after 200 h of usage, possibly due to passivation.
- the major mineralization end-products after mineralization treatment at 120 mA are short-chain carboxylic and inorganic ions.
- initial AMX solution shows relatively high inhibition to *V. fischeri* bacteria, which further increased at the early stage of electrooxidation due to formation of cyclic intermediates but sharply decreased at the later stage of electrolysis.

Since the  $\text{Ti}_4\text{O}_7$  is produced mainly from  $\text{TiO}_2$  which is very cheap and highly abundant, this anode could be an interesting alternative in industrial wastewater treatment by electrooxidation

### 6.1.2 Substoichiometric titanium oxides as suitable anode materials for electro-Fenton degradation of pharmaceuticals

Electro-Fenton process with  $\text{Ti}_4\text{O}_7$  anode shows excellent mineralization of pharmaceutical PPN without the formation of yellowish  $\text{Ti-H}_2\text{O}_2$  complex, indicating that the anode is highly stable at acidic pH and is suitable for EF treatment. Comparative studies with AO at similar experimental conditions shows lower efficiency (82% TOC removal) compared to EF (96% TOC removal) (chapter 4). However, similar studies (AO and EF) with commercial DSA anode demonstrated inferior efficiency compared to  $\text{Ti}_4\text{O}_7$  anode, implying high oxidation ability of  $\text{Ti}_4\text{O}_7(\cdot\text{OH})$  than  $\text{DSA}(\cdot\text{OH})$ .

The PPN concentration decay followed pseudo-first order kinetics and the apparent rate constant increased with applied current but decreased with PPN concentration during both AO and EF treatment and the absolute rate constant for the reaction between  $\cdot\text{OH}$  and PPN was determined as  $(2.99 \pm 0.02) \times 10^9 \text{ L mol}^{-1} \text{ s}^{-1}$ . The final end products always found in the treated solution were carboxylic acids and inorganic ions.

### *6.1.3 Heterogeneous electro-Fenton process – an efficient alternative*

Excellent mineralization of azo-dye AO7 has been achieved over a pH range of 2 – 7.1 with heterogeneous EF using CoFe-LDH modified carbon-felt cathodes (Chapter 5). Two main mechanisms of oxidation of the pollutant were observed depending on the pH at which the EF is being carried out. Both  $\text{Fe}^{2+}/\text{Fe}^{3+}$  cyclic redox homogeneous catalyzed and surface-catalyzed process occur at pH 2 and 3 and only surface-catalyzed process was prevalent at pH 5.83 and 7.1 (chapter 5). The efficiency of the heterogeneous process was found to depend on pH and hydrothermal treatment parameters – temperature, time and concentration (during synthesis). The efficiency decreased as the pH increases due to the minimal contribution of the homogeneous catalyzed process, while best mineralization was obtained with CoFe-LDH/CF synthesized at 90°C, 7 h and 25:12.5 (Co:Fe) initial molar concentration (chapter 5).

Comparative studies with homogeneous EF using raw carbon-felt cathode and 0.2 mM  $\text{Fe}^{2+}$  and/or  $\text{Co}^{2+}$  showed lower efficiency and the TOC removal by heterogeneous EF was 1.7 and 3.5 times higher than homogeneous system with  $\text{Fe}^{2+}/\text{Co}^{2+}$  at pH 5.83 and 7.1 respectively (Fig. 5-5b, chapter 5). The CoFe-LDH/CF showed relatively good stability and reusability at pH 3 with mineralization of 61% still achievable after 7<sup>th</sup> cycle.

## **6.2 Future perspectives**

### *6.2.1 High current density application of plasma $\text{Ti}_4\text{O}_7$ electrode*

The  $\text{Ti}_4\text{O}_7$  prepared by plasma deposition was only tested at low current density ( $\leq 10 \text{ mA cm}^{-2}$ ) due to fear of delamination of the thin film  $\text{Ti}_4\text{O}_7$  from the Ti substrate. Other studies

that have investigated this class of electrode were also carried out at low current density. For commercial and industrial applications this electrode should be studied at high applied current densities ( $\geq 10 \text{ mA cm}^{-2}$ ). However, high current density may accelerate the formation of thin passivation layer at the surface of the electrode. The passivation layer is form as a result of the oxidation of  $\text{Ti}_4\text{O}_7$  by  $\text{O}_2$ . The mechanism of the formation of the passivation layer has not been investigated. Further studies are also necessary to find an economic way to minimize the passivation of the anode or method of completely remove the passivation and restore the activity of the electrode.

### *6.2.2 Coupling of membrane nanofiltration and EAOPs using reactive membranes*

Although some studies have employed the formability of  $\text{Ti}_4\text{O}_7$  powder to produce reactive membranes that is capable of performing filtration and electrochemical degradation simultaneously under the application of both current and pressure, but the obtained mineralization for the model pollutants studied is relatively low. Studies are required to fully understand the mechanism of the combined process as well as enhancing the efficiency of such process. A highly stable and electrochemically active  $\text{Ti}_4\text{O}_7$  membrane necessary for such studies is feasible plasma process. Beside the reactive  $\text{Ti}_4\text{O}_7$  membrane has not been test in electro-Fenton process. Further, pre-pilot scale experiment is required to better understand the combined process and its adaptability for commercial applications.

### *6.2.3 Enhancing the stability of the modified cathode and assessing the toxicity of the solution*

The stability of the prepared CoFe-LDH/CF cathode is an important characteristic required for the efficiency of the heterogeneous process studied because it not only enhance the efficiency of the process by preventing the leaching of the LDH but also eliminate the toxicity that may emanate from Co leached into the solution. As such there is necessity to enhance the stability of the CoFe-LDH to ensure zero percent leaching. The possibility of using Fe[II]/Fe[III] and Cu[II]Fe[III] LDH should be considered because of non-toxicity of Fe compared to Co.

Beside the heterogeneous system should be investigated for other pollutants especially pharmaceuticals residues.

#### *6.2.4 Treatment of real wastewater effluents*

The thesis work has been achieved by studying synthetic solutions of the selected pollutants, therefore it is important to test the experiments realized here with real wastewater effluents. The real effluents behave differently when treated by electrochemical techniques because of the multicomponent nature of its organic content, varying pH and its significant quantities of inorganic ions.

## **ANNEXES**

## Annex 1

### Valorization of the PhD research

#### Publications

- [1] **Ganiyu, S.O.**, Oturan, N., Raffy, S., Cretin, M., Esmilaire, R., van Hullebusch, E.D., Esposito, G., Oturan, M.A. (2016). Sub-stoichiometric titanium Oxide ( $Ti_4O_7$ ) as a suitable ceramic anode for electrooxidation of organic pollutants: A case study of kinetics, mineralization and toxicity assessment of amoxicillin. *Water Research* 106, 171-181. DOI:10.1016/j.watres.2016.09.056
- [2] **Ganiyu, S.O.**, van Hullebusch, E.D., Cretin, M., Esposito, G., Oturan, M.A. (2015). Coupling of membrane filtration and advanced oxidation processes for the removal of pharmaceutical residues. *Separation and Purification Technol.* 156, 891-914. DOI: 10.1016/j.seppur.2015.09.059.
- [3] **Ganiyu, S.O.**, Le, T.X.H., Bechelany, M., Esposito, G., van Hullebusch, E.D., Oturan, M.A., Cretin, M., (2016). Hierarchical CoFe-layered double hydroxide modified carbon-felt cathode for heterogeneous electro-Fenton. *Journal of Material Chemistry A (Accepted)* DOI: 10.1039/C6TA09100H
- [4] **Ganiyu, S.O.**, Oturan, N., Raffy, S., Esposito, G., van Hullebusch, E.D., Cretin, M., Oturan, M.A., (2016). Use of sub-stoichiometric titanium oxide as a ceramic electrode in anodic oxidation and electro-Fenton degradation of the beta-blocker propranolol: Degradation kinetics and mineralization pathway (*to be submitted to Electrochimica Acta*)

### Conferences

- Oral presentation
- ❖ **Ganiyu, S.O.**, Le, T.X.H., Bechelany, M., van Hullebusch, E.D., Oturan, M.A., Cretin, M., Hierarchical CoFe-layered double hydroxide modified carbon-felt cathode: Synthesis, characterization and application in heterogeneous electro-Fenton degradation of organic pollutants at circumneutral pH. 1<sup>st</sup> International Conference on Sustainable Water Processing, Sitges (Spain), September, 2016.
- ❖ **Ganiyu, S.O.**, Oturan, N., Hullebusch, E.D., Oturan, M.A., Removal of antibiotic amoxicillin from water by Electrochemical advanced oxidation processes: Influence of anode materials and applied current, Indo-French Water Workshop, Karaikudi (India), February, 2015
- Poster presentation
- ❖ **Ganiyu, S.O.**; Le, T.X.H., Bechelany, M., van Hullebusch, E.D., Oturan, M.A., Cretin, M., Synthesis, characterization and application of self-catalyzed layered double hydroxide coated carbon-felt cathode in electro-Fenton's degradation of organic pollutants, 67<sup>th</sup> Annual Meeting of International Society of Electrochemistry, Den Haag (The Netherlands), August, 2016.

### Summer school presentations

- ❖ **Ganiyu, S.O.**, Le, T.X.H., Bechelany, M., Esposito, G., van Hullebusch, E.D., Oturan, M.A., Cretin, M., Hierarchical CoFe-layered double hydroxide modified carbon-felt cathode: Synthesis, characterization and application in heterogeneous electro-Fenton wastewater treatment, Summer school on contaminated sediments: Characterization and remediation, Delft (The Netherlands), May, 2016.
- ❖ **Ganiyu, S.O.**, van Hullebusch, E.D., Oturan, N., Cretin, M., Esposito, G., Oturan, M.A., Degradation of paracetamol by electrochemical advanced oxidation processes using platinum or boron doped diamond anode and carbon felt cathode: Kinetics and mineralization, Summer school on contaminated soils: From characterization to remediation, Paris-Est (Champs-sur-Marne, France), June, 2015



- ❖ **Ganiyu, S.O.**, van Hullebusch, E.D., Oturan, N. Cretin, M. Esposito, G., Oturan, M.A., Coupling of membrane nanofiltration and electrochemical advanced oxidation processes for removal of pharmaceutical residues from wastewater, Summer school on biological treatment of municipal solid waste, Cassino and Gaeta, (Italy), June, 2014.

## Annex 2

## Curriculum Vitae



## Personal data

<b>Name</b>	<b>Soliu Oladejo GANIYU</b>
<b>Email</b>	<a href="mailto:oladejosoliu@gmail.com">oladejosoliu@gmail.com</a>
<b>Nationality</b>	<b>Nigerian</b>
<b>Date of birth</b>	<b>23/09/1983</b>

## Education and training

2013 – 2016	PhD degree in Environmental Chemistry, ERASMUS Mundus Joint Doctoral Degree “Environmental Technologies for Contaminated Solids, Soils and Sediments” ETeCoS <sup>3</sup> . University Paris-Est, France and University of Cassino and Southern Lazio, Italy
2011 – 2013	Masters of Science, specializing in nanomaterial, ERASMUS Mundus Master Programme “International Masters in Advanced Clay Science” IMACS. University de Poitiers, France, University of Ottawa, Canada and University of Aveiro, Portugal.
2002 – 2007	Bachelor degree in Metallurgical and Materials Engineering, Federal University of Technology Akure, Nigeria.

---

**Publications**

---

- [1] **Ganiyu, S.O.**, Oturan, N., Raffy, S., Cretin, M., Esmilaire, R., van Hullebusch, E.D., Esposito, G., Oturan, M.A. (2016). Sub-stoichiometric titanium Oxide ( $Ti_4O_7$ ) as a suitable ceramic anode for electrooxidation of organic pollutants: A case study of kinetics, mineralization and toxicity assessment of amoxicillin. *Water Research* 106, 171-181. DOI:10.1016/j.watres.2016.09.056
- [2] **Ganiyu, S.O.**, van Hullebusch, E.D., Cretin, M., Esposito, G., Oturan, M.A. (2015). Coupling of membrane filtration and advanced oxidation processes for the removal of pharmaceutical residues. *Separation and Purification Technol.* 156, 891-914. DOI: 10.1016/j.seppur.2015.09.059.
- [3] **Ganiyu, S.O.**, Bispo, C., Bion, N., Ferreira, P., Batonneau-Gener, I.: Periodic mesoporous organosilicas as adsorbent for removal of organic pollutants from aqueous phase, *Microporous and Mesoporous Mater.* 200 (2014) 117-123. DOI: 10.1016/j.micromeso.2014.07.047
- [4] Hajjaji, W., **Ganiyu, S.O.**, Tobaldi, D.M., Andrejkovicova, S., Pullar, R.C., Rocha, F., Labrincha, J.F.: Natural Portuguese clayey materials and derived  $tio_2$ -containing composites used for decolouring methylene blue (MB) and orange ii (OII) solution, *Applied Clay Sci.* 83-84 (2013) 91-98; DOI: 10.1016/j.clay.2013.08.013